AD-A186 579

DTIC FILE COPY

# XEROX WEBSTER RESEARCH CENTER

## ELECTRONIC AND CHEMICAL STRUCTURE OF III-V/ METAL AND Si / METAL INTERFACES

DTIC
ELECTE
OCT 1 9 1987
S D
D

ANNUAL SUMMARY REPORT

L.J.Brillson, Principal Investigator
Xerox Webster Research Center
800 Phillips Rd 114/41D
Webster, NY 14580
Telephone (716) 422-6468

October 1. 1987

Office of Naval Research
800 North Quincy Street
Arlington, VA 22117

Sponsored by

Office of Naval Research
NR #372-098
Proposal No. 80-10-199
Contract No. N00014-80-C-0778

DISTRIBUTION STATEMENT A
Approved for public release
Distribution Unlimited

87 10 6 096

SECURITY CLASSIFICATION OF THIS PAGE *(When Data Entered)*

# REPORT DOCUMENTATION PAGE

READ INSTRUCTIONS BEFORE COMPLETING FORM

| | |
|---|---|
| 1. REPORT NUMBER | 2. GOVT ACCESSION NO. - |
| 3. RECIPIENT'S CATALOG NUMBER - | |
| 4. TITLE *(and Subtitle)*<br>Electronic and Chemical Structure of III-V/ Metal and Si/Metal Interfaces | 5. TYPE OF REPORT & PERIOD COVERED<br>Annual Summary Report |
| | 6. PERFORMING ORG. REPORT NUMBER |
| 7. AUTHOR(s)<br>L.J. Brillson | 8. CONTRACT OR GRANT NUMBER(s)<br>N00014-80-C-0778 |
| 9. PERFORMING ORGANIZATION NAME AND ADDRESS<br>Xerox Webster Research Center<br>800 Phillips Rd 114/41D<br>Webster, NY 14580 | 10. PROGRAM ELEMENT, PROJECT, TASK AREA & WORK UNIT NUMBERS<br>NR #372-078 |
| 11. CONTROLLING OFFICE NAME AND ADDRESS<br>Office of Naval Research<br>800 North Quincy Street<br>Arlington, VA 22117-5000 | 12. REPORT DATE<br>September 30, 1987 |
| | 13. NUMBER OF PAGES |
| 14. MONITORING AGENCY NAME & ADDRESS *(if different from Controlling Office)*<br>Office of Naval Research | 15. SECURITY CLASS. *(of this report)*<br>Unclassified |
| | 15a. DECLASSIFICATION/DOWNGRADING SCHEDULE - |

16. DISTRIBUTION STATEMENT *(of this Report)*

Approved for public release, Distribution unlimited.

17. DISTRIBUTION STATEMENT *(of the abstract entered in Block 20, if different from Report)*

18. SUPPLEMENTARY NOTES

19. KEY WORDS *(Continue on reverse side if necessary and identify by block number)*

20. ABSTRACT *(Continue on reverse side if necessary and identify by block number)*

An annual report of research performed under Office of Naval Research Grant No. N00014-80-C-0778

DD FORM 1 JAN 73 1473 EDITION OF 1 NOV 65 IS OBSOLETE

S/N 0102-LF-014-6601

SECURITY CLASSIFICATION OF THIS PAGE *(When Data Entered)*

## I. Overview

Over the past year, we have carried out an experimental program to investigate the electronic states and band structure at GaAs, InP, $In_xGa_{1-x}As$, GaP, and Si / metal interfaces and their relationship to the chemical reactions and interdiffusion which evolve at room temperature and elevated temperatures. We have used soft x-ray photoemission spectroscopy to determine Fermi level movements and atomic redistribution during initial states of Schottky barrier formation and conventional electrical techniques to characterize transport mechanisms across these junctions. We have used cathodoluminescence spectroscopy to observe optical emission from interface states and their evolution with metal coverages. Surface photovoltage spectroscopy measurements complemented the identification of interface states on a nanometer scale. Combined cathodoluminescence and photoluminescence spectroscopy measurements provided a measure of the influence which bulk trap states exert on the Schottky barrier formation. These measurements revealed new relationships between the semiconductor band bending, electronic states within the band gap localized near the interface, bulk trap states, and the atomic redistribution which occurs under various conditions of clean and "real" surface preparation, including oxidation and thermal processing.

This annual report for the period October 1, 1986 through September 30, 1987 defines (Sec. II) and summarizes (Sec.III) the bulk of this research and includes the papers published or in press as a result of this effort. A list of the papers published under Navy Contract #N00014-80-C-0778 (NR #372-078) as well as the papers

themselves are included in Sec. IV of this report. Also attached are: the cumulative list of publications (Sec.V) serially numbered, a list of postdoctoral fellows involved in the contract (Sec. VI), a list of Publications/Patents/Presentations/Honors (Sec. VII), money spent on equipment (Sec. VIII), transitions of research to industry (Sec. IX), and a list of collaborations with workers from academic institutions(Sec. X).

## II. Background

Over the last decade, surface science techniques have yielded considerable new information on the chemical, geometrical, and electronic structures of metal-semiconductor interfaces.[1-7] In particular, researchers have devoted substantial effort to improving our understanding of rectification at the metal-semiconductor interface ( e.g., Schottky barrier formation). It is now recognized that (1) the first few monolayers or less of deposited metal on a semiconductor produce large electronic changes in and below the semiconductor surface which can in fact dominate the electrical properties of the macroscopic junction, and that (2) the surface chemistry before and after metallization can have a major effect on the ultimate electronic states and electrical barriers formed. The former realization has justified the use of surface-sensitive techniques with atomic-scale depth resolution for probing semiconductor surfaces and interfaces. The latter discovery has led to a more general picture of the energy band structure at the microscopic metal-semiconductor interface than is commonly represented in solid - state electronics textbooks. Rather than an abrupt interface between metal and semiconductor, the electronic band structure must now take into account the possibilities of: a reacted region between metal and semiconductor with new dielectric properties, a nonparabolic band bending region within the semiconductor surface space charge

Codes
Dist | Avail and/or Special
A-1
QUALITY INSPECTED 2

region with electrically-active sites due to semiconductor outdiffusion and/or metal indiffusion, and a metal layer at the intimate semiconductor contact with altered chemical composition and work function.[1,8] Even this picture fails to take into account the possibility of chemical and morphological inhomogeneity.[9] The existence , extent, and electronic effects of such reacted and/or interdiffused regions will depend on the strength and nature of chemical bonding between the semiconductor and metal constituents.

Our understanding of interface electronic structure is far from complete. Analysis of metal - semiconductor band structure by surface science techniques has centered on measurements of band bending and localized electronic states - primarily by photoemission and electron loss spectroscopies. Such measurements are limited to overlayer thicknesses only a few nanometers or less due to the electron scattering length.[10] On the other hand, deep level capacitance spectroscopies can detect states within the semiconductor surface space charge region, but only indirectly for states located within a few atomic layers of the intimate interface.[11-13] Similarly, conventional laser-excited and high energy electron beam luminescence spectroscopies lack sufficient sensitivity to the intimate interface region.

In order to characterize the electronic band structure of states more than a few monolayers below the free metal-semiconductor interface plane yet confine such measurements to the near-interface region, one can make use of an optical technique with intermediate depth excitation - low energy cathodoluminescence spectroscopy (CLS).[14] The CLS technique allows us to monitor electronic structure (deep levels within the band gap, new band structure) of the semiconductor interface as it evolves into a truly metallic contact and to compare these features with the electronic and chemical properties extracted by other near-surface

techniques under ultrahigh vacuum (UHV) conditions. Such techniques include soft x-ray photoemission spectroscopy (SXPS) to monitor Fermi level ($E_F$) movements *via* rigid core level and valence band shifts as well as to monitor chemical reaction and diffusion via core level intensities and chemical shifts. In some cases, these spectroscopic techniques are coupled to J-V and C-V measurements to obtain Schottky barrier heights, doping densities, ideality factors, and interface state densities.This complement of experimental techniques can be used successfully to relate electronic and chemical structure for clean or carefully processed semiconductor surfaces with deposited metal overlayers.

Prime candidates for analysis by this battery of techniques are the III-V compounds. For this family of compound semiconductors, it is commonly believed that the $E_F$ "pins" in a narrow range of energies near mid-gap, thereby compromising the device capabilities of these materials.[15,16] On the other hand, the correlation of Schottky barrier heights with stoichiometry of anion versus cation outdiffusion indicates the formation of chemically-based, electrically-active sites within the semiconductor.[17] Likewise, a number of studies have now shown that chemical treatments of the semiconductor surface prior to deposition, i.e., interlayers[17,18], photoelectrochemical washing[19], gas exposure[20], can effectively expand the range of $E_F$ movement for some of these compounds. Furthermore, there exists only limited information on electronic properties of molecular-beam-epitaxy (MBE)-grown III-V / metal interfaces. Hence, these techniques and materials provide opportunities to understand and better control the Schottky barrier formation of clean as well as non-ideal metal-semiconductor junctions.

## III. Results

The work under this contract can be grouped into three related areas: (1) the electronic structure of the metal-semiconductor interface as it evolves from the monolayer chemisorption regime to truly metallic coverages; (2) the extension of these studies to ternary III-V semiconductor materials ; and (3) the systematics of Schottky barrier formation for III-V compounds in general and its relation to microscopic interface chemistry.

In the first area, we have measure optical emission from interface states formed by metal deposition of UHV-cleaved InP(110) and GaAs (110) surfaces by means of low energy CLS.[21-24] This is the first direct observation of discrete states associated with the formation of the metal - semiconductor interface. Our results show discrete levels distributed over a wide range of energies and localized at the microscopic interface. These features show qualitative differences between metals, especially with different chemical reactivity. These studies demonstrate the influence of the metal, the semiconductor and its surface morphology on the energy distributions. The detailed evolution of optical emission energies and intensities with multilayer metal deposition exhibits a strong correlation between the deep gap levels, the Fermi level movements and Schottky barrier heights. The results demonstrate that in general electronic states deep within the band gap continue to evolve beyond monolayer coverage into the metallic regime.

CLS studies of partially-stepped surfaces reveal that the optical emission of deep level surface and interface states depend on the semiconductor surface morphology.[25] Spatially-resolved measurements reveal metal-induced interface states at cleavage steps whose optical emission properties depend on electron beam injection level. Such nonlinear behavior requires both surface roughness and the presence of a metallic overlayer. The density and spatial distribution of such metal-

cleavage-related states may account for variations in electrical transport measurements reported for clean III-V compound semiconductor -metal interfaces.[26,27]

These low energy CLS results help provide a new perspective on the dominant mechanisms of Schottky barrier formation. First of all, discrete gap states at the semiconductor-metal interface can be observed directly. The CLS technique supports the observations made by various less-direct techniques of the existence of metal-induced interface states. The existence of these states, their coupling with the semiconductor band bending, and the correspondence between their energies of emission and $E_F$ pinning in the band gap are evidence for their dominant role in Schottky barrier formation. Conversely, the existence of such states with their metal-dependent energies and densities means that gap states, virtual or otherwise, which depend primarily on the band structure of the semiconductor[28-30] are not needed to account for electrical properties of metal-semiconductor interfaces. The evolution of the discrete states with metal coverage beyond a few monolayers for most metals indicates that $E_F$ stabilization is not determined by a monolayer surface mechanism[5,31] but rather by extended chemical interaction between the metal and the semiconductor.[1,17] Thus low energy CLS confirms the formation of defects with initial metal chemisorption but also demonstrates that defects, impurities, or other electronically-active sites evolve at multilayer and metallic coverages at different energies which are more consistent with the $E_F$ movements. Low energy CLS also confirms the electrical activity of excess anion concentration at the semiconductor surface,[32,33] a major consideration in the chemical redistribution which can occur at the metal-semiconductor interface.

We have also analyzed the temperature dependence of the current and capacitance responses for Al contacts on UHV-cleaved n-type InP (110) surfaces.[12] The variations in J-V ideality factor and C-V barrier height with temperature preclude a simple analysis based on thermionic emission theory.[34] Instead, the results can be analyzed self-consistently on the basis of acceptor-like electron traps distributed within a few hundred Å of the semiconductor surface and at energies close to those observed by CLS. Laser annealing reduces the thickness of this interfacial layer by a factor of five.

In the second area of activity, we have performed SXPS measurements of $E_F$ position at metal interfaces with ternary III-V compound semiconductors to investigate the range of pinning behavior. SXPS measurements of metals on clean, ordered $In_xGa_{1-x}As$ (100) surfaces reveal that $E_F$ pinning depends strongly on the particular metal and that, for $In_xGa_{1-x}As$ ($x>0$), the range of $E_F$ movement is comparable to or greater than the semiconductor band gap.[35,36] In other words, $E_F$ is not pinned. For the same metal on different alloys, we observe regular trends in stabilization energies. The trend for Au is strikingly different from previous, air-exposed values. The latter can be reproduced by intentionally contaminating the interfaces with air exposure. For In and Al on the $In_xGa_{1-x}As$ alloy series, the $E_F$ pinning position follows the conduction band edge and are distinctly different from the Au trend as well. The SXPS data effectively contradicts Schottky barrier models based on simple vacancy or antisite defect formation, metal-induced gap states, or the "common-anion "rule. These first SXPS measurements on a ternary III-V compound semiconductor also reveal striking chemical interactions with metals which differ from binary compounds. Observed variations in semiconductor outdiffusion provide a chemically-modified interface work function model which accounts for the barrier variations across the alloy series. Overall, the results demonstrate that

barrier height can be controlled effectively over a wide range - from ohmic to rectifying -with different metals on clean surfaces of these prime technological materials.

In the third area of activity, we have extended our SXPS measurements beyond InGaAs to investigate the strength of $E_F$ pinning for other III-V compound semiconductors. We have measured the $E_F$ movements and chemical interactions as a function of metal coverage on UHV-cleaved GaP (110) surfaces.[37,38] Valence band and core level spectra taken for deposition of Au, Al, Cu, Ge, and In reveal a range of $E_F$ stabilization which extends over 1.2 ev for the GaP band gap of 2.26 ev. The $E_F$ positions for Au and Cu are in agreement with Schottky barrier heights reported for vacuum-cleaved and chemically-treated GaP reported earlier, whereas substantial disagreement exist with results for the more reactive metal Al. Comparison of $E_F$ stabilization energies with the absolute metal work functions and GaP ionization potential indicate a reasonably good correspondence, permitting a classical work function model to describe the Schottky barrier formation. Defect and metal-induced interface state models which predict a narrow stabilization range are not consistent with the wide range of $E_F$ energies observed nor the good agreement with classical barrier predictions.

The GaP band gap is the largest for a conventional, binary III-V compound semiconductor and permits a wide range of $E_F$ movements, unlike those of many other III-V compounds. Coupled with previous data for InAs and the $Ga_xIn_{1-x}As$ ($0 \leq x \leq 1$) pseudobinary alloy series as well as the absence of narrow ranges of $E_F$ stabilization for all but cleaved or chemically-etched GaAs, the GaP-metal results demonstrate that strong $E_F$ pinning is not in general characteristic of III-V compounds.[37,38]

In general, the results obtained by a complement of interface techniques over this reporting period provide a new perpective on Schottky barrier formation, especially for III-V compound semiconductors. Direct evidence for discrete interface states show that such states indeed exist near the junction and change in energy and density as the chemical interaction between metal and semiconductor proceeds. By controlled preparation of such interfaces under UHV conditions, we find that $E_F$ pinning is far less prevalent than commonly assumed for III-V compounds. These results suggest that further understanding of the relationship between chemical interactions on a microscopic scale and the macroscopic electronic properties will yield even greater control of Schottky barrier properties.

## References


1. L.J. Brillson, Surface Sci. Repts. 2, 123 (1982) and references therein.
2. G. Margaritondo, Solid-State Electron. 26, 499 (1983).
3. R.Z. Bachrach, in Metal-Semiconductor Schottky Barrier Junctions and Their Applications (Plenum, New York, 1984) p. 61-112.
4. R.H. Williams, Contemp. Phys. 23, 329 (1982).
5. W.E. Spicer and S.J. Eglash, in VLSI Electronics: Microstructure Science, Vol. 10 (Academic, New York, 1985) p. 79.
6. J.H. Weaver, Treatise on Materials Science and Technology, Vol. 28. Analysis and Characterization of Thin Films, edited by K.N. Tu and R. Rosenberg (Academic Press, New York, 1985).
7. A. Kahn, Surface Sci. Repts. 3, 193 (1983).
8. L.J. Brillson, J. Vac. Sci. Technol. 20, 652 (1982); Appl. Surface Sci. 11/12, 249 (1982).
9. R. Ludeke, Surface Sci. 132, 143 (1983).
10. M.P. Seah and W.A. Dench, Surface Interface Analysis 1, 2 (1979).
11. P.S. Ho, E.S. Yang, H.L. Evans, and X. Wu, Phys. Rev. Lett. 56, 177 (1986).
12. J.H. Slowik, H.W. Richter, and L.J. Brillson, J. Appl. Phys 58, 3154 (1985).
13. C. Barret, F. Chekir, and A. Vapaille, J. Phys. C: Solid State Phys. 16, 2421 (1983).
14. L.J. Brillson, H.W. Richter, M.L. Slade, B.A. Weinstein, and Y. Shapira, J. Vac. Sci. Technol. A3, 1011 (1985).
15. S. M. Sze, Physics of Semiconductor Devices (John Wiley & Sons, New York, 1969).
16. C.A. Mead, Solid State Electron. 9, 1023 (1966).
17. L.J. Brillson, C.F. Brucker, A.D. Katnani, N.G. Stoffel, and G. Margaritondo, Appl. Phys. Lett. 38, 784 (1981).
18. C.F. Brucker and L.J. Brillson, Appl. Phys. Lett. 39, 67 (1981).
19 S.D. Offsey, J.M.Woodall, A.C. Warren, P.D.Kirchner, T.I. Chappell, and G.D.Pettit, Apppl. Phys. Lett. 48, 475 (1986).
20. V. Montgomery, R.H. Williams, and G.P. Srivastava, J. Phys. C (Solid State Phys.) 14, L191 (1981).

21. R.E. Viturro, M.L. Slade, and L.J. Brillson, Phys. Rev. Lett. 57, 487 (1986).

22. R.E. Viturro, M.L. Slade, and L.J. Brillson, in Proceedings of the 18th International Conference on the Physics of Semiconductors (Stockholm, 1986), p. 371.

23. R.E. Viturro, M.L. Slade, and L.J. Brillson, J. Vac. Sci . Technol. A5, 1516 (1987).

24. L.J. Brillson and R.E. Viturro, Scanning Electron Microsc., in press.

25. R.E. Viturro and L.J. Brillson, J. Vac. Sci. Technol. B5, 1125 (1987).

26. J.L. Freeouf, T.N. Jackson, S.E. Laux, and J.M. Woodall, J. Vac. Sci. Technol. 21, 570 (1982).

27. J. Y. -F. Tang and J.L. Freeouf, J. Vac. Sci. Technol. B2, 459 (1984).

28. J. Tersoff, Phys. Rev. Lett. B32, 6968 (1985).

29. J. Tersoff, Phys. Rev. Lett. 52, 465 (1984).

30. W.A. Harrison and J. Tersoff, J. Vac. Sci. Technol. B4, 1068 (1986).

31. W.E. Spicer, I. Lindau, P. Skeath, and C.Y. Su, J. Vac. Sci. Technol. 17, 1019 (1980).

32. J.L. Freeouf and J.M. Woodall, Appl. Phys. Lett. 39, 727 (1981).

33. J.M. Woodall and J.L. Freeouf, J. Vac. Sci. Technol. 19, 794 (1981).

34. N. Newman, W.E. Spicer, and E.R. Weber, J. Vac. Sci. Technol. B5, 1020 (1987).

35. L.J. Brillson, M.L. Slade, R.E. Viturro, M. Kelly, N. Tache, G. Margaritondo, J. Woodall, G.D. Pettit, P.D. Kirchner, and S.L. Wright, Appl. Phys. Lett. 48, 1458 (1986).

36. L.J. Brillson, M.L. Slade, R.E. Viturro, M. Kelly, N. Tache, G. Margaritondo, J. Woodall, G.D. Pettit, P.D. Kirchner, and S.L. Wright, J. Vac. Sci. Technol. B4, 919 (1986).

37. L.J. Brillson, R.E. Viturro, M.L. Slade, P. Chiaradia, D. Kilday, M. Kelly, and G. Margaritondo, Appl. Phys. Lett. 50, 1379 (1987).

38. P. Chiaradia, R.E. Viturro, M.L. Slade, L.J. Brillson, D. Kilday, M. Kelly, N. Tache, and G. Margaritondo, J. Vac. Sci. Technol. B5, 1075 (1987).

## IV. Papers Published and Submitted under Navy Contract #N00014-80-C-0778 during the Period October 1, 1986 to September 30, 1987

80-C-0778-33. **Titanium-Silicon and Silicon Dioxide Reactions Controlled by Low Temperature Rapid Thermal Annealing**, L.J. Brillson, M.L. Slade, H.W. Richter, H. Vander Plas, and R.T. Fulks, Journal of Vacuum Science and Technology A4, 993 (1986).

80-C-0778-34. **Chemical Reaction and Interdiffusion at III-V Compound Semiconductor-Metal Interfaces** L.J. Brillson, Materials Research Society Symposium Proceedings 54, 327 (1986).

80-C-0778-35. **Acceptor-like Electron Traps Control Effective Barrier for UHV-Cleaved and Laser Annealed Al/InP**, J. Slowik, L.J. Brillson, and H. Richter, Journal of Vacuum Science and Technology B4, 974 (1986).

80-C-0778-36. **Fermi Level Pinning and Chemical Interactions at Metal - $In_xGa_{1-x}As$ (100) Interfaces,** L.J. Brillson, M.L. Slade, R.E. Viturro, M. Kelly, N. Tache, G. Margaritondo, J. Woodall, G.D. Pettit, P.D. Kirchner and S.L. Wright, Journal of Vacuum Science and Technology B4, 919 (1986).

80-C-0778-37. **Absence of Fermi Level Pinning at Metal - $In_xGa_{1-x}As$ (100) Interfaces,** L.J.Brillson, M.L. Slade, R.E. Viturro, M.Kelly, N. Tache, G. Margaritondo, J.M. Woodall, G.D. Pettit, P.D. Kirchner, and S.L. Wright, Applied Physics Letters 48, 1458 (1986).

80-C-0778-38. **Optical Emission Properties of Metal/III-V Compound Semiconductor Interface States,**R. E. Viturro, M. L. Slade, and L. J. Brillson, Physical Review Letters 57, 487 (1986).

80-C-0778-39. **Metallization of III-V Compounds**, L. J. Brillson, in Semiconductor-Based Heterostructures: Interfacial Structure and Stability, ed. J.E.E.Baglin, G.Y.Chin, H. W. Deckman, W. Mayo, and D. Narasinham (The Metallurgical Society,Inc.Warrendale,PA,1986) p.387.

80-C-0778-40. **Cathodoluminescence Spectroscopy of Metal/III-V Compound Semiconductor Interface States,** R. E. Viturro, M. L. Slade, and L. J. Brillson, Proceedings of the 18th International Conference on the Physics of Semiconductors (Stockholm, 1986) p. 371.

80-C-0778-41. **Optical Emission Properties of Metal / InP and GaAs Interface States,** R. E. Viturro, M. L. Slade, and L. J. Brillson, Journal of Vacuum Science and Technology, A5, 1516 (1987).

80-C-0778-42. **Near-Ideal Schottky Barrier Formation at Metal-GaP Interfaces,** L.J.Brillson, R.E.Viturro, M.L.Slade, P. Chiaradia, D. Kilday, M. Kelly, and G. Margaritondo, Applied Physics Letters 50, 1379 (1987).

80-C-0778-43. **Unpinned Schottky Barrier Formation at Metal-GaP Interfaces: A Representative III-V Compound Case,** P. Chiaradia, R. E. Viturro, M.L.Slade, L.J.Brillson, D.Kilday, M.Kelly, N.Tache, and G.

Margaritondo, Journal of Vacuum Science and Technology B5, 1075 (1987).

80-C-0778-44. **Cleavage-Related Electronic States of Al - InP (110) Interfaces,** R.E.Viturro and L.J.Brillson, Journal of Vacuum Science and Technology B5, 1125 (1987).

80-C-0778-45. **Low Energy Cathodoluminescence Spectroscopy of Semiconductor Interfaces,** L.J.Brillson and R.E.Viturro, Scanning Electron Microscopy, in press.

# TITANIUM-SILICON AND SILICON DIOXIDE REACTIONS CONTROLLED BY LOW TEMPERATURE RAPID THERMAL ANNEALING

L.J. Brillson, M.L. Slade, and H.W. Richter
Xerox Webster Research Center
800 Phillips Road
Webster, NY 14580

and

H. VanderPlas and R.T. Fulks
Xerox Palo Alto Research Center
3333 Coyote Hill Road
Palo Alto, CA 94304

## Abstract

Auger electron spectroscopy measurements coupled with sputter depth profiling demonstrate that titanium silicide forms between Ti and $SiO_2$ at conventional annealing temperatures in UHV and that rapid thermal annealing at relatively low temperatures can enhance silicide formation at Ti-Si relative to Ti-$SiO_2$ interfaces within the same thin film structure. Reactions and diffusion at these interfaces occur on a short time scale (seconds) at low temperatures (400-700°C), yet resemble interactions obtained at multimicron thicknesses. UHV fabrication and analysis reveals that these reactions are sensitive to interface contamination and sputter-induced disorder.

## 1. Introduction

The titanium silicon interace has attracted considerable interest in recent years due to the microelectronic applications of titanium silicide, whose resistivity is the lowest of all refractory metal silicides.[1] Because of its low resistivity and compatibility with metal-oxide-semiconductor (MOS) processing, titanium silicide finds use as interconnects for very-large-scale-integrated (VLSI) circuits and as gate electrodes for MOS devices.[2-7] An example of current concern is the formulation of self-aligned silicide structures involving the simultaneous reaction of elemental Ti with polycrystalline Si (polysilicon) gates and with crystalline Si in the source and drain of an MOS transistor. An $SiO_2$ spacer layer prevents shorting between gate and source/drain. High temperature annealing promotes silicide formation at the Ti-Si interface so that the resultant silicide pattern forms a self-aligned gate and source/drain for MOS transistors. In order to promote formation of a low resistivity titanium silicide without extensive dopant redistribution or Si-metal interdiffusion, researchers have focused on relatively new annealing techniques such as rapid thermal annealing[8] and low temperature sputter deposition.[9] Futhermore, the chemical interactions which occur at the Ti-$SiO_2$ interface are now receiving attention since the Si- and $SiO_2$-metal interfaces are frequently formed together on the same Si wafer.[10-11] Nevertheless, the chemical evolution of these interfaces is relatively unexplored at short times, at low temperatures, under clean and controlled conditions, and especially for the thin film structures increasingly employed.

In this paper we present results obtained for thin film Ti-Si and Ti-$SiO_2$ interfaces formed under ultrahigh vacuum (UHV) conditions and annealed *in situ* using a low temperature, rapid thermal annealing technique. We find that a) reactions and diffusion occur at these interfaces on a short time scale (seconds) at conventional processing temperatures and not over the course of tens of minutes or hours, b) these

chemical interactions evolve for thin films (e.g., less than 1000 Å) in a manner similar to multimicron thicknesses, c) Ti silicide forms at the Ti-$SiO_2$ interface due to the dissociation of $SiO_2$, d) at low temperatures (< 500°C), titanium silicide forms faster at Ti-Si than at Ti-$SiO_2$ interfaces on the same substrate and can be enhanced preferentially by annealing for short durations (tens of seconds), e) reactions at the Ti-Si interface are quite sensitive to interface contamination, which can form a strong barrier to Si diffusion into Ti, and f) ion sputter-cleaning of Si and $SiO_2$ before Ti deposition accelerates dissociation of $SiO_2$ and outdiffusion of Si into Ti overlayers. In the next section, we describe the experimental techniques employed for this study. Following sections deal in turn with each of the findings a) through e) above.

## 2) Experimental

We prepared Ti-Si and Ti-$SiO_2$ interfaces by evaporating Ti from carefully outgassed sublimation filaments on to 6x12 mm sections of Si(100) wafer (intrinsic, p-type, near room temperature and patterned with thermally-grown 1400 Å nm $SiO_2$ areas across the surface. These surfaces were heated prior to Ti deposition by passing current through the wafer section via Ta support clips after a 1050°C anneal for two minutes. Auger electron spectroscopy (AES) analysis revealed no detectable (< 1%) C or O contamination. Base pressure of our stainless steel UHV chamber was $p = 1x10^{-10}$ torr rising during Ti evaporation to the mid-$10^{-9}$ torr range. Deposition rates ranged from 30-80 Å/min. AES results yielded no evidence (< 1%) for O incorporation within the Ti film.

We used the same resistive heating geometry for rapid thermal annealing of the Ti-covered wafer sections. For both high temperature precleaning and post-deposition, low temperature annealing, we measured the surface temperature with a Barnes Engineering Optitherm radiometer focussed on the heated surface through a

sapphire vacuum viewpoint. Only a portion of each substrate received a Ti deposit in order to prevent resistive heating through the metallic film and to provide a metal-free region for radiometer measurements. Our emissivity values for the exposed Si are based on values reported previously.[12] In addition, we localized our AES analysis to Ti-Si and Ti-$SiO_2$ interfaces within a few tens of microns laterally of the exposed Si surface to minimize any possible temperature discrepancy between the probe area and the bare surface. With standard, high current power supplies, the specimen temperature could be ramped up to temperature of 1000°C in a matter of seconds. Radiant cooling limited the rate of temperature decrease such that 15-30 sec were required for temperatures to sink below 200°C.

We performed AES measurements using a PHI 15-110A single pass cylindrical mirror analyzer with 3$\mu$m spatial resolution. Hence, direct chemical comparisons were possible between Ti-Si and Ti-$SiO_2$ interfaces separated by only a few microns on the same wafer substrate. AES combined with 3 keV $Ar^+$ sputtering allowed us to obtain depth profiles of these interfaces after thermal processing. AES intensities presented here correspond to peak-to-peak heights of LMM, KLL, and LMM features for Si, O, and Ti, respectively.

## 3. Rapid Diffusion and Reaction: Thin Film Ti on Si

AES characterization of 400 Å Ti films deposited on clean Si (100) substrates reveal that a range of silicide formation occurs at temperatures of 500-100°C after only a few tens of seconds or less. With increasing anneal temperature, the silicon concentration near the free Ti surface increases, consistent with the proportions of TiSi and $TiSi_2$ formed[1], as well as with the reported Si surface segregation.[10,13] Annealing the 40 nm Ti-Si interface for 15 seconds at 1045°C leads to a Si/Ti intensity ratio characterization of $TiSi_2$. This result is consistent with rapid thermal annealing of thicker titanium silicide films for comparable times using commercially

available equipment.[2] This intensity ratio provides a normalization for our AES results at lower temperatures. Thus, annealing an as-deposited 400°A Ti-Si interface for 15 sec at 600°C yields a normalized Si/Ti ratio of 0.85 which asymptotes to 1.0 after 150 seconds. AES shows that the Ti is completely consumed by silicide formation, as evidenced by Ti LMM features charactistic of only reacted vs. metallic Ti. According to x-ray diffraction intensities obtained by Murarka and Fraser[14], conventional annealing at 600°C for considerably longer times yields predominately TiSi mixed with only a small proportion of $TiSi_2$. Assuming a uniform distribution, their results suggest an Si/Ti ratio < 1.15, close to the observed AES rapid thermal annealing result. After annealing at 740°C for up to 45 seconds, the Si/Ti ratio observed with AES reaches 1.2, consistent with the diffraction results[14] showing an increase in $TiSi_2$ relative to TiSi concentration and an associated Si/Ti ratio of 1.26. These low temperature, rapid annealing findings complement thinner film, longer annealing studies of Butz *et al.*[11] and demonstrate chemical reactions characteristic of bulk films after furnace annealing for extended periods.

## 4. Diffusion and Reaction of Thin Film Ti on $SiO_2$

Low temperature, rapid thermal annealing produces not only rapid silicidation at the Ti-Si interface but also strong dissociation, diffusion, and reaction at the Ti-$SiO_2$ interface. Using AES, we observe reactions between Ti and $SiO_2$ which begin slowly near and above 500°C. At a temperature of 700°C for only 2 minutes, considerable interaction takes place. The AES sputter profile shown in Fig. 1 illustrates three distinct regions for a 400 Å Ti layer deposited on a 1400 Å thermally-grown $SiO_2$ film on Si (100). The entire Ti film appears to be consumed by Si and O produced by $SiO_2$ dissociation, yielding a Ti oxide outer layer separated from the remaining $SiO_2$ by a Ti silicide layer. The abrupt dip in Si Auger signal between the Ti-Si and $SiO_2$ layer is due to a sharing of intensity between Si bonded to both Ti and O.

The Ti oxide layer is not associated with ambient contamination since Ti on Si interfaces adjacent to the Ti on $SiO_2$ area of the same substrate exhibit no such oxidation. The presence of a Ti-O phase is consistent with a surface segregation of the phase with the lowest heat of vaporization,[15] since Kuiper *et al.*[13] found $TiO_2$ desorption from O-exposed Ti occurring at 500°C *vs.* higher temperatures for $SiO_2$ desorption.[13,16] Indeed we observe removal of oxide with a 1045°C anneal for only 15 seconds.

The Ti silicide layer in Fig. 1 which forms above $SiO_2$ is noteworthy because it can form a low resistance film across an otherwise insulating layer. Such a film must be avoided in forming device structures, e.g., the self-aligned gate for MOS transistors.

Tanielian *et al.*[9] have obtained an analogous depth profile for medium-vacuum ($10^{-7}$ torr), sputter-deposited Ti on $SiO_2$ held at 520°C or furnace annealed at 520°C for 30 minutes. Our AES studies at 425°C-700°C reveal O outdiffusion due to $SiO_2$ dissociation as well, albeit at slower rates. These results are in contrast with those of Maa *et al.*[17] who find no Ti-$SiO_2$ reaction below 700°C, and with those of Taubenblatt and Helms[10], who reported no significant chemical changes in the temperature range 300-500°C.

The stoichiometry of the Ti-O and Ti-Si phases can be derived in two ways - from the Ti-O-Si ternary phase diagram recently published by Beyers *et al.*[18] and from the $TiSi_2$ film normalization extracted from our high temperature Ti-Si interface in Sec. 3. The tie lines illustrated in Fig. 2 correspond to phase couples which are in stable equilibrium, i.e., no reaction will take place. The solid lines have been established experimentally[17,19,20], whereas the dashed lines are inferred from calculations of free energy change.[18,21] In Fig. 2, the Ti-O-Si system is at thermodynamic equilibrium, which is likely in Fig. 1 since Si and O have diffused throughout the Ti and discrete regions have formed. The phase diagram shows that several Ti silicides are stable in

contact with $SiO_2$ but only $Ti_5Si_3$ is stable with both $SiO_2$ and a Ti oxide. Thus, the $Ti_5Si_3$ AES intensities establish the Ti-Si intensity normalization. Given the Si:O normalization from the $SiO_2$ region, one can then obtain the Ti:O stoichiometry for the outer Ti oxide. Figure 2 has been so normalized and yields a metal-rich TiO layer. This is precisely the conclusion derived from electron and x-ray diffraction studies for Ti films on $SiO_2$ substrates annealed at 950°C for 30 minutes. The absence of an O-rich surface layer precludes $Ti_2O_3$, $Ti_3O_5$ or $TiO_2$ phases, all of which are thermodynamically more stable than Ti-rich TiO plus additional oxygen. Consistent with this result, Taubenblatt and Helms[10] report a $TiO_{0.93}$ surface stoichiometry for Ti on $SiO_2$ at 800°C.

Alternatively, the Si:Si normalization based on the 1045°C 15 second anneal can provide the stoichiometry of the two Ti regions. The result is a $Ti_5Si_3$ silicide layer and a TiO surface layer which are 3-5 percent richer in Ti than the result derived from the ternary diagram alone. The sigificance of this phase analysis is first, that a 2 minute, 700°C anneal yields essentially the same result as an extended time, elevated temperature result, and second, that a 15 second anneal at 1045°C indeed promotes $TiSi_2$ formation.

## 5. Preferential Enhancement of Ti-O *vs.* Ti-$SiO_2$ Interface Reactions

Figure 1 shows that the appearance of Ti oxide on Ti over $SiO_2$ is indicative of $SiO_2$ dissociation and subsurface silicide formation. Similarly, the appearance of Si on Ti over Si is an indication of Ti silicide formation. At relatively low temperatures and anneal times, a process window exists such that Ti silicide forms faster at the Ti/Si interface than $SiO_2$ dissociates at an adjacent Ti/$SiO_2$ interface. Figure 3 shows the evolution of Ti, O, and Si Auger intensities as a function of 475°C anneal time for Ti over Si (a) and for Ti over $SiO_2$ (b). Differences in surface chemical composition between a) and b) evolve from areas spaced less than 20 microns apart laterally on

the same substrate. In Fig. 3a, Si appears at the Ti/Si free surface with the first 30 second anneal, whereas the Ti/$SiO_2$ interface requires more than 240 seconds for O to diffuse to the free surface. At this latter stage, the Si concentration has already reached a broad, gradually increasing plateau.

Figure 4 demonstrates that the slightly lower temperature of 425°C serves to widen the window in time between the Ti/Si silicide formation and the $SiO_2$ dissociation at the Ti/$SiO_2$ interface. Here the Si Auger signal appears almost immediately at the Ti/Si free surface (Fig. 4a) whereas the appearance of O on the Ti/$SiO_2$ free surface in Fig. 4b requires between 8 and 12 minutes. After this time interval, almost the entire Ti film on Si has reacted to form various silicides, whereas the $SiO_2$ dissociation has only begun. The rapid changes of diffusion and dissociation with only modest temperature changes indicate the need to avoid any thermal overshoot in this annealing treatment. Given careful temperature control, rapid thermal annealing at low temperatures provides a new technique for limiting such dissociation while promoting silicide reaction where desired.

Butz *et al.*[11] have shown from transmission electron microscopy (TEM) analyses that Ti films on Si annealed at ~ 300°C can form a nonuniform distribution of silicides with very fine grains. Likewise, after only 10 minutes at 425°C, the Ti silicide layer evident in Fig. 4a is not yet $TiSi_2$. Hence, etches used to remove residual Ti from a conformal Ti film over both $SiO_2$ and Si may well remove some Ti from the $TiSi_x$ ($x \leq 2$) as well. However, after Ti is removed from such an array, additional anneals at higher temperature could complete the $TiSi_2$ formation.

6. Influence of Contamination and Sputter Damage

One requires interfaces free of contamination in order to obtain the results of Figs. 3 and 4. Contamination of the Si surface by C and O prior to Ti deposition forms a

diffusion barrier to silicide formation[7,23] requiring higher temperatures, typically 700°C or more, to initiate diffusion and reaction. At such temperatures, dissociation of $SiO_2$ at the $Ti/SiO_2$ interface can no longer be controlled.

Ion bombardment of Si surfaces prior to Ti deposition represents an alternative to high temperature annealing[12] for obtaining clean surfaces. Figure 5 illustrates the evolution of Auger peak intensities for Ti on ion-bombarded Si (a) and $SiO_2$ (b). Again, a process window in time exists for Ti silicide formation *vs.* $SiO_2$ dissociation, but it is considerably shorter than for heat-cleaned Si. As shown in Fig. 5b, O appears on the free $Ti/SiO_2$ surface after only 120 seconds. The disorder introduced by sputtering accelerates the Ti-Si interaction as well.

## 7. Conclusions

Section 3-5 underscore the importance of annealing time in silicide processing at relatively low temperatures (400-700°C) where reaction products are obtained which resemble these at much longer anneal times. The results indicate that rapid thermal annealing can provide a new avenue for controlling competitive reactions. This approach may also prove useful in promoting new chemical structures at compound semiconductor/metal interfaces, where changing the balance of cation, anion, and metal diffusion may alter the Schottky barrier properties.

## Acknowledgements

The authors wish to thank C.B. Duke, J. Knights, and J. Mort for their encourangement. This work was supported in part by Office of Naval Research Grant N00014-80-C-0778 (G.B. Wright).

## Figure Captions

Fig. 1. Auger depth profile of 400 Å Ti over 1400 Å $SiO_2$ thermally-grown on Si, annealed at 700°C for 2 minutes.

Fig. 2. Tie lines determined (solid) and inferred (dashed) from the observed Ti-$SiO_2$ reaction products at T = 700 - 1000°C. After Beyers *et al.*, ref. 18. Reprinted with permission.

Fig. 3. Evolution of Auger intensities (unnormalized) as a function of 475°C anneal time for 40 nm Ti on heat-cleaned Si (a) and $SiO_2$ (b).

Fig. 4. Evolution of Auger intensities (unnormalized) as a function of 425°C anneal time for 40 nm Ti on heat-cleaned Si (a) and $SiO_2$ (b).

Fig. 5. Evolution of Auger intensities (unnormalized) as a function of 475°C anneal time for 40 nm Ti on sputter-cleaned Si (a) and $SiO_2$ (b).

## References


1. S.P. Murarka, Silicides for VLSI Applications (Academic, New York, 1983).

2. R.A. Powell, R. Chow, C. Thridandam, R.T. Fulks, T.A. Blech, and J.-D.T. Pan, IEEE Electron Device Letters EDL-4, 380 (1983).

3. M. Tanielian, S. Blackstone, and R. Lajos, Appl. Phys. Lett. 45, 444 (1984).

4. C.S. Wei, J. VanderSpiegel, J.J. Santiago, and L.E. Seiberling, Appl. Phys. Lett. 45, 527 (1984).

5. M. Tanielian and S. Blackstone, Appl. Phys. Lett. 45, 673 (1985).

6. T.P. Chow, W. Katz, and G. Smith, Appl. Phys. Lett. 46, 41 (1985).

7. G.G. Bentini, R. Nipoti, A. Armigliato, M. Berti, A.V. Drigo, and C. Cohen, J. Appl. Phys. 57, 270 (1985).

8. R.T. Fulks, C.J. Russo, P.R. Hanley, and T.I. Kamines, Appl. Phys. Lett. 39, 604 (1981).

9. M. Tanielian and S. Blackstone, J. Vac. Sci. Technol. A3, 714 (1985).

10. M.A. Taubenblatt and C.R. Helms, J. Appl. Phys. 53, 6308 (1982).

11. R. Butz, G.W. Rubloff, T.Y. Tan, and P.S. Ho, Phys. Rev. B30, 5421 (1984).

12. L.J. Brillson, M.L. Slade, A.D. Katnani, M. Kelly, and G. Margaritondo, Appl. Phys. Lett. 44, 110 (1984).

13. A.E.T. Kuiper, G.C.J. vanderLigt, W.M. van de Wijgert, M.F.C. Willemsen, and

F.H.P.M. Habraken, J. Vac. Sci. Technol. B3, 830 (1985).

14. S.P. Murarka and D.B. Fraser, J. Appl. Phys. 51, 342 (1980).

15. H.H. Brongersma, M.J. Sparnaay, and T.M. Buck, Surface Sci. 71, 657 (1978).

16. M. Berti, A.V. Drigo, C. Cohen, J. Siejka, G.G. Bentini, R. Nipoti, and S. Guerri, J. Appl. Phys. 55, 3558 (1984).

17. J.-S. Maa, C.-J. Lin, J.-H. Liu, and Y.-C. Liu, Thin Solid Films 64, 439 (1979).

18. R. Beyers, R. Sinclair, and M.E. Thomas, J. Vac. Sci. Technol. B2, 781 (1984).

19. H. Krautle, M.-A. Nicolet, and J.W. Mayer, Phys. Stat. Sol. (a) 20, K33 (1973).

20. R. Pretorius, J.M. Harris, and M.-A. Nicolet, Solid State Electro... 21, 667 (1978).

21. R. Beyers, J. Appl. Phys. 56, 147 (1984).

22. C.Y. Ting, M. Wittmer, S.S. Iyer, and S.B. Brousky, in *VLSI Science and Technology 1984*, edited by K.E. Bean and G.A. Rozgonyl (Electrochemical Society, Princeton, NJ, 1984), p. 397.

23. M.A. Taubenblatt, D. Thomson, and C.R. Helms, Appl. Phys. Lett. 44, 895 (1984).

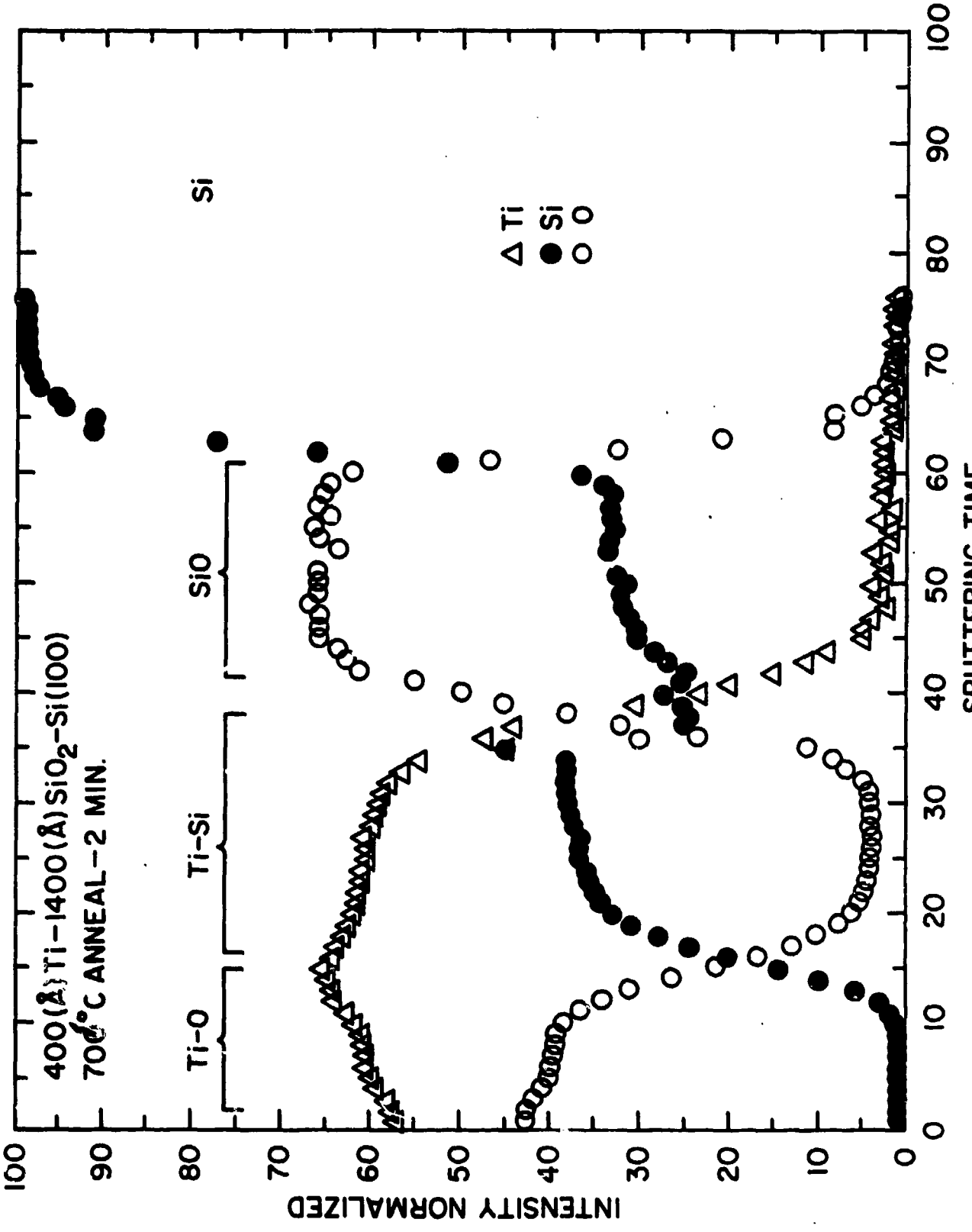
400(Å)Ti-1400(Å)SiO2-Si(100)
700°C ANNEAL-2 MIN.
Ti-O
Ti-Si
SiO
Si
Ti
Si
O
INTENSITY NORMALIZED
SPUTTERING TIME
0
10
20
30
40
50
60
70
80
90
100

Fig. 1

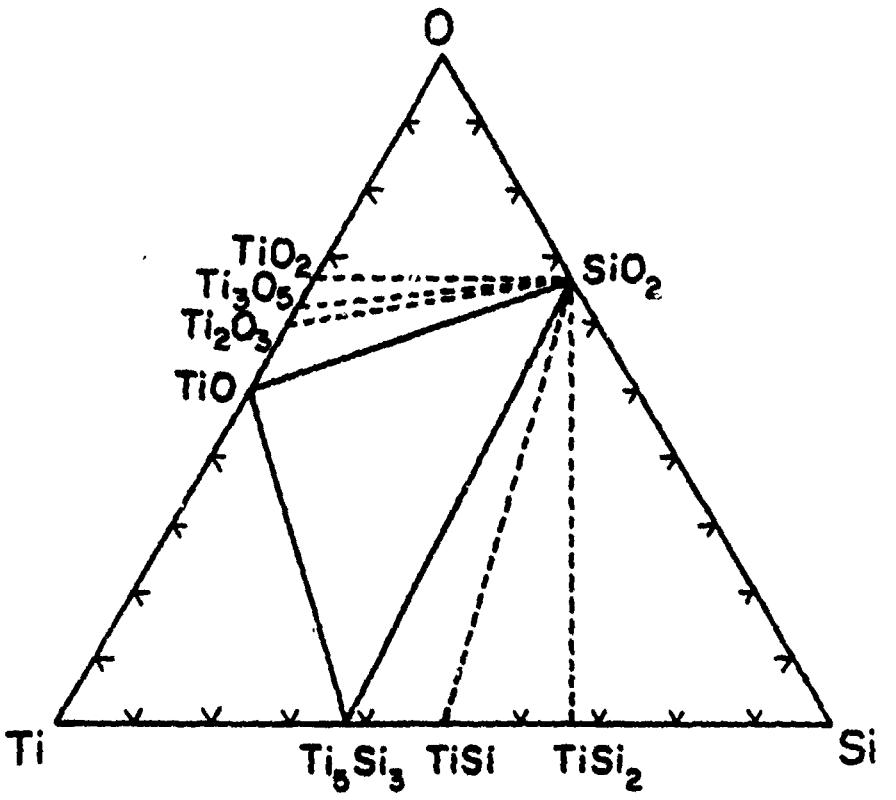


Fig. 2

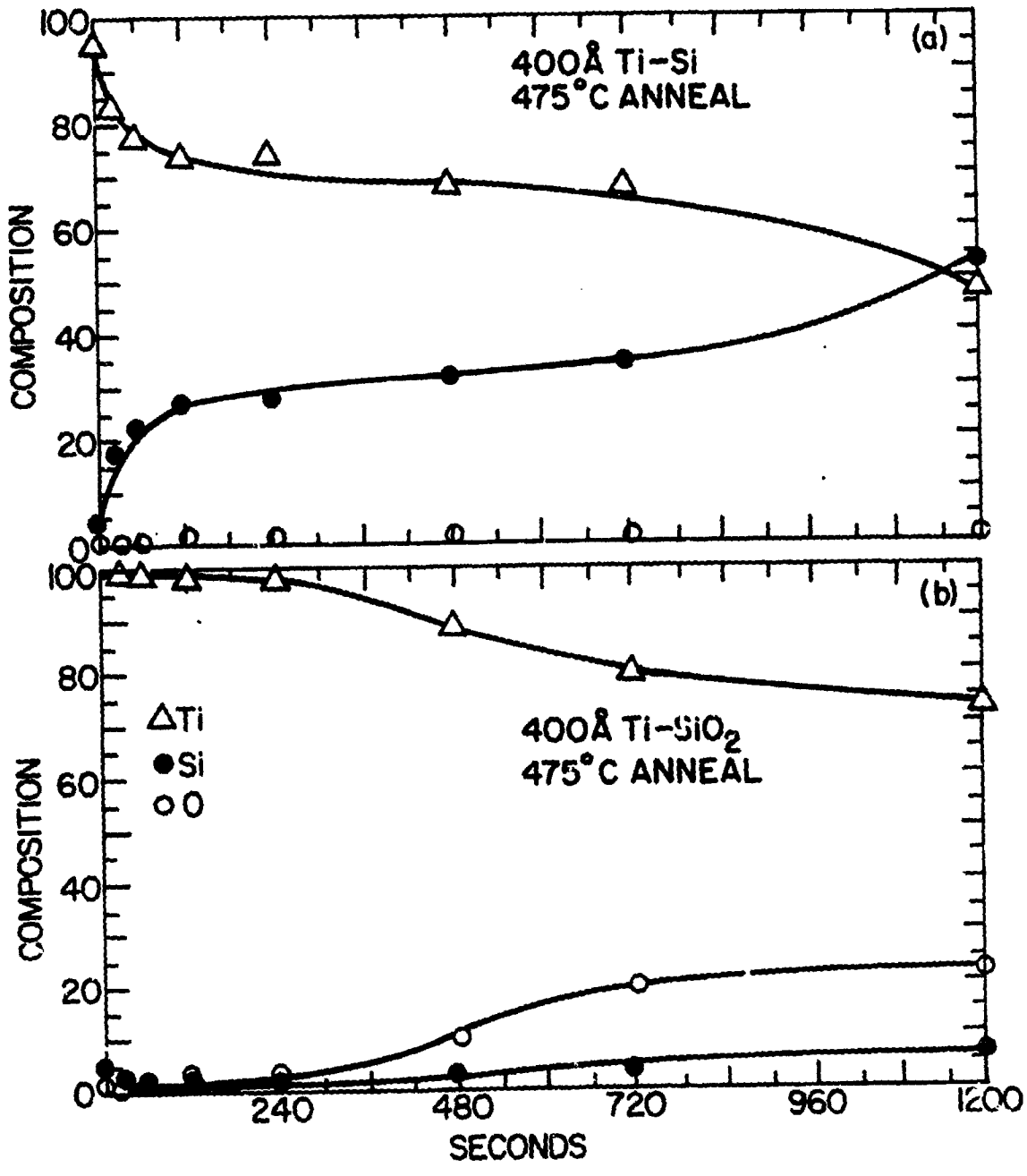
100
80
60
40
20
0
COMPOSITION
400Å Ti-Si
475°C ANNEAL
(a)
100
80
60
40
20
0
COMPOSITION
ΔTi
●Si
○O
400Å Ti-SiO2
475°C ANNEAL
(b)
240
480
720
960
1200
SECONDS

Fig. 3

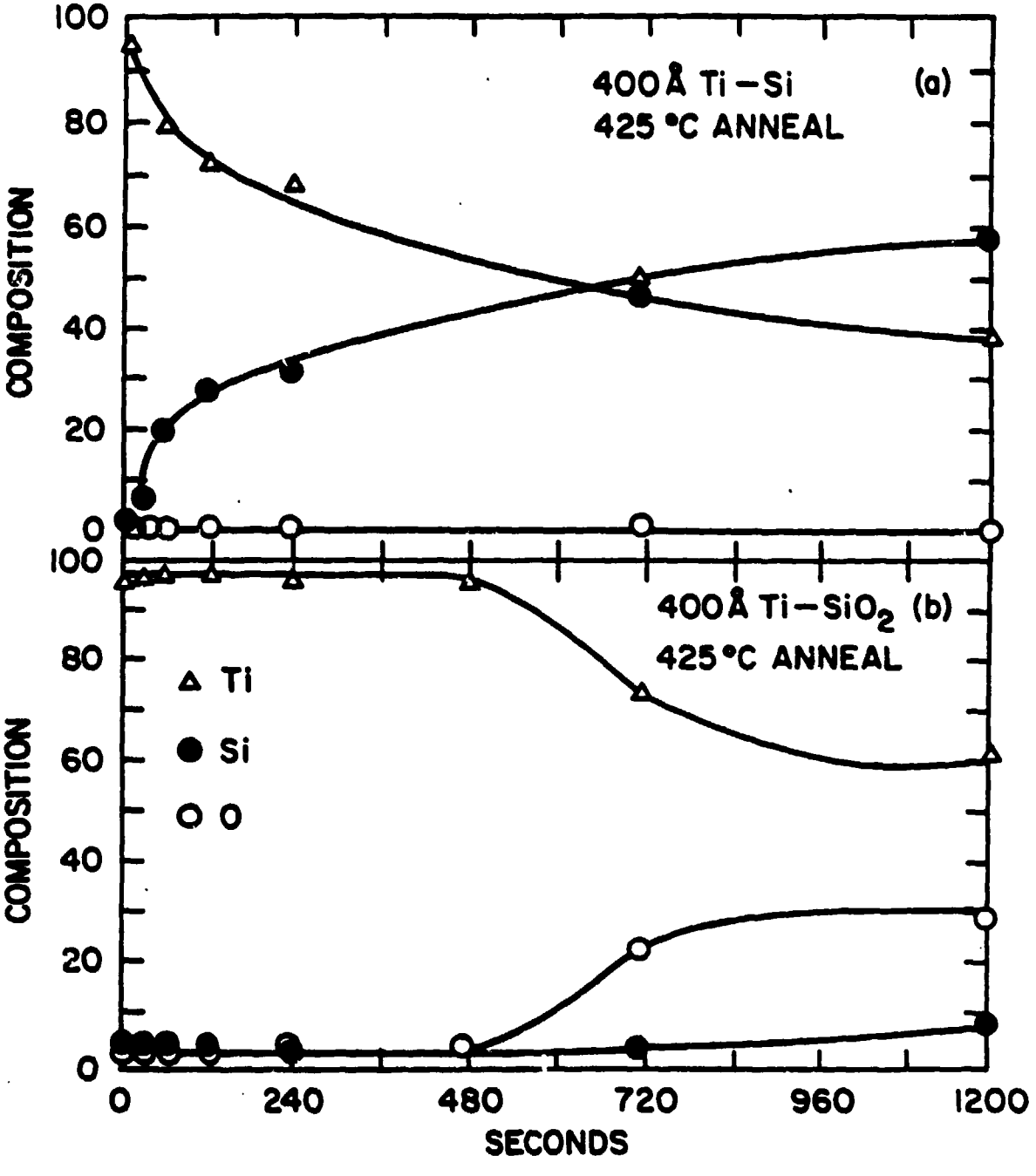
400Å Ti–Si
425 °C ANNEAL
(a)
400Å Ti–SiO2
425 °C ANNEAL
(b)
Ti
Si
O
COMPOSITION
COMPOSITION
100
80
60
40
20
0
0
240
480
720
960
1200
SECONDS

Fig. 4

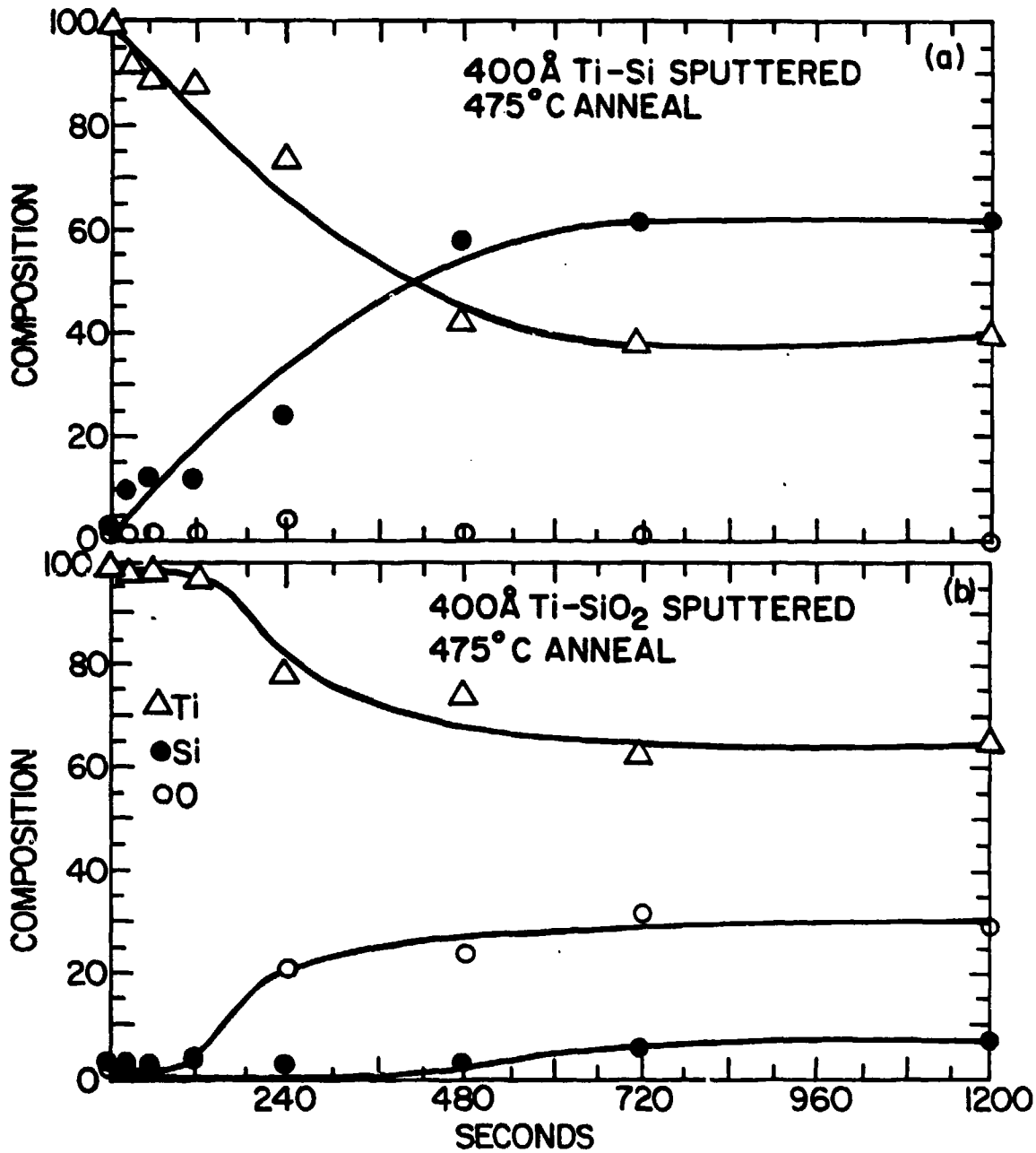
400Å Ti-Si SPUTTERED
475°C ANNEAL
(a)
400Å Ti-SiO2 SPUTTERED
475°C ANNEAL
(b)
ΔTi
●Si
○O
COMPOSITION
SECONDS
0
20
40
60
80
100
240
480
720
960
1200

Fig. 5

# REACTION AND INTERDIFFUSION AT III-V COMPOUND SEMICONDUCTOR-METAL INTERFACES

L.J. Brillson, Xerox Webster Research Center, 800 Phillips Road 114-41D, Webster, N.Y. 14580.

## ABSTRACT

The characterization of III-V compound semiconductor-metal interfaces by surface science techniques has led to new relationships between interfacial chemistry and Schottky barrier formation. These and recent results on ternary alloy III-V compounds suggest a greater control of Schottky barrier heights by atomic scale techniques and advanced III-V materials than previously believed.

## INTRODUCTION

Studies of metal-semiconductor interfaces over the past decade using surface science techniques have revealed that reaction and interdiffusion play a major role in the formation of electrical barriers [1-5]. While such chemical interactions were widely recognized by the materials science community since the early 1970's [6-8], it is only with the advent of surface science techniques that such interface chemistry could be observed near room temperature and with sub-monolayer sensitivity. Moreover, such techniques have proven useful in characterizing the earliest stages of Schottky barrier formation. Among the interfaces receiving the most attention have been metals on the III-V compound semiconductors, due in part to their application in high-speed electronic devices. However contacts to III-V compounds have electrical barriers which are generally insensitive to different metals due to a high density of interface change which "pins" the Fermi level in a relatively narrow energy range [9]. While a number of models involving defects [10-12], interface dipoles and reacted layers [1-13], effective work functions [14,15] and metal-induced surface states [16-19] have been advanced, the detailed evolution of interface structure is far from understood.

Here, I review several aspects of the interface chemistry between metals and III-V compound semiconductors as obtained with soft X-ray photoemission spectroscopy (SXPS) and Auger electron spectrocsopy (AES) depth profiling. This includes a brief discussion of the extended metal semiconductor interface as modified by chemical interactions, evidence for such interactions, the systematics of semiconductor outdiffusion and the role of chemical bonding in controlling this process, the observed relation between outdiffusion stoichometry and measured Schottky barrier height, as well as recent measurements on ternary III-V compounds which suggest a greater degree of barrier control than hitherto believed.

## THE EXTENDED METAL-SEMICONDUCTOR INTERFACE

Considerable evidence for reaction and interdiffusion at compound semiconductor interfaces on a micron scale stems from AES, ion backscattering, and electron microscopy work in the mid 1970's [6-8]. For compound semiconductors, the correlation of Schottky barrier heights with the strength of metal-semiconductor bonding was indicative of the influence of chemical interactions on interface electronic structure [13]. In Figure 1, barrier heights measured by internal photoemission [20] are plotted versus interface heat of reaction $\Delta H_R$, the difference between heats of formation [21] for the bulk semiconductor and metal-anion reaction product, assuming a dissociated cation. This correlation appears to be applicable to a wide range of semiconductors and metals [1], with few exceptions [22]. Indeed, strong metal-cation bonding can account for the latter [23,24].

As shown in Figure 2, metal-semiconductor interactions can influence electronic structure in a number of ways, including reactions to form new interfacial phases with unique dielectric properties, band structure, and internal electric fields (e.g., dipoles), alloying to form metal contact layers with new effective work functions, as well as semiconductor outdiffusion and metal indiffusion to form electrically-active sites (e.g., native defects, impurities, and their complexes) which modify the band structure within the surface space change region [1]. In addition , the possibility of lateral inhomogeneties parallel to the interface can further complicate this picture [25].

## SYSTEMATICS OF SEMICONDUCTOR OUTDIFFUSION

Chemical reactions involving metal-semiconductor bonding are commonly observed at semiconductor surfaces with metal absorbates. Such reactions can extend monolayers to microns in thickness, depending on the temperature and the particular system [1,8]. For unreactive metals, which form no strong anion and cation compounds with high bond strength, room-temperature outdiffusion of semiconductor constituents into the metal overlayer can occur which is strongly influenced by the strength of interfacial bonding. SXPS measurements reveal that the extent of outdiffusion depends on the semiconductor stability - the lower the heat of formation, the greater the anion and cation outdiffusion [26]. This phenomena applies both III-V and II-VI materials and is measurable due to the extreme surface sensitivity available with the SXPS technique. Futhermore, the relative stoichiometry of anion and cation outdiffusion depends sensitively on the strength of metal-semiconductor bonding. Interlayers of reactive metal (e.g., Al,Ti, and Ni) between Au and overlayers on III-V compounds can change the outdiffusion from anion to cation-rich [27]. Such effects scale with increasing interlayer thickness, yet only a few monolayers or less are sufficient to produce orders-of-magnitude change in anion/cation surface-segregated concentration. Constant interlayer thickness with metals of different reactivity indicate a "chemical trapping" of outdiffusing anions as they bond with metal atoms near the intimate metal-semiconductor interface [28].

AES depth profiling measurements of "buried" metal-III-V semiconductor interfaces confirm this chemical trapping effect. Figure 3 illustrates the effect of a Ti interlayer at the Au-InP interface [29]. Here the P spectral intensity detected by AES decreases

to zero abruptly at the internal interface, whereas In atoms appear to diffuse through the Au overlayer and segregate at the free Au surface. The 10Å interlayer also serves to mark the original interface. In contrast, the Au-InP (110) interface without a reactive interlayer exhibits both cation and anion outdiffusion with preferential P surface segregation. Significantly this difference in outdiffusion results in a reversal of stoichiometry at the buried interface as well--anion-rich at the chemically-trapped interface and cation-rich at the unreactive interface. Such differences can affect any native defects left behind by the outdiffusion - i.e., their donor/acceptor character, energies, and densities. For example, a P-rich interface for reactive junctions with low n-type Shottky barriers argues against P vacancies playing a strong role in the Fermi level pinning, contrary to theoretical calculations of simple native defects [30]. The importance of outdiffusion stoichiometry versus measured barriers [32] for metals on ultrahigh vacuum (UHV)-cleaved InP (110) is underscored by the correspondence between the P-to-In stoichiometry versus measured barriers [32] for metals on ultrahigh vaccum (UHV)-cleaved InP (110) [31]. As shown in Figure 4, reactive metals such as Al, Ti, and Ni produce In-rich outdiffusion and low barriers, whereas relatively unreactive metals such as Ag, Cu, and Au lead to P-rich outdiffusion and high barriers. Similar effects are apparent for the same metals on GaAs, albeit over a smaller energy range [33]. Cr and Pd may be exceptions to these relations [22], but in both cases metal-cation bonding complicates the interface chemistry [23,24]. Diffusion of metal atoms into the semiconductor can also occur. For example, marker experiments reveal Au diffusion into GaAs and InP near room temperature [26]. Overall, figure 4 suggests that semiconductor outdiffusion leaves behind electrically-active sites and that the stoichiometry of outdiffusion can change the nature of such sites [31].

## ATOMIC SCALE CONTROL OF SCHOTTKY BARRIERS

The use of interlayers to alter interface stoichiometry has led to significant effects on measured electrical properties of metal/III-V compound semiconductor interfaces. A 10Å Al interlayer deposited between Au and a UHV-cleaved InP (110) surface produces an order-of-magnitude increase in forward and reverse current-voltage charcteristics relative to the same Au film on the same InP surface without the Al interlayer [31]. Exposure to $H_2S$ and Cl can also alter the InP and GaAs electrical properties substantially [34,35], presumably by adding or removing chemical species which change the interface chemistry and the residual sites of electric activity. Recently, Waldrop [36] has employed S and Se interlayers to produce reacted chalcogenides and to move the pinning energy over 0.4eV. Slowik et al. [37] have identified interface states located within the InP band gap which are close in energy to Fermi level pinning positions and which are sensitive to preparation conditions.

## FERMI LEVEL PINNING ON InGaAs (100)

Recent SXPS studies of Fermi level pinning at ternary III-V compound semiconductor interfaces indicate that the narrow range of pinning positions for metals on the GaAs (110) face is not characteristic of III-V compounds in general.

These measurements, the first for a ternary III-V compound, involved $In_x Ga_{1-x} As$, $0 \leq x \leq 1$, ($n = 10^{17} cm^{-3}$ Si) grown by molecular beam epitaxy (MBE) and capped by an As overlayer [38]. After thermal removal of these caps and prior to deposition of metal overlayers, these surfaces exhibited clean, ordered (lxl) characteristics. SXPS spectra with the deposited metals Au, Al, In, and Ge exhibit feature characteristics if their binary counterparts - i.e. reactions and interdiffusion near room temperature. As an example, Figure 5 illustrates spectra obtained with increasing Al coverage on clean $In_{.25} Ga_{.75} As$ (100). Spectra exhibit Ga3d and (spin-orbit split) In4d features which change with increasing Al coverage. A new set of In4d peaks appear, shifted to lower binding energy, characteristic of dissociated In. Al2p spectra (not shown) demonstrate that the first few Al monolayers bond with the semiconductor substrate, suggesting an exchange reaction between Al and In within the outer layers of the InGaAs. Hence, In segregation to the surface and formation of an InAlGaAs or AlGaAs near-interface layer appear near room temperature. This apparent exchange reaction favors the breaking of the weaker In-As versus the GaAs component of the ternary bonding. This is analogous to the dissociation of HgCdTe with metal deposition observed by Davis et al. [39] using SXPS., where the weaker Hg bonds break initially and lead to a Hg depletion near the interface.

The SXPS core levels in Figure 5 also reveal rigid shifts associated with band bending (e.g., movement of the Fermi level with respect to surface conduction and valence bands). Significantly, this shift for Al is opposite to that of Al on GaAs [10], e.g., toward the conduction band. Absolute energies of the complete alloy series core and valence band levels suggest no significant band bending prior to metal deposition on clean, ordered (100) surfaces. Figure 6 illustrates the Fermi level movement as a function of coverage for Au, and In on clean surfaces of the same $In_{.25}Ga_{.75}As$ (100) specimen. Each of the three metals exhibits a different movement both in energy and rate [38]. The spread of final pinning energies is over half that of the $In_{.25}Ga_{.75}As$ alloys exhibit even larger energy ranges relative to their band gaps. Furthermore, the pinning positions for a given metal across the InGaAs band gap energy. Analogous mesurements for the same metals on more In-rich InGaAs alloy series are systematic yet quite unlike previous lower vacuum results as well as theoretical predictions for simple defects [40]. Overall, these results for a ternary compound semiconductor alloy demonstrate that clean III-V surfaces can provide a wide range of controllable Schottky barrier heights. This result is particularly satisfying, given that (100) surfaces are used for actual devises.

## CONCLUSIONS

Chemical reaction and interdiffusion produce significant changes in chemical and electronic structure at metal interfaces with III-V compound semiconductors. Surface science techniques can monitor these phenomena even at room temperature and within a few monolayers or less of the interface. The close relationship between chemical and electronic structure lends itself to modification of macroscopic Schottky barrier heights by atomic scale techniques. New results for ternary III-V compounds reveal similar phenomena as well as much greater ranges of Fermi level pinning relative to their binary counterparts.

## ACKNOWLEDGEMENTS

The author gratefully acknowledges support in part from the Office of Naval Research (Contract N00014-80-C-0778). SXPS results were obtained at the Physical Sciences Laboratory , University of Wisconson, which is supported by the National Science Foundation.

## REFERENCES

1. L.J. Brillson, Surface Sci. Repts. 2, 123 (1982); Intern. J. Phys. Chem. Solids 44, 703 (1983); Handbook of Synchrotron Radiation II, edited by G.V. Marr (North-Holland,Amsterdam, 1986), in press.
2. G. Margaritondo, Solid State Electron. 26, 499 (1983).
3. R.H. Williams, Contemp. Phys. 23, 329 (1982).
4. M. Schluter, Thin Solid Films 93, 3 (1983); A. Zunger, ibid. 104, 301 (1983)
5. R.Z. Bachrach, in Metal-Semiconductor Schottky Barrier Junctions, edited by B.L. Sharma (Plenum, New York, 1984).
6. A. Hiraki, M.A. Nicolet, and J.W. Mayer, Appl. Phys. Lett. 18, 178 (1971).
7. A.K. Sinha and J.M. Poate, Appl. Phys. Lett. 23, 666 (1973).
8. See, for example, Thin Films - Interdiffusion and Reactions, edited by J.M. Poate, R.N.Tu, and J.W. Mayer (Wiley-Interscience, New York, 1978), and references there in.
9. S.M. Sze, Physics of Semiconductor Devises, 2nd ed. (Wiley-Interscience, New York, 1981), Ch.5.
10. W.E. Spicer, I. Lindau, P.W.Chye, C.Y. Su, J. Vac. Sci. Technol. 16, 1422 1979).
11. R.H. Williams, J. Vac Sci. Technol. 16, 1418 (1979).
12. H.H. Wieder, J. Vac. Sci. Technol. 15, 1498 (1978).
13. L.J. Brillson, Phys. Rev. Lett. 40, 260 (1978).
14. J.L. Freeouf and J. M. Woodall, Appl. Phys. Lett. 39, 727 (1981).
15. J.M. Woodall and J.L. Freeouf, J. Vac. Sci. Technol. 21, 574 (1982).
16. M.L. Cohen, Adv. Electron. Electon Phys. 51, 1 (1980) and references therein.
17. J. Tersoff, Phys. Rev. Lett. 57, 465 (1984).
18. J. Tersoff, J. Vac. Sci. Technol. B3, 1157 (1985).
19. R.Ludeke, T.-C Chiang, and T. Miller, J. Vac. Sci.Technol. B1 581 (1985).
20. C.A. Mead, Solid State Electron. 9, 1023 (1966)
21. D.D. Wagman, W.H. Evans, V.B. Parker, I Halow, S.M. Bailey, and R.H. Schumm, NBS Technical Notes 270-3-270-7 (USGPO Washington, D.C., 1968-1971)
22. T. Kendelewicz, N. Newman, R. List, I. Lindau, and W.E. Spicer, J.Vac. Sci. Technol. B3, 1206 (1985).

23. J. McGilp, J. Phys. C17, 2249 (1984).
24. J.H. Weaver, M. Grioni and J. Joyce, Phys. and J. Joyce, Phys. Rev. B31, 5348 (1985).
25. R. Ludeke, Surface Sci. 132, 143 (1983).
26. L. J. Brillson, C.F. Brucker, N.G. Stoffel, A.D. Katnani, R. Daniels, and G. Margaritondo, Surface Sci. 132, 212 (1983).
27. L.J. Brillson, G. Margaritondo, and N.G. Stoffel, Phys. Rev. Lett. 44, 667 (1980).
28. L.J. Brillson, C.F. Brucker, G. Margaritondo, J. Slowik, and N.G. Stoffel J. Phys. Sci. Soc. Japan 49, 1089 (1980).
29. Y. Shapira, and L.J. Brillson, J. Vac Sci. Technol. B1, 618 (1983).
30. J.D. Dow, O.F. Sankey, and R.E. Allen, Appl. Surf. Sci. 22/23, 937 (1985).
31. L.J. Brillson, C.F. Brucken, A.D. Katnani, N.G. Stoffel, and G. Margaritondo, Appl. Phys. Lett. 38, 784 (1981).
32. R.H. Williams, V. Montgomery, and R.R. Varina, J. Phys. C11, L735 (1978)
33. N. Newman, T. Kendelwicz, D. Thompson, S.H. Pan, S.J. Eglash, and W.E. Spicer, Solid State Electron. 28, 307 (1985).
34. V. Montgomery, R.H. Williams, and G.P Srivastava, J. Phys. C14, L191 (1981).
35. J. Massies, J. Chaplart, M. Laviron, and N.T. Linh, Appl. Phys. Lett. 38, 693 (1981).
36. J. Waldrop, J. Vac. Sci. Technol. B3, 1197 (1985).
37. J. Slowik, L.J. Brillson, and H.W. Richter, J. Appl. Phys. 58, 3154 (1985)
38. L.J. Brillson, M.L. Slade, J.M. Woodall, P.Kirchner, G.D. Pettit, M. Kelly, N. Tache, and G. Margaritondo, unpublished.
39. G.D. Davis, W.A. Beck, N.E. Byer, R.R. Daniels, and G. Margaritondo, J. Vac. Sci. Technol. A2, 546 (1984).
40. K. Kajiyama, Y. Mizushima, and S. Sakata, Appl. Phys. Lett. 23, 458 (1973); H.H. Wieder, ibid. 38, 170 (1981).

## FIGURE CAPTIONS

1. Schematic energy band diagram of the extended metal-semiconductor interface, as modified by chemical reaction and interdiffusion. After Brillson [1].

2. Schottky barrier heights measured by internal photoemission [20], plotted as a function of interface heat of reaction. After Brillson [13].

3. AES depth profiles for (a) 70A Ti - InP (110) and (b) 70A Au - InP (110) interfaces. Arrows indicate the reversal in cation-anion stoichiometry near the buried interfaces. After Shapira and Brillson [29].

4. SXPS ratio of surface anion/cation core local intensities $I_{P2p}/I_{In\ 4d}$ versus Ag, Pd, Cu, Au, Al, Ti, or Ni coverages on InP (110) relative to its UHV-cleaved surface ratio. Barrier $\varnothing_{SB}$ versus $\Delta H_r$ is plotted in the inset (after Williams et al. [32] and illustrates the correspondence between $\varnothing_{SB}$ and stoichiometry of outdiffusion. After Brillson et al. [31].

5. SXPS Ga 3d and In 4d core level spectra of $In_{.25}Ga_{.75}As$ (100) obtained at $h\nu = 40ev$ as a function of Al deposition. New In 4d features indicate In dissociation by absorbed Al. Rigid core level shifts correspond to Fermi level movement toward the vacuum level. After Brillson et al. [38].

6. Fermi level movements of $In_{.25}Ga_{.75}As$ (100) as a function of Au, Al and In metal deposited thickness from SXPS rigid core level shifts. The range of Fermi level stalilization energies is more than half the semiconductor band gap. After Brillson et al. [38].

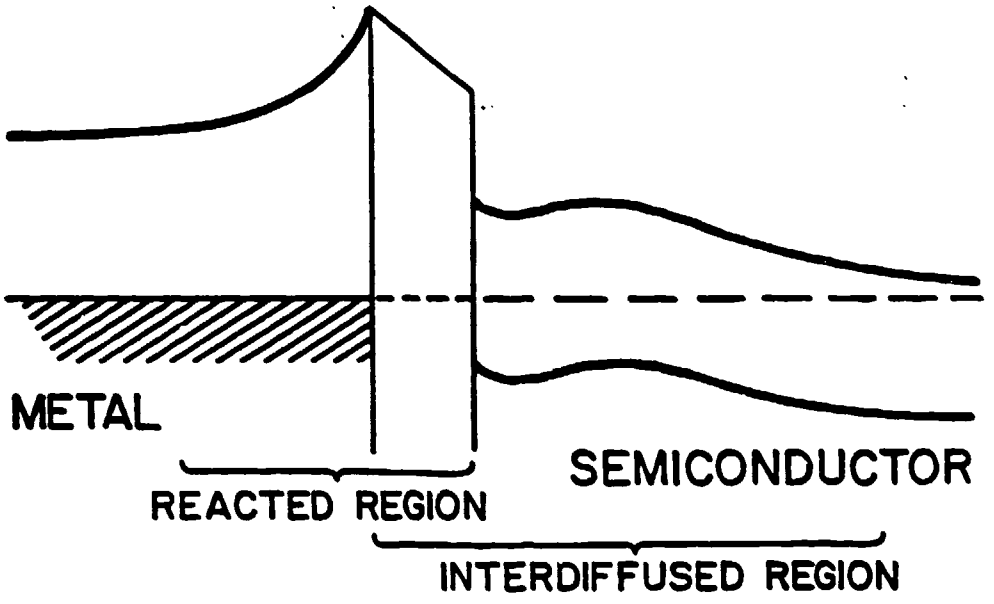
METAL
SEMICONDUCTOR
REACTED REGION
INTERDIFFUSED REGION

Fig. 1

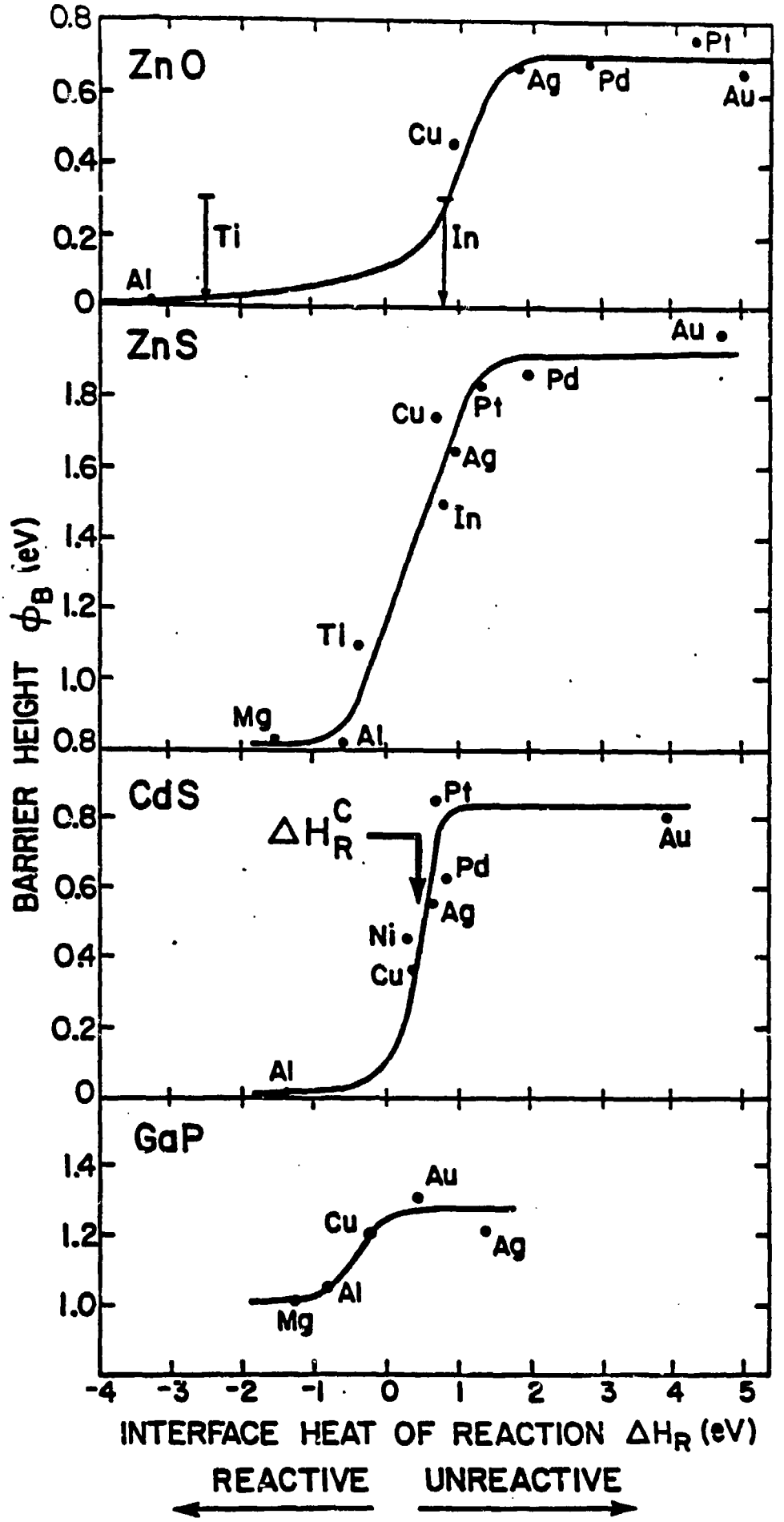
ZnO
Pt
Ag
Pd
Au
Cu
Ti
In
Al
ZnS
Au
Pd
Cu
Pt
Ag
In
Tl
Mg
Al
CdS
Pt
$\Delta H_R^C$
Au
Pd
Ag
Ni
Cu
Al
GaP
Au
Cu
Ag
Al
Mg
BARRIER HEIGHT $\phi_B$ (eV)
0.8
0.6
0.4
0.2
0
1.8
1.6
1.4
1.2
1.0
0.8
0.8
0.6
0.4
0.2
0
1.4
1.2
1.0
-4 -3 -2 -1 0 1 2 3 4 5
INTERFACE HEAT OF REACTION $\Delta H_R$ (eV)
REACTIVE
UNREACTIVE

Fig. 2

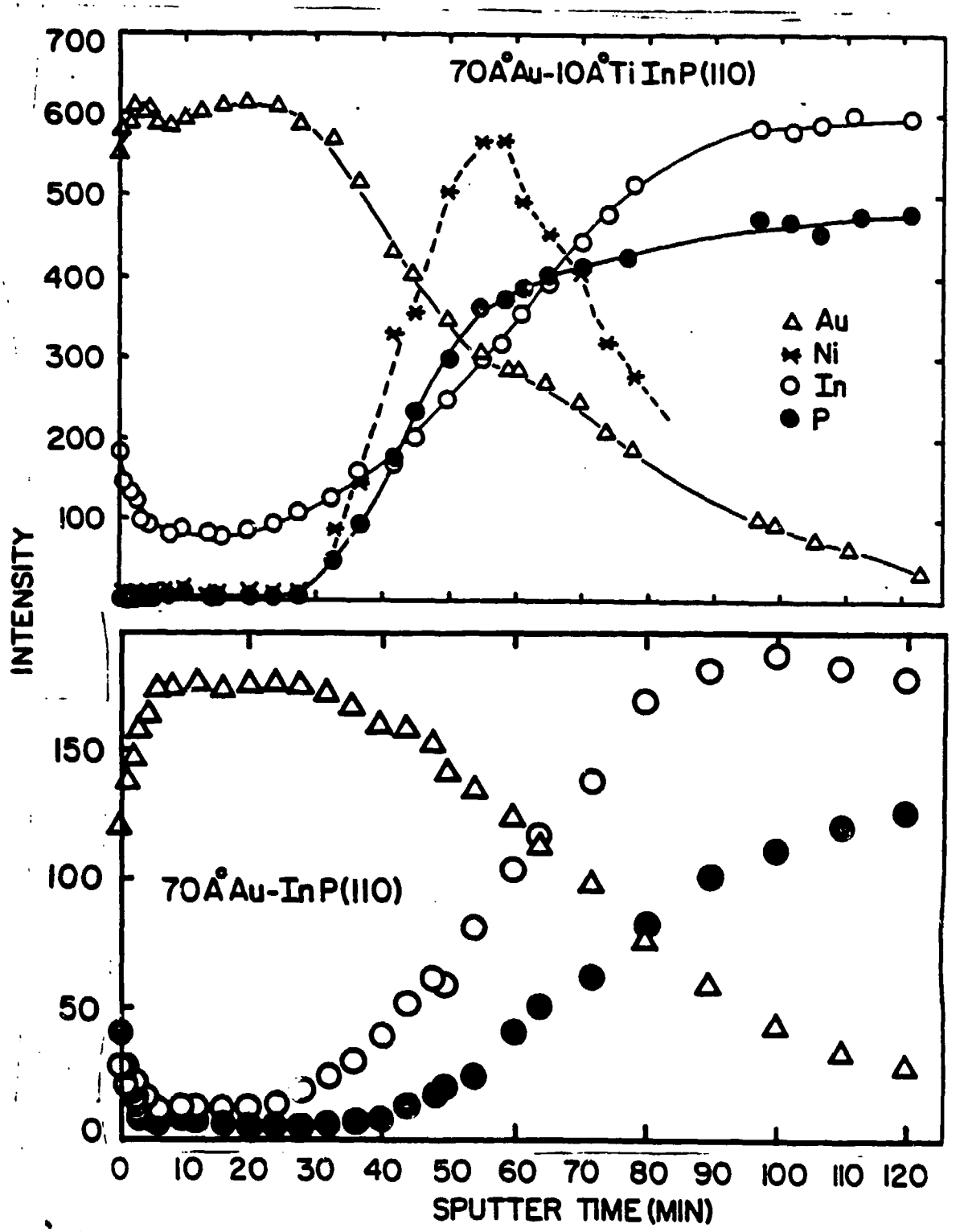
70Å Au-10Å Ti InP(110)
Au
Ni
In
P
INTENSITY
700
600
500
400
300
200
100
70Å Au-InP(110)
150
100
50
0
0 10 20 30 40 50 60 70 80 90 100 110 120
SPUTTER TIME (MIN)

Fig. 3

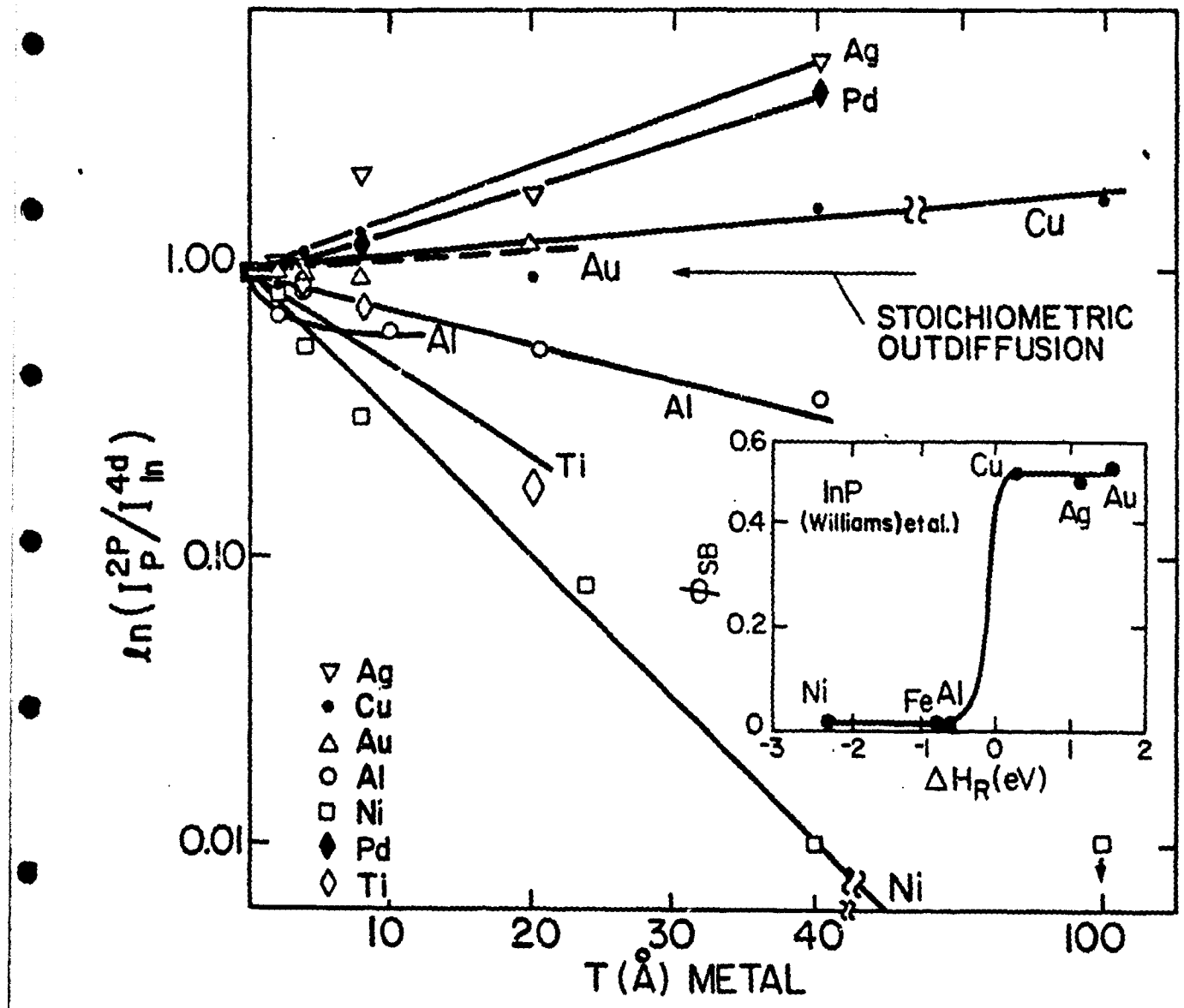
Ag
Pd
Cu
Au
Al
Ti
Ni
STOICHIOMETRIC
OUTDIFFUSION
1.00
0.10
0.01
$\ln(I_P^{2P}/I_{In}^{4d})$
10
20
30
40
100
T (Å) METAL
▽ Ag
• Cu
△ Au
○ Al
□ Ni
♦ Pd
◇ Ti
InP
(Williams)et al.
$\phi_{SB}$
0.6
0.4
0.2
0
Ni
Fe
Al
Cu
Ag
Au
-3
-2
-1
0
1
2
$\Delta H_R$(eV)

Fig. 4

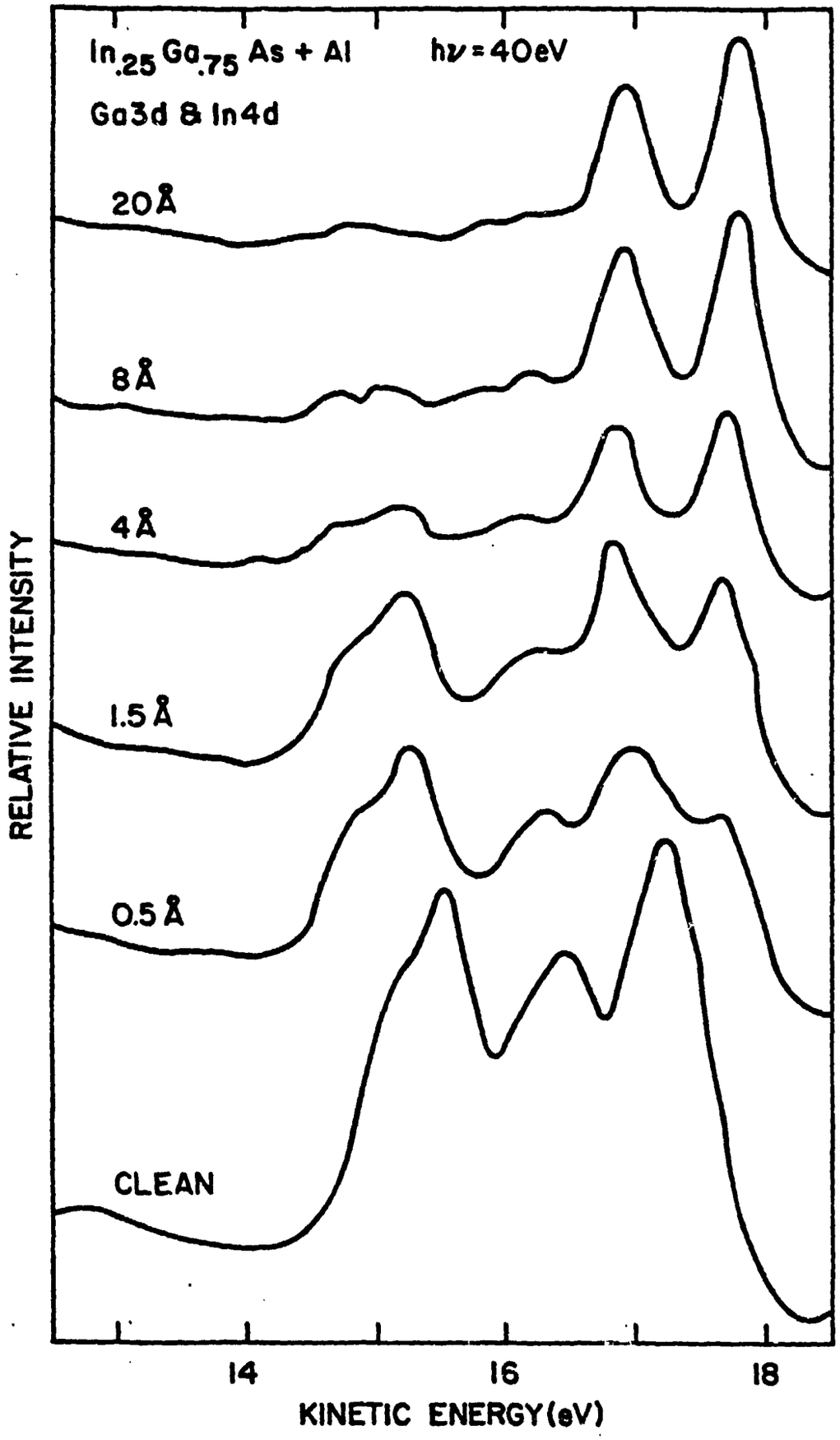
$In_{.25}Ga_{.75}As$ + Al
hν = 40eV
Ga3d & In4d
20Å
8Å
4Å
1.5Å
0.5Å
CLEAN
RELATIVE INTENSITY
14
16
18
KINETIC ENERGY(eV)

Fig. 5

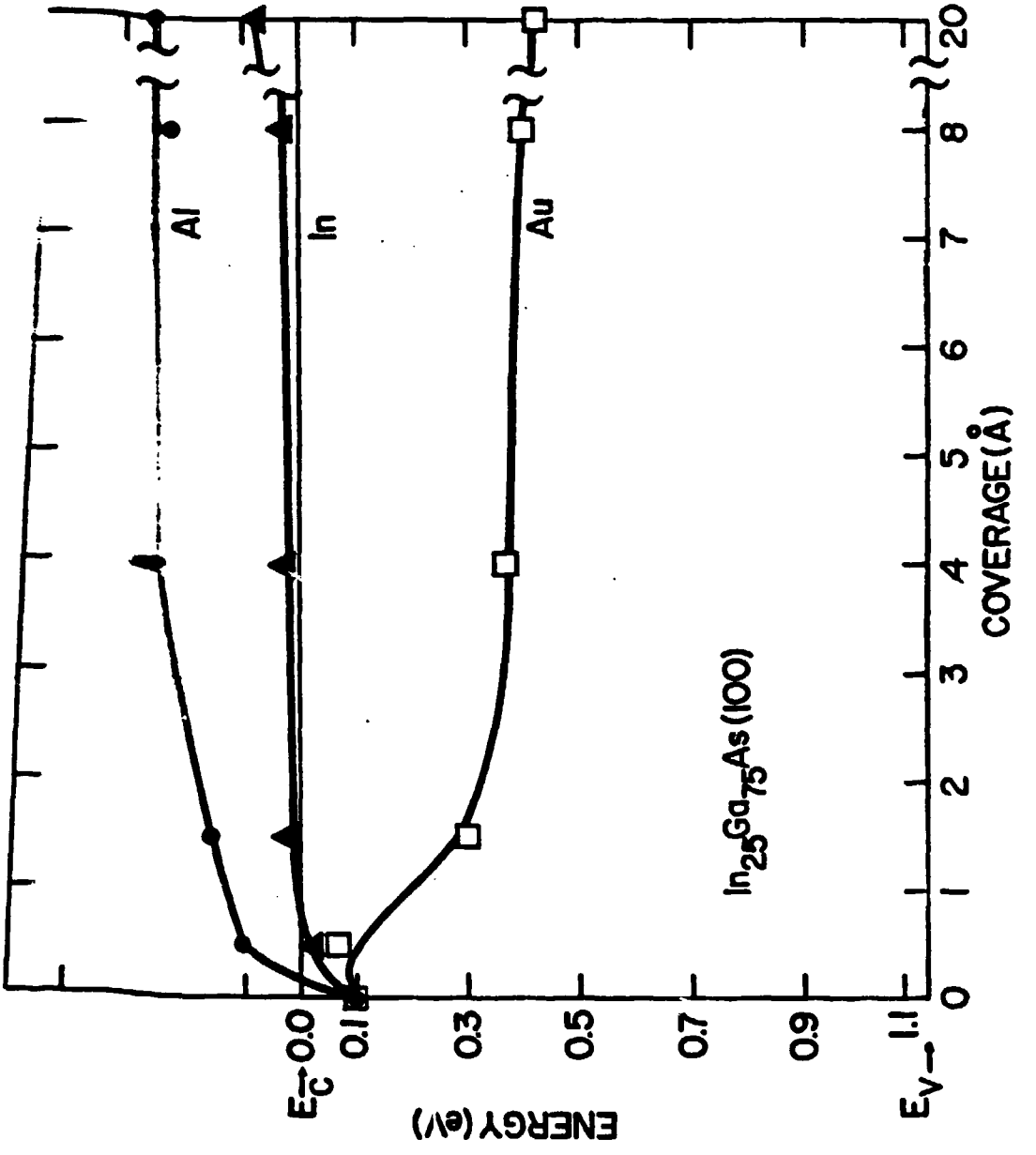
Al
In
Au
$In_{25}Ga_{75}As$ (100)
COVERAGE (Å)
ENERGY (eV)
$E_C$ 0.0
0.1
0.3
0.5
0.7
0.9
$E_V$ 1.1
0
1
2
3
4
5
6
7
8
20

Fig. 6

# Acceptor-like Electron Traps Control Effective Barrier for UHV-cleaved and Laser-annealed Al/InP

John H. Slowik, L.J. Brillson, and H. Richter[a]

Xerox Webster Research Center, Webster, N.Y. 14580

## ABSTRACT

We analyze the temperature dependence of the current and capacitance responses for Al contacts on UHV-cleaved (110) n-InP. We compare pulse-laser-annealed contacts to unannealed contacts formed concurrently on the opposite half of each freshly-cleaved InP surface. Acceptor-like electron traps lying 0.10eV below the conduction band (a level sometimes ascribed to donors in the unified defect model) dominate electronic behavior. These traps occur in an interfacial layer whose thickness is reduced from ~160Å to ~34Å by laser-annealing. Both laser-pulsed and unannealed contacts have a 0.22eV barrier height. The fact that the 0.5eV barrier of Al reported on treated InP also decreases to 0.22eV upon heating suggests that the barrier stabilizes between two states with a stable, reproducible concentration ratio.

## I. INTRODUCTION

Much effort is being devoted to exploiting the potential of InP for high frequency oscillators and injection lasers. Contact stability is crucial in these devices. Two categories of contacts on pure (doping density, $N_D = 5 \times 10^{15}cm^{-3}$) n-InP have been found to produce highly reproducible 0.5eV Schottky barriers: 1) unreactive metals[1] deposited on vacuum-cleaved InP,[2] and 2) reactive metals such as Al, if the InP surface is processed by etching and heating before metallization.[3] The reproducibility of these barriers is understood on the basis of a defect level[2,4] 0.5eV below the conduction band edge, $E_C$. However, the details of barrier formation, and the issue of their stability are still subjects for investigation. For example, the barrier of Al on etched and heated InP decreases progressively to 0.22eV following successively more intense annealing treatments.[5] If the InP surface is left unprocessed before Al deposition, a low[2,3,6] thermally reversible effective barrier is formed, whose electronic behavior indicates a real barrier height of[7] 0.21 to 0.26eV.

The barrier formed by Al on InP is investigated here by studying an intermediate contact. Al is deposited on an unprocessed InP surface, but subsequently annealed with a laser. Other Al contacts on the same InP surface are formed simultaneously, except that they are left unannealed. These unannealed contacts have been reported in detail elsewhere.[7] We find that the laser-annealed contacts exhibit electronic behavior intermediate between the above-mentioned processed and unprocessed contacts. Acceptor-like electron traps[7] at 0.10eV below $E_C$ control the electronic response. The effect of laser-annealing is to confine their distribution in InP to within ~34Å of the interface. We propose that interaction between the level at 0.10eV and a deeper level may be the reason why a 0.22eV barrier results from several distinctly different Al/InP barrier formation techniques.

Experimental detail is contained in Section II, and results in Section III. capacitance and current characteristics are analyzed in Sections IV and V. Section VI discusses the significance of the results for understanding the details of the electronic structure of the barrier. Results are summarized in Section VII.

## II. EXPERIMENT

Laser-annealed contacts were formed concurrently with the clean untreated contacts described earlier.[7] Oriented crystals of n-InP, $N_D$ = 1-5 x $10^{15}cm^{-3}$, were cleaved (110) in ultrahigh vacuum. A 60-65Å layer of Al was deposited on the freshly cleaved face. With a mask protecting half of the face, 308nm light from a xenon chloride excimer laser annealed the Al/InP contact throughout the unmasked half. The pulsed laser beam scanned the surface so that each spot received 3 pulses. Total energy was approximately 2.3 $J/mm^2$. Deposition of a 5x5 pattern of Al electrodes, covering the cleavage face, resulted in 5-8 usable electrodes on both the annealed and unannealed areas. These electrodes were 200Å thick and 500μm diam. Additional electrodes were used to guard against surface currents[8] or to determine spreading and residual resistances.[9]

Current and capacitance measurements were made within the range 80-360K. Forward currents were kept sufficiently low so that the known spreading and residual resistances were negligible. When interpreting the current response to applied potentials less than 3kT/q, special care was taken to handle exponential terms containing kT correctly.[10] Capacitance response was measured at 1 MHz and was not significantly affected by the series resistance.[11] However, at higher temperatures, capacitance measurements were limited when reverse currents became too large for the Boonton 72B capacitance meter.

## III. CAPACITANCE AND CURRENT RESULTS

The capacitive response of the laser-annealed contacts to applied reverse bias, and the stray capacitance contribution, were measured at a variety of fixed temperatures. After subtracting stray capacitance, $(A/C)^2$ *vs* V was plotted as in Fig. 1, where A is the electrode area. The curves are linear between zero and about -50mV, but become flat at stronger bias. This behavior is similar to that reported for the unannealed contacts,[7] except that the magnitude of the capacitance is larger for annealed contacts. Data distorted by excessive reverse-bias currents are deleted from Fig. 1.

Typical forward-bias current characteristics are shown in Fig. 2. These characteristics are qualitatively similar to those reported for the unannealed contacts,[7] in that both are highly non-ideal. There is, however, an important

difference. Characteristics of the unannealed contacts converged below ~130K, a good indication of the onset of a tunneling mechanism. Such a convergence is not obvious down to 80K in the annealed contacts reported here, which indicates that the barrier is less conducive to tunneling.

## IV. ANALYSIS OF CAPACITANCE CHARACTERISTICS

The capacitance characteristics in Fig. 1 indicate the presence of acceptor-like electron traps at 0.10eV below the conduction band edge. If these traps were restricted to the surface of the InP, their space charge could not account for the nonlinearity of the characteristics.[12] But if the traps are distributed over some distance between the contact and some depth within the semiconductor, then they are decoupled from the metal and the nonlinearity can be explained.[7,12] At large reverse bias, the metal electrode injects a significant tunneling current which interacts with the traps. Although the slope of the characteristic at high bias reflects the doping density, the extrapolated voltage intercept is offset to a large value because of a potential drop across the trap layer. At small values of reverse bias the slope of the capacitance characteristics, given by

$$\partial(C^{-2})/\partial(-V) = 2/q\varepsilon_s n_{oo}, \qquad (1)$$

is large.[10] This indicates an effective donor density, $n_{oo}$, which is considerably less than the bulk free carrier density, $n_o$. We attribute this to partial population of the traps. A populated trap has a negative charge, as would an ionized acceptor in the space charge region, and acts to compensate shallow donors. The value of $n_{oo}$ at different temperatures is shown in Fig. 3. As the temperature increases, the traps fully ionize and $n_{oo}$ approaches $n_o$ as indicated by the dashed line. The slope of this rise indicates the depth of the trap, 0.10eV below the conduction band edge, $E_C$. Although this trap provides the simplest interpretation of the data, note that a more complex distribution could be present.

The relatively linear region in the capacitance characteristics near zero bias indicates a regime within which $n_{oo}$ is constant, so that the barrier height can be estimated from

$$(A/C)^2 = 2(\phi_{CO} - qV - \zeta - kT)/q^2\varepsilon_s n_{oo}, \qquad (2)$$

where

$$\zeta = E_C - E_F = kT \ln(U_C/n_o), \quad (3)$$

$E_F$ is the Fermi level, and $U_C$ is the effective density of states in the conduction band. The resulting barrier estimate, $\phi_{CO}$, can differ significantly from the true value, $\phi_O$, of the barrier at the metallurgical junction, since $\phi_{CO}$ results from extrapolating parabolic bands to the junction.[13] In reality, spatially non-uniform trapped charge makes the band bending non-parabolic. Trapped majority/minority carriers result in a $\phi_{CO}$ which is too large/small. Thus large $\phi_{CO}$ values at low temperatures, as seen in Fig. 3, arise from majority carriers (electrons) in the acceptor-like traps at 0.10eV. The capacitance results contain two additional indications of such trapping. First, note that $\phi_{CO}$ approaches a constant value above ~170K, although the transition is not sharp. This transition may be due to decreased trapped space charge since 170K marks the onset of ionization in $n_{oo}$. Secondly, there is a strong decrease in the value of the zero-bias capacitance at low temperature in Fig. 1, presumably due to majority carrier trapping.

The region of constant $\phi_{CO}$ values in Fig. 3 should thus most closely approximate the true barrier, $\phi_O$. From the figure, $\phi_{CO} = 0.19 \pm 0.02$eV near room temperature.

## V. ANALYSIS OF CURRENT CHARACTERISTICS

As in the case of the unannealed contacts,[7] we found it necessary to analyze current characteristics for the laser-annealed contacts by using Levine's model.[14] This model makes specific allowance for the presence of interfacial traps which need not be restricted to the surface of the semiconductor, but rather may be distributed within an interfacial layer.

The dashed line in Fig. 2 shows the slope of the current characteristic which would be expected at low temperature if the ideality factor, n, were unity. The characteristics in Fig. 2, even eliminating the effects of spreading and residual resistances, correspond to effective n values which are too large for thermionic emission, or space charge region recombination, or thermionic-field emission[9] models. Also, the calculated value of the minority carrier injection ratio[15,16] is far too small to account for the magnitude of the observed current. Finally, unlike the unannealed contacts, under forward bias and above 80K there is little evidence of the temperature-independent current which would indicate true tunneling.

Satisfactory analysis of the current characteristics require a model which includes an interfacial layer of trapped charge. Levine's model[14] proved successful for analysis of the unannealed contacts,[7] and is used again here. In the model, the traps modify the current response in a way that is mathematically equivalent to defining an effective temperature, $T_e$, according to

$$T_e = q/k[\partial(\ln J)/\partial V]. \quad (4)$$

The temperature and field dependence of $T_e$ are fully determined by a set of current characteristics such as in Fig. 2. The model predicts an effective barrier, $\phi_B$, given by

$$\phi_B - qV - \zeta - kT = (T_e - T)qT/(\partial T_e/\partial V)T_e, \quad (5)$$

if certain additional conditions[17] are satisfied. Values of $\phi_B$ obtained from Eq. (5) are shown in Fig. 4. Extrapolation of $\phi_B$ produces values for $\phi_{BO}$, the effective barrier height at zero bias. The variation with temperature of $\phi_{BO}$ for annealed contacts is shown in Fig. 3. It varies from 0.20 to 0.22eV over the 80-360K range. This is a much weaker temperature variation than was observed for unannealed contacts.[7] Unannealed contacts increased with temperature monotonically and reversibly from 0.04 to 0.21 over the identical temperature range.

The interfacial trap layer is physically different from a thin interfacial insulator layer. Nevertheless, the resulting band distortions have similarities,[7,18] and it is instructive to analyze the current characteristics of the Al/InPcontacts as if they were those of an MIS device. Thus, the current characteristics are replotted as a Richardson plot in Fig. 5. As was the case for the unannealed contacts,[7] there is a regime at high temperature which corresponds to Schottky emission in an MIS device, and a low temperature regime where other transport mechanisms contribute. The low temperature regime was a clear case of tunneling for unannealed contacts,[7] since a plot of $\ln(J/V^2)$ *vs* $V^{-1}$ showed temperature independence at low temperature, as predicted by the MIS tunneling expression:[18]

$$J \sim V^2 \exp(-1.89 m^{*1/2} \phi_{BO}^{3/2} d/q\hbar V), \quad (6)$$

where d is the insulator thickness. As can be seen from Figs. 2 and 6, no such convergence is evident for the case of the laser-annealed contacts, even though the currents are four orders of magnitude lower than the tunneling currents in

unannealed contacts. This suggests that annealing removes those traps which are spatially deeper within the space charge region, and which otherwise could facilitate a multistep tunneling process.

Returning to the high temperature regime in Fig. 5, one finds further evidence that the interfacial trap layer is thinner following annealing. According to the expression for Schottky emission current in an MIS device,[18] which is

$$J = A^*T^2\exp\{[q(qV/4\pi\varepsilon_i d)^{1/2} - \phi_{BO}]/kT\}, \quad (7)$$

the slopes, S, at high temperature in Fig. 5 are given by

$$S = [q(qV/4\pi\varepsilon_i d)^{1/2} - \phi_{BO}]/k. \quad (8)$$

A plot of S *vs* $V^{1/2}$ is shown in Fig. 7. From the slope of the line in Fig. 7, d can be extracted according to Eq. (8). The resulting value is 34Å for the laser-annealed contacts, compared to 160Å without annealing. In both cases the insulator dielectric constant $\varepsilon_i$ in Eq. (8) has been set equal to that of InP. It should be emphasized that d in Eqs. (7) and (8) refers to a true insulator thickness and is merely analogous to the trap penetration depth. The values of d extracted from Al/InP data may well depend on trap occupancy, whereas d would be invariant for the case of an MIS device. The change in d values does point, however, to a thinner interfacial trap layer as a consequence of the laser-annealing, in agreement with the earlier tunneling discussion.

Equation (8) also indicates that the intercept in Fig. 7 may be used to estimate $\phi_{BO}$, again within the limitations of the MIS analog. The resulting value is $\phi_{BO}$ = 184meV, which agrees well with values in Fig. 3 obtained from the interfacial trap model. The agreement in $\phi_{BO}$ values provides a measure of confidence that d values obtained from the MIS analog approximate the thickness of the interfacial trap layer.

Without laser-annealing, the current characteristics showed some sensitivity to the immediately preceding bias conditions, particularly at low temperature. No such sensitivity is observed after annealing. This observation is consistent with a trap layer thickness which is reduced by annealing, since traps closer to the metal contact could be more readily emptied by emission into the metal.

## VI. DISCUSSION

The current and capacitance responses to applied bias indicate the presence of a thin region at the Al/InP interface which contains acceptor-like electron traps. This type of penetrating trap distribution has been proposed by Williams,[19] who went on to point out the relevancy of Levine's model. The principal effect of laser-annealing the Al/InP contact is to reduce the thickness of this region. Analysis of the current characteristics according to an MIS model suggest a reduction by a factor of five, to ~34Å. This interpretation is consistent with the observations that laser-annealing 1) drastically lowers the contribution to current due to tunneling, 2) eliminates dependence of the current upon preceding bias conditions, 3) eliminates strong thermal variation of $\phi_{BO}$, 4) doubles the magnitude of the zero-bias capacitance, and 5) decreases the band distortion which causes $\phi_{CO}$ to exceed $\phi_{BO}$.

Strong thermally reversible lowering of $\phi_{BO}$ due to tunneling is eliminated by laser-annealing. A weak reversible lowering remains. We propose an explanation which is illustrated in Fig. 8. Because of the low bulk free carrier density, there is a strong temperature dependence of the separation between the conduction band, at $E_C$, and the Fermi level, at $E_F$. If $\phi_{BO}$ is slightly less than $\phi_O$, due to tunneling through the tip of the barrier or image-force lowering, then the shift of $E_C$-$E_F$ would cause a weaker correlated shift in $\phi_{BO}$, as illustrated. The true barrier height would slightly exceed the maximum observed $\phi_{BO}$, $\phi_O \approx 0.22$eV.

Capacitance data indicates that the interfacial acceptor-like electron traps are 0.10eV below $E_C$ for both unannealed[7] and laser-annealed Al/InPcontacts. It has been noted that such states are closely related[7] to those invoked by the unified defect model.[20]

Traps at 0.10eV clearly cannot pin the barrier at $\phi_O$ = 0.22eV. Either other states are present at 0.22eV, or else there is an interaction with a deeper lying level such as the level at ~0.5eV which accounts[6,21] for the barrier formed by less reactive metals on InP. Interaction of two defect levels could be expected to reproducibly stabilize $\phi_O$ at a level between them only if they shared a common chemical or physical source, so that their concentrations were correlated. Regardless of what pins $\phi_O$ at 0.22eV, there is further evidence that it does represent a stable, reproducible value. A stable 0.5eV barrier is universally produced on InP by etching and heating the InP surface before depositing metal.[2,3,5,22] This is understood as a

consequence of pinning by a 0.5eV defect level. However, when an Al contact on this type of InP surface is heated, the barrier decreases[5] to 0.22eV. Thus this annealing treatment of Al on etched InP, and the distinctly different laser annealing of Al on vacuum-cleaved InP, result in the same barrier height. Presumably a fixed ratio of defect levels is present in the two cases. Although vacant states were once reported[23] on cleaved (110) InP at 0.2eV, no defect level is commonly reported at 0.22eV. A level at about 0.3eV (assuming 1.4eV gap) was recently used to fit contact potential difference measurements.[24] An acceptor is found in photoluminescence at 0.21eV and with activation energy 0.08eV. These numbers are intriguingly like the $\phi_o$ and $E_a$ reported here. However this 0.21eV is measured from $E_V$, not $E_C$. The absence of a level at 0.22eV below $E_C$ suggests that, at least in the case of Al contacts, the 0.22eV barrier may result from a stable, reproducible ratio of the concentrations of the acceptor-like electron trap and a deeper level.

## VII. SUMMARY

Al contacts on n-InP which are formed in different ways share a common barrier height of ~0.22eV at room temperature. These contacts include those formed by 1) deposition of Al on UHV-cleaved InP, 2) laser-annealed Al on InP, and 3) annealing an Al contact on InP where the InP is first etched and heated before deposition. Capacitance and current characteristics of at least the first two contacts are controlled by acceptor-like electron traps in an interfacial layer 30 to 200Å thick. These traps are 0.10eV below $E_C$, and may interact with a deeper level in a fixed concentration ratio to produce the 0.22eV barrier which is common to these three types of Al/InP contacts. Laser annealing reduces the thickness of the interfacial trap layer and removes tunneling as a channel of charge transport under forward bias.

## ACKNOWLEDGMENTS

We thank Dr. C.B. Duke, Professor A. Kahn, Professor M. Shaw, and Dr. H. Wieder for helpful discussions. One of the authors (LJB) acknowledges partial support by the Office of Naval Research (Contract N00014-80-0778).

## REFERENCES


a. Present address: Max-Planck Institut für Festkörperforschung, Stuttgart, West Germany.

1. L.J. Brillson, Phys. Rev. Lett. 40, 260 (1978).

2. R.H. Williams, R.R. Varma, and V. Montgomery, J. Vac. Sci. Technol. 16, 1418 (1979).

3. B. Tuck, G. Eftekhari, and D.M. deCogan, J. Phys. D 15, 457 (1982).

4. W.E. Spicer, I. Lindau, P. Skeath, and C.Y. Su, J. Vac. Sci. Technol. 17, 1019 (1980).

5. R.H. Williams, R.R. Varma, and A. McKinley, J. Phys. C 10, 4545 (1977).

6. R.H. Williams, V. Montgomery, and R.R. Varma, J. Phys. C 11, L735 (1978).

7. J.H. Slowik, H.W. Richter, and L.J. Brillson, J. Appl. Phys. 58, 3154 (1985).

8. F.A. Padovani, in Semiconductors and Semimetals, edited by R.K. Willardson and A.C. Beer, (Academic, New York, 1971), Vol. 7A, p. 75.

9. M. Shaw, in Handbook on Semiconductors, edited by T.S. Moss and C. Hilsum, (North-Holland, New York, 1981), Vol. 4, p. 1.

10. E.H. Rhoderick, Metal-Semiconductor Contacts (Clarendon, Oxford, 1980).

11. A.M. Goodman, J. Appl. Phys. 34, 329 (1963).

12. A.M. Cowley, J. Appl. Phys. 37, 3024 (1966).

13. C.R. Crowell and G.I. Roberts, J. Appl. Phys. 40, 3726 (1969).

14. J. Levine, J. Appl. Phys. 42, 3991 (1971).

15. D.L. Scharfetter, Sol. St. Electron. 8, 299 (1965).

16. M.A. Green and J. Shewchun, Sol. St. Electron. 16, 1141 (1973).

17. One should test that $T_e$-T and $(T_e-T)^2/(\partial Te/\partial V)T_e$ are essentially independent of temperature at constant current.

18. S.M. Sze, Physics of Semiconductor Devices, (Wiley, New York, 1969).

19. R.H. Williams, Surf. Sci. 132, 122 (1983).

20. W.E. Spicer, I. Lindau, P. Skeath, C.Y. Su, and P. Chye, Phys. Rev. Lett. 44, 420 (1980).

21. R.H. Williams, A. McKinley, G.J. Hughes, V. Montgomery, and I.T. McGovern, J. Vac. Sci. Technol. 21, 594 (1982).

22. H.B. Kim, A.F. Lovas, G.G. Sweeney, and T.M.S. Heng, in Proceedings of Sixth International Symposium on GaAs and Related compounds, Inst. Phys. Conf. Ser. No. 33b, p. 145 (1976).

23. W.E. Spicer, P.W. Chye, P.E. Gregory, T. Sukegawa, and I.A. Babalola, J. Vac. Sci. Technol. 13, 233 (1976).

24. A. Ismail, A. Ben Brahim, L. Lassabatere, and I. Lindau, J. Appl. Phys. 59, 485 (1986).

25. H. Temkin, B.V. Dutt, and W.A. Bonner, Appl. Phys. Lett. 38, 431 (1981).

## FIGURE CAPTIONS

1. Reverse-bias capacitance characteristics of laser-annealed Al contact on (110) n-InP, at (top to bottom) 127, 145, 159, 181, 216 and 245K.

2. Forward-bias current characteristics of laser-annealed Al contacts on (110) n-InP, at (top to bottom) 359, 300, 219, 147 and 84K. If the ideality factor at 84K were unity, the slope would equal that of the dashed line.

3. Temperature dependence of effective barrier height $\phi_{BO}$ determined from forward current characteristics, and $\phi_{CO}$ and $n_{oo}$ from reverse capacitance characteristics according to Eq. (2), for laser-annealed Al/InP contact. As traps ionize, $n_{oo}$ rises (dashed line) to bulk free carrier density, $n_o$. Slope of dashed line yields trap depth $E_a$ = 0.10eV.

4. $\phi_B$ vs forward bias resulting from analysis of laser-annealed Al/InP contact current characteristics according to interfacial trap model. Intercepts equal zero-bias effective barrier, $\phi_{BO}$. Upper data at 359K (line) and 300K (points) are essentially colinear. Middle line at 219K. Lower data at 147K (points) and 84K (line) are essentially colinear. Temperature-dependence is reversible.

5. Richardson plot of current response of laser-annealed Al/InP, at (top to bottom) 0.75, 0.65, 0.5, 0.4, 0.3, 0.2, 0.1V forward bias.

6. Current response data of laser-annealed Al/InP replotted according to Eq. (6) to test for tunneling. Data are at (top to bottom) 359, 300, 220, 147, and 84K.

7. High temperature slopes, S, from Fig. 5, plotted according to Eq. (8). This treats the laser-annealed Al/InP contact as an MIS analog. Thickness of interfacial trap layer can be estimated from the slope, and barrier height from the intercept.

8. Electronic structure of laser-annealed Al/InP interface showing an interfacial layer of acceptor-like electron traps (neutral when empty) at $E_a$ = 0.10eV below $E_C$. Dashed part of conduction band signifies possible tunneling or barrier-lowering region. Strong change in $E_C$-$E_F$ between high (a) and low (b) temperatures results in a weak temperature dependence for effective barrier $\phi_{BO}$ if true barrier $\phi_O$ remains constant.

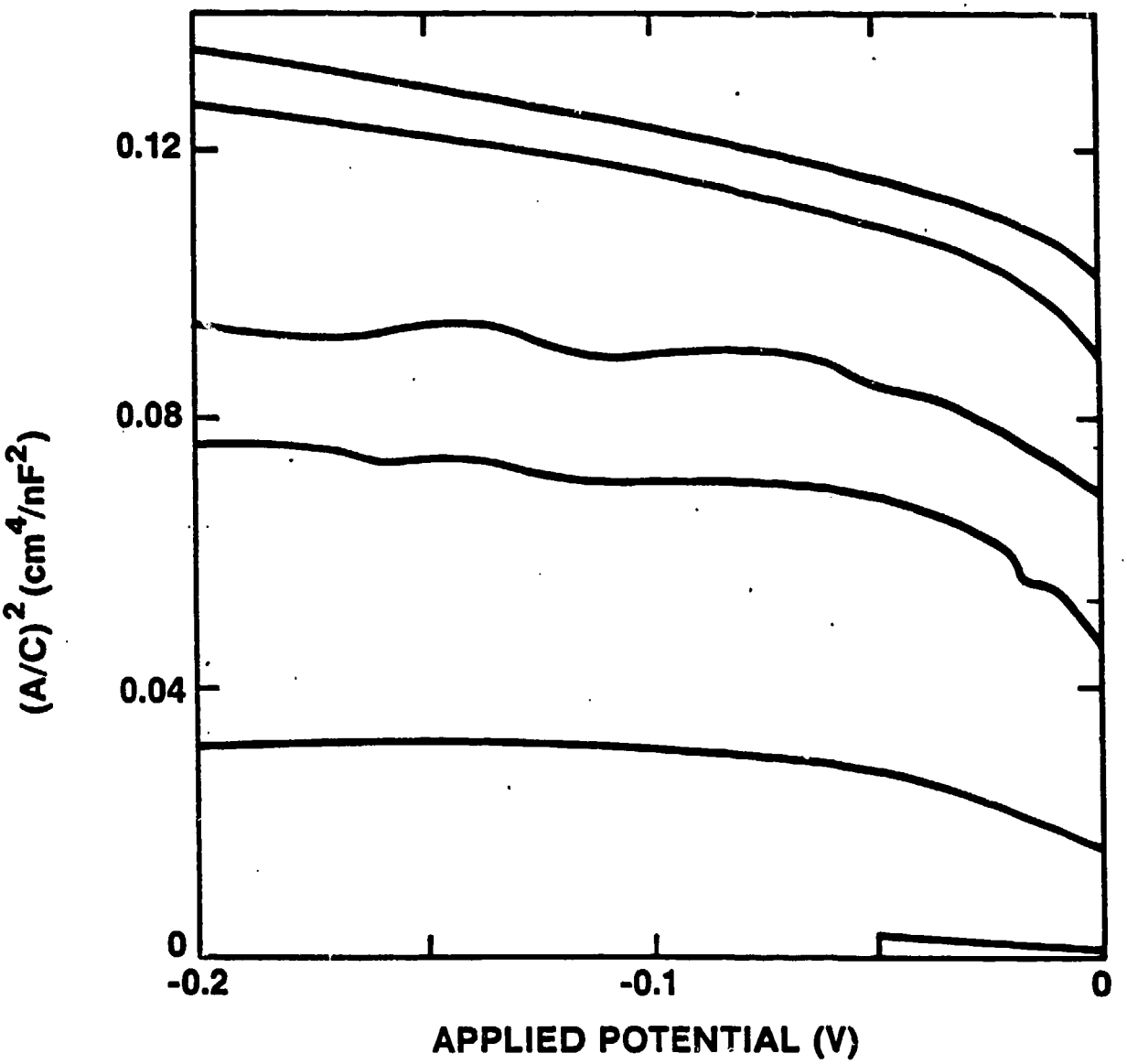


Figure 1.

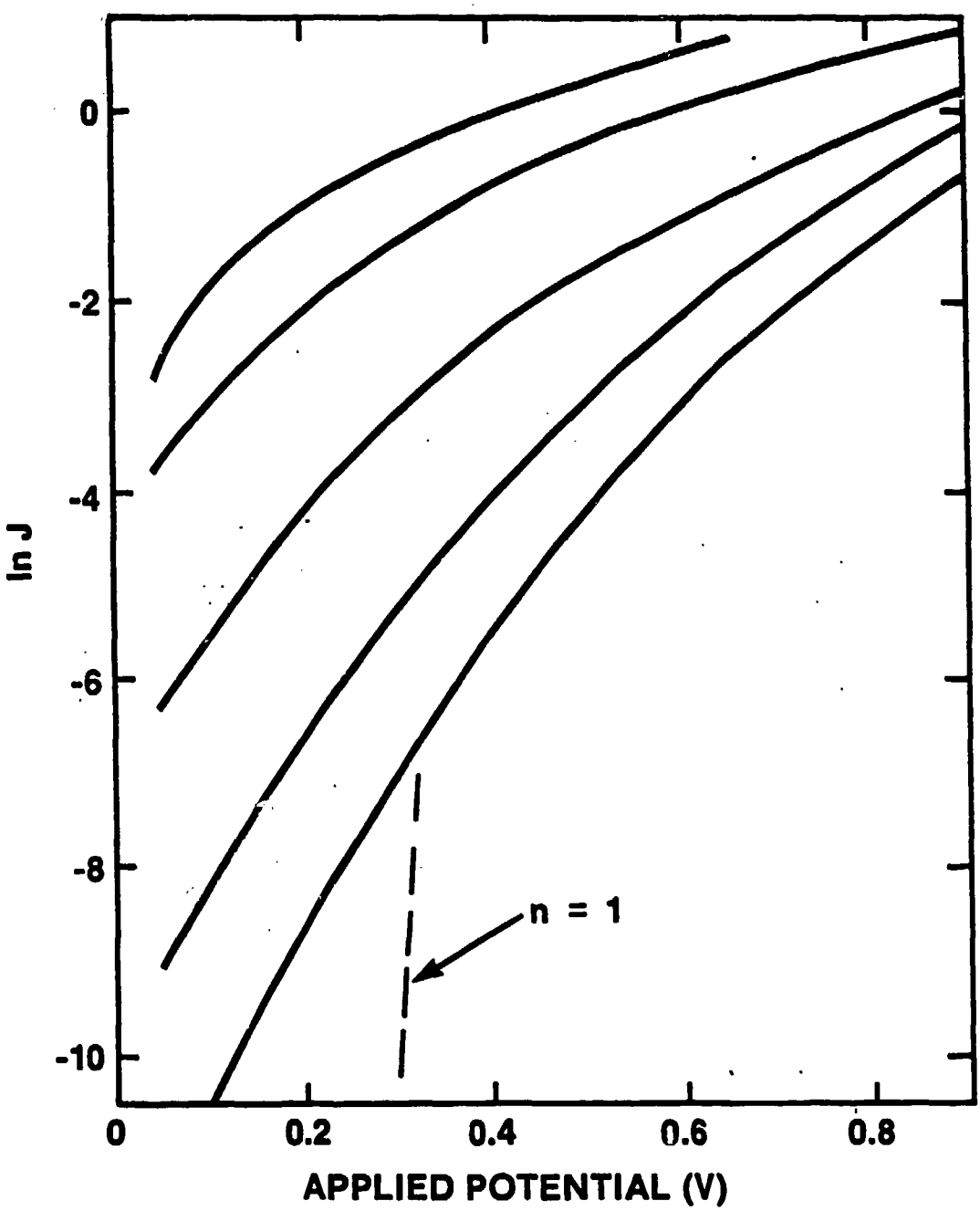


Figure 2.

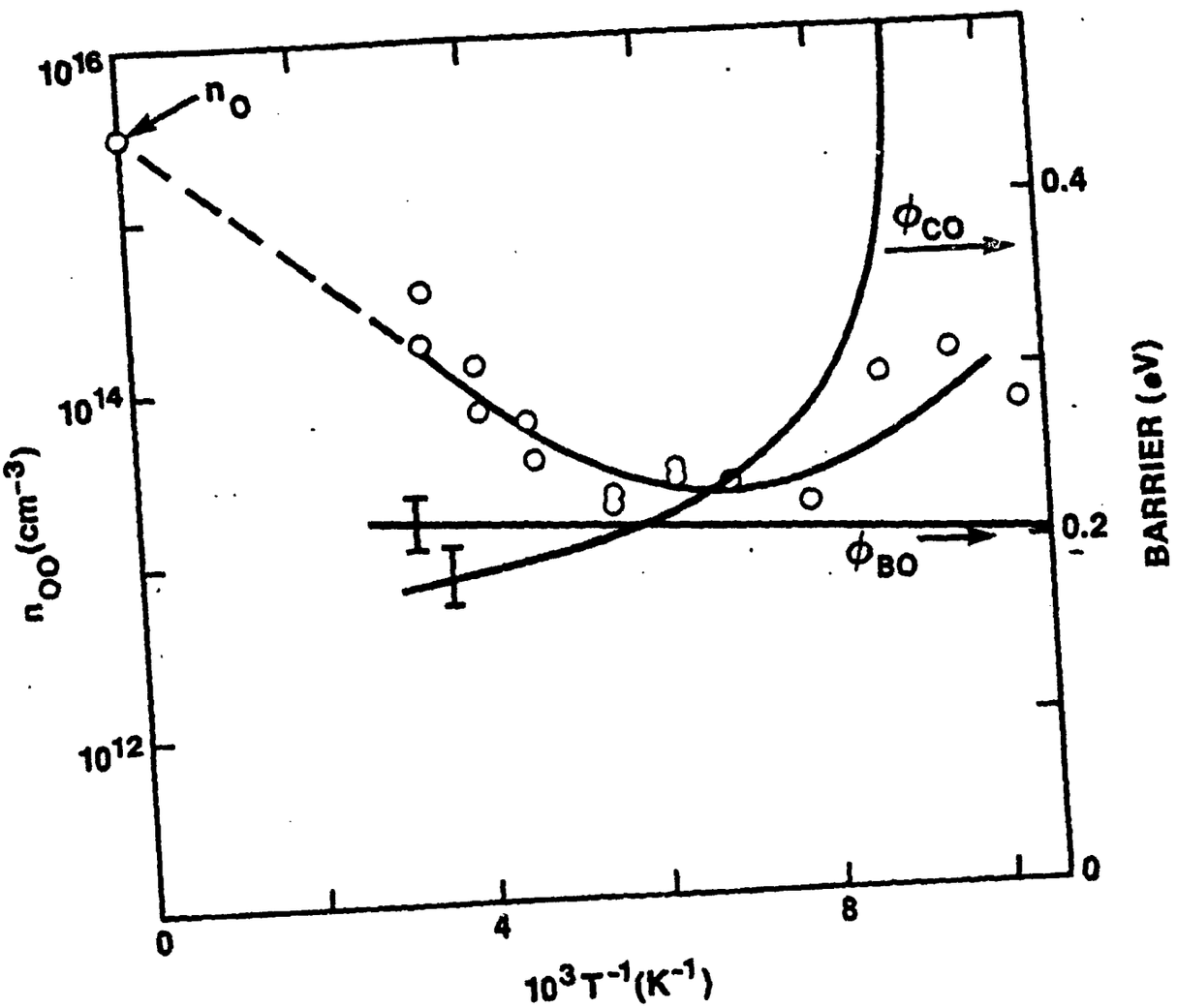
$10^{16}$
$n_o$
$10^{14}$
$10^{12}$
$n_{oo}(cm^{-3})$
0.4
$\phi_{co}$
0.2
$\phi_{BO}$
BARRIER (eV)
0
0
4
8
$10^3 T^{-1}(K^{-1})$

Figure 3.

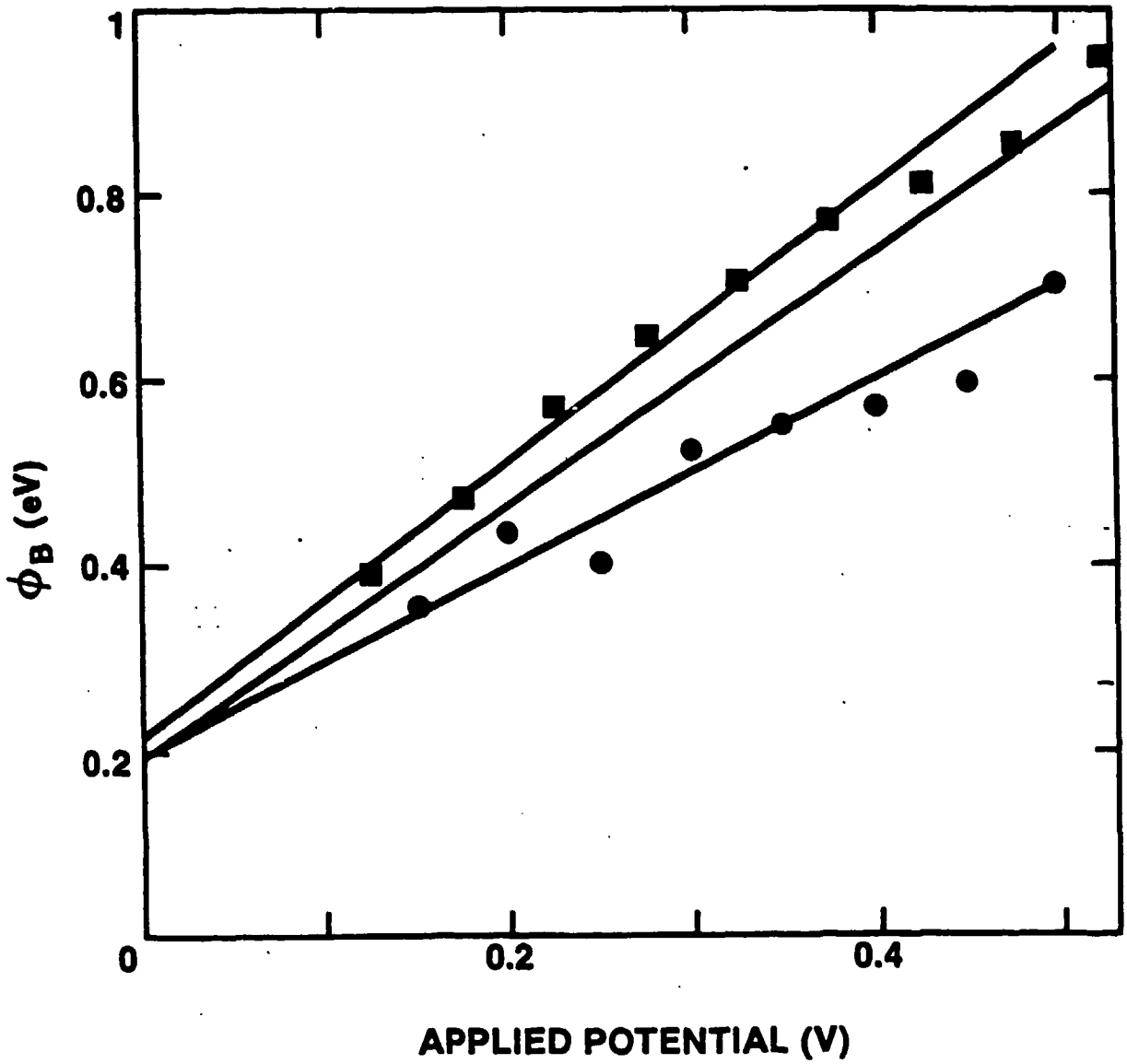


Figure 4.

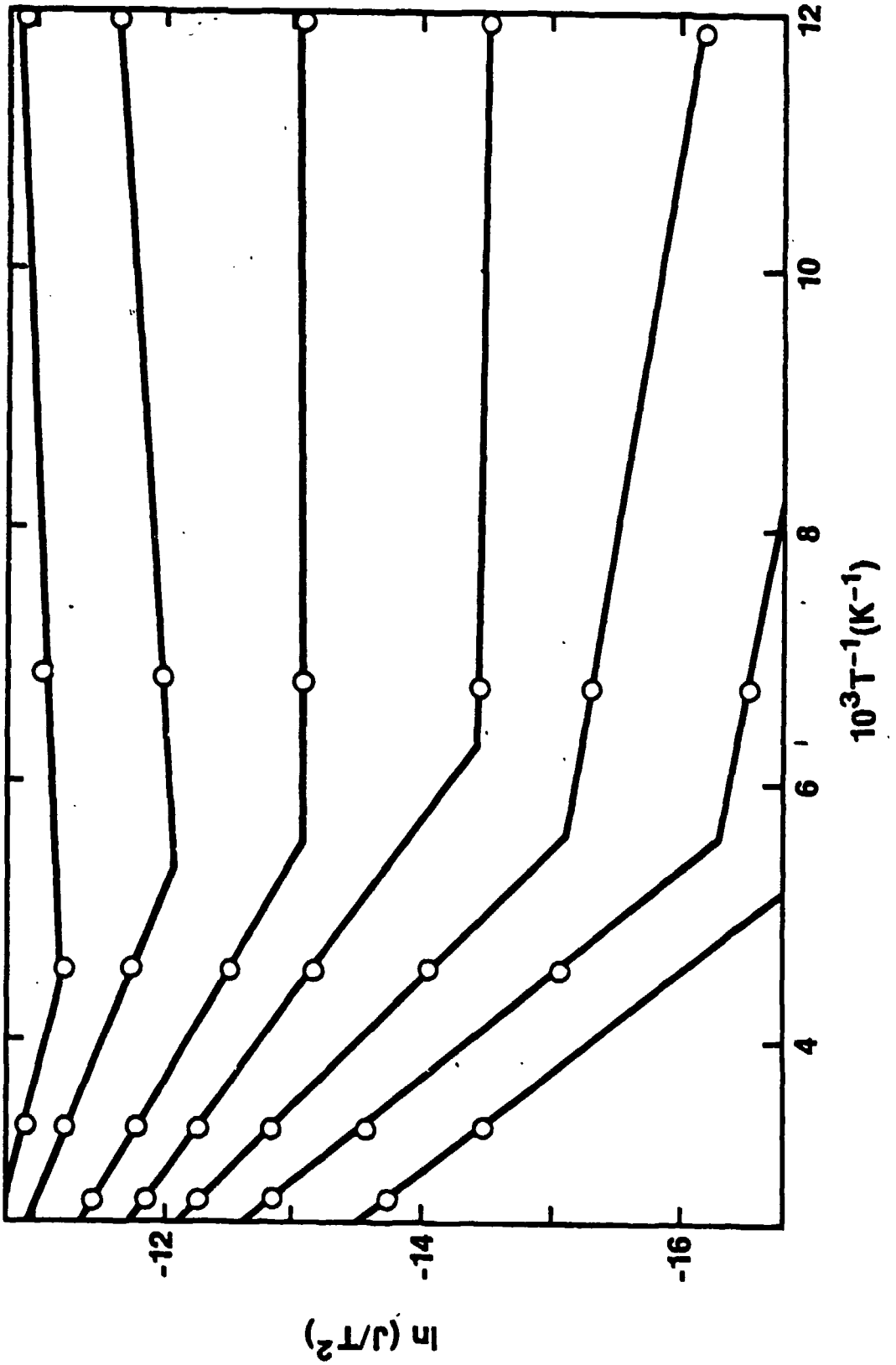


Figure 5.

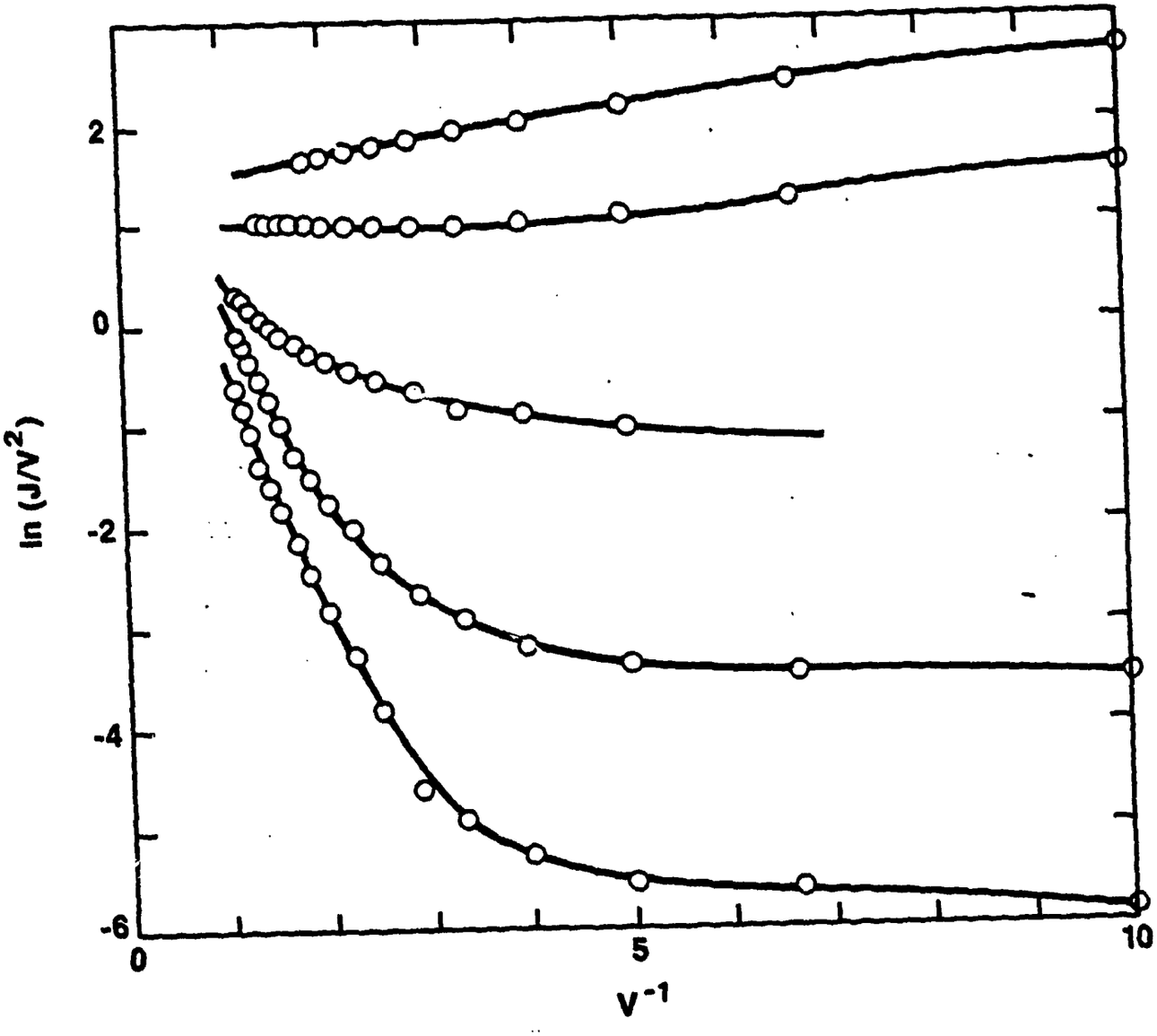


Figure 6.

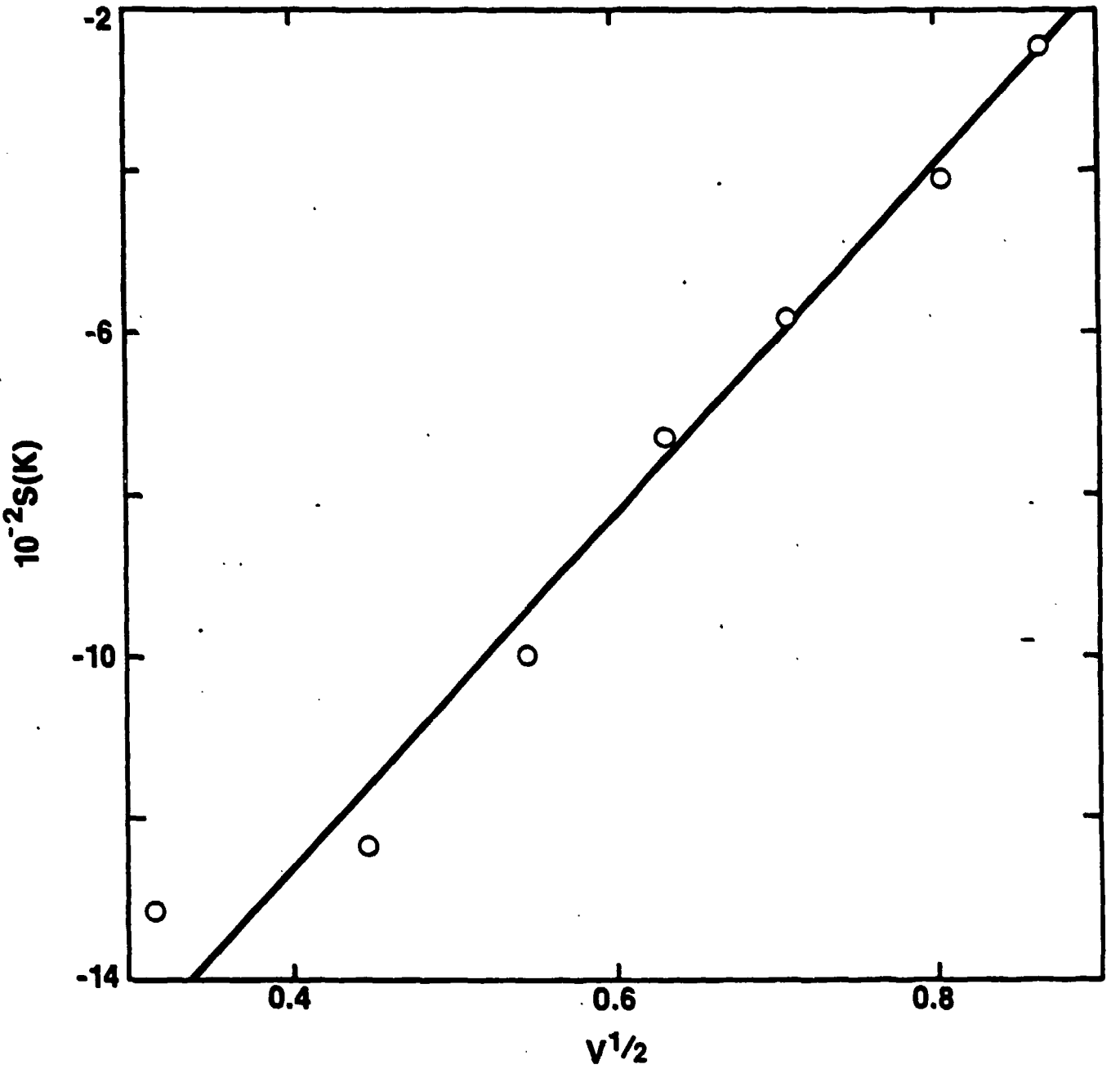


Figure 7.

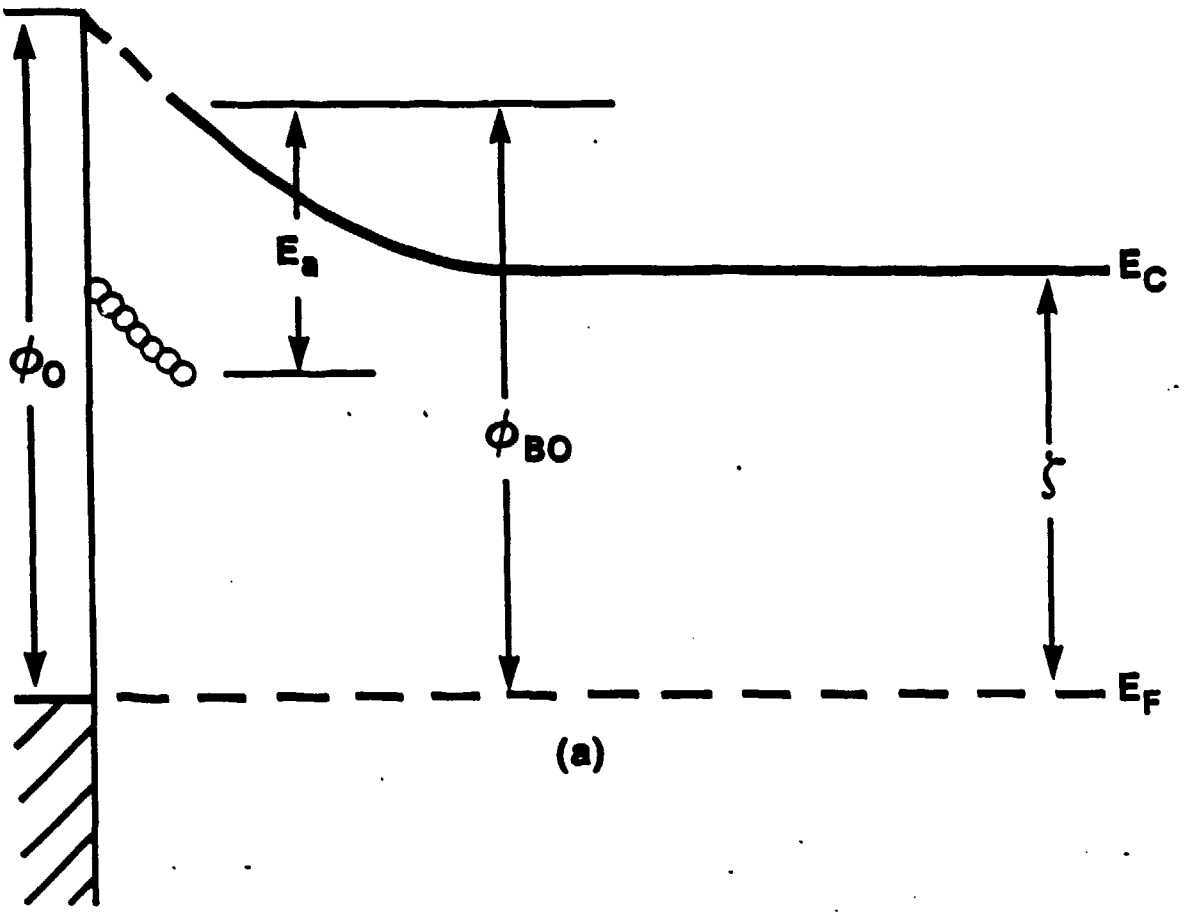


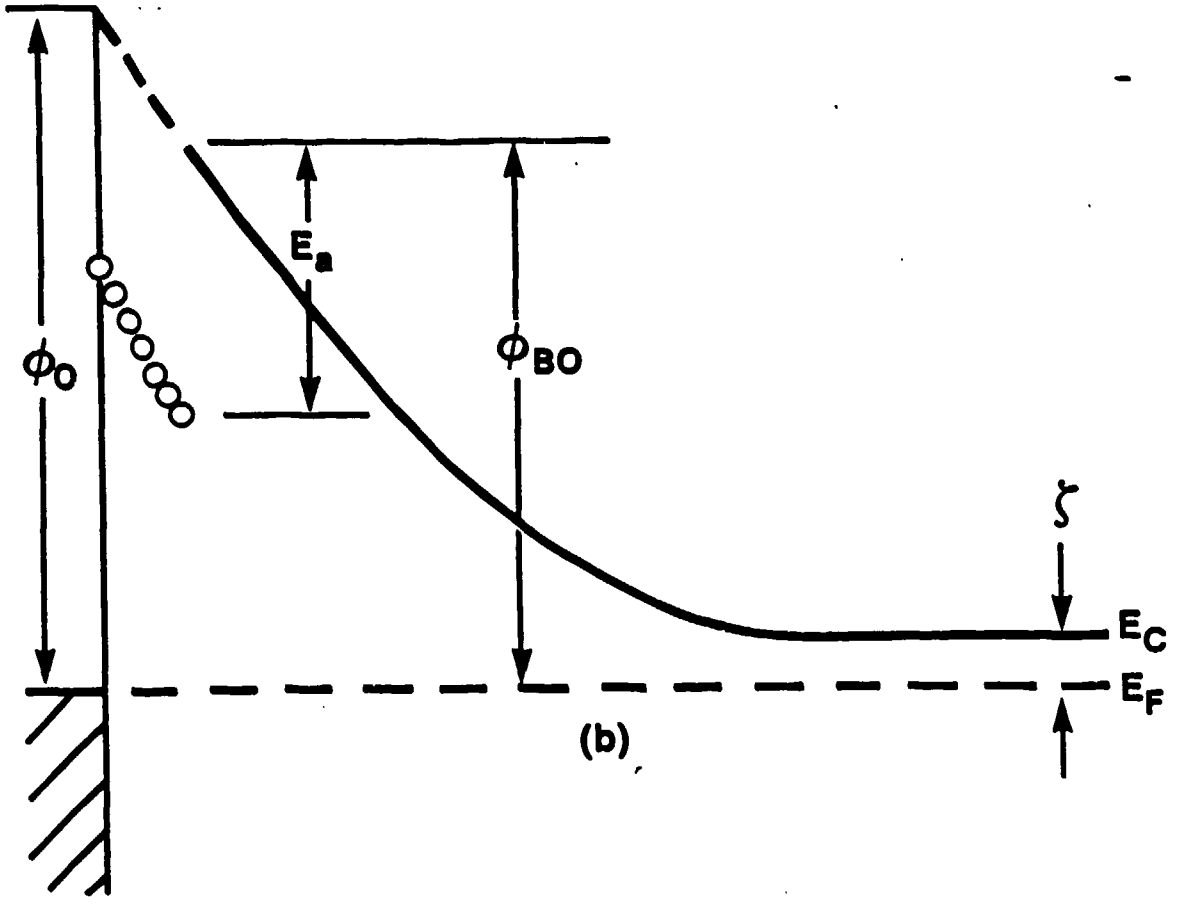


Figure 8.

# Fermi Level Pinning and Chemical Interactions at Metal - $In_xGa_{1-x}As$ (100) Interfaces

L.J. Brillson, M.L. Slade, and R.E. Viturro
Xerox Webster Research Center, Webster, N.Y. 14580.

M.K. Kelly, N. Tache, and G. Margaritondo
Physics Dept., University of Wisconson-Madison, WI 53706.

J.M. Woodall, P.D. Kirchner, G.D. Pettit, and S.L. Wright
IBM Thomas J. Watson Research Center, Yorktown Heights, N. Y. 10598.

## ABSTRACT

Soft X-ray photoemission spectroscopy (SXPS) measurements of metals on clean, ordered $In_xGa_{1-x}As$ (100) surfaces reveal that Fermi level stabilization energies depend strongly on the particular metal - i.e., the Fermi level is not pinned. For $In_xGa_{1-x}As$, $x > 0$, the range of Fermi level movement is comparable to or greater than the semiconductor band gap. For the same metal on different alloys, we observe regular trends in stabilization energies. The trend for Au is strikingly different from previous, air-exposed values. Our results rule out Schottky barrier models based on simple native defects, metal-induced gap states, or the "common-anion" rule. Observed variations in semiconductor outdiffusion provide a chemically-modified interface work function model which accounts for the data across the alloy series.

## 1. Introduction

The mechanisms by which Schottky barriers form at metal / III-V compound semiconductor interfaces has been of considerable interest over the past two decades because of the apparently weak dependence of the band bending on different metal contacts.[1,2,3] This insensitivity presents serious difficulties to the designer of GaAs-based high-speed and opto-electronic devices.[4] Historically, fundamental studies of Schottky barrier formation on III-V compounds have been directed primarily at GaAs and its (110) cleavage face in particular. In this case, the energy at which the surface Fermi-level $E_F$ stabilizes appear to be relatively insensitive to the chemical nature of the metal contact or to ambient contamination, falling into a range of only a few tenths of eV near the center of the GaAs band gap.[5,6] To account for this "pinning" behavior, researchers have proposed a variety of microscopic models, including gap states due to defects formed by metal atom condensation[7], metal-induced gap states defined by the semiconductor band structure[8] or by chemisorption and change transfer involving metal atoms and clusters,[9] chemically-formed dipole layers,[10] and effective work functions of interface alloys involving As precipitates.[11,12] Studies of InP (110)[13,14] and GaAs (100)[13] suggest that a somewhat wider range of $E_F$ gap positions are possible. Nevertheless, it is not yet clear whether the nature of the metal contact has a major or minor influence for the III-V compounds in general.

The electrical behavior of the ternary alloy series $In_xGa_{1-x}As$ has until now used to support a defect pinning model of Schottky barrier formation with a narrow range of $E_F$ stabilization energies.[16-20] The data is based upon capacitance versus voltage (C-V) measurements on Schottky barrier diodes[21] and gate-controlled galvanometric

measurements on metal-insulator-semiconductor (MIS) capacitor and transistor test structures.[22] The metal-semiconductor experiments were performed on air exposed, etched $In_xGa_{1-x}As$ (100) surfaces with Au contacts.[21] These data have been used to support theoretical calculations of anion vacancies[17], antisite (cation replacing anion) defects[18,19], and cation dangling bonds[20] as the cause of the $E_F$ "pinning".

In this paper, we report on the initial stages of Schottky barrier formation for metal deposition on clean, ordered surfaces of $In_xGa_{1-x}As$ under ultrahigh vacuum (UHV) conditions. Soft X-ray photoemission spectroscopy (SXPS) measurements of rigid shifts in core level spectra demonstrate that the surface $E_F$ stabilizes at energies which depend strongly on the particular metal. For $x>0$, the range of $E_F$ movement and the resultant band bending is comparable to or greater than the semiconductor band gap. For the same metal on different alloys, we observe regular trends in $E_F$ position with respect to the conduction and valence band edges. The major influence of the metal overlayer on $E_F$ position and the specific trends across the alloy series rule out Schottky barrier models based on simple vacancy or antisite defects as well as the "common-anion rule" of III-V barrier formation. Instead, SXPS measurements of semiconductor outdiffusion reveal significant changes in near-interface composition between different metal-semiconductor systems and suggest that chemical modification of the interface leads to a range of metal-alloy compositions whose work functions determine the barrier formation.

## 2. Experimental

The study of clean, ordered GaInAs surfaces is complicated by the absence of bulk single crystals for cleaving in UHV. We circumvented this problem by growing

thick films by molecular beam epitaxy (MBE), then "capping" the freshly grown film with several thousand monolayers of As. In all cases reported here, $In_xGa_{1-x}As$ layers 7500 Å thick ($n=5x10^{16}$ Si/cm$^3$) were grown over 2000 Å $In_xGa_{1-x}As$ ($n=10^{19}$/cm$^3$) and on top of 1000 Å GaAs ($n=10^{19}$/cm$^3$) and an $n^+$ GaAs (100) substrate. This multilayer film structure yielded an unstrained $In_xGa_{1-x}As$ (100) outer film and an Ohmic contact through the degenerately-doped base layers and substrate. By desorbing the As "cap" under high vacuum conditions,[23] we obtain a clean and ordered (1x1) surface as determined from valence band photoemission spectroscopy and low energy electron diffraction (LEED) respectively. Even though the resultant surface is likely to be As-stabilized,[24] a comparison of surface versus bulk-sensitive SXPS core level intensities revealed no apparent excess of surface As. For example, As 3d/Ga3d core level intensity ratios were compared for photoelectron kinetic energies of 50-100 eV (surface-sensitive[26]) versus 10-20 eV (bulk-sensitive) using appropriate excitation energies. They showed no systematic deviations with depth sensitivity.

The energies of SXPS spectral features appear reproducibly from surface to surface of the same alloy concentration and the energies vary systematically with different compositions across the alloy series. For each alloy composition, the SXPS core level peaks and valence band edge are reproducible to within ±0.05 eV and ±0.15 eV respectively. Assuming the same $E_F$ position with respect to the band edges for each clean alloy (for $n=5x10^{16}$/cm$^3$, $E_c$-$E_F$ ~ 0.1 eV), the SXPS valence band edges exhibit the correct decrease in band gap with increasing In composition to within ±0.17 eV. A valence band spectrum of a thick (220 Å) Au film deposited on InAs established the initial $E_F$ position of clean InAs to be $E_c$-$E_F$=0.1 eV. Metal evaporation took place in a UHV chamber (base pressure $P=8x10^{-11}$ torr) from W

filaments with a pressure rise no higher than mid-$10^{-9}$ torr. A quartz crystal oscillater monitored the thin film depostions.

3. Results

We have measured the SXPS peak energies and intensities for the Ga3d, In4d, and As3d core levels as a function of Au, In, Al, and Ge deposition on $In_xGa_{1-x}As$ (100) surfaces, where $x=0$, 0.25, 0.50, 0.75, and 1.00. We obtained bulk-sensitive spectra in order to monitor core level shifts while minimizing lineshape changes due to chemical bonding effects near the surface. In this case, we used $h\nu=40$ eV for the Ga3d and In4d spectra and $h\nu=60$ eV for the As3d spectra in order to produce photoelectrons in the 10-20 eV kinetic energy range. Figure 1 illustrates these core level shifts for Au deposition on clean $In_{0.5}Ga_{0.5}As$. The rigid shift to higher kinetic energy corresponds to an $E_F$ movement of 0.3 eV toward the valence band maximum $E_V$. In general the sharp In4d and Ga3d peak features provide a clearer indication of $E_F$ movement than the As3d feature. In many cases such as that of Fig. 1, the As3d peak feature becomes distorted by multiple components with different chemical bonding, even for the bulk-sensitive spectra. We also obtained surface-sensitive spectra in order to monitor outdiffusion of dissociated semiconductor species as well as chemical bonding changes of the metal adsorbates. Here, we used $h\nu=80$ eV for the Ga3d and In4d spectra and $h\nu=100$ eV for the As3d spectra in order to obtain photoelectrons in the 50-60 eV kinetic energy range. Integrated peak areas for the semiconductor constituents at the free metal surface provide a measure of the change in stoichiometry at the metal-semiconductor interface. Lineshape changes also reveal the presence of dissociated species. Thus, for Au on $In_{0.5}Ga_{0.5}As$, surface-sensitive spectra (not shown) display a dissociated As3d feature displaced to higher binding energy, corresponding to As outdiffusion. In general,

core level shifts In4d and Ga3d peak for substrate features in the surface-sensitive spectra were in agreement with those of the corresponding bulk-sensitive spectra.

The $E_F$ movements induced by metal deposition on $In_xGa_{1-x}As$ (100) indicate a wide range of Schottky barrier positions for each of the In alloys. Figure 2 illustrates the different $E_F$ behavior produced by Au, Al, and In deposition on $In_{.25}Ga_{.75}As$ (100). Each metal exhibits a different $E_F$ movement with increasing metal coverage. The thickness over which each curve approaches an asymptotic value is in all cases more than one or two monolayers. Differences in the rate, sign, and magnitude of $E_F$ movement are apparent, indicative of differences in the chemical interaction between metal and semiconductor. At 20 Å metal coverage, the final $E_F$ positions extend from 0.25 eV above $E_c$ to 0.42 eV below $E_c$ - an energy range of 0.67 eV compared to the band gap of 1.05 eV.[26]

Differences between metals are even more apparent for $E_F$ movement on clean InAs (100) surfaces, as shown in Fig. 3. At 20 Å metal coverage, the final $E_F$ positions extend from 0.1 eV above $E_c$ to 0.14 eV below $E_v$ - a range of 0.6 eV compared to the InAs band gap of 0.36 eV.[26] Furthermore, the $E_F$ stabilization positions for Al, In, Ge, and Au appear to be distributed in energy, rather than clustered around particular positions. Analogous plots for other alloy semiconductors yield ranges of 0.85 eV for $In_{.75}Ga_{.25}As$ ($E_g$=0.53 eV) and 0.65 eV for $In_{.50}Ga_{.50}As$ ($E_g$=0.76 eV). For GaAs, we studied only Au and In overlayers on GaAs (100), which yielded a range of ~0.4 eV ($E_g$=1.43 eV). Thus, moving away from GaAs, one obtains larger ranges of $E_F$ movement which are comparable to or larger than the semiconductor band gap.

The $E_F$ stabilization energies obtained by SXPS show large differences for clean $In_xGa_{1-x}As$ (100) surfaces with and without subsequent air exposure. For this comparison, we exposed thermally-cleaned InGaAs (100) surfaces to 50 torr air (10 torr $O_2$) for 100 sec in a stainless steel reaction chamber attached to the UHV analysis chamber. No hot filaments were present. For the same initially clean InAs (100) surface, Fig. 4a illustrates a striking difference in $E_F$ behavior between air-exposed versus clean cases with Au deposition. The immediate effect of air exposure is to move $E_F$ up into the conduction band. Whereas $E_F$ for the clean surface moves down into the valence band, $E_F$ for the air-exposed surface remains near the conduction band edge. Figure 4b provides an example for which air exposure produces the opposite shift with respect to the clean interface. Here initial air exposure shifts $E_F$ down into the band gap where it remains with In deposition. In contrast, $E_F$ for the clean surface rises into the conduction band with In coverage. Significantly, the $E_F$ positions for the two air-exposed cases shown in Fig. 4 are in agreement with the electrical data of Kayiyama,[21] which were based on air-exposed material.

## 4. Discussion

The $E_F$ stabilization energies for Au, Al, In, and Ge on clean $In_xGa_{1-x}As$ (100), $0 \leq x \leq 1$ surfaces provide sufficient data to evaluate the applicability of various Schottky barrier models. In Fig. 5, the energy levels for the entire InGaAs alloy series are plotted relative to the GaAs valence band maximum (left-hand scale) and to the vacuum level (right-hand scale). The valence band edges of InAs and GaAs are determined from photoemission threshold measurements of van Laar et al.[27] (e.g., 5.42 eV for InAs and 5.56 eV for GaAs). The small difference $\Delta E_v$ between the two alloy extrema allow us to approximate $E_V$ at intermidiate alloy compostiions by a linear ramp. On the other hand, the compositional dependence of the lowest energy

direct gaps measured by electroreflectance[26] indicates a distinct bowing, which is indicated in Fig. 5 by the curvature of the conduction band edge. The data points are in reasonable agreement with what little results have been measured previously for clean metal-$In_xGa_{1-x}As$ interfaces. For Au on GaAs (100), Grant et al. measured $E_c$-$E_F$=0.75 eV (0.75 eV in Fig. 5) as well as a range of $E_c$-$E_F$ energies ranging from 0.75 eV to 0.2 eV with surface treatment.[15] For In on GaAs (100), the high position ($E_c$-$E_F$=0.35 eV) relative to that of Au agrees with SXPS work of Daniels et al.[28] for cleaved GaAs (110) (e.g., 0.4 versus 0.9 eV[7]). Schottky barrier height data for MBE-grown Al on n-$In_5Ga_5As$ (100) also support the SXPS results, exhibiting Ohmic behavior[29] (e.g., $E_c$-$E_F$ < 0).

The first conclusion reached upon inspection of the wide $E_F$ ranges in Fig. 5 is that $E_F$ is not "pinned". These large energy differences with metals invalidate models based on pinning in a narrow energy range, where the effect of the metal is secondary. Included are the Unified Defect model involving high densities of closely-spaced defect energy levels[7] and metal-induced state "pinning" at a mid-gap position defined primarily by the semiconductor band structure.[8] In fact, the metal-induced gap state model leads to a large error for the Au-InAs $E_F$ position,[8] even after taking the metal electronegativity and band structure effects (i.e., spin-orbit splitting, in direct gaps) into account. It should be emphasized that the $E_F$ ranges for each semiconductor composition in Fig. 5 are internally consistent. They each involve clean surfaces of the same material with the same starting position for $E_F$ with respect to the band edges.

For a given metal on different alloy semiconductors, the $E_F$ stabilization positions follow regular trends as indicated by the fitted curves in Fig. 5. Besides exhibiting a

sizable variation in energy, each curve appears to parallel the conduction band, especially In and Al. These movements are contrary to theoretical calculations of native defects reported thus far. Simple vacancies,[17] anion-on-cation antisite defects[18,19], and cation dangling bonds[20] all display trends which parallel the valence rather than the conduction band and which lie above the conduction band for $x_{In}<0.5$. Within a localized state model, the conduction band trends may be consistent only with cation-derived bulk states. The strong variation of $E_F$ with respect to the valence band both for the same metal with different alloys and for different metals on the same alloy argues conclusively against a "common-anion rule".[30] In this model, the same $E_F$-$E_v$ would have to appear for all III-V compounds with the same anion. Finally, the conduction band trends in Fig. 5 do not support an anion work function dominated, for example, by As precipitates. In this case, $E_F$ energies would also be at constant energies below the vacuum level.

One possible explanation of our data invokes defect levels which are widely spaced and of variable density.[23,31] Studies of $Ga_{.47}In_{.53}As$ MIS structures suggest that the densities of any interface states on dielectric-coated GaInAs surfaces are relatively low and are further reduced by thermal annealing.[22,32,33] The observed $E_F$ excursions in C-V and field-effect-controlled galvanomagnetic measurements are interpreted in terms of the position and density of donor and acceptor levels near the interface.

Without involving localized interface states, it is possible to account for the observed $E_F$ stabilization energies in terms of differences in overlayer work function due to changes in interface chemical composition. SXPS core level intensities provide a measure of the relative composition of outdiffusion species to the free metal surface

and, by extension, a measure of the stoichiometry at the metal-semiconductor interface. For Au on $In_xGa_{1-x}As$ (100) and increasing $x_{In}$, the SXPS spectra indicate an increasing proportion of dissociated As, i.e., a trend from an As-rich to an As-deficient interface.[23] Assuming that the interface work function varies from $\varphi_{AS}$ ~ 4.8[12] eV to $\varphi_{AS}$ = 5.2-5.4 eV[34] under these conditions, the resultant trend agrees with the Au data points in Fig. 5 both in range and in absolute values. For In on $In_xGa_{1-x}As$ (100), we observe a chemical trend from a As-deficient to an As-rich interface with increasing $x_{In}$.[23] These values agree with the In points in Fig. 5 in range, although their absolute values appear to be 0.1-0.2 eV too low. The In-GaAs (100) point may deviate from the otherwise near-linear trend in part because of the absence of lower-$\varphi$ In versus Ga at the interface.[34] For Al on $In_xGa_{1-x}As$ (100), As accumulation at the interface increases with $x_{In}$[23]. For GaAs, this As may be bound up as reacted AlAs, with a work function different from $\varphi_{As}$. With additional accumulation, the excess As may forms precipitates, thereby dominating the interface work function. Given $\varphi_{Al}$~4.2 eV[34], the variation in local $\varphi$ may then approximate that of In. Hence by using observations of interface chemical compositions and a classical work function model, we are able to account for a large set of interface data on both an absolute and relative scale.

## 5. Conclusions

We have performed (the first) SXPS core level measurements for metals on clean, ordered surfaces of a ternary III-V compound semiconductor $In_xGa_{1-x}As$ (100). We find that the Fermi level exhibits no "pinning" across the entire In alloy series. Air exposure of the clean ternary surfaces prior to metal deposition produces major changes in the subsequent $E_F$ level movements. The wide variations in $E_F$ stabilization energy for different metals on the same semiconductor as well as the

same metal across the alloy series preclude a number of leading Schottky barrier models. Chemically-modified changes in metal-alloy composition rather than interface defect levels appear to be the most straightforward explanation for the barrier formation at $In_xGa_{1-x}As$ (100) - metal interfaces.

## 6. Acknowledgements

We gratefully acknowledge partial support by the Office of Naval Research (ONR N00014-80-C-0778). The Synchrotron Radiation Center is supported by the National Science Foundation. We wish to give particular thanks to the staff of the Aladdin Storage Ring Facility for their outstanding efforts in implementing these experiments.

## REFERENCES


1. C.A. Mead, Solid State Electron. 9, 1023 (1966)

2. S.M. Sze, Physics of Semiconductor Devices, 2nd (Wiley-Interscience, New York, 1981) ch. 5.

3. L.J. Brillson, Surface Sci. Rept. 2, 123 (1982).

4. A.G. Milnes, Semiconductor Devices and Integrated Electronics, (Van Nostrand Reinhold Co., New York, 1980).

5. I. Lindau, P.W. Chye, C.M. Garner, P. Pianetta, C.Y. Su, and W.E. Spicer, J. Vac. Sci. Technol. 15, 1332 (1978).

6. W.E. Spicer, I. Lindau, P. Skeath, C.Y. Su, and P.W. Chye, Phys Rev. Lett. 44, 420 (1980).

7. W.E. Spicer, I. Lindau, P. Skeath, and C.Y. Su, J. Vac Sci. Technol. 17, 1019 (1980).

8. J. Tersoff, Phys. Rev. B32, 6968 (1985); Phys. Rev. Lett., 52, 465 (1984); J. Vac. Sci. Technol. B3, 1157 (1985).

9. R. Ludeke, T.-C. Chiang, and T. Miller, J. Vac. Sci. Technol. B1, 581 (1983).

10. L.J. Brillson, J. Vac. Sci. Technol. 16, 1137 (1979).

11. J.L. Freeouf and J.M. Woodall, Appl. Phys. Lett. 39, 727 (1981).

12. J.M. Woodall and J.L. Freeouf, J. Vac. Sci. Technol. 19, 794 (1981).

13. R.H. Williams, V. Montgomery, and R.R. Varma, J. Phys. Chem. 11, L735 (1978); V. Montgomery, R.H. Williams, and G.P. Srivastava, ibid. 14, L191 (1981).

14. L.J. Brillson, C.F. Brucker, A.D. Katnani, N.G. Stoffel, and G. Margaritondo, Appl. Phys. Lett., 38, 784 (1981); C.F. Brucker and L.J. Brillson, ibid. 39, 67 (1981).

15. R.W. Grant, J.R. Waldrop, S.P. Kowalczyk, and E.A. Kraut, J. Vac. Sci. Technol. 19, 477 (1981).

16. W.E. Spicer and S.J. Eglash, in VLSI Electronics: Microstructure Science, Vol. 10 (Academic, New York 1985) p.79.

17. M.S. Daw and D.L. Smith, Appl. Phys. Lett. 8, 690 (1980).

18. R.E. Allen and J.D. Dow, Phys. Rev. B25, 1423 (1982).

19. R.E. Allan, T.J. Humphreys, J.D. Dow, and O.F. Sankey, J. Vac. Sci. Technol. B2, 449 (1984).

20. O.F. Sankey, R.E. Allen, S.-F. Ren, and J.D. Dow, J. Vac Sci. Technol. B3, 1162 (1985).

21. K. Kajiyama, Y. Mizushima, and S. Sakata, Appl. Phys. Lett. 23, 458 (1973).

22. H.H. Wieder, Appl, Phys. Lett. 38, 170 (1981).

23. L.J. Brillson, M.L. Slade, R.E. Viturro, M. Kelly, N. Tache, G. Margaritondo, J.M. Woodall, P.D. Kirchner, G.D. Pettit, and S.L. Wright, unpublished.

24. R.Z. Bachrach, R.S. Bauer, P. Chiaradia, and G.V. Hansson, J. Vac. Sci. Technol. 18, 797 (1981).

25. M.P. Seah and W.A. Dench, Surface Interface Analysis 1, 2 (1979).

26. E.W. Williams and V. Rehn, Phys. Rev. 172, 798 (1969).

27. J. van Laar, A. Huijser, and T.L. van Rooy, J. Vac. Sci. Technol. 14, 894 (1977).

28. R.R. Daniels, T.-X. Zhao, and G. Margaritondo, J. Vac. Sci. Technol. A2, 831 (1984).

29. K.H. Hsieh, M Hollis, G. Wicks, C.E. Wood, and L.F. Eastman, Inst. Phys. Conf. Ser. 65, 165 (1983).

30. J.O. McCaldin, T.C. McGill, and C.A. Mead, Phys. Rev. Lett. 36, 56 (1976).

31. A. Nedoluha, J. Vac. Sci. Technol. 21, 429 (1982).

32. H.H. Weider, A.R. Clawson, D.I. Elder, and D.A. Collins, IEEE Electron Device Lett. EDL-2, 73 (1981).

33. H.H. Weider, Surface Sci. 132, 390 (1983).

34. H.B. Michaelson, J. Appl. Phys. 48, 4729 (1977) and references therein.

# FIGURE CAPTIONS

1. SXPS core level spectra for As3d at $h\nu = 60$eV and Ga3d and In4d at 40eV as a function of increasing Au deposition. Arrows indicate spin-orbit split components. The rigid core level shifts provide a measure of $E_F$ movement relative to the band edges.

2. Fermi level movements for clean $In_{.25}Ga_{.75}As$ (100) (band gap = 1.05 eV) as a function of Au, In, or Al deposition in ultrahigh vacuum.

3. Fermi level movements for clean InAs (100) (band gap = 0.36 eV) as a function of Au, In, Ge, or Al deposition in ultrahigh vacuum.

4. Fermi level movements for a) clean and air-exposed InAs (100) as a function of Au deposition and b) clean and air-exposed $In_{.5}Ga_{.5}As$ (100) as a function of In deposition. Clean semiconductor surfaces provide the starting point in all cases.

5. Fermi level stabilization energies for Au, In, Ge, and Al deposited on clean $In_xGa_{1-x}As$ (100), $0 \leq x \leq 1$, in ultrahigh vacuum. Left (right)-hand scale is relative to the GaAs valence band maximum (the vacuum level).

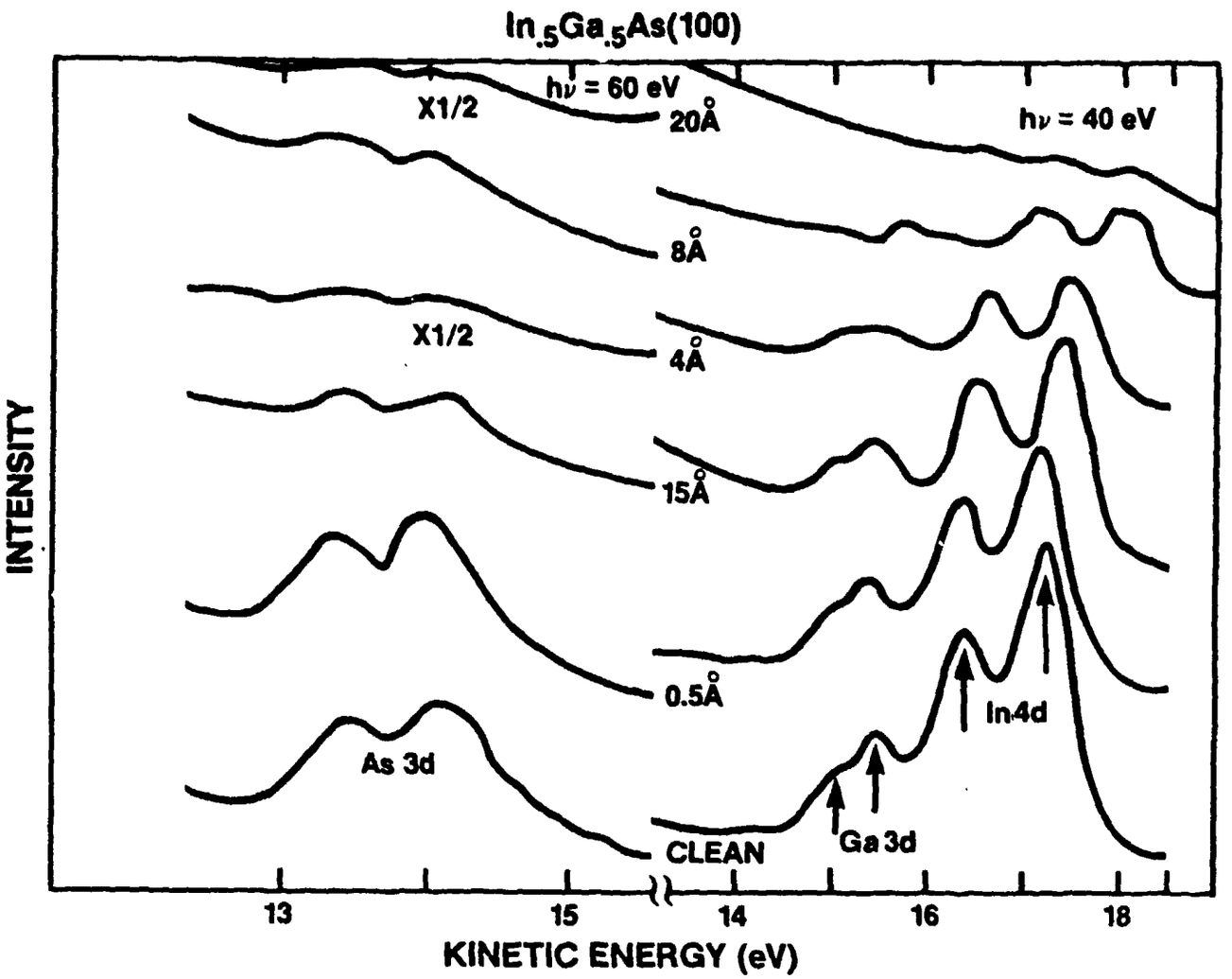
In.5Ga.5As(100)
hν = 60 eV
X1/2
20Å
hν = 40 eV
8Å
X1/2
4Å
15Å
INTENSITY
0.5Å
In4d
As 3d
CLEAN
Ga 3d
13
15
14
16
18
KINETIC ENERGY (eV)

Fig. 1

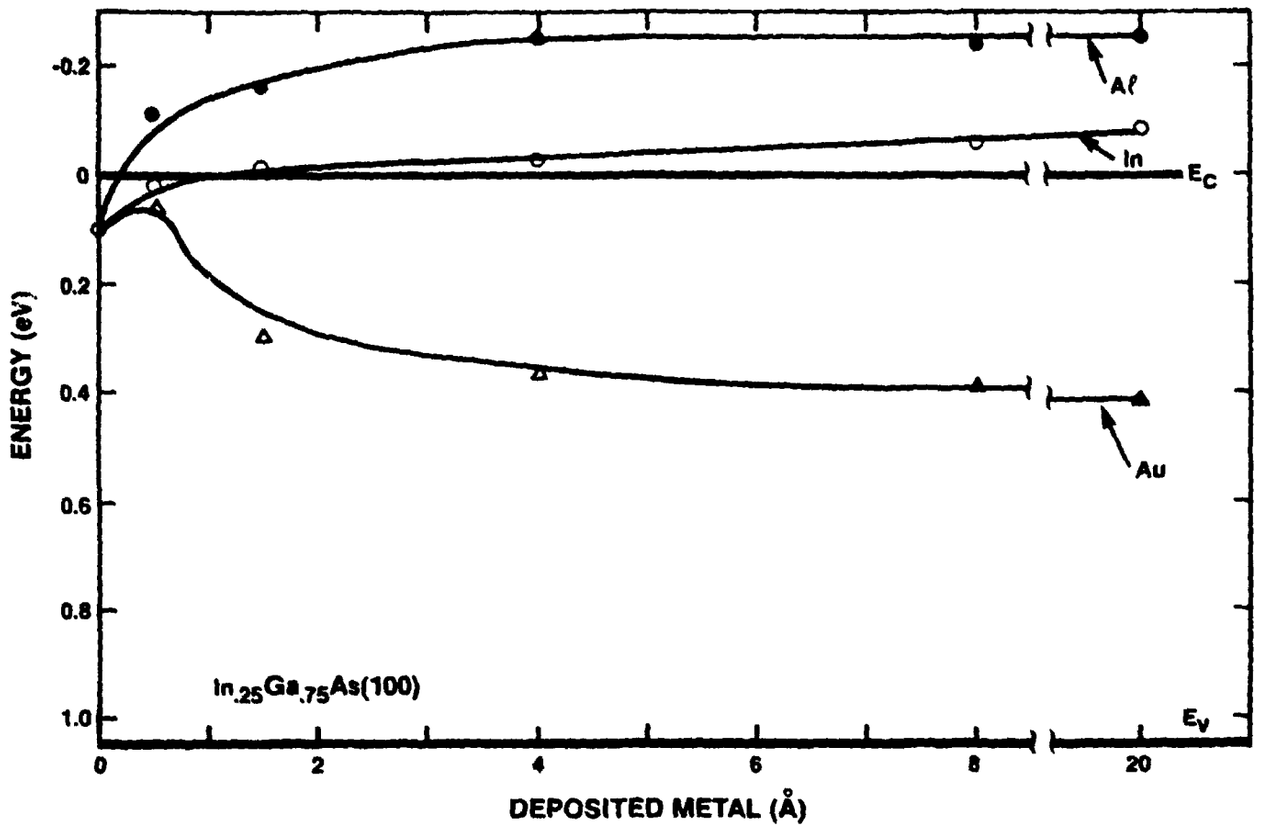
-0.2
0
0.2
0.4
0.6
0.8
1.0
ENERGY (eV)
Al
In
$E_C$
Au
$E_V$
$In_{.25}Ga_{.75}As(100)$
0
2
4
6
8
20
DEPOSITED METAL (Å)

Fig. 2

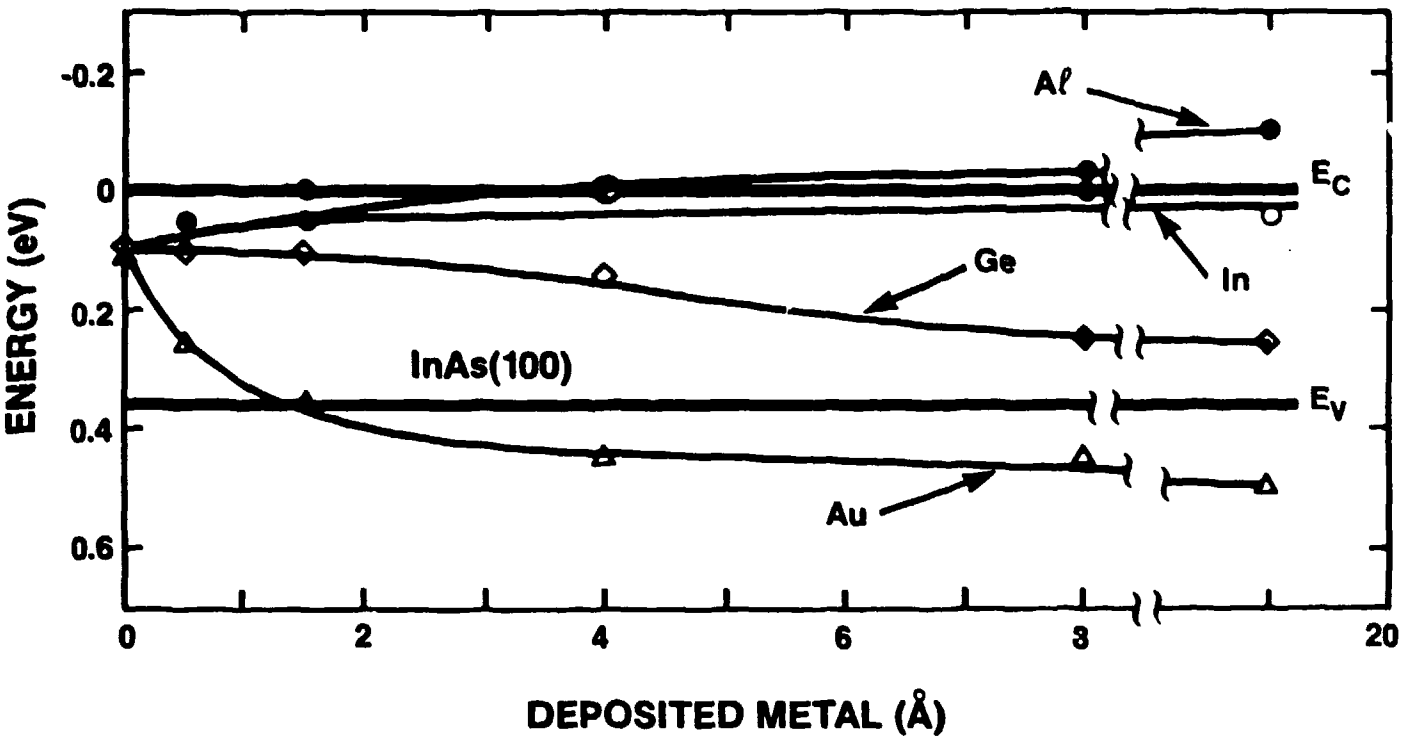
-0.2
0
0.2
0.4
0.6
ENERGY (eV)
Aℓ
$E_C$
In
Ge
InAs(100)
$E_V$
Au
0
2
4
6
3
20
DEPOSITED METAL (Å)

Fig. 3

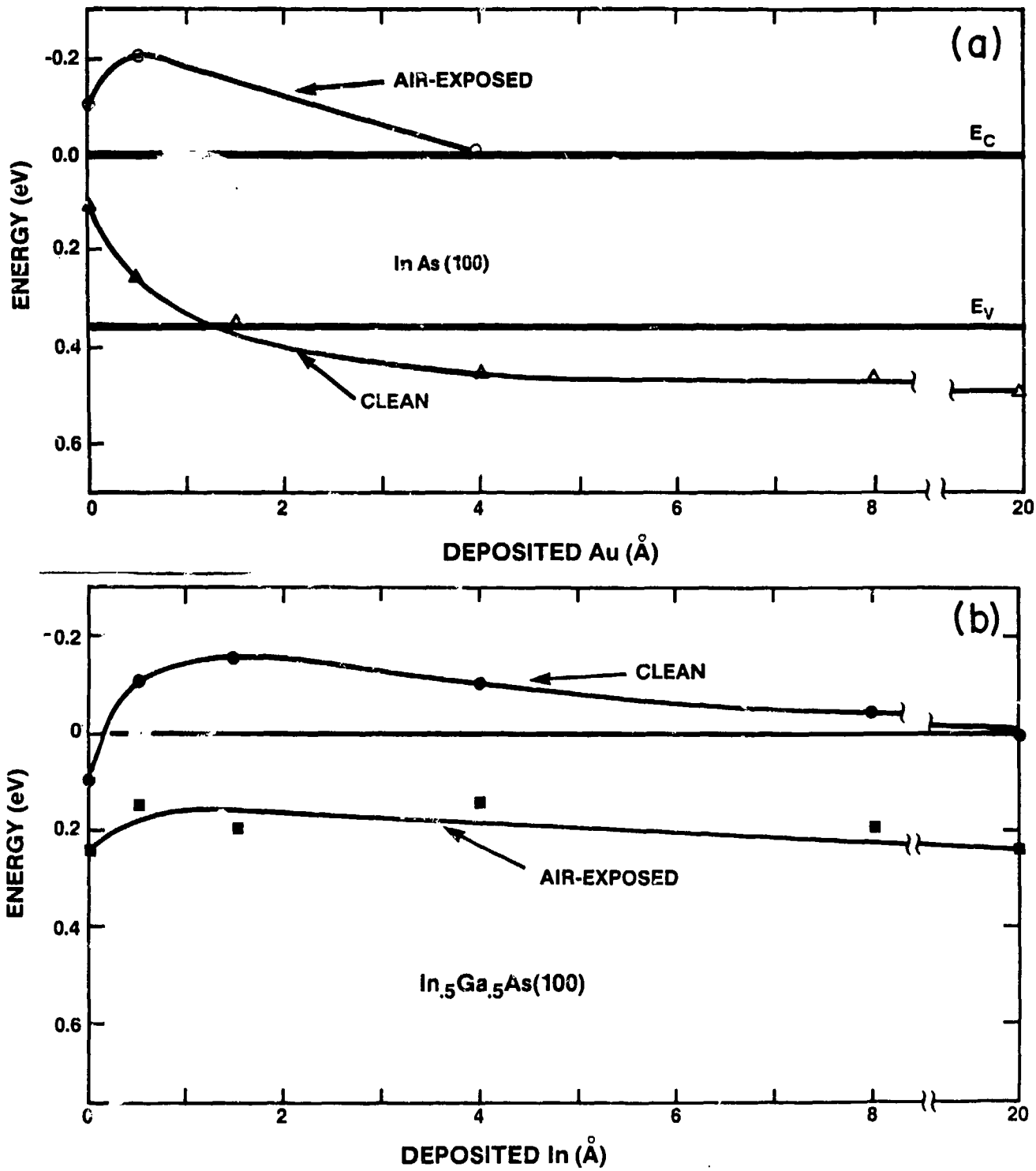
(a)
AIR-EXPOSED
$E_C$
$E_V$
In As (100)
CLEAN
ENERGY (eV)
-0.2
0.0
0.2
0.4
0.6
0
2
4
6
8
20
DEPOSITED Au (Å)
(b)
CLEAN
AIR-EXPOSED
$In_{.5}Ga_{.5}As(100)$
ENERGY (eV)
-0.2
0
0.2
0.4
0.6
0
2
4
6
8
20
DEPOSITED In (Å)

Fig. 4

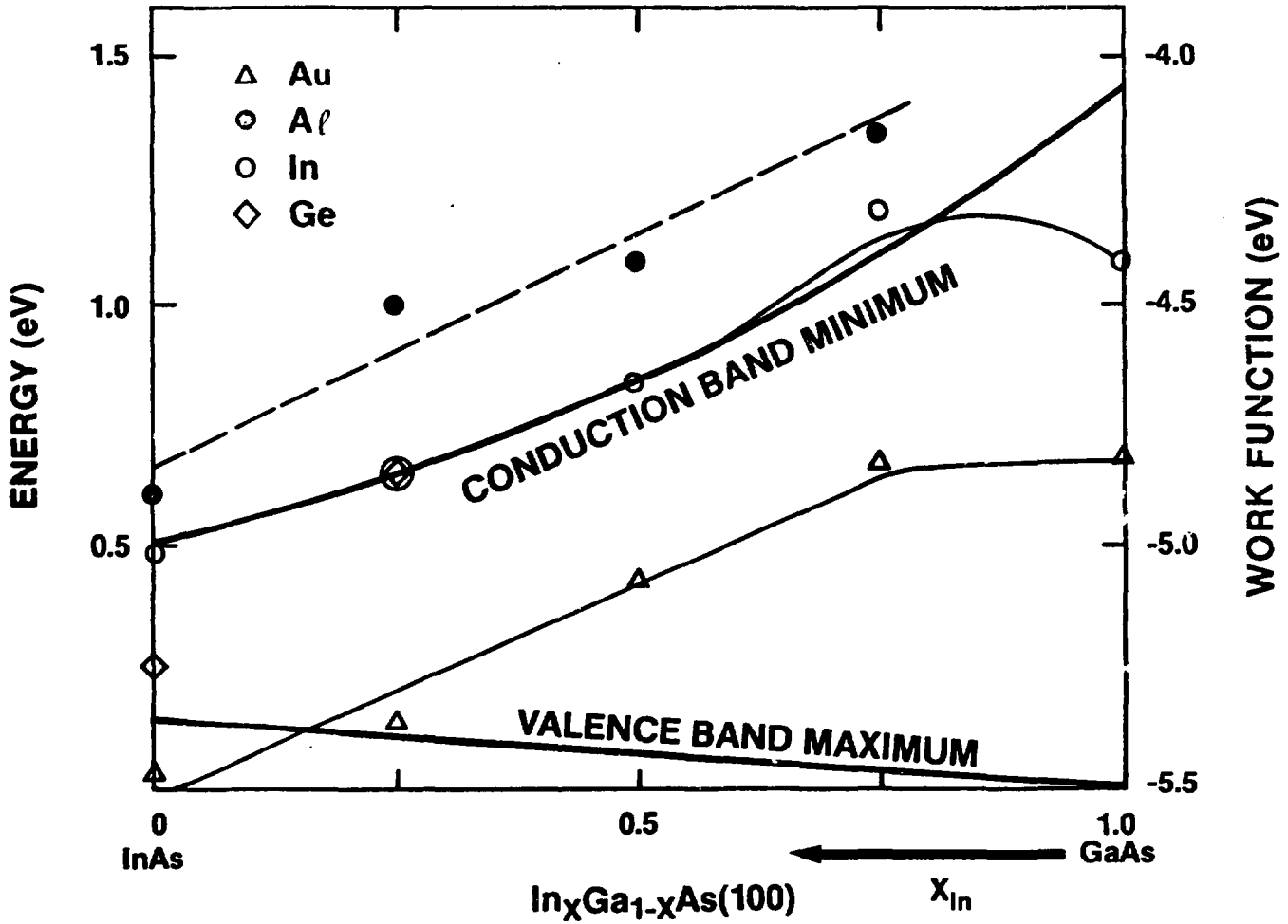
1.5
1.0
0.5
ENERGY (eV)
Au
Aℓ
In
Ge
CONDUCTION BAND MINIMUM
VALENCE BAND MAXIMUM
-4.0
-4.5
-5.0
-5.5
WORK FUNCTION (eV)
0
InAs
0.5
1.0
GaAs
InXGa1-XAs(100)
XIn

Fig. 5

# Absence of Fermi Level Pinning at Metal - $In_xGa_{1-x}As$ (100) Interfaces

L.J. Brillson, M.L. Slade, and R.E. Viturro
Xerox Webster Research Center, Webster, NY 14580

M. K. Kelly, N. Tache, and G. Margaritondo
Physics Dept., University of Wisconsin - Madison, WI. 53706

J.M. Woodall, P.D. Kirchner, G.D. Pettit and S. L. Wright
IBM Thomas J. Watson Research Center, Yorktown Heights, N.Y. 10598

## ABSTRACT

Soft X-ray photoemission spectroscopy measurements of clean, ordered $In_xGa_{1-x}As$ (100) surfaces with Au, In, Ge, or Al overlayers reveal an unpinned Fermi level across the entire In alloy series. The Fermi level stabilization energies depend strongly on the particular metal and differ dramatically from those of air-exposed interfaces. This wide range of Schottky barrier height for III-V compounds is best accounted for by a chemically - induced modification in metal - alloy composition.

PACS numbers: 68.20, 73, 71.55, 79.40

Schottky barrier formation at metal interfaces with III-V compound semiconductors has been of considerable ongoing interest because of the apparently weak dependence of barrier height on metal work function and its consequences for high-speed and opto-electronic devices.[1] Fundamental studies of Schottky barrier mechanisms for III-V compounds have been directed primarily to GaAs and especially the (110) cleavage surface of bulk single crystals., In this case, the energy at which the surface Fermi level $E_F$ stabilizes appears to be relatively insensitive to the particular metal contact and to ambient contamination, lying in a range of only a few tenths of eV near the band gap center. To account for this $E_F$ "pinning", researchers have proposed gap states due to defects formed by metal atom condensation,[2] alloy work functions involving As precipitates[3], chemically-formed dipole layers,[4] and metal-induced gap states defined by the semiconductor band structure[5] or by chemisorption and charge transfer involving metal atoms and clusters.[6] Studies of InP (110)[7] and GaAs (100)-metal interfaces suggest somewhat wider ranges of $E_F$ gap position which are sensitive to chemical changes on an atomic scale.[8-10]

Until now, the ternary alloy series $In_xGa_{1-x}As$ has also been viewed in terms of a narrow $E_F$ "pinning" range.[11] This is suggested by capacitance versus voltage (C-V) measurements on Schottky barrier diodes[12] (air-exposed, etched $In_xGa_{1-x}As$ (100) surfaces with Au contacts) and gate-controlled galvanometric measurements on metal-insulator-semiconductor (MIS) capacitor and transistor test structures.[13] These data have been used to support theoretical calculations of anion vacancies[14] or antisite (cation replacing anion)[15] defect states.

Here we use soft X-ray photoemission spectroscopy (SXPS) measurements of metals on clean, ordered $In_xGa_{1-x}As$ (100) surfaces to demonstrate that the surface

$E_F$ stabilization energy (and thereby the band bending) depends strongly on the particular metal and that, for $x > 0$, the range of $E_F$ movement is comparable to or greater than the band gap. For the same metal on different alloys, we observe regular trends in $E_F$ position with respect to the band edges which effectively contradict the models based on simple vacancy or antisite defects as well as the "common-anion rule"[16] of III-V barrier formation. Instead, the results suggest that $E_F$ is not "pinned" by interface states but that interface chemical reaction and diffusion lead to a range of metal-alloy compositions whose work functions determine the $E_F$ gap position.

$In_xGa_{1-x}$ As layers 7500 Å thick ($n = 5 \times 10^{16}$ Si/cm$^3$) were grown by molecular beam epitaxy (MBE) over 2000 Å $In_xGa_{1-x}$ As ($n = 10^{19}$ Si/cm$^3$) on top of 1000 Å GaAs ($n = 10^{19}$/cm$^3$) and an $n^+$ GaAs (100) substrate. This configuration provided unstrained $In_xGa_{1-x}As$ (100) films with Ohmic contacts. Following growth, the specimens were capped with As as protection against ambient contamination. Using a sequence of vacuum annealing steps,[17] we desorb this As cap, leaving clean and ordered (1x1) surfaces as determined from valence band photoemission spectroscopy and low energy electron diffraction respectively. The resultant surface appeared not to have an excess of surface As as gauged by surface versus bulk (photoelectron kinetic energy 50-100 eV versus 10-20 eV)[18] ratios of Ga3d and As3d SXPS core level intensities at appropriate excitation energies. The energies of SXPS features with varying alloy concentration agree systematically and reproducibly with the changes in semiconductor band gap.[19] Thus, if we assume a constant $E_F$ position with respect to the band edges for each clean alloy (for $n = 5 \times 10^{16}$/cm$^3$, $E_C$-$E_F$ ~ 0.1eV), the SXPS valence band edges exhibit the correct decrease in band gap with increasing $x_{In}$ to within $\pm$0.17eV. For each alloy composition, $E_C$-$E_V$ is reproducible to within $\pm$0.05eV. We evaporated metals in ultrahigh vacuum (base pressure 8

x$10^{-11}$torr) from W filaments (pressure rise no higher than mid-$10^{-9}$ torr) and monitored depositions with a quartz crystal oscillator.

We have measured the rigid As3d, Ga3d, and In4d core level shifts as a function of Au, Al, In, and Ge depositions for $In_x Ga_{1-x}$ As where x = 0, 0.25, 0.50, 0.75, and 1.00. Figure 1 illustrates surface-sensitive spectra for As3d and Ga3d/In4d core levels obtained with 100 eV and 80eV respectively. Rigid shifts of all core levels with increasing metal deposition correspond to $E_F$ shifts with respect to the band edges. In general, the relatively sharp In4d and Ga3d peak features provided clearer indications of $E_F$ movement than the As3d feature. Figure 1 illustrates these features for atoms localized within the top few Å of the deposited surface. The 0.3eV rigid shift to higher kinetic energy corresponds to an $E_F$ movement toward the valence band maximum $E_V$. Integrated peak areas of these three structures reveal a slower attenuation of the As3d peak with Au coverage, indicating As outdiffusion. Indeed the As3d spectra display at least one additional component at lower kinetic energy due to Au deposition, corresponding to dissociated As. The As3d and Ga3d/In4d spectra obtained with $h\upsilon = 60$eV and 40 eV respectively yield more bulk-sensitive spectra which minimize any surface chemical effects on core lineshape and whose rigid spectral shifts agree with those of Fig.1. In general, we used both surface and bulk-sensitive spectra to determine the rigid core level shifts reported here.

The $E_F$ shifts with metal coverage extracted from SXPS features indicate a wide range of Schottky barrier positions for metals on $In_xGa_{1-x}As$ (100). For example, Figure 2 illustrates $E_F$ position as a function of metal coverage on InAs (100) for Au, Al, In, and Ge deposition. Each metal exhibits a different $E_F$ movement with increasing metal coverage. Furthermore, the thickness over which each $E_F$ position evolves to its final value range from 1-10 Å, reflecting chemical and electronic differences in the metal-semiconductor interaction., At 20 Å metal coverage, the

final $E_F$ positions extend from above the conduction band minimum $E_C$ to below $E_V$ over a range of 0.5eV. By comparison, the InAs band gap $E_g$ is only 0.36 eV. Analogous plots for other alloy semiconductors yield ranges of 0.85 eV for $In_{.75}Ga_{.25}As$ ($E_g$=0.53 eV), 0.65eV for $In_{.50}Ga_{.50}As$ ($E_g$=.76eV), 0.67eV for $In_{.25}Ga_{.75}As$ ($E_g$=1.05 eV), and ~ 0.4 eV for GaAs ($E_g$=1.43eV). Thus the range of $E_F$ stabilization energies becomes comparable to or greater than the semiconductor band gap with increasing In alloy concentration.

The $E_F$ stabilization energies for a given metal on different alloy semiconductors follow regular trends with respect to the band edges. Figure 3 illustrates these trends for Au, Al, and In across the $In_xGa_{1-x}As$ (100) alloy series. Here, the valence band energies are referred to a common vacuum level as determined by photoemission threshold measurements[20] (e.g., 5.42 eV for InAs and 5.56 eV for GaAs). The wide $E_F$ ranges for each In alloy demonstrate that $E_F$ is not "pinned". Furthermore, the $E_F$ trends appear to parallel the conduction band, especially for In and Al. The data are in reasonable agreement with what little results have been measured previously for clean interfaces. Grant et al. measured an $E_C$-$E_F$ of 0.75eV for Au on GaAs(100) as well as a range of $E_C$-$E_F$ energies ranging from 0.75 to 0.2eV with surface treatment[8]. The significantly higher position of In versus Au ($E_c$-$E_F$=0.35 versus 0.75ev) for GaAs (100) agrees with SXPS results of Daniels et al[21] for cleaved GaAs (110) (e.g., 0.4 versus 0.9 eV[2]).

There is a large discrepancy between these ultrahigh vacuum results for InAs and InGaAs alloys and the previous air-exposed results[12-13], which showed $E_F$ pinning within the conduction band for Au on InAs and a relatively constant position with respect to $E_V$ across the entire alloy series. Also, Baier et al.[22] have measured an $E_F$ position 0.13ev above the conduction band edge for both cleaved and oxidized InAs(110). To address these apparent differences, we have performed SXPS experiments for Au on MBE-grown InAs (100), thermally cleaned and then exposed

to air. Under these conditions, $E_F$ indeed stabilized within the conduction band. Similarly, we measured for In on thermally cleaned air-exposed $In_{.50}Ga_{.50}As$ (100) an $E_F$ stabilization 0.25eV below $E_C$, again in agreement with Kajiyama et al.[12]. Also supporting our results are Schottky barrier data for MBE-deposited Al on n-$In_{.50}Ga_{.50}As$ (100), which display Ohmic behavior.[23] The apparent discrepancy between our clean InAs(100) and Baier's cleaved (110) results is likely due to the different surface preparations - *i.e.*, As passivation and subsequent reevaporation for (100) MBE-grown *versus* cleavage for (110) melt-grown InAs. An analogous difference in $E_F$ movement between (110) melt- and (100) MBE-grown surfaces has already been reported for GaAs[24].

The $E_F$ trends for different metals in Fig. 3 are at variance with a number of Schottky barrier models. The large energy differences with metals does not support models based on "pinning" in a narrow energy range, where the effect of the metal is secondary. These include models involving high densities of closely-spaced defect energy levels[2] or metal-induced state "pinning" at a mid-gap position[5]. Indeed, the latter yields a large error for the Au-InAs(100) $E_F$ position, even after taking the metal electronegativity and band structure effects into account. The $E_F$ movements parallel to the conduction band are contrary to theoretical calculations of native defects reported thus far. Both simple vacancies[14] and anion-on-cation antisite defects[15] display trends which parallel the valence rather than the conduction band and which lie above the conduction band for $x_{In}<0.5$. Within a localized state model, the conduction band trends are consistent only with cation-derived states. Finally, the conduction band trend in Fig. 3 is contrary to a common anion rule[16], where the same $E_C$-$E_F$ would obtain for all III-V compounds with the same anion. Hence, a unified theoretical model of all experimental observations to date (let alone a predictive model) is not yet at hand.

Several studies of $Ga_{.47}In_{.53}As$ MIS structures suggest that the densities of any interface states on dielectric-coated GaInAs surfaces are relatively low and are reduced further by thermal annealing[25,26]. Nevertheless, it was argued that the $E_F$ position depended on the position and density of surface donors and acceptors. Without involving such surface charge states, one can account for the observed $E_F$ stabilization energies via differences in overlayer work function. The trends in Fig. 3 do not reflect pure metal work function values, for which the stabilization energies would be at constant energies below the vacuum level. Instead they are accounted for by overlayer work functions of changing composition.

Based on the relative composition of outdiffusing species observed via SXPS, we observe a trend with Au on $In_x Ga_{1-x}$ As (100) from an As-rich to an *As-deficient* interface with increasing $x_{In}$[17]. This is in sharp contrast to both In and Al on $In_xGa_{1-x}As(100)$, where we observe a trend toward an increasingly *As-rich* interface with increasing $x_{In}$.[17] On the premise that the interface work function varies with increasing $x_{In}$ from $\varphi_{As} = 4.8ev$[3] to $\varphi_{Au} = 5.2\text{-}5.4ev$[27] for Au overlayers and varies from $\varphi_{In,Al,Ga} \sim 4.1\text{-}4.3ev$[27] to $\varphi = 4.8ev$ for In or Al overlayers, one obtains reasonable fits to the data points in Fig. 3 using only straight lines (not shown) between end point values of work function (right-hand scale). Higher-$\varphi$ interfacial Ga versus In may account for the In-GaAs variation[17]. Thus, we are able to account for a large set of interface data on both an absolute and relative scale using only a classical work function approach and observations of interface chemical species. Hence, chemically-induced changes in metal-alloy composition rather than interface defect levels appear to be the most direct explanation for the large range of $E_F$ stabilization energies for metals on $In_xGa_{1-x}As$ alloys.

Beyond any theoretical model relating the position of the equilibrium Fermi level and Schottky barrier formation, the data presented here yields an unambiguous

result: within the $In_xGa_{1-x}As$ alloy system, the metal-semiconductor barrier depends upon the chemically-induced modification of the interface.

Partial support by the Office of Naval Research (ONR N00014-80-C-0778) is gratefully acknowledged. The Synchrotron Radiation Center is supported by the National Science Foundation. We wish to express special appreciation to the Aladdin staff for their outstanding efforts in implementing these experiments.

## FIGURE CAPTIONS

1. SXPS core level spectra for As 3d at $h\upsilon = 100eV$ and Ga 3d and In 4d at $h\upsilon = 80eV$ as a function of increasing Au deposition.

2. Fermi level movements for clean InAs (100) as a function of Au, In, Ge, or Al deposition.

3. Fermi level stabilization energies for Au, In, Ge, and Al deposited on clean $In_xGa_{1-x}As$ (100), $0 \leq x \leq 1$. Left-hand scale relative to GaAs valence band maximum. Right-hand scale relative to vacuum level.

## REFERENCES


1. A.G. Milnes, Semiconductor Devices and Integrated Electronics (Van Nostrand Reinhold Co., New York, 1980).

2. W.E. Spicer, I. Lindau, P. Skeath, C.Y. Su, and P. Chye, Phys. Rev. Lett. 44, 420 (1980).

3. J.L. Freeouf and J.M. Woodall, Appl. Phys. Lett. 39, 727 (1981).

4. L.J. Brillson, J. Vac. Sci. Technol. 16, 1137 (1979)

5. J. Tersoff, Phys. Rev. B32 6968 (1985).

6. R. Ludeke, T.-C. Chiang, and T. Miller, J. Vac. Sci. Technol. B1, 581 (1983).

7. R.H. Williams, V. Montgomery, and R.R. Varma, J. Phys. C. 11, L735 (1978).

8. R.W. Grant, J.R. Waldrop, S.P. Kowalczyk, and E.A. Kraut, J. Vac. Sci. Technol. 19, 477 (1981).

9. L.J. Brillson, C.F. Brucker, A.D. Katnani, N.G. Stoffel, and G. Margaritondo, Appl. Phys. Lett. 38, 784 (1981); C.F. Brucker and L.J. Brillson, ibid. 39, 67 (1981).

10. V. Montgomery, R.H. Williams, and G.P. Srivastava, J. Phys. C. 14, L191 (1981).

11. W.E. Spicer and S.J. Eglash, in VSLI Electronics : Microstructure Science, Vol. 10 (Academic, New York, 1985) p. 79.

12. K. Kajiyama, Y.Mizushima, and S. Sakata, Appl. Phys. Lett. 23, 458 (1973).

13. H.H. Wieder, Appl. Phys. Lett. 38, 170 (1981).

14. M.S. Daw and D.L. Smith, Appl. Phys. Lett. 8, 690 (1980).

15. R.E. Allen and J.D. Dow, Phys. Rev. B25, 1423 (1982).

16. J.O. McCaldin, T.C. McGill, and C.A. Mead, Phys. Rev. Lett. 36, 56 (1976).

17. L.J. Brillson, M.L. Slade, R.E. Viturro, M. Kelly, N. Tache, G. Margaritondo, J.M. Woodall, P.D. Kirchner, G.D. Pettit and S. Wright, unpublished.

18. M.P. Seah and W.A. Dench, Surface Interface Analysis 1,2 (1979).

19. E.W. Williams and V. Rehn, Phys. Rev. 172, 798 (1969).

20. J. van Laar, A.Huijser, and T.L. van Rooy, J. Vac. Sci. Technol. 14, 894 (1977).

21. R.R. Daniels, T.-X Zhao, and G. Margaritondo, J. Vac. Sci. Technol. A2, 831 (1984).

22. H.-U. Baier, L. Koenders, and W. Mönch, J.Vac. Sci. Technol., to be published.

23. K.H. Hsieh, M. Hollis, G. Wicks, C. E. C. Wood, and L. F. Eastman, Inst. Phys. Conf. Ser. 65, 165 (1983).

24. P.Chiaradia, A.D.Katnani, H.W.Sang, Jr., and R.S. Bauer, Phys. Rev. Lett. 52,1246(1984).

25. H.H. Weider, A.R. Clawson, D.I. Elder, and D.A. Collins, IEEE Electron Device Lett. EDL-2, 73 (1981).

26. H.H. Weider, Surface Sci. 132, 390 (1983).

27. H.B. Michaelson, J. Appl. Phys. 48, 4729 (1977) and references therein.

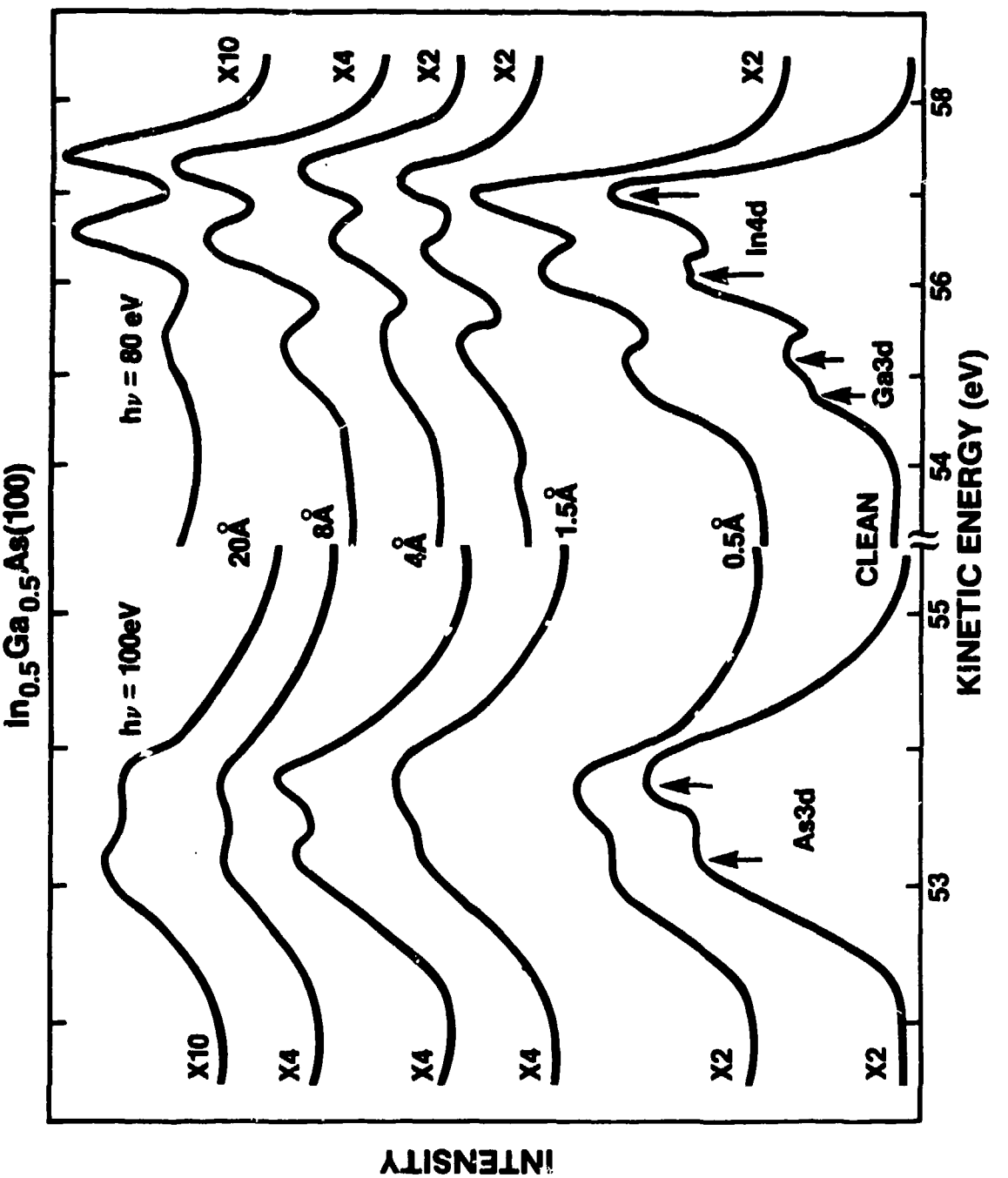
In0.5Ga0.5As(100)
hν = 100eV
hν = 80 eV
X10
X4
X4
X4
X2
X2
X2
X2
X2
20Å
8Å
4Å
1.5Å
0.5Å
CLEAN
As3d
In4d
Ga3d
53
54
55
56
58
KINETIC ENERGY (eV)
INTENSITY

Fig. 1

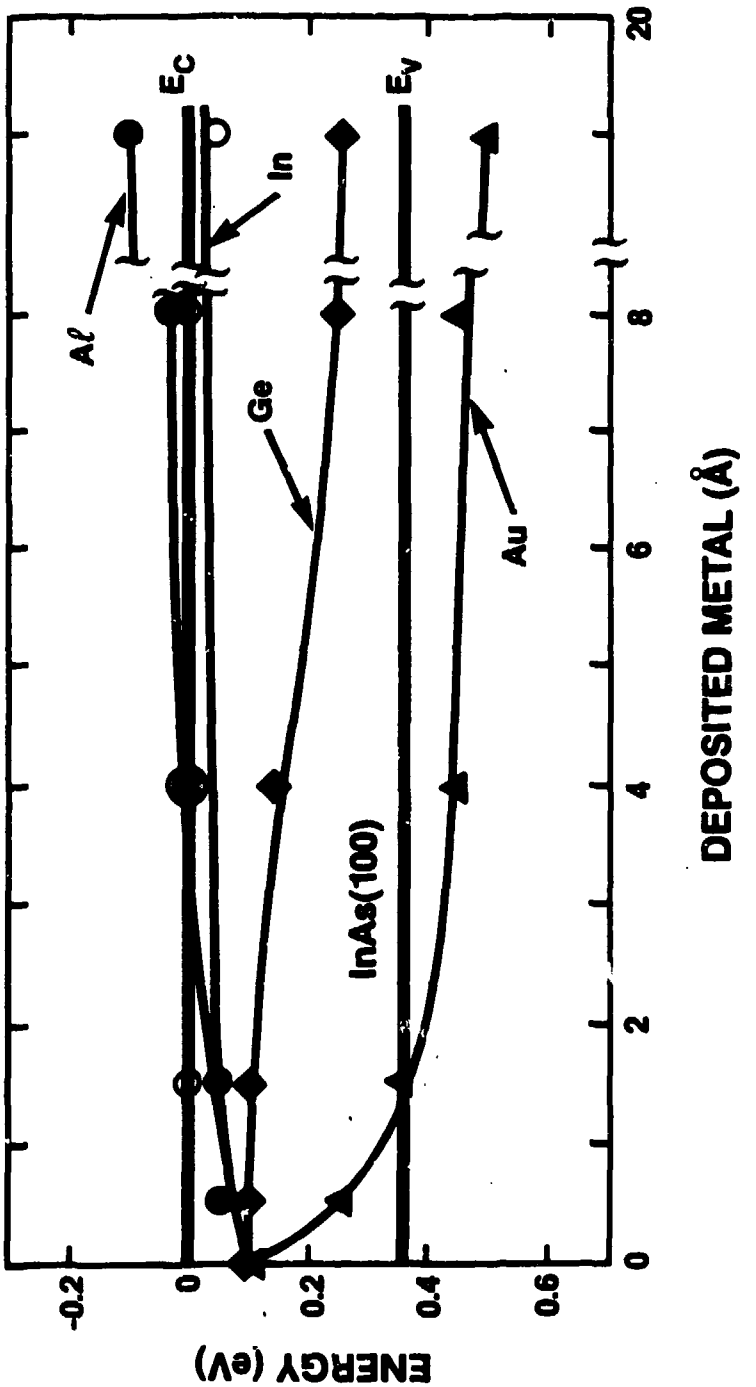
E_C
E_V
In
Al
Ge
Au
InAs(100)
ENERGY (eV)
-0.2
0
0.2
0.4
0.6
DEPOSITED METAL (Å)
0
2
4
6
8
20

Fig. 2

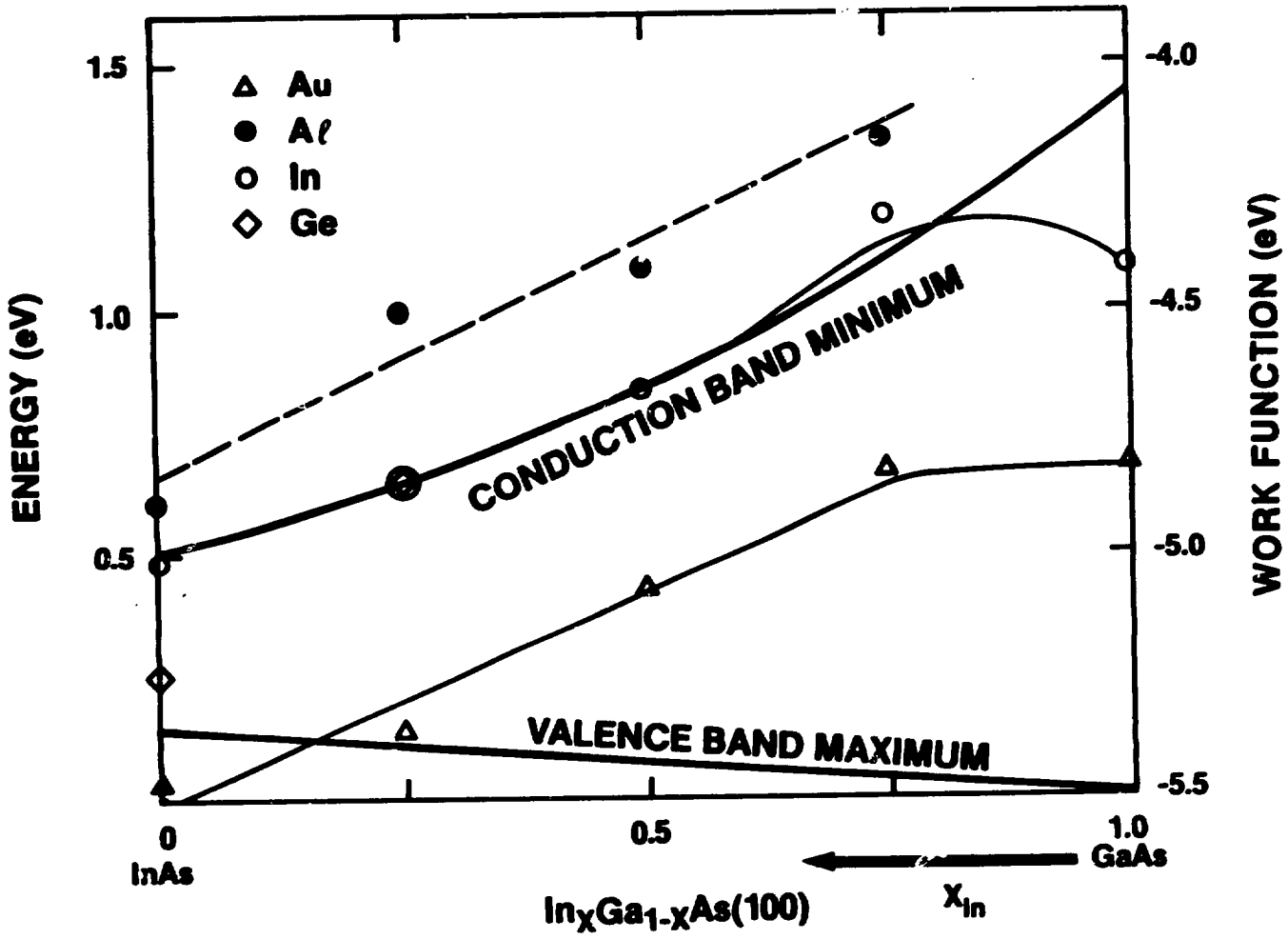
Au
Al
In
Ge
CONDUCTION BAND MINIMUM
VALENCE BAND MAXIMUM
ENERGY (eV)
WORK FUNCTION (eV)
1.5
1.0
0.5
-4.0
-4.5
-5.0
-5.5
0
InAs
0.5
1.0
GaAs
InχGa1-χAs(100)
Xin

Fig. 3

# Optical Emission Properties of Metal/III-V Semiconductor Interface States

R. E. Viturro, M. L. Slade, and L. J. Brillson

Xerox Webster Research Center, Webster, NY 14580

## Abstract

We report the first study of optical emission properties associated with formation of metal/III-V semiconductor interface states. Cathodoluminescence spectroscopy reveals discrete levels distributed over a wide energy range and localized at the microscopic interface. Our results demonstrate the influence of the metal, the semiconductor and its surface morphology on the energy distributions. Evolution of spectral features with interface formation, particularly above monolayer metal coverage, is correlated with Fermi level movements and Schottky barrier heights.

The identification of interface states and their role in Schottky barrier formation have long been key issues in understanding electronic properties of metal/semiconductor (SC) junctions[1]. For clean, ordered InP or GaAs (110), intrinsic gap surface states are absent, and a few monolayers of deposited metal create new charge states which stabilize the Fermi level ($E_F$) in a limited range within the band gap[2]. Considerable spectroscopic evidence suggests that chemical effects (e.g., reaction and interdiffusion) take place concurrently which promote localized charge formation. Physical models for the localized charge states which influence metal/compound SC contact rectification vary from gap states due to defects formed by metal atom condensation[3], to metal-induced gap states defined by the SC band structure[4], to chemisorption and charge transfer involving metals atoms and clusters[5], to chemically formed dipole layers[6] and effective work functions of interface alloys[7]. Nevertheless, except for isolated absorption studies of surface and interface states by total internal reflection[8] or surface photovoltage spectroscopy[9] and near edge photoluminescence of mechanically-damaged surfaces[10], the presence and energies of interface states have been inferred largely from measurements of capacitance[1,11], current[1,12], and $E_F$ movement[2-5].

Here we report the most direct observation of metal/SC interface states thus far. We have detected luminescence from interface states by means of cathodoluminescence spectroscopy[13] (CLS), a technique common to bulk studies and recently applied to laser-annealed metal/SC interfaces[14] and to GaAs/GaAlAs multilayer structures[15]. We have characterized the formation and evolution of interface states with metal deposition on UHV-cleaved (110) III-V SC surfaces of submonolayers up to several monolayers, where the metallic state of the overlayer is well defined. We show that dramatic changes are produced in the optical emission properties of III-V SC's upon metal deposition, both broad and discrete emission

bands at energies below the band gap. Our studies reveal the influence of the particular metal, the SC, its morphology and bulk growth quality on the spectral distribution. Furthermore, the evolution of electron-excited optical emission spectra of metal/InP or GaAs interfaces show qualitative differences at submonolayer *vs.* multilayer metal coverages which can be correlated to their $E_F$ movements and macroscopic Schottky barrier heights (SBH).

The CLS excitation was produced by a chopped electron beam from a glancing incidence electron gun impinging on a (110) crystal face. The room-temperature luminescence was focussed into a monochromator and the transmitted signal was phase-detected using a $LN_2$-cooled Ge detector (North Coast) and a lock-in amplifier. Excitation depths on a scale of nanometers were achieved using low (500- 3000 eV) incident electron energies at glancing angles[14,16,17]. As expected, interface specific features exhibited monotonic intensity increases relative to bulk features with decreasing excitation energy[18]. We evaporated metals on cleaved (110) single crystal surfaces of InP ($n = 4.3 \times 10^{15}$ cm$^{-3}$, $p = 10^{18}$cm$^{-3}$) and GaAs ($n = 4 \times 10^{15}$ cm$^{-3}$) from Metal Specialties. A quartz crystal oscillator positioned next to the cleaved surface monitored film thicknesses. Injected electron concentration ranged from $10^{15}$- $10^{17}$ cm$^{-3}$. We raised injection levels to $10^{18}$ cm$^{-3}$ in order to identify any effects of electron beam damages (which we found to be distinct from the spectral features reported here)[18]. Additionally, *in situ* photoluminescence spectra provided evidence for any bulk related features[18].

Figure 1 shows CL spectra which illustrate the effect of submonolayer coverage on clean UHV-cleaved InP(110) surface for different metals and their similarity with step-cleaved features. We observe new emission features which indicate that metal deposition modifies the SC surface and forms new states. Similar features are observed for both p-type and n-type (not shown) InP (110). Within the energy range

0.6-1.6 eV, the CL spectra of clean InP shows only one emission centered at 1.35 eV, which corresponds to a near-band-gap (NBG) transition. Whereas for mirror-like areas there is no detectable emission in the energy region below the NBG transition over two orders of magnitude of injection level, the CL spectrum of step-cleaved areas shows weak emission at sub-band gap energies. The similarities in CL spectral shapes of step-cleaved areas and those from chemisorbed metals on mirror-like areas suggest that the initial metal deposition causes the formation of broken bonds, such as those formed during a step-cleavage process.

Multilayer metal deposition produces new spectral features which evolve differently for several metals. Fig. 2(a)-(d) demonstrate that the changes produced in the optical emission properties of InP upon metal deposition are strongly dependent on the particular metal. For Au deposition, Fig 2(a) exhibits significant new peak features at 0.8 eV and 0.96 eV, and a broad band whose energies extend up to the onset of the NBG transition. Deposition of 15 Å of Au dramatically reduces the relative emission intensity at energies higher than 0.9 eV. Relative to Au, Cu deposition on InP(110), Fig. 2(b), produces interface states which exhibit a different spectral dependence on metal thickness, *i.e.*, these interface states evolve faster with Cu *versus* Au thickness. This result is consistent with $E_F$ movements extracted from photoemission core level shifts for these interfaces, which showed a faster movement and stabilization for Cu versus Au[19] over similar thickness ranges. The 0.78 eV emission is a common feature between the Au and Cu/InP interfaces. However, spectral differences are apparent at higher energies. In contrast, Fig. 2(c) shows that for Al deposition the NBG transition dominates the spectra even after deposition of 20 Å, whereas the low energy emissions are similar to those of Fig. 1. The overall luminescence intensity is drastically reduced, but Al deposition does not substantially change the spectrum. Similar low energy emission are found for Pd

deposition, Fig. 2(d), although the NBG transition is now totally suppressed. The p-InP specimens display lower overall luminescence efficiency than the n-type crystals, but the behavior of reactive metals such as Al, Pd, and Ni (not shown) differs only in the persistence of the NBG transition for Al. Sub-band gap spectral features appears to be roughly independent of doping.

Fig. 3 shows CL spectra of Au on cleaved GaAs (110). The mirror-like cleaved surface exhibits three strong emissions, a 1.42 eV emission corresponding to a NBG transition and lower energy peaks whose intensities depend on cleavage quality, doping, and doping level[18]. Deposition of Au causes a small shift of the 0.8 eV emission to lower energies, following by development of a peak centered at 0.75 eV which dominates the spectral shape after 15 Å of Au. The evolution of spectral features with metal deposition in both Figs. 2 and 3 demonstrate that strong changes in electronic state energies and densities take place at multilayer coverage which are not apparent in the lower coverage regime.

Metal deposition reduces the NBG luminescence intensity for all systems investigated, due in part to electron beam attenuation by the overlayer and to formation of a surface "dead layer" (ca.1000 - 4000Å) in which increasing band bending and width of the surface space charge region reduces bulk radiative recombination[20,21]. For coverages of only a few atomic layers, overlayer attenuation of 500-3000 eV electrons depends only weakly on the particular metal[15]. In contrast, the magnitude and rate of band bending changes depend sensitively on specific metal, and the NBG intensity attenuation in Figs 2(a)-(d) correlate strongly with $E_F$ movement with metal deposition measured by photoemission[19]. Thus, $E_F$ shifts slowly (rapidly) with Au (Cu) coverage[19], producing large n-type band bending with 10-20 Å (2-4 Å) deposition, which reduces NBG luminescence intensity at a corresponding rate. Al deposition produces relatively little band bending[12,19],

consistent with the NBG feature dominant after 20 Å coverage. The NBG intensity reduction observed for Pd/p-InP is also consistent with the large $E_F$ movement expected[19].

Several possibilities exist for the physical nature of the observed metal-induced transitions. Initially, metal deposition perturbs the surface bonding and thereby the electronic structure of the semiconductor surface. However, with multilayer metal coverage, these states evolve into interface states with different energies and densities. At submonolayer coverages, these states can not be ascribed to metal-induced gap states[4] since the overlayers are not yet metallic. At higher coverages, the spectral shape also rules out surface amorphization, which would produce a structureless optical emission spectrum or a broad NBG wing. On the other hand, diffusion of the metal in the SC may cause the formation of a highly doped surface layer, which may account for the observed optical emission spectra. The high diffusion coefficient and macroscopic transport of Cu in InP, even at temperatures as low as 400°C[22] suggests that an indiffusion process may form a similar albeit microscopic layer even near room temperature. The qualitative difference between unreactive[6] metals such as Au or Cu *versus* reactive metals such as Al or Ni may be attributed to the formation of a reacted interfacial layer which inhibits metal indiffusion in the latter case. However, we have not found clear correlation between the emission energies of the metal/InP interfaces and optical emission from the same metal-doped InP[22,23]. A recent luminescence investigation of Cu metal diffusion in InP[23] at various temperatures displayed formation of a neutral complex at 400°C which evolved with increasing temperature, giving rise to an intense band at ca. 1.0 eV *versus* our 0.78 eV band. The results suggest that isolated metal impurities within the SC are alone insufficient to account for the observed optical emission. More likely, metal indiffusion coupled with semiconductor outdiffusion of the

different species forms defect complexes (*e.g.*, impurity-native defects) which are responsible for the optically-detected interface states.

The dominant CLS features at multilayer coverages in Figs. 2 and 3 can account for the reported SBH's of Au and Cu on n-InP (110) and Au on n-GaAs (110). Transitions from interface states into (out of) the valence (conduction) band as well as between localized states can contribute to the CL spectrum. Of these, transitions which have the valence band maximum as the final state have the highest probability since the upward band bending of n-type SC's results in accumulation of injected beam-excited valence holes at the interface. This fact also accounts for the lower overall CL efficiency observed for p-type specimens, where such hole accumulation is not in general expected. Thus, assuming that localized state transitions to the valence band maximum produce the dominant contribution to the n-type CL spectra and that recombination cross sections do not vary discontinuously with energy, the pronounced peak feature at 0.78 eV in Figs. 2(a) and (b) suggest a relatively high density of states located 0.58 eV below the conduction band edge. This value is close to the 0.43-0.5 eV[1] SBH reported for Au and Cu on InP (110) and can account for the observed $E_F$ stabilization. Surface photovoltage spectra of Au on InP (110) supports this spectral interpretation[9], *although CLS alone provides optical evidence at metallic coverages.* Similarly, the evolution of CLS peaks in Fig. 3 to a single emission feature at 0.75 eV indicates a high density of states located 0.7 eV below the conduction band edge, compared with the reported SBH of 0.8-0.9 eV[1]. Of course, $E_F$ stabilization need not be precisely at a density-of-states peak but rather may be weighted or averaged toward such a value from the bulk $E_F$ position.

On the other hand, the more reactive Al/InP system displays a SBH ≤ 0.2 eV[12,19] which correlates well with the persistence of the NBG transition and weak sub-band gap emission detected.

We have observed the formation and evolution of metal/SC interface states by optical emission techniques. We were able to distinguish between interface states promoted by metal deposition from those of step-cleaved areas. The CL spectra show qualitative differences between metals, especially with different chemical reactivity. These metal-induced states are distributed over a wide energy range, are localized at the interface, and can differ substantially from those produced by only submonolayer metal coverages. Dominant CL features show interface levels at energies which can account for Schottky barrier heights.

Partial support by the Office of Naval Research (ONR N00014-80-C-0778) and fruitful discussions with Christian Mailhiot are gratefully acknowledged.

## References


1. S. M. Sze, **Physics of Semiconductor Devices**, 2nd ed. (Wiley-Interscience, New York, 1981) ch.5.

2. L. J. Brillson, Surf. Sci. Rept. **2**, 123 (1982), and references therein.

3. W. E. Spicer, I. Lindau, P. Skeath, and C. Y. Su, J. Vac. Sci. Technol. **17**, 1019 (1980); H. H. Wieder, *ibid.* **15**, 1498 (1978).; R. H. Williams, *ibid.* **18**, 929 (1981).

4. J. Tersoff, Phys. Rev. Lett., **52**, 465 (1984).

5. R. Ludeke, T. C. Chiang, and T. Miller, J. Vac. Sci. Technol. **B1**, 581 (1983).

6. L. J. Brillson, J. Vac. Sci. Technol. **16**, 1137 (1979).

7. J. L. Freeouf and J. M. Woodall, Appl. Phys. Lett. **39**, 727 (1981).

8. G. Chiarotti, S. Nannarone, R. Pastore, and P. Chiaradia, Phys. Rev. **B4**, 3398 (1971).

9. Y. Shapira, L. J. Brillson, and A. Heller, Phys. Rev. **B29**, 6824 (1984).

10. R. A. Street, R. H. Williams, and R. S. Bauer, J. Vac. Sci. Technol. **17**, 1001 (1980).

11. P. S. Ho, E. S. Yang, H. L. Evans, and X. Wu, Phys. Rev. Lett. **56**, 177 (1986).

12. J. H. Slowik, H. W. Richter, and L. J. Brillson, J. Appl. Phys. **58**, 3154 (1985).

13. B. G. Yacobi and D. B. Holt, J. Appl. Phys. **59**, R1 (1986), and references therein.

14. L. J. Brillson, H. W. Richter, M. L. Slade, B. A. Weinstein, and Y.Shapira, J. Vac. Sci. Technol. A3, 1011 (1985).

15. J. Christen, D. Bimberg, A. Steckenborn and G. Weimann, appl. Phys. Lett. 44, 84 (1984)

16. D. B. Wittry, in **Electron Beam Interactions With Solids**, ed. D.F. Kyser, H. Niedrig, D. E. Newbury and R. Shimizu (SEM, Inc., Chicago, 1984) p. 99 and references therein.

17. K. Murata, Phys. Status Solidi A36, 527 (1976).

18. R. E. Viturro, M. L. Slade, and L. J. Brillson, unpublished.

19. L. J. Brillson, C. F. Brucker, A. D. Katnani, N. G. Stoffel, R. Daniels, and G. Margaritondo, J. Vac. Sci. Technol. 21, 564 (1982).

20. D. B. Wittry and D. F. Kyser, J. Appl. Phys. 38, 375 (1967).

21. R. E. Hollingsworth and J. R. Sites, J. Appl. Phys. 53, 5357 (1982).

22. M. S. Skolnick, E. J. Foulkes, and B. Tuck, J. Appl. Phys. 55, 2951 (1984).

23. H. Temkin, B. V. Duff, W. A. Bonner, and V. G. Keramidas, J. Appl. Phys. 53, 7526 (1982).

## Figure Captions

1. CL spectra of clean, mirror-like p-InP (110) surfaces before and after submonolayer Ni, Pd, or Cu deposition, and the clean step-cleaved surface.

2. CL spectra of (a) Au, (b) Cu and (c) Al on clean, mirror-like n-InP (110) and (d) Pd on clean mirror-like p-InP (110) as a function of deposition.

3. Cl spectra of clean, mirror-like n-GaAs (110) with increasing Au deposition.

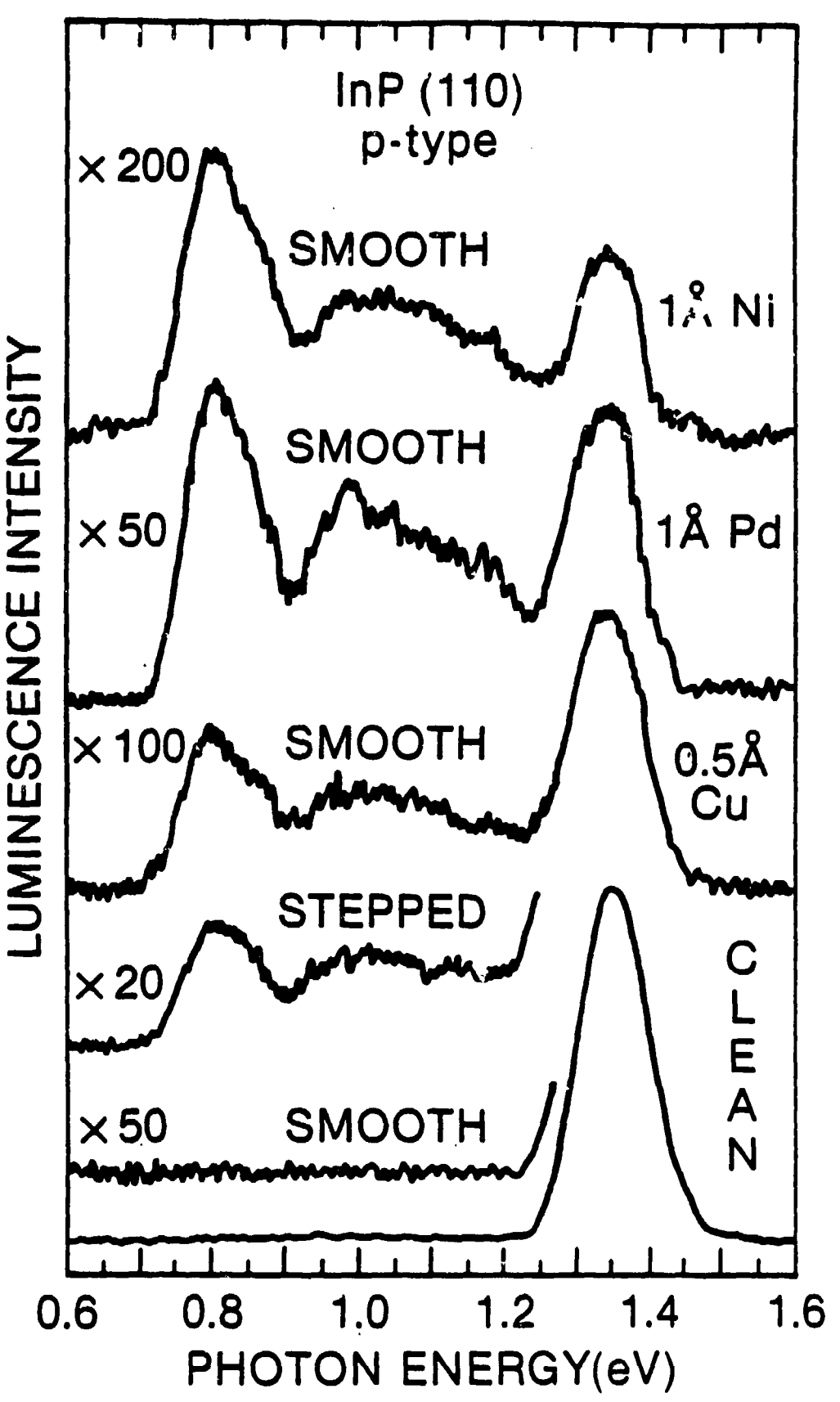
InP (110)
p-type
×200
SMOOTH
1Å Ni
SMOOTH
×50
1Å Pd
×100
SMOOTH
0.5Å
Cu
STEPPED
×20
CLEAN
×50
SMOOTH
LUMINESCENCE INTENSITY
0.6
0.8
1.0
1.2
1.4
1.6
PHOTON ENERGY(eV)

Fig. 1

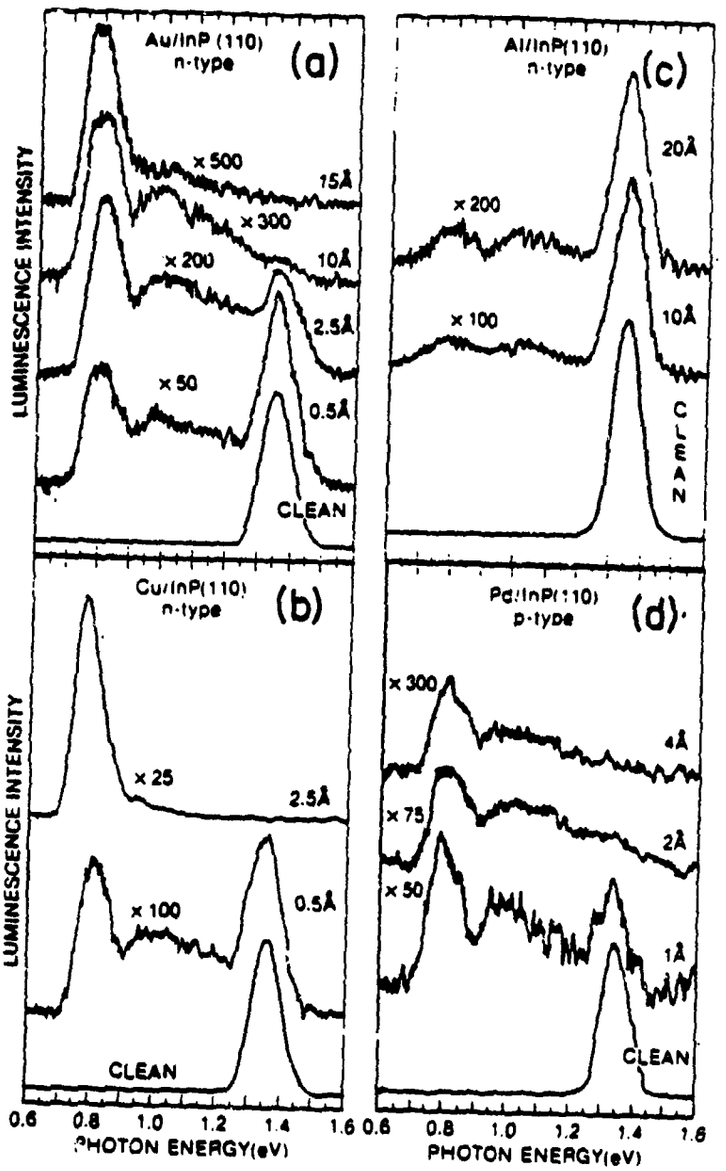
Au/InP (110)
n-type
(a)
× 500
15Å
× 300
10Å
× 200
2.5Å
× 50
0.5Å
CLEAN
Al/InP(110)
n-type
(c)
20Å
× 200
× 100
10Å
CLEAN
Cu/InP(110)
n-type
(b)
× 25
2.5Å
× 100
0.5Å
CLEAN
Pd/InP(110)
p-type
(d)
× 300
4Å
× 75
2Å
× 50
1Å
CLEAN
LUMINESCENCE INTENSITY
LUMINESCENCE INTENSITY
0.6 0.8 1.0 1.2 1.4 1.6
PHOTON ENERGY(eV)
0.6 0.8 1.0 1.2 1.4 1.6
PHOTON ENERGY(eV)

Fig. 2

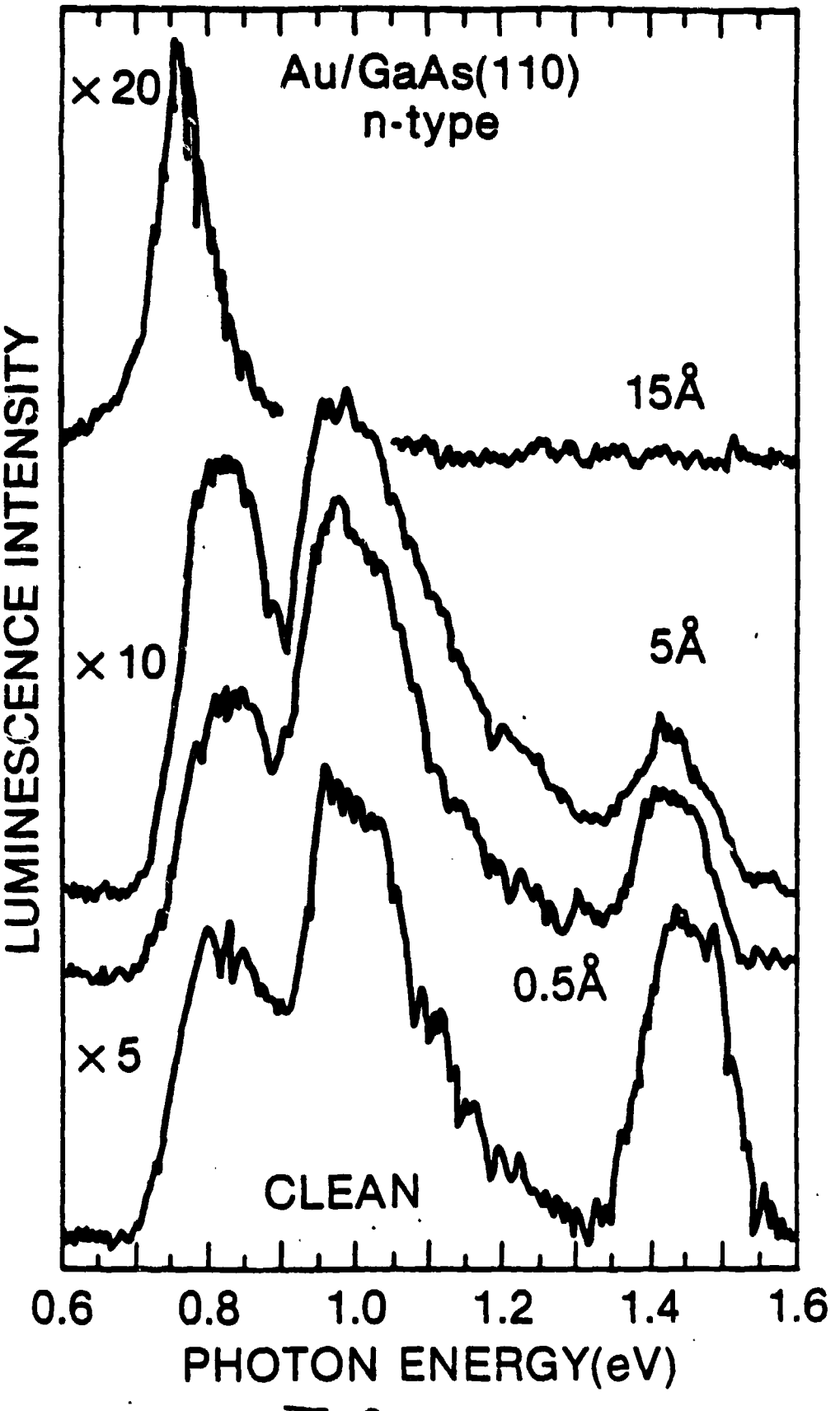
Au/GaAs(110)
n-type
×20
15Å
×10
5Å
0.5Å
×5
CLEAN
LUMINESCENCE INTENSITY
0.6
0.8
1.0
1.2
1.4
1.6
PHOTON ENERGY(eV)

Fig. 3

# METALLIZATION OF III-V COMPOUNDS

L. J. Brillson

Xerox Webster Research Center
800 Phillips Road, 0114/41D
Webster, NY 14580

## Abstract

Electronic and chemical characterization of III-V compound semiconductor-metal interfaces on an atomic scale reveals that chemical reactions and interdiffusion play a major role in Schottky barrier formation. A complement of electron and optical spectroscopies provides evidence for a rich, systematic array of metal-semiconductor interactions. These results for InP, GaAs, and $In_xGa_{1-x}$ As indicate that atomic scale techniques may provide a greater degree of Schottky barrier control than hitherto believed.

## Introduction

The characterization of chemical and electronic structure at III-V compound semiconductor-metal interfaces by surface science techniques reveals that chemical interactions on an atomic scale have a major effect on Schottky barrier formation. Thus, soft x-ray photoemission spectroscopy (SXPS) and Auger electron spectroscopy (AES) depth profiling on thin film/semiconductor interfaces highlight the role of bulk semiconductor stability and interface "chemical trapping" in determining the anion/cation stoichiometry of outdiffusion and the composition of the buried interface. Surface photovoltage spectroscopy (SPS) and cathodoluminescence spectroscopy (CLS) provide direct evidence of localized electronic states due to surface and interface chemical interactions. SXPS measurements of clean, ordered $In_xGa_{1-x}As$ (100) surfaces with metal overlayers indicate an unpinned Fermi level($E_F$) across the entire In alloy series. The strong dependence of $E_F$ stabilization energies on specific metal and dramatic differences from air-exposed interfaces are accounted for by a chemically-induced modification in metal-alloy composition. The chemical basis for Schottky barrier formation observed for III-V compound metallization suggest a greater degree of electrical control may be possible than hitherto believed.

## Microscopic Chemical and Macroscopic Electronic Structure

Considerable evidence now exists that chemical interactions on a microscopic scale can manifest themselves in electronic properties on a macroscopic scale. Early indications of this relationship followed from the Schottky barrier height (SBH) dependence of transition metal silicides on their heats of formation(1) and the SBH dependence of ionic and covalent compound semiconductors on their heats of reaction with various metals(2).

Early experimental work showed that SBH changes of Au-GaAs interfaces with annealing were linked to pronounced interdiffusion of the constituents(3). With the application of surface science techniques to metal-semiconductor interface studies, it was found in general that considerable atom and change rearrangement takes place with the initial few monolayers of metal deposition on a clear semiconductor surface and that intrinsic surface states played no role in the Fermi level ($E_F$) stabilization(4).

Figure 1 illustrates the low coverage electronic effects of Au deposition on an ultrahigh vacuum (UHV)-cleaved GaAs (110) surface and their relation to the SBH. Here, discrete metal-induced states with the band gap are monitored by a surface photovoltage spectroscopy (SPS) technique(5) (indicated schematically in the upper inset). Figure 1 shows no photopopulation or depopulation of such states for the metal-free surface,

but new subgap transitions occurring with submonolayer Au deposition(6). These transitions evolve with metal coverage and display a pronounced depopulation of states located 0.9eV below the conduction band minimum. Since this corresponds to the ultimate $E_F$ position of the macroscopic contact, the metal-induced states appear to be related to the Schottky barrier formation. The SPS technique has provided evidence for a wide range of interface states on III-V compounds, notably the chemically-treated and metallized InP (100) surface(7).

Complementary to detection of subband transitions by SPS, cathodoluminescence spectroscopy (CLS) yields evidence of optical emission from interface states, sub-surface defects, impurities, and new band structure(8). Recently, CLS has been extended to III-V compounds with metal overlayers and reveals new interfacial electronic structure which evolves with coverage at metallic (multilayer) thicknesses(9). Similarly, SXPS studies of UHV-cleaved InP (110) with various metal overlayers display thickness dependencies of $E_F$ movement and chemical interaction which correlate on a scale of monolayers(10).

## Chemical Systematics of III-V Metallization

SXPS and AES measurements of metals on UHV-cleaved III-V binary compound semiconductors reveal pronounced interdiffusion of semiconductor and metal which exhibit systematic behavior(11). Thus the extent of semiconductor anion and cation dissociation and outdiffusion through a thin (20Å) Au overlayer increases monotonically with decreasing heat of formation, i.e., semiconductor stability. Furthermore, the diffusion of such dissociated species through the metal overlayer depends sensitively on the bond strength between metal and anion (or, in some cases, metal and cation)(12). For example, metals which bond strongly to outdiffusing anions lead to a "chemical trapping" or accumulation of anions at the metal-semiconductor interface even if the reactive metal is an interlayer only a few Å thick(12). Figure 2 illustrates AES depth profilic for Au on UHV-cleaved InP(110) showing how Ti and Ni interlayers only 10 or 20Å thick retard P outdiffusion, causing a P accumulation at the interface and no segregation to the free metal surface(13). Significantly, the interface stoichiometry changes from In-rich to P-rich with addition of the reactive interlayer. Comparison of Figs. 2a and 2b suggests that different interlayers can influence the metal indiffusion as well.

Figure 3 indicates SXPS In4d and As3d core level spectra at the Au-UHV-cleaved InAs (110) interface, showing the dramatic effect of a reactive Al interlayer on the semiconductor outdiffusion. Whereas in Fig. 3a, an excess of (dissociated) As segregates to the free Au surface, addition of a 10Å Al interlayer strongly Attenvates such outdiffusion while enhancing free Ga

segregation(12). Similar effects are observed for GaSb, In As, InSb, and InP(4).

## Microscopic Chemical Effects on Macroscopic Electronic Structure

The reversal in stoichiometry of outdiffusion for a particular metal on III-V compound semiconductors can be related to the magnitude of the SBH and indicates a chemical basis for the Schottky barrier formation. Figure 4 displays the ratio of integrated P2p *versus* In4d SXPS core level intensities as a function of metal deposition on UHV-cleaved InP(14). Whereas reactive(2) metals produce In-rich outdiffusion, less-reactive metals lead to the reverse stoichiometry. SBH's measured by Williams *et. al.*(15) for many of these metals and plotted *versus* heat of reaction appear in the Fig. 4 inset. The correspondence between P-rich (In-rich) outdiffusion and high (low) SBH suggests that electrically-active sites produced by the semiconductor anion and cation outdiffusion and dependent upon the stoichiometry are responsible for the $E_F$ stabilization(14). This reversal in stoichiometry is not observed for metals on ionic II-VI compound semiconductors such as CdS, CdSe, or ZnS(11). Coupled with the tendency to form degenerate n-type layers with preferential anion outdiffusion, the absence of stoichiometry reversal can account for the wider range of SBH's observed for the class of II-VI *versus* III-V compound semiconductors.

Figure 5 illustrates the change in current-voltage characteristic produced by a reactive interlayer at a metal-InP interface. Here both Au-InP and Au-10Å Al-InP diode measurements were performed on the same InP single crystal surface in UHV(14). The diodes with interlayers have an order of magnitude larger extrapolated forward and reverse saturation currents - indicating a macroscopic electrical effect from the atomic-scale interlayer. Recent temperature-dependent current-voltage and capacitance-voltage measurements for the Al-UHV-cleaved InP(110) interface indicate a 0.21-0.26eV SBH with interfacial charge residing in states 0.10eV below the conduction band edge(16). These states are distributed 100-200Å into the surface space charge region, consistent with the picture of room temperature outdiffusion and associated electrical activity described above. Exposure of InP to $H_2S$, Cl, and $H_2O$(17,18) and of GaAs to $H_2S$(19,20) also has pronounced effects the Schottky barrier properties as well as on the chemical interdiffusion(4). Likewise, a variety of surface treatments for GaAs (100)(21) and InP (100)(22) produce ranges of $E_F$ stabilization respectively 0.6eV and 0.7eV wide within the semiconductor bandgap. Hence atomic-scale treatments of the interface chemical structure appear to be effective in affecting substantially the SBH's at III-V compound semiconductor-metal interfaces.

## Un-"pinned" $E_F$ Stabilization at $In_x Ga_{1-x} As$ (100) - Metal Interfaces

Recently, we have observed a wide range of $E_F$ stabilization energies with different metals on the ternary III-V compounds $In_x Ga_{1-x} As$ across the entire In alloy series(23,24). We obtained SXPS results from $In_x Ga_{1-x} As$ (100) surfaces using the film structure pictured schematically in Fig. 6. The multilayer structure provides for an Ohmic back contact and for an unstrained n-type InGaAs outer layer. In addition, these specimens were capped with an As overlayer as protection from ambient gases during transfer from the molecular beam epitaxy (MBE) chamber (in New York) to the analysis chamber (in Wisconsin). After thermal desorption of the As cap under UHV conditions, we could obtain clean, ordered surfaces as determined from SXPS valence band spectra and low energy electron diffraction (LEED).

SXPS core level spectra exhibited evidence for pronounced chemical interactions at metal-$In_x Ga_{1-x} As$ (100) $0 \leq x \leq 1$ interfaces which depended strongly upon the particular metal. Thus, as illustrated by Figure 7, Au on $In_{0.50} Ga_{0.50} As$ (100) exhibits an accumulation of dissociated As at the free Au surface and no analogous effects for In or Ga. From depth profiles such as Figure 2, we may conclude that such interfaces are not likely to have an As excess relative to In or Ga. In contrast, Al on the $In_{0.50} Ga_{0.50} As$ (100) surface produces an excess of dissociated In which segregates to the free Al surface. As outdiffusion is retarded relative to both In and Ga, analogous to the results of Figs. 2, 3, and 4. Interestingly, the Ga sublattice appears virtually unaffected by the Al overlayer, suggesting that Al disrupts the weaker In-As *versus* Ga-As bonds preferentially. Comparison of surface- and bulk-sensitive SXPS spectra for Au, Al, In, and Ge and $In_x Ga_{1-x} As$ (100) $0 \leq x \leq 1$ surfaces indicates the following chemical trends: for Au, the buried interface *decreases* in As richness as x increases (e.g., the Au-InAs (100) interface is As-deficient, the Au-GaAs (100) interface is As-rich; for Al and In, the buried interface *increases* in As richness with increasing x.

The rigid core level shifts pictured in Fig. 7 permit us to determine the $E_F$ movement with metal coverage and the stabilization energy with respect to the band edges(23,24). Figure 8 presents these results for the metals Au, Al, In, and Ge, revealing systematic variations across the alloy series and demonstrating the strong dependence on the metal for a particular alloy. Both the relative and absolute behavior shown are incompatible with a variety of Schottky barrier "pinning" models. Instead the results are consistent with a chemically-modified interface work function model, given the chemical trends already mentioned. Assuming that the interface work function varies from 4.8eV for As to 5.2-5.4eV for Au as x increases, the resultant trend agrees with the Au data points in Figure 7 both in range and in absolute values. Similarly, assuming that the interface work function varies from ca 4.2eV for In or Al to 4.8eV for As as x increases, the work

function trend agrees with the data for In and Al in range and magnitude (although the In points are 0.1-0.2eV too low). Thus by using interface chemical compositions and a simple work function model, we are able to account for a large set of interface data on both an absolute and relative scale.

In conclusion, we have used surface science techniques to establish that microscopic chemistry influences (or dominates) macroscopic electronic structure. The systematics of interface behavior correlate with differences in Schottky barrier formation. Indeed, we have now identified atomic-scale techniques with which to control interdiffusion, chemical reaction, and thereby electronic properties. The surprisingly large electronic changes now apparent using these techniques provides us with new opportunities for understanding and controlling Schottky barrier formation.

## Acknowledgements

We gratefully acknowledge partial support by the office of Naval Research (ONR N00014-80-C-0778) and the assistance of the Aladdin Storage Ring Facility. The Synchrotron Radiation Center is supported by the National Science Foundation.

## References


1. J. M. Andrews and J. C. Phillips, Phys. Rev Lett. 35, 56 (1975).

2. L. J. Brillson, Phys. Rev. Lett. 40, 260 (1978).

3. A. K. Sinha and J. M. Poate, Appl. Phys. Lett. 23, 666 (1973).

4. L. J. Brillson, Surf. Sci. Repts. 2, 123 (1982).

5. L. J. Brillson, Surf. Sci. 51, 45 (1975).

6. L. J. Brillson, J. Vac. Sci. Technol. 16, 1137 (1979).

7. L. J. Brillson, Y. Shapira, and A. Heller, Appl. Phys. Lett. 43, 174 (1983).

8. L. J. Brillson, H. W. Richter, M. L. Slade, B. A. Weinstein, and Y. Shapira, J. Vac. Sci. Technol. A3, 1011 (1985).

9. R. E. Viturro, M. L. Slade, and L. J. Brillson, unpublished.

10. L. J. Brillson, C. F. Brucker, A. D. Katnani, N. G. Stoffel, R. Daniels, and G. Margaritondo, J. Vac. Sci. Technol. 21, 564 (1982).

11. L. J. Brillson, C. F. Brucker, N. G. Stoffel, A. D. Kanani, R. Daniels, and G. Margaritondo, Surf. Sci. 132, 212 (1983).

12. L. J. Brillson, C. F. Brucker, A. D, Kanani, N. G. Stoffel, and G. Margaritondo, Appl. Phys. Lett. 38, 784 (1981).

13. Y. Shapira and L. J. Brillson, J. Vac. Sci. Technol. B1, 618 (1983).

14. L. J. Brillson, C. F. Brucker, A. D. Kanani, N. G. Stoffel, and G. Margaritondo, Appl. Phys. Lett. 38, 784 (1981).

15. R. H. Williams, V. Montgomery, and R. R. Varma, J. Phys. C (Solid State Phys.) 11, L735 (1978).

16. J. H. Slowik, H. W. Richter, and L. J.Brillson, J. Appl. Phys. 58, 3154 (1985).

17. V. Montgomery, R. H. William,s and G. P. Srivastava, J. Phys. C. (Solid State Phys.) 14, L191 (1981).

18. V. Montgomery and R. H. Williams, J. Phys. C. (Solid State Phys.) 15, 5887 (9183).

19. J. Massies, J. Chaplart, M. Laviron, and N. T. Linh, Appl. Phys. Lett. 38, 693 (1981).

20. J. Massies, F. DeZaly, and D. T. Lonh, J. Vac. Sci. Technol. 17, 1134 (1980).

21. R. W. Grant, J. R. Waldrop, S. P. Kowalczyk, and E. A. Kraut, J. Vac. Sci. Technol. 19, 477 (1981).

22. J. W. Waldrop, S. P. Kowalczyk, and R. W. Grant, Appl. Phys. Lett. 42, 454 (1983).

23. L. J. Brillson, M. L. Slade, R. E. Viturro, M. K. Kelly, N. Tache, G. Margaritondo, J. M. Woodall, P. D. Kirchner, G. D. Pettit, and S. L. Wright, Appl. Phys. Lett., in press.

24. L. J. Brillson, M. L. Slade, R. E. Viturro, M. K. Kelly, N. Tache, G. Margaritondo, J. M. Woodall, P. D. Kirchner, G. D. Pettit, and S. L. Wright, J. Vac. Sci. Technol., in press.

## Centered Figure Captions

Figure 1 Surface photovoltage spectra of UHV-cleaved GaAs(110) as a function of increasing Au deposition. Inset shows corresponding energy band diagram for 0.9eV transition induced by monolayer Au coverages(6).

Figure 2 Auger electron spectroscopy sputter profile of atomic composition normal to the 70Å Au-InP interface with (a) a 20 Å Ni interlayer, (b) a 10 Å Ti interlayer, and (c) no interlayer. Chemical trapping of outdiffusing P reverses the interface stoichiometry and may reduce Au indiffusion(13).

Figure 3 Soft x-ray photoemission spectra of UHV-cleaved InAs (110) as a function of Au deposition (a) with and (b) without a reactive interlayer, showing reversal in outdiffused In *versus* As stoichiometry(11).

Figure 4 In/P stoichiometry of outdiffusion as a function of different metal coverage. Inset displays Schottky barriers for many of these metals (after Williams(15)) and indicates correspondence between high (low) barrier and P (In)-rich out diffusion(14).

Figure 5 Current-voltage characteristics for Au/UHV-cleaved InP (110) interfaces (a) without and (b) with a reactive 10Å Al interlayer(14).

Figure 6 Schematic geometry of epitaxially-grown $In_x Ga_{1-x} As$ (100) with an Ohmic back contact and on As capping layer to prevent ambient contamination(23).

Figure 7 Soft x-ray photoemission spectra of clean $In_{0.50} Ga_{0.50} As$ (100) as a function of Au deposition. The changes in relative As/In, Ga intensities and the As lineshape with coverage indicate preferential As outdiffusion.

Figure 8 Fermi level stabilization energies for various Au, Al, In, and Ge depositions on $In_x Ga_{1-x} As$ (100) for $0 \leq x \leq 1$. Left-hand scale is relative to the GaAs valence band maximum. Right-hand scale is relative to the vacuum level. The variations in $E_F$ stabilization are accounted for by a chemically-modified interface work function(23,24).

## SURFACE PHOTOVOLTAGE SPECTROSCOPY

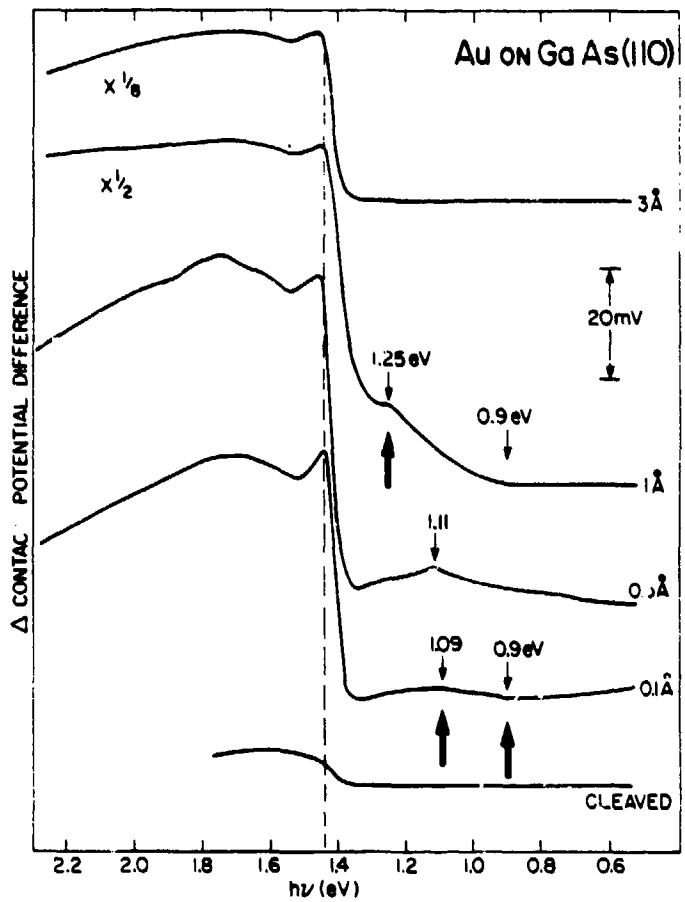


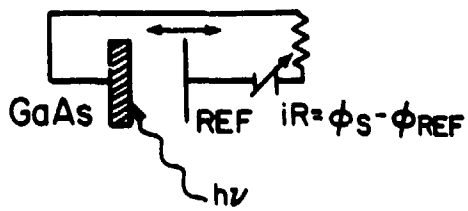


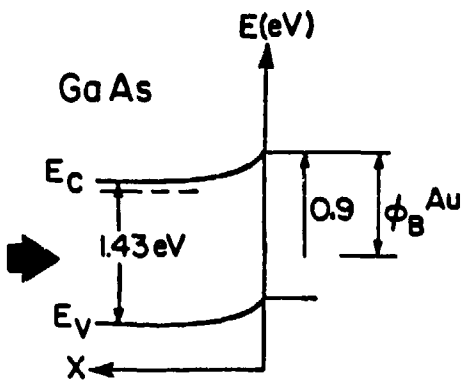

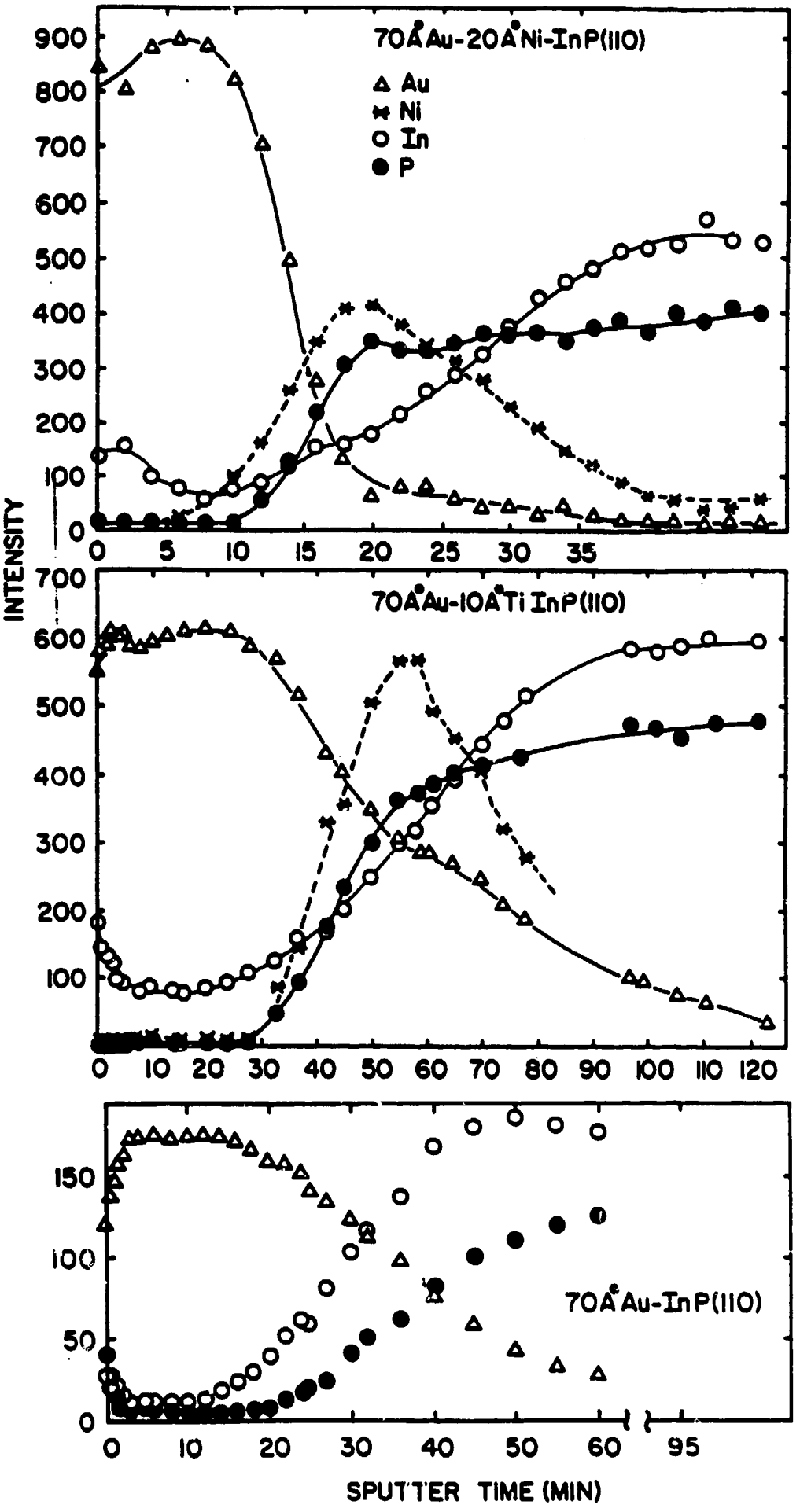
70Å Au-20Å Ni-InP(110)
Au
Ni
In
P
INTENSITY
70Å Au-10Å Ti InP(110)
70Å Au-InP(110)
SPUTTER TIME (MIN)

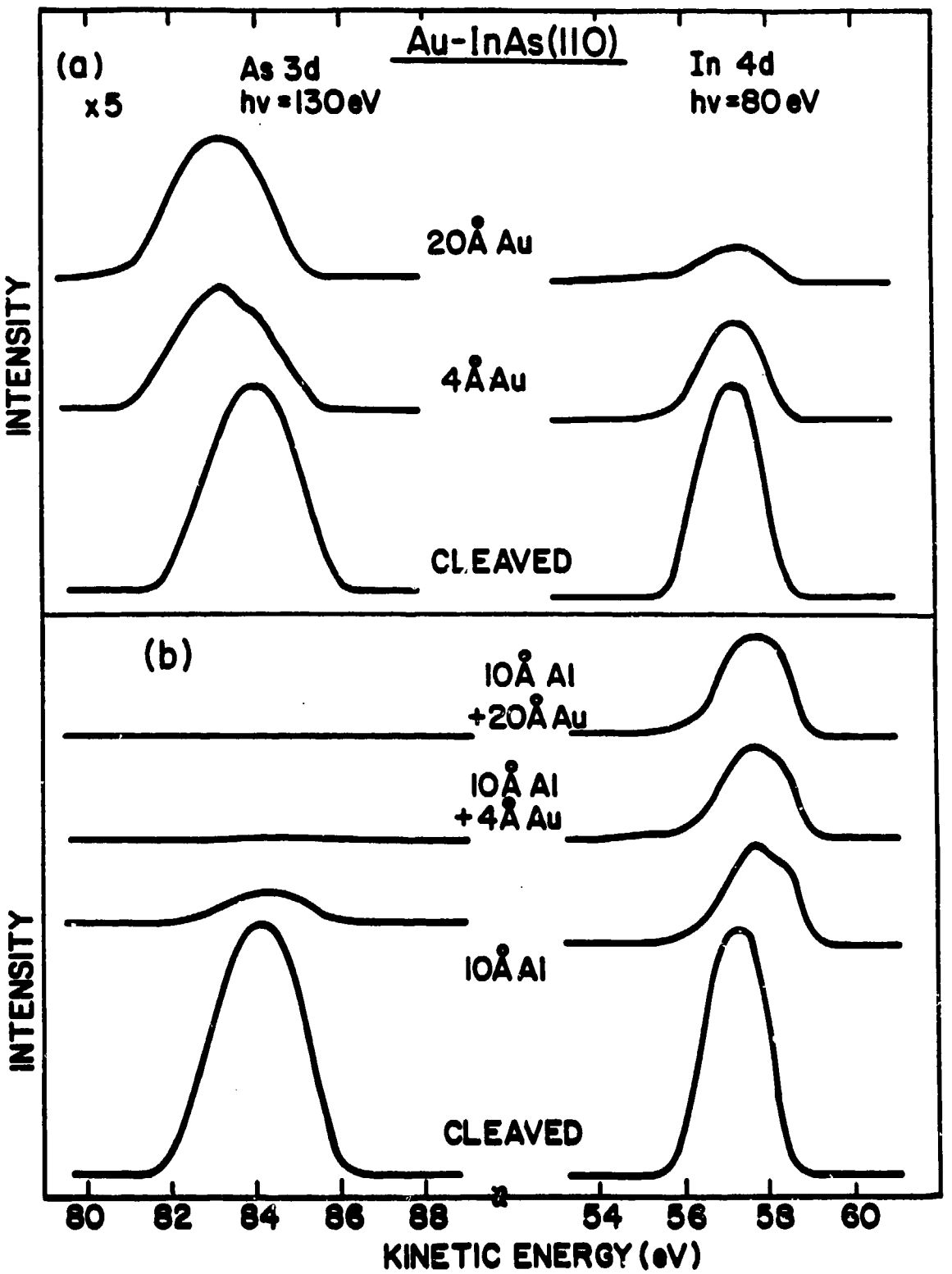
Au-InAs(110)
(a)
x5
As 3d
hv=130eV
In 4d
hv=80eV
20Å Au
4Å Au
CLEAVED
INTENSITY
(b)
10Å Al
+20Å Au
10Å Al
+4Å Au
10Å Al
CLEAVED
INTENSITY
80
82
84
86
88
54
56
58
60
KINETIC ENERGY (eV)

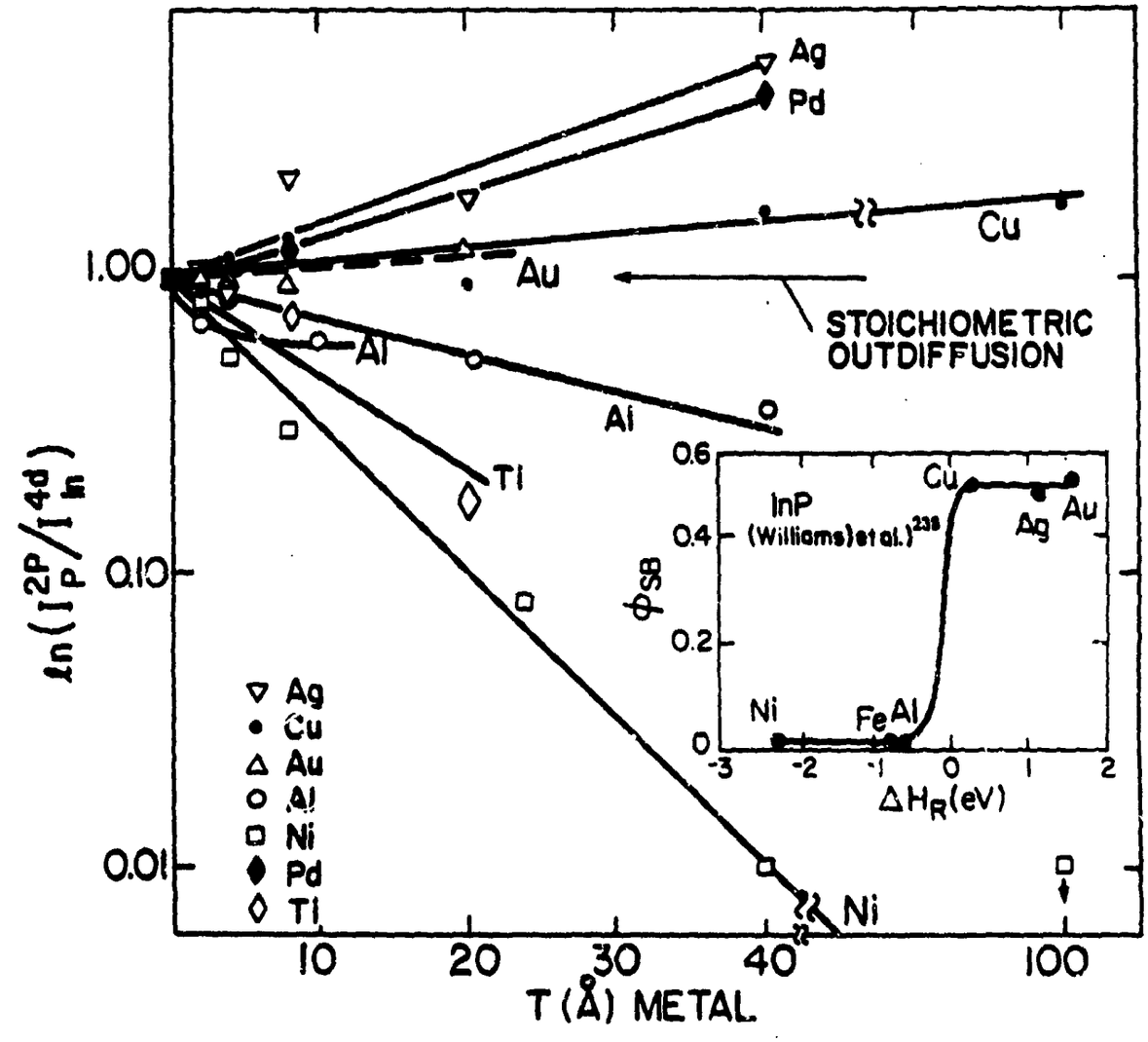
Ag
Pd
Cu
Au
STOICHIOMETRIC
OUTDIFFUSION
Al
Al
Tl
Ni
1.00
0.10
0.01
$\ln(I_P^{2P}/I_{In}^{4d})$
Ag
Cu
Au
Al
Ni
Pd
Tl
10
20
30
40
100
T (Å) METAL
0.6
0.4
0.2
0
$\phi_{SB}$
InP
(Williams) et al.[238]
Cu
Ag
Au
Ni
Fe
Al
-3
-2
-1
0
1
2
$\Delta H_R$(eV)

(4)

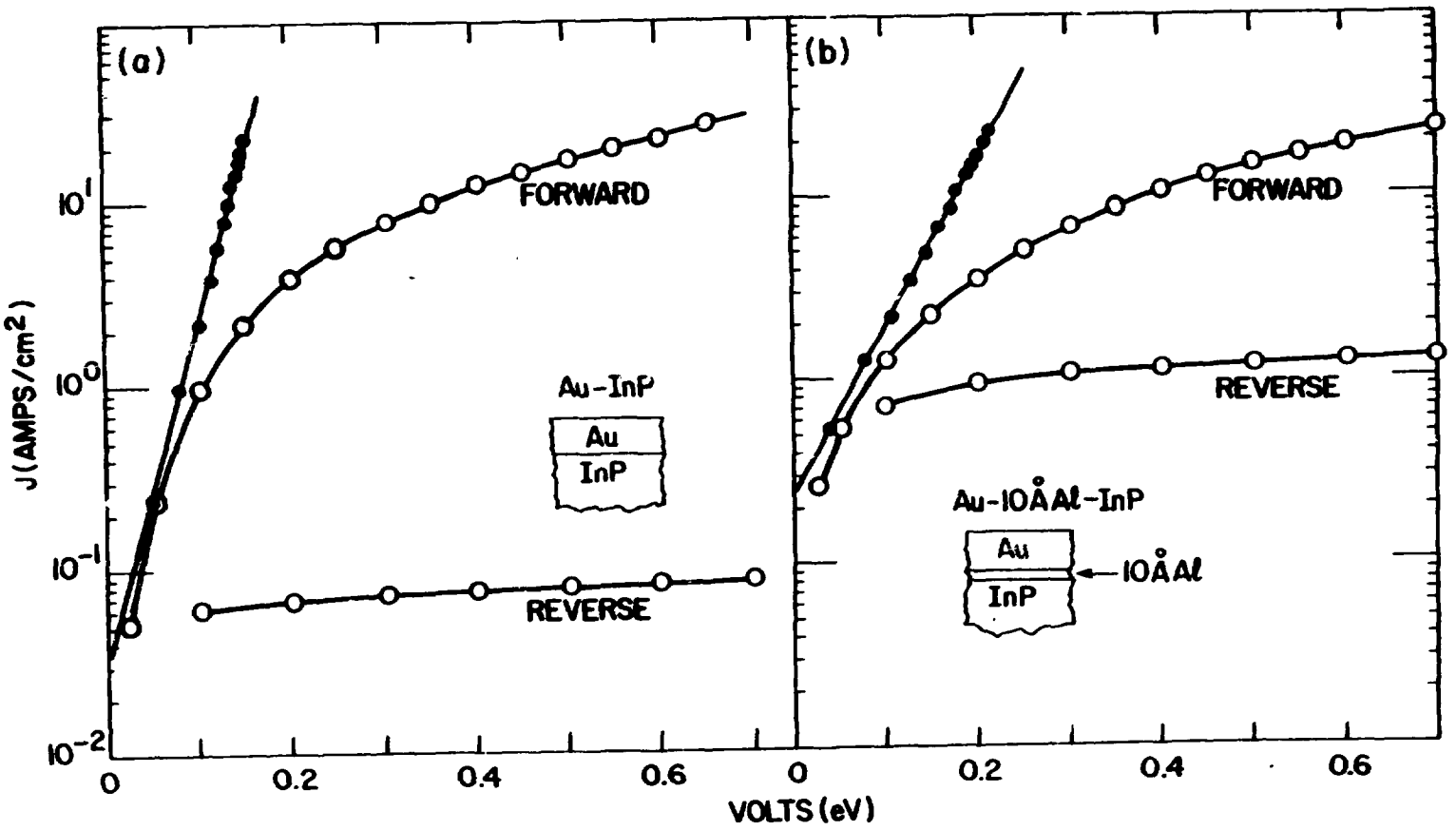
(a)
(b)
FORWARD
REVERSE
Au-InP
Au
InP
Au-10ÅAl-InP
10ÅAl
J(AMPS/cm²)
VOLTS(eV)
10¹
10⁰
10⁻¹
10⁻²
0
0.2
0.4
0.6

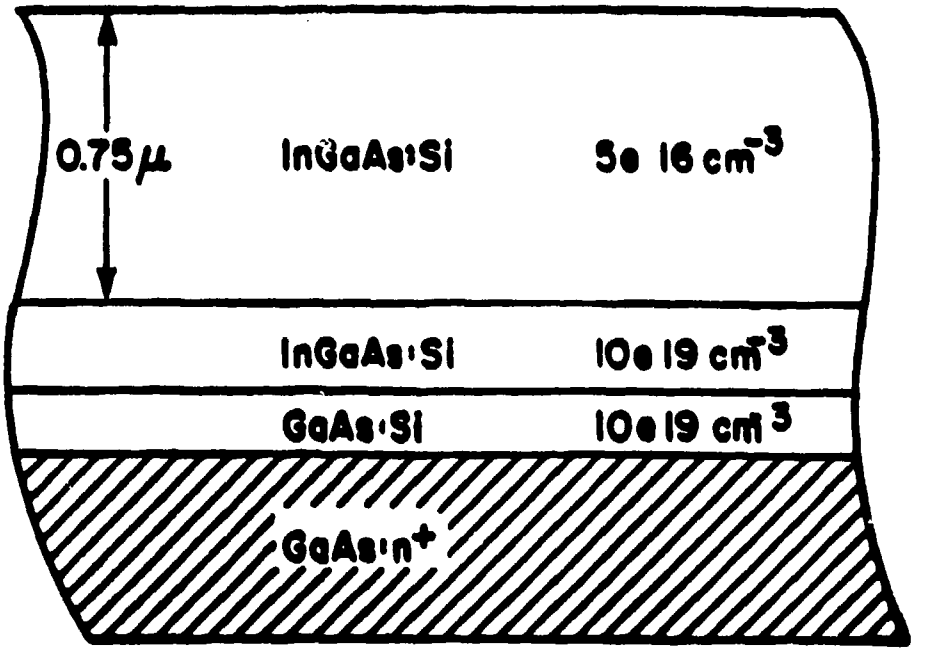
0.75 μ
InGaAs:Si
5e 16 cm⁻³
InGaAs:Si
10e 19 cm⁻³
GaAs:Si
10e 19 cm⁻³
GaAs:n+

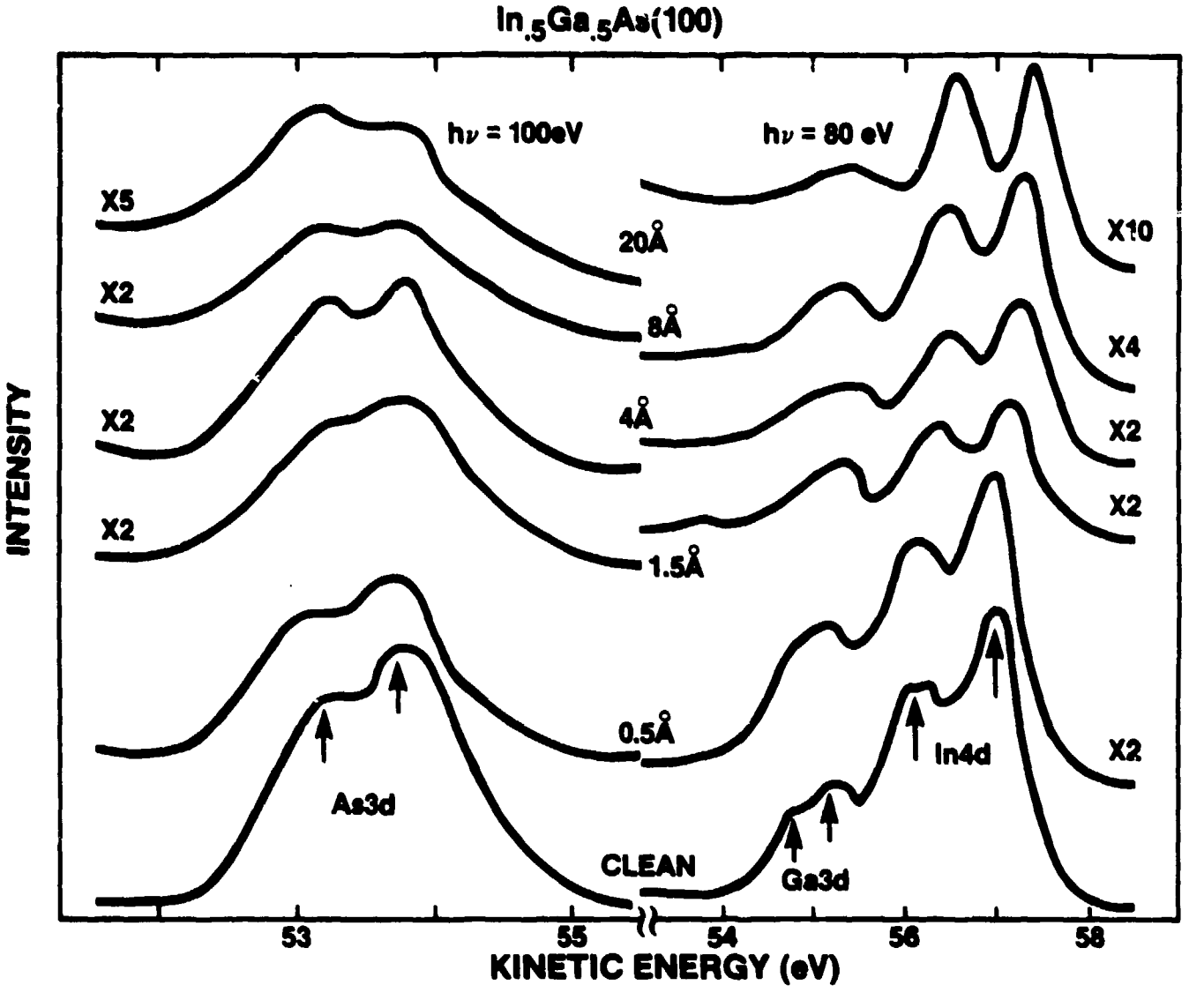
In.5Ga.5As(100)
hν = 100eV
hν = 80 eV
X5
X2
X2
X2
20Å
8Å
4Å
1.5Å
X10
X4
X2
X2
X2
0.5Å
As3d
CLEAN
Ga3d
In4d
X2
INTENSITY
53
55
54
56
58
KINETIC ENERGY (eV)

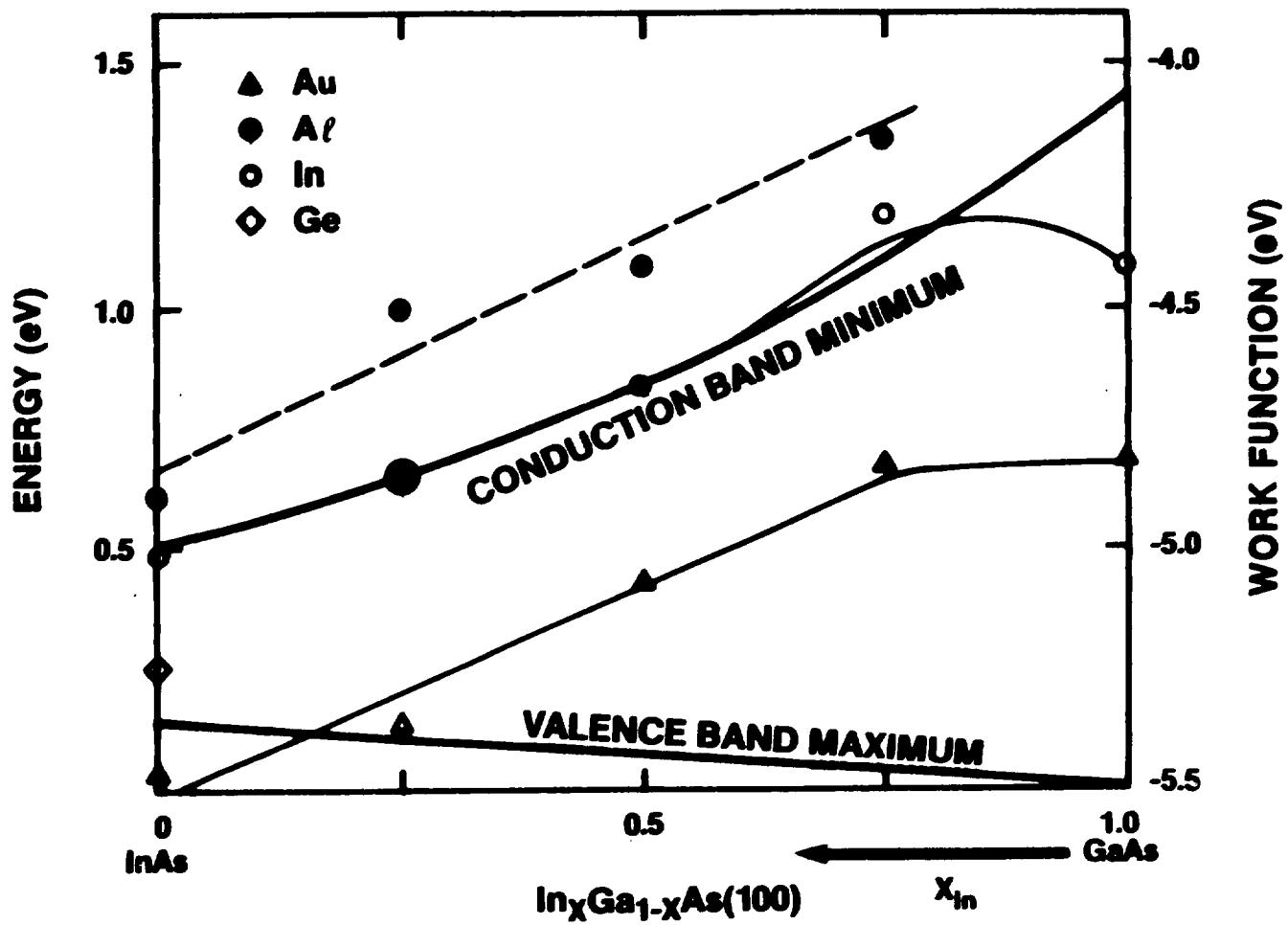
1.5
1.0
0.5
ENERGY (eV)
Au
Aℓ
In
Ge
CONDUCTION BAND MINIMUM
VALENCE BAND MAXIMUM
-4.0
-4.5
-5.0
-5.5
WORK FUNCTION (eV)
0
InAs
0.5
1.0
GaAs
$In_XGa_{1-X}As(100)$
$X_{In}$

# CATHODOLUMINESCENCE SPECTROSCOPY OF METAL/III-V SEMICONDUCTOR INTERFACE STATES

R. E. Viturro, M. L. Slade, and L. J. Brillson,
Xerox Webster Research Center, Webster, NY 14580, USA.

We have employed optical emission techniques to characterize the formation and evolution of interface states with metal deposition on UHV cleaved (110) III-V semiconductor surfaces from submonolayer to multilayer coverages. We show that the evolution of the electron excited optical emission spectra of metal/InP and GaAs interfaces can be correlated to their $E_F$ movements and macroscopic Schottky barrier heights.

Metal/semiconductor (M/SC) interfaces have attracted considerable attention over the past few decades for both scientific and technological reasons[1]. Still, the nature of the interface electronic states and basic mechanism of Schottky barrier formation are not yet well understood [2]. For clean, ordered InP or GaAs (110), intrinsic gap surface states are absent, and a few monolayers of deposited metal create new interface states which stabilize the Fermi level ($E_F$) in a limited range within the band gap[3]. Here we report the most direct observation of these metal/SC interface states thus far. We have detected luminescence from interface states by means of cathodoluminescence spectroscopy[4](CLS), using a chopped electron beam from a glancing incidence electron gun and a $LN_2$ cooled Ge detector (North Coast)[4,5].

Figure 1 shows CL spectra from p-type InP(110), for mirror-like areas and step cleaved areas, and for submonolayer coverage of different reactive and unreactive metals deposited on the mirror-like InP cleavage. The CL spectra of clean InP shows only one emission centered at 1.35 eV within the energy range 0.6-1.6 eV, corresponding to the near-band gap (NBG) of InP at room temperature. On the other hand, the CL spectrum of step-cleaved areas shows weak emission at sub-band gap energies. This spectrum is similar to those obtained from submonolayer deposits of metals on mirror-like areas. Thus, the initial metal deposition disrupts the (110) surface, causing the formation of broken bonds, such as those formed during a step-cleavage process. Figure 2 shows the CL spectra of clean InP(110) and GaAs(110) with a series of metal overlayer thicknesses. We observe new emission features which reflect the modification of the SC surface upon metal deposition and the consequent formation of new states.

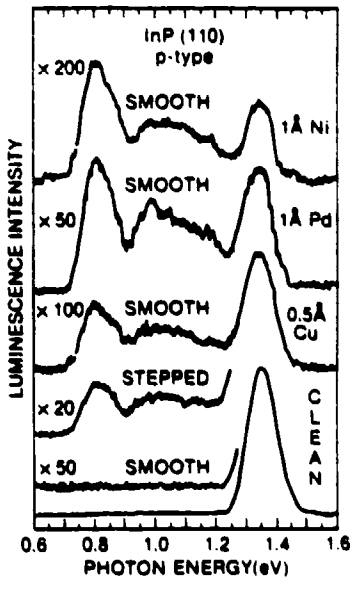


1. CL spectra of UHV mirror-like cleaved InP(110) surfaces before and after submonolayer Ni, Pd, or Cu deposition, and the step-cleaved surface

THIS PAGE IS MISSING IN ORIGINAL DOCUMENT

FIG 2

An overall reduction in NBG luminescence intensity with metal deposition appears in all the studied systems. The formation of a "surface dead layer" due to band bending in the SC depletion region reduces the radiative recombination[9]. In our case, we modify the surface potential of the SC by metal deposition, thus changing the width of the depletion region. Photo-emission experiments[10] show that the $E_F$ shifts are both a large but relatively slow function of the Au thickness and fast function of the Cu thickness.

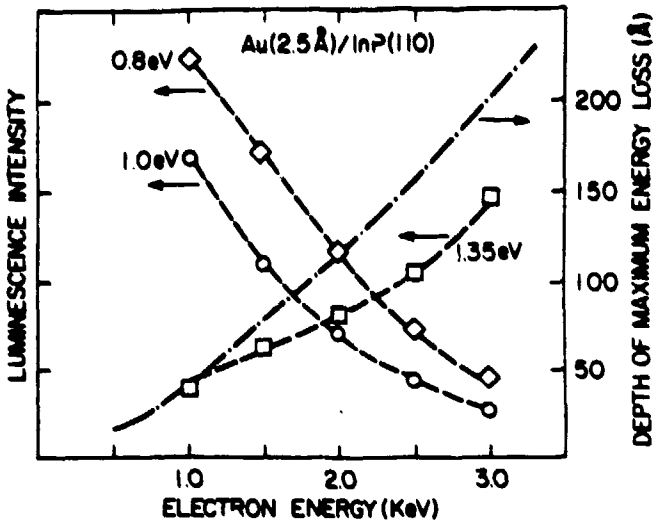


3. Dependence of the luminescence peak intensity on incident electron energy and excitation depth for 0.8 eV, 1.0 eV, and 1.35 eV emissions for 2.5 Å Au on InP(110).

These results correlate well with the observed evolution of the CL spectra upon Au and Cu deposition, and explains the corresponding disappearance of NBG emission. On the other hand, the deposition of Al on InP causes the formation of only a small band bending which builds up slowly with Al coverage[10], and the NBG transition is still detected after deposition of about 20 monolayers of Al.

Several possibilities exist for the origin and properties of the new detected transitions in the CL spectra of the metal/SC interface. Evidently, the perturbation caused by the initial metal deposition modifies the semiconductor surface structure and, consequently, the surface electronic structure. As more metal is deposited and the metal and SC interact, these states evolve into the interface states. These states cannot be assigned to metal induced gap states[11], because at such low coverage the overlayer is not yet metallic. At higher coverages, the spectral shape rules also out possibilities such as surface amorphization which would produce structureless optical emission spectrum or a broad NBG wing.

Diffusion of the metal in the SC, on the other hand, may cause the formation of a highly doped thin layer, which may account for the obeserved optical emission spectra. The high diffusion coefficient of Cu in InP, even at temperatures as low as 400 C[12], suggests that an in-diffusion process may form a thin highly doped layer, even near room temperature. However, we have not found clear correlation between the emission energies of the metal/InP interfaces and optical emission from the same metal-doped InP [12,13]. The results suggest that simple diffusion of the metal deep into the semiconductor is not the process which causes the formation of centers that give rise to the obeserved optical emission. More likely, interdiffusion of the different species and the formation of an interlayer with particular electronic properties will be responsible for the optically detected interface states.

# Optical Emission Properties of Metal / InP and GaAs Interface States

R. E. Viturro, M. L. Slade, and L. J. Brillson
Xerox Webster Research Center, Webster, NY 14580

## ABSTRACT

We have measured optical emission from interface states formed by metal deposition on UHV-cleaved InP(110) and GaAs(110) surfaces by means of cathodoluminescence spectroscopy. Our study reveals discrete levels distributed over a wide range of energies and localized at the microscopic interface. Our results demonstrate the influence of the metal, the semiconductor and its surface morphology on the energy distributions. The detailed evolution of optical emission energies and intensities with multilayer metal deposition exhibits a strong correlation between the deep gap levels, the Fermi level movements and Schottky barrier heights. The results demonstrate that in general electronic states deep within the band gap continue to evolve beyond monolayer coverage into the metallic regime.

## I. INTRODUCTION

The detection of metal-semiconductor (M/SC) interface states and the role they can play in the formation of Schottky barrier are central issues of research on condensed matter physics[1]. Research performed in the last few years using modern surface science techniques has uncovered a variety of systematics in the formation and evolution of Schottky barrier heights (SBH) upon metal deposition.[2]. The results obtained by these techniques strongly suggest that modifications of the chemical structure near the interface occur which can influence or even dominate the electronic structure and formation of the M/SC junction. For clean, ordered InP or GaAs (110), intrinsic gap surface states are absent, and a few monolayers of deposited metal create new charge states which stabilize the Fermi level ($E_F$) in a

limited range within the band gap[2]. Considerable spectroscopic evidence suggests that chemical effects (e.g., reaction and interdiffusion) take place concurrently which promote localized charge formation. Accordingly, several models have been proposed for the localized charge states which influence metal-compound semiconductor contact rectification, including gap states due to defects formed by metal atom condensation[3-5], metal-induced gap states defined by the semiconductor band structure[6] or by chemisorption and charge transfer involving metals atoms and clusters[7], chemically formed dipole layers[8] and effective work functions of interface alloys[9]. However, except for absorption studies of surface and interface states by total internal reflection[10] or surface photovoltage spectroscopy[11] and near edge photoluminescence of mechanically-damaged surfaces[12], the presence and energies of interface states have been inferred largely from measurements of capacitance[1,13], current[1,14], and $E_F$ movement[2-7,9].

We have performed cathodoluminescence spectroscopy (CLS)[15,16,17] and photoluminescence (PL) studies of the formation and evolution of interface states with metal deposition on UHV-cleaved (110) InP and GaAs semiconductor surfaces from submonolayer up to several monolayers, where the metallic state of the overlayer is well defined. We show that dramatic changes are produced in the optical emission properties of III-V SC upon metal deposition, causing the formation of both broad and structured emission bands at energies lower than the band gap. The study reveals the influence of the particular metal, the semiconductor, its morphology and bulk growth quality on the spectral distribution. Furthermore, we also show that the evolution of electron-excited optical emission spectra of metal/InP or GaAs interfaces can be correlated to their $E_F$ movements and macroscopic Schottky barrier heights (SBH).

## II. EXPERIMENTAL

Figure 1 shows a schematic diagram of the UHV chamber (base pressure = $5 \times 10^{-11}$torr) used in our experiments. It incorporates a variety of surface science techniques. The CLS excitation was produced by a chopped electron beam from a glancing incidence electron gun impinging on a (110) crystal face. The electron beam energy can be varied between 500-3500 eV to vary the depth of electron excitation. PL excitation was produced by a HeNe laser ( photon energy = 1.96 eV). The luminescence was focussed into a monochromator and the transmitted signal was phase-detected by means of a $LN_2$ cooled Ge detector (North Coast, $D^* = 5 \times 10^{14}$ cm $Hz^{1/2}$ $W^{-1}$) and a lock-in amplifier. Both the monochromator scan energies and the signal acquisition were controlled by a Data General Nova 2/10 minicomputer. We used single crystals InP ($n = 4.3 \times 10^{15}$ $cm^{-3}$, $p = 10^{18} cm^{-3}$) and GaAs ($n = 4 \times 10^{15}$ $cm^{-3}$, $p = 1.8 \times 10^{18} cm^{-3}$) from Metal Specialties. The specimen was mounted in a manipulator in such a way the (110) crystal face could be moved in a plane perpendicular to the focal axis of the monochromator. This set up allowed us to scan the whole crystal area under identical excitation and detection conditions, and to investigate optical emission properties from different patches of the (110) cleaved crystal, mirror-like as well as step cleaved and rough areas. Metals were evaporated on cleaved (110) surfaces and film thicknesses were monitored by means of a quartz crystal oscillator positioned next to the cleaved surface. The values of the maximum steady state excess carrier concentration at the near surface region (N) were estimated following Pankove.[18] Briefly N is equal to the generation rate (G) times the carrier lifetime at the surface ($\tau$):

$$N = \frac{I}{1.6 \times 10^{-19} Ad} \cdot \frac{E_p}{E_o} \cdot \tau \quad \text{carriers cm}^{-3}$$

where I is the beam current, A the bombarded area, d the effective penetration depth, $E_p$ is the beam energy and $E_o$ is the energy needed to create an electron-hole pair. The beam current were usually in the range 0.1 - 4 μA. In order to search for possible electron beam induced effects electron beam currents of 25 μA were used. The area A ranges between $10^{-2}$ - $10^{-4}$ $cm^2$, depending on $E_p$. Depth d is energy-dependent and is estimated to range from below 50Å to above several hundred Å, as discussed below. $E_o$ is about 4.5 eV for InP and GaAs.[18] The carrier lifetime is about $10^{-9}$ sec, but could be much longer for trap states. These numbers give values of N ranging between $10^{14}$ - $10^{18}$ carriers per $cm^3$. No electron beam effects were found in the metal/SC results reported here.

## III. RESULTS

Fig. 2 shows CL spectra from p-type InP(110), for mirror-like areas and step cleaved areas, and for submonolayer coverage of different reactive and unreactive metals deposited on the mirror-like InP cleavage. Within the energy range 0.6-1.6 eV, only one emission centered at 1.35 eV appears, which corresponds to the energy band gap of InP at room temperature. Accordingly, we assign this peak to a near-band-gap (NBG) transition. For mirror-like areas there is no detectable emission in the energy region below the NBG transition over two orders of magnitude of injection level. However, the CL spectrum of step-cleaved areas (bottom spectra of Fig. 2) shows weak emission at sub-band gap energies. Small amount of metals deposited on top of the mirror-like InP surfaces causes drastic changes in the optical emission spectra, a strong decrease in the NBG emission intensity and the formation of a broad emission band at energies lower than the band gap. The similarities in the spectral shape between CL spectrum of step-cleaved areas and those from chemisorbed metals on mirror-like areas (upper spectra of Fig. 2) shows that the initial metal deposition cause the formation of broken bonds such as those formed during a step-cleavage process.

Figure 3 shows the CL spectra of the clean InP(110) and of the metal/SC interfaces formed with a series of metal overlayer thicknesses. We observe new emission features which reflect the modification of the SC surface upon metal deposition and the consequent formation of new states. In each series the bottom spectrum corresponds to a clean mirror-like cleavage InP(110). Fig. 3(a)-(d) show that the changes produced in the optical emission properties of InP upon metal deposition are strongly dependent on the particular metal. Figures 3(a), (b), (c), and (d) show CL spectra from Au, Cu, and Al, on n-type InP, and Pd on p-type InP respectively. For Au deposition, Fig. 3(a), exhibits a broad band whose energies extend up to the onset of the NBG transition. Deposition of 15 Å of Au reduces the relative intensity of the emissions at energies higher than 0.9 eV drastically. In comparison to the Au/InP system, Cu deposition on InP Fig. 3(b) shows a different dependence on metal thickness. These interface states evolve faster with metal thickness than the Au/InP case. This result is consistent with $E_F$ movements extracted from photoemission core level shifts for these interfaces[19], which showed similar rates of change and differences between Au and Cu.

The mid-gap emission is a common feature between the Au and Cu/InP interfaces. However, there are differences in the spectral shape at higher energies. On the other hand, the CL spectra of increasing Al thicknesses on InP show that the NBG transition dominates the spectral shape even after deposition of 20 A of Al on InP, whereas the low energy emissions, similar to those of bottom of Fig. 3(a), are formed at low metal thickness and does not evolve with further Al deposition. The overall luminescence intensity is drastically reduced, but the spectral shape is not substantially changed by Al deposition. Similar low energy emission shape is shown in the Pd/p-InP case ( Fig. 3(d)) even though the NBG transition is totally supressed. The p-type InP samples shows lower overall luminescence efficiency than the n-type samples, but the behavior of reactive transition metals such as Pd, Ni (not shown) and Al on the p-type specimen is different only in the persistence of the NBG

transition at multilayer coverages. The spectral shape is roughly independent of doping type.

Fig. 4 shows CL spectra of the Au/GaAs(110) system. The bottom spectrum corresponds to a mirror-like cleaved surface and shows broad emission structure at energies lower than the band gap, as well as the 1.42 ev peak of the NBG transition. The deposition of Au on mirror-like n-type GaAs(110), depicted in Fig. 4, causes first a small shift of the 0.8 eV emission to lower energies. This new feature develops with increasing metal thickness and dominates the spectral shape after 15 Å of Au. The appearance of strong spectral features on the UHV-cleaved GaAs(110) surface differs sharply from the analogous InP spectra. Furthermore, the intensity of these features appears to depend on bulk doping.[20] Nevertheless, the changes in spectral features with Au thickness in Fig. 4 permit a distinction to be made between bulk and metal-induced features.

Figure 5 shows the dependence of peak intensity on excitation energy for Au(2.5 Å)/InP(110), which corroborates the surface localized nature of the low energy transitions, since the excitation depth increases with incident energy. The intensity of three emission peaks are plotted: the NBG transition, the broad band emission at 1.0 eV and that at 0.8 ev. The experimental data have been normalized to constant excitation power. This is justified because there is no dependence of the spectral shape on injection level for the Au/InP(110) system. The excitation depth was varied by changing the electron beam energy between 1 KeV and 3 KeV. The intensities of the two lower energy transitions decay and that of the NBG transition increase with increasing energy / excitation depth.

Figure 6 depicted Cl spectra for Pd (4Å)/p-InP(110) for several electron beam energies/excitation depths at constant electron beam current of 4 μA. Clearly, as the electron energy/excitation depth is increased, electron-hole pairs are generated

beyond the depletion layer and can radiatively recombine, giving rise to a relative increase in NBG transition intensity (see below).

A more quantitative analysis of excitation depth requires consideration of the maximum of the energy loss per unit length.[21] This parameter gives the depth below the surface at which the energy loss to the plasmon, the fastest energy loss mechanism within our energy range,[22] is a maximum. Unfortunately there is no experimental data for such low electron energies. The experimental, as well as the theoretical results, are given for electron energies higher than 5 kV.[21] For those energies, Gaussian models for the spatial distribution of the electron beam excitation and simple scaling in energy for the distribution of the excitation with depth have proven to reflect accurately the experimental results.[21,23] We have extrapolated these results to the energy range 500-4000 eV, and computed the depth of the maximum energy loss. The extrapolation is justified since the change of the electron energy loss rate to the plasmon with increasing energy is slow over a wide range of energies.[22] The results of the calculation are depicted in Fig. 5, referred to the right side scale. The calculation applies to normal incidence of the electron beam. For glancing incidence, one expects a still lower depth of the maximum energy loss[24].

## IV. DISCUSSION

An overall reduction in NBG luminescence intensity with metal deposition is observed in all the studied systems. The relative efficiency of the radiative recombination process between different systems cannot be estimated without knowing the attenuation of the electron beam within the particular metal overlayer. This attenuation will depend mainly on the type of film that is formed by a particular metal. However, for coverages of only several layers, we can assume that the attenuation of the electron beam is similar to all the systems, and a qualitative correlation between the diminution of NBG luminescence intensity and

the particular metal can be done. The dependence of the NBG luminescence intensity on surface quality was reported in the past.[25] It was qualitatively explained in terms of surface potential, which causes the formation of a "surface dead layer", roughly the SC depletion region, in which little radiative recombination occurs.[25] In our case, we modify the surface potential of the SC by depositing different metals at different thicknesses, thus changing the width of the depletion region. The photoemission experiments show that the $E_F$ shifts are a relatively slow function of the Au thickness and a fast function of the Cu thickness[19]. These results correlate well with the observed evolution of the CL spectra upon Au and Cu deposition. Thus, the fast and large movement of $E_F$ with deposition of 2.5 A of Cu on InP causes a large depletion region and explains the corresponding absence of NBG emission. Deposition of Al on InP causes the formation of only a small band bending.[14,19] Hence the NBG transition is still detected after deposition of about 20 monolayers of Al. The NBG intensity reduction observed for Pd/p-InP is also consistent with the large $E_F$ movement expected.[19]

Several possibilities exist for the origin and properties of the new detected transitions in the CL spectra of the metal/SC interface. Evidently, the perturbation caused by the initial metal deposition modifies the semiconductor surface structure and consequently the surface electronic structure. As more metal is deposited and the interface between metal and SC forms, these states evolve into the interface states. These states cannot be assigned to metal induced gap states[6], because at such low coverage the overlayer is not yet metallic. At higher coverages, the spectral shape rules also out possibilities such as surface amorphization which would produce structureless optical emission spectrum or a broad NBG wing. Diffusion of the metal in the SC, on the other hand, may cause the formation of a highly doped thin layer, which may account for the observed optical emission spectra. The high diffusion coefficient of Cu in InP, even at temperatures as low as 400 $^0$C,[26] suggests that an in-diffusion process may form a thin highly doped layer, even near room

temperature. However, we have not found clear correlation between the emission energies of the metal/InP interfaces and optical emission from the same metal-doped InP.[26,27] A recent luminescence investigation of Cu metal diffusion in InP[26] at various temperatures showed the formation of a neutral complex at 400 $^0$C, which evolved with increasing temperature, giving rise to an intense band at ca. 1.0 eV, versus our band at 0.78 eV. The results suggest that simple diffusion of the metal deep into the semiconductor is not the process that causes the formation of centers that give rise to the observed optical emission. More likely, interdiffusion of the different species and the formation of an interlayer with particular electronic properties will be responsible for the optically - detected interface states.

The energy levels involved in the optical emission spectra can be established only with respect to either conduction or valence band edges. The modification of the surface SC band structure by metal deposition results in the formation of a interface density of states which shows dominant features at particular energies. Because of the localized nature of these interface states, the associated levels must act as either electron traps (et) or hole traps (ht). Then, for a n-type SC, the observed features correspond to et-to-VBM, et-to-ht, CBM-to-ht, and NBG transitions. The NBG transition is strongly dependent on band bending, as it was discussed above. In principle, we can also include the CBM-to-ht in this category, because both require free electrons moving against the electric field produced by the band bending. The et-to-ht transition cannot ruled out on the basis of spatial localization arguments, because we expect both traps to be localized on the metal/SC interface, and we have no cause to assume greatly different concentrations of electron versus hole traps. However, for a n-type SC, because of the hole accumulation on the interface region, transitions that have as final state the valence band maximum are more likely to occur. Thus, we assume that the et-to-VBM transitions have the highest probability of occurrence and that the cross section for radiative recombination is constant within the energy range of interest. Under this assumption, the optical

emission spectrum of metal/InP and GaAs can be aligned in energy with respect to the semiconductor VBM or CBM. We now can correlate this analysis with the evolution of $E_F$ and the values of the SBH measured in the metal/InP and GaAs systems. A high density of states at a particular energy will influence the movements of $E_F$ and "pin" the Fermi level. For Au and Cu/InP systems, as more metal is deposited, the interface density of states evolves and peaks at about 0.58 eV below the CBM. The SBH of those systems are about 0.43-0.5 eV [3-5]. This value is close to the energy distance between the 0.78 eV emission, which dominates the spectral shape, and the CBM. Surface photovoltage spectra of Au on InP(110) support this spectral interpretation[11], although CLS alone provides optical evidence at metallic coverages. The Al/InP system, on the other hand, shows a SBH of about 0.2 eV or smaller.[14,19] This correlates well with the persistence of the NBG transition and weak sub-band gap emission detected. For Au/GaAs, a similar analysis results in a SBH of about 0.7 eV, whereas electric measurements gives a value of 0.8-0.9 eV[3]. Of course, $E_F$ stabilization need not be precisely at density-of-states peak but rather may be weighted or averaged toward such a value from the bulk $E_F$ position. Significantly the states formed by initial metal deposition are <u>not</u> the same as those which evolve at multilayer coverage. Hence these results emphasize the importance of measuring interface electronic structure beyond monolayer coverages.

## V. CONCLUSIONS

The experimental data presented above clearly shows that it is possible to observe the formation and evolution of metal/SC interface states by optical emission techniques. We were able to distinguish between interface states promoted by multilayer metal deposition from those of step-cleaved areas. The CL spectra show qualitative differences between metals, especially with different chemical reactivity. The experiments demonstrate that these new states are distributed over a wide range of energies, and that they are localized on the metal/SC interface. Dominant features of the CL spectra of metal/SC show interface

levels at energies which can account for Schottky barrier heights. These features of the "buried" metal-semiconductor interface show striking differences from the electronic structure induced by only monolayer metal coverages.

## ACKNOWLEDGMENTS

Partial support by the Office of Naval Research (ONR N00014-80-C-0778) and fruitful discussions with Christian Mailhiot are gratefully acknowledged.

## REFERENCES


1. S. M. Sze, **Physics of Semiconductor Devices**, 2nd ed. (Wiley-Interscience, New York, 1981) ch.5.

2. L. J. Brillson, Surf. Sci. Rept. **2**, 123 (1982), and references therein.

3. W. E. Spicer, I. Lindau, P. Skeath, and C. Y. Su, J. Vac. Sci. Technol. **17**, 1019 (1980).

4. H. H. Wieder, J. Vac. Sci. Technol. **15**, 1498 (1978).

5. R. H. Williams, J. Vac. Sci. Technol. **18**, 929 (1981).

6. J. Tersoff, Phys. Rev. Lett., **52**, 465 (1984).

7. R. Ludeke, T. C. Chiang, and T. Miller, J. Vac. Sci. Technol. **B1**, 581 (1983).

8. L. J. Brillson, J. Vac. Sci. Technol. **16**, 1137 (1979).

9. J. L. Freeouf and J. M. Woodall, Appl. Phys. Lett. **39**, 727 (1981).

10. G. Chiarotti, S. Nannarone, R. Pastore, and P. Chiradia, Phys. Rev. **B4**, 3398 (1971).

11. Y. Shapira, L. J. Brillson, and A. Heller, Phys. Rev. **B29**, 6824 (1984).

12. R. A. Street, R. H. Williams, and R. S. Bauer, J. Vac. Sci. Technol. **17**, 1001 (1980).

13. P. S. Ho, E. S. Yang, L. Evans, and X. Wu, Phys. Rev. Lett. **56**, 177 (1986).

14. J. H. Slowik, H. W. Richter, and L. J. Brillson, J. Appl. Phys. **58**, 3154 (1985).

15. R. E. Viturro, M. L. Slade, and L. J. Brillson, Phys.Rev.Lett. **54**, 490(1986).

16. L. J. Brillson, H. W. Richter, M. L. Slade, B. A. Weinstein, and Y. Shapira, J. Vac. Sci. Technol. **A3**, 1011 (1985).

17. B. G. Yacobi and D. B. Holt, J. Appl. Phys. **59**, R1 (1986), and references therein.

18. J. I. Pankove, **Optical Process in Semiconductors**, page 255 (Dover Publications, 1975).

19. L. J. Brillson, C. F. Brucker, A. D. Katnani, N. G. Stoffel, R. Daniels, and G. Margaritondo, J. Vac. Sci. Technol. **21**, 564 (1982).

20. R. E. Viturro and L. J. Brillson. Unpublished results.

21. D. B. Wittry, **Electron Beam Interactions With Solids**, 99 (1984), and references therein.

22. A. Rose, **RCA Review**, March, 98(1966) and December, 600(1966).

23. J. D. Brown, **Electron Beam Interactions With Solids**, 137 (1984).

24. K. Murata, Phys. Status Solidi **A36**, 527 (1976).

25. D. B. Wittry and D. F. Kyser, J. Appl. Phys. **38**, 375 (1967).

26. M. S. Skolnick, E. J. Foulkes, and B. Tuck, J. Appl. Phys. **55**, 2951 (1984).

27. H. Temkin, B. V. Duff, W. A. Bonner, and V. G. Keramidas, J. Appl. Phys. **53**, 7526 (1982).

## FIGURE CAPTIONS

1. Schematic diagram of the experimental apparatus for optical emission spectroscopies.

2. CL spectra of clean, mirror-like p-InP(110) surfaces before and after submonolayer Ni, Pd, or Cu deposition, and the clean step-cleaved surface.

3. CL spectra of (a) Au, (b) Cu, and (c) Al on clean mirror-like n-InP (110), and (d) Pd on clean, mirror-like p-InP (110) as function of incresing metal thicknesses.

4. CL spectra of clean, mirror-like n-GaAs (110) with increasing Au deposition.

5. Dependence of the luminescence intensity on incident electron energy and excitation depth for 0.8 eV, 1.0 eV and 1.35 eV emissions for 2.5 A of Au on n-InP(110).

6. CL spectral shape dependence on incident electron energy for Pd (4Å)/p-InP (110). Electron beam current 4 μA.

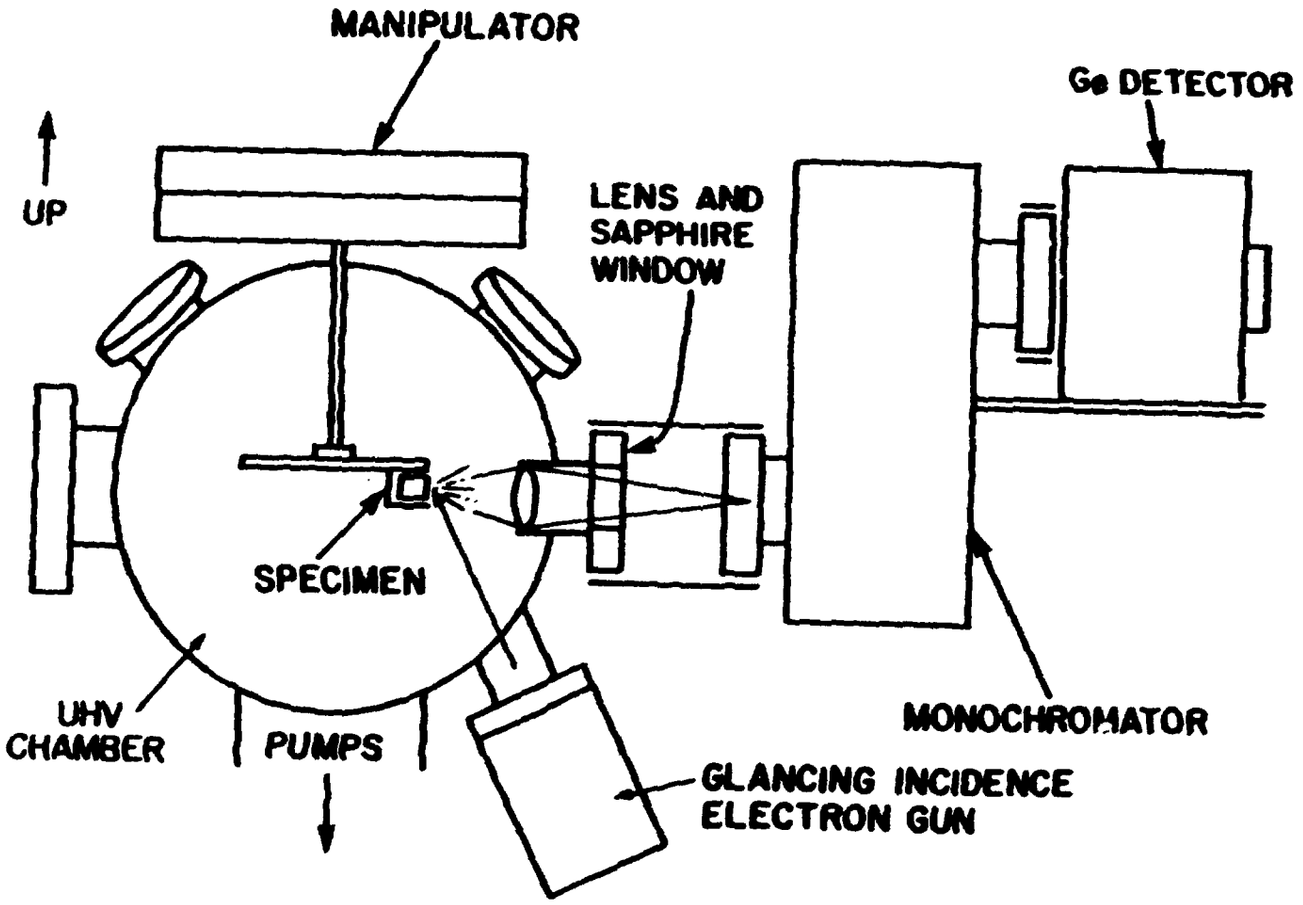
MANIPULATOR
Ge DETECTOR
UP
LENS AND
SAPPHIRE
WINDOW
SPECIMEN
UHV
CHAMBER
PUMPS
MONOCHROMATOR
GLANCING INCIDENCE
ELECTRON GUN

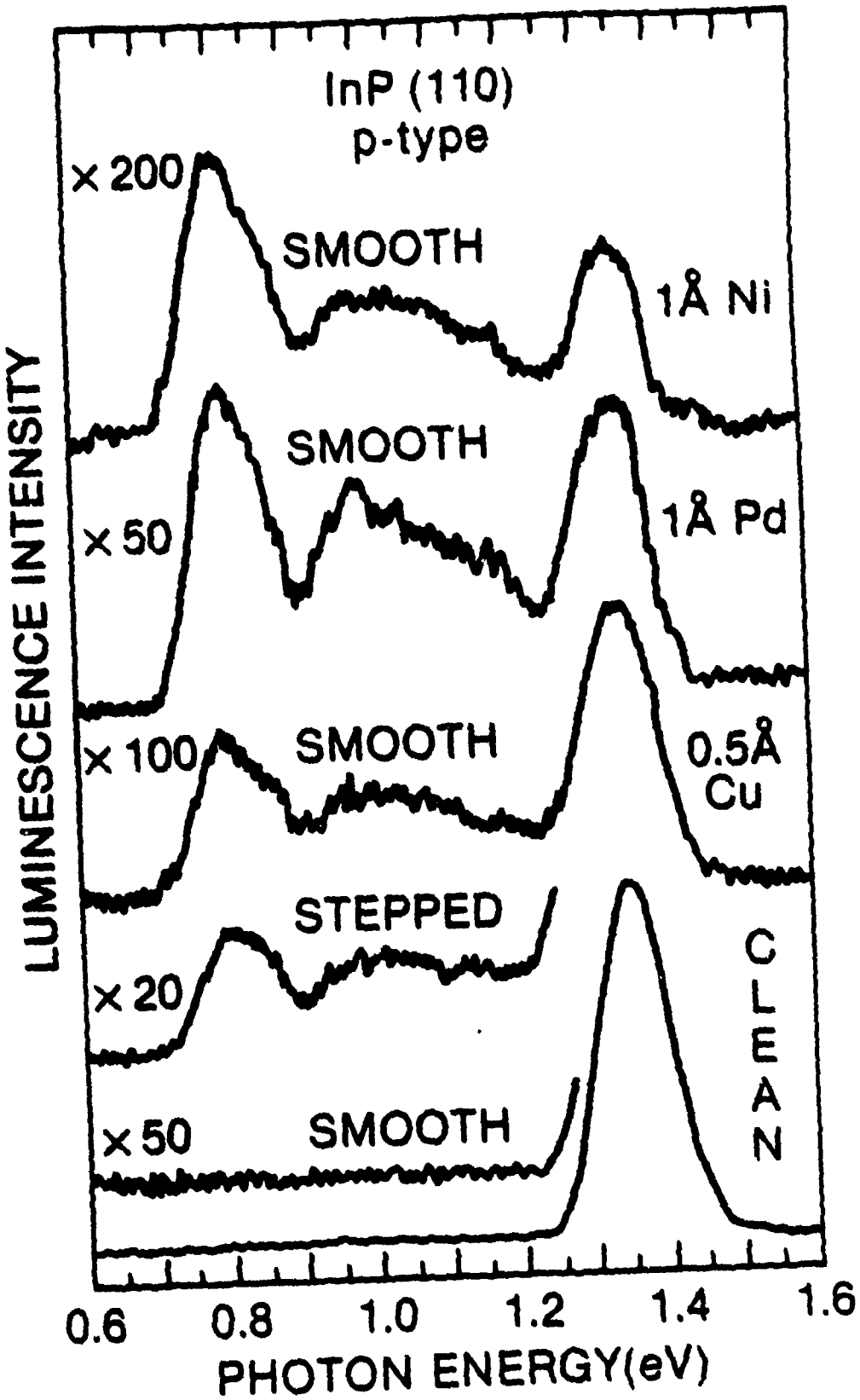
InP (110)
p-type
× 200
SMOOTH
1Å Ni
SMOOTH
× 50
1Å Pd
× 100
SMOOTH
0.5Å
Cu
STEPPED
× 20
CLEAN
× 50
SMOOTH
LUMINESCENCE INTENSITY
0.6
0.8
1.0
1.2
1.4
1.6
PHOTON ENERGY(eV)

Fig. 2

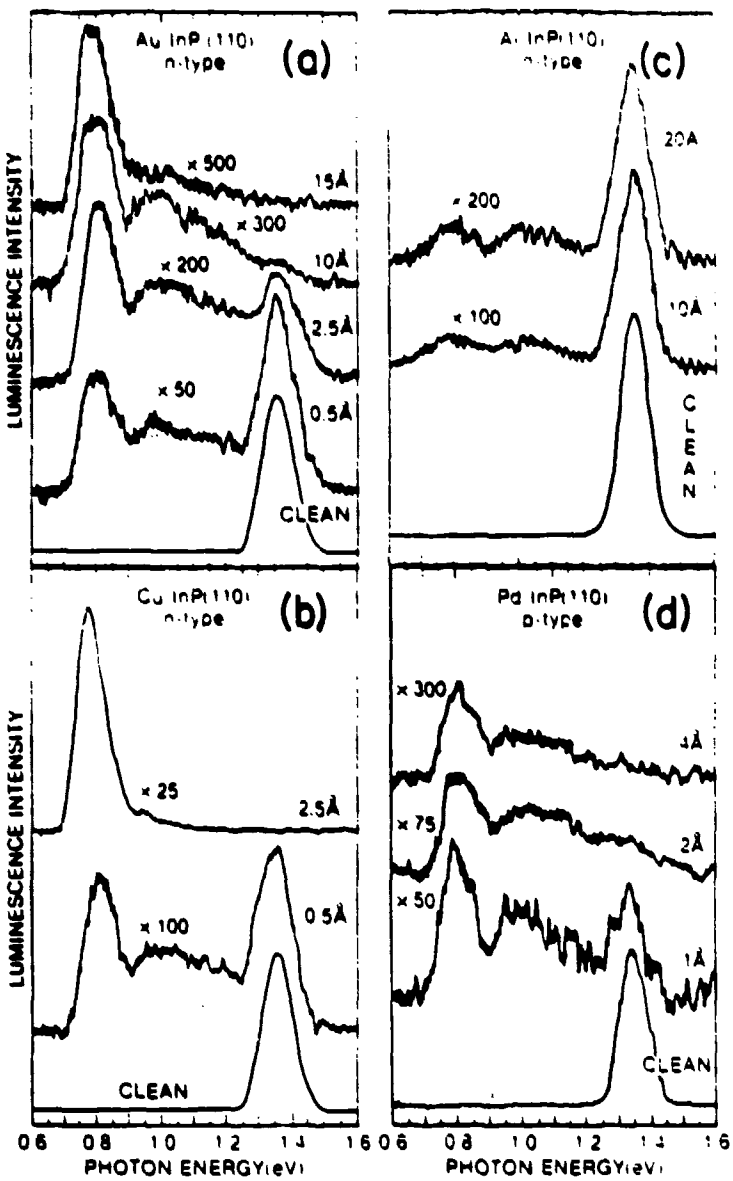
Au InP(110)
n-type
(a)
× 500
15Å
× 300
10Å
× 200
2.5Å
× 50
0.5Å
CLEAN
Al InP(110)
n-type
(c)
20Å
× 200
10Å
× 100
CLEAN
Cu InP(110)
n-type
(b)
× 25
2.5Å
× 100
0.5Å
CLEAN
Pd InP(110)
p-type
(d)
× 300
4Å
× 75
2Å
× 50
1Å
CLEAN
LUMINESCENCE INTENSITY
LUMINESCENCE INTENSITY
0.6 0.8 1.0 1.2 1.4 1.6
PHOTON ENERGY(eV)
0.6 0.8 1.0 1.2 1.4 1.6
PHOTON ENERGY(eV)

Fig. 3

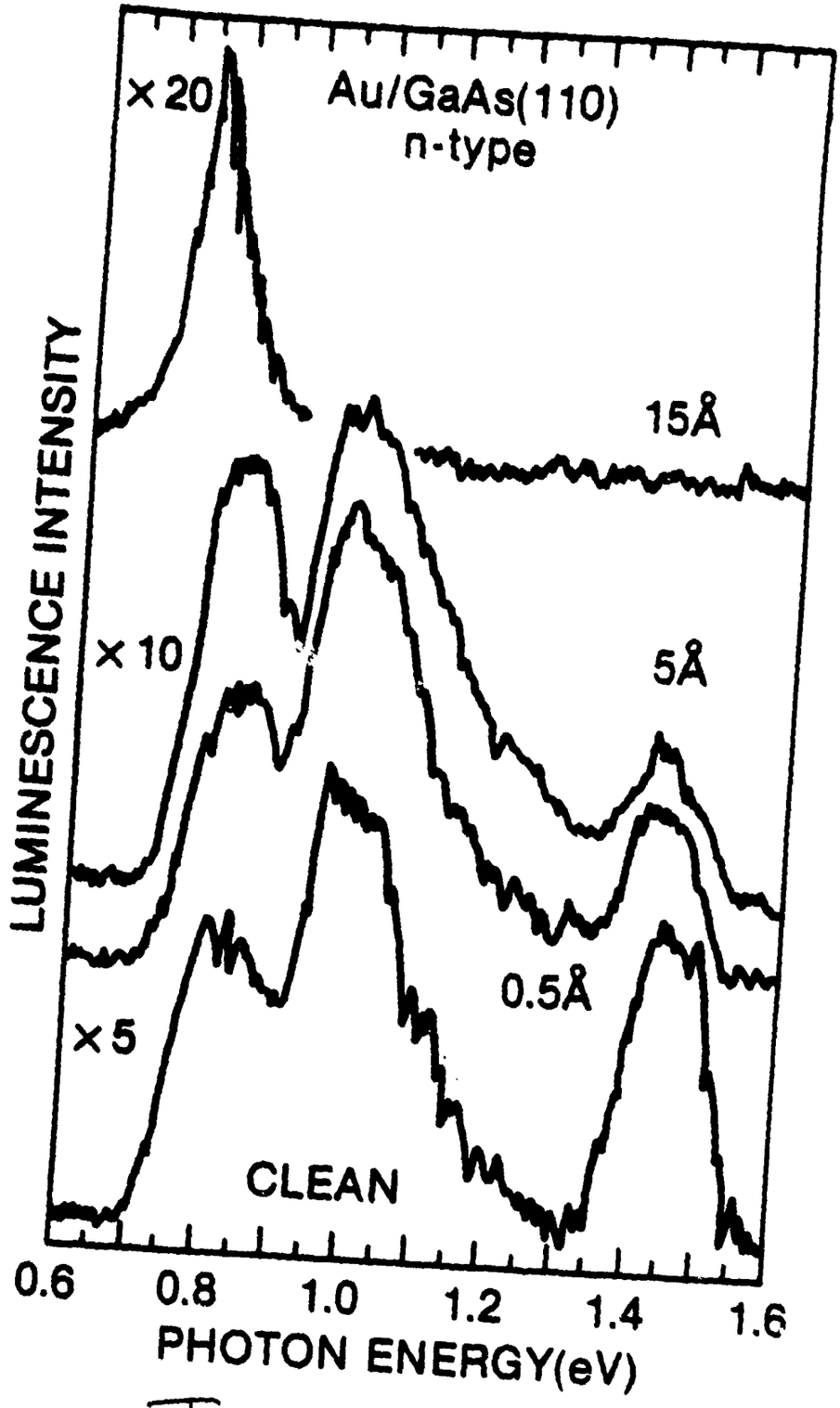
Au/GaAs(110)
n-type
×20
15Å
×10
5Å
0.5Å
×5
CLEAN
LUMINESCENCE INTENSITY
0.6
0.8
1.0
1.2
1.4
1.6
PHOTON ENERGY(eV)

Fig. 4

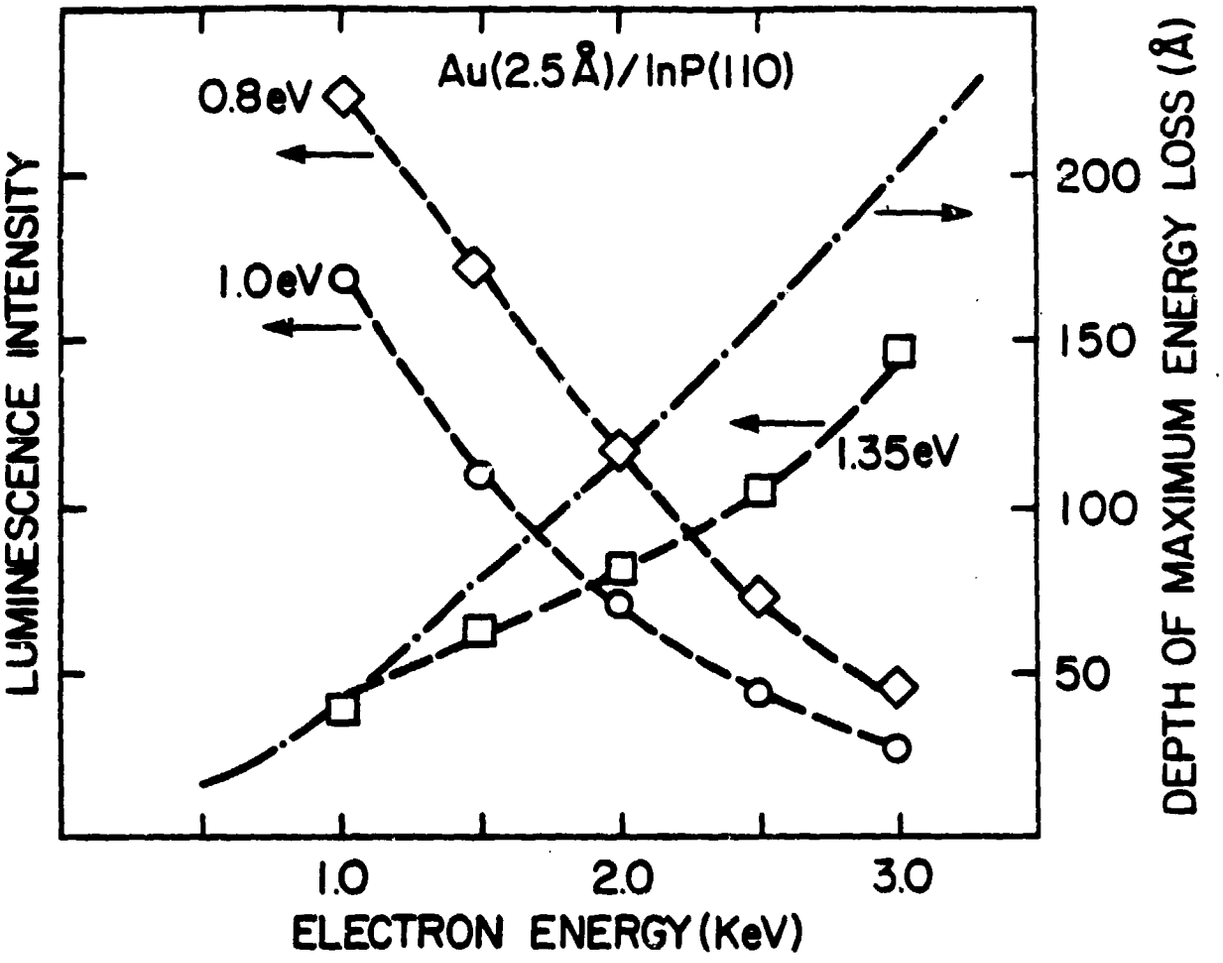
Au(2.5 Å)/InP(110)
0.8eV
1.0eV
1.35eV
LUMINESCENCE INTENSITY
DEPTH OF MAXIMUM ENERGY LOSS (Å)
200
150
100
50
1.0
2.0
3.0
ELECTRON ENERGY (KeV)

Fig. 5

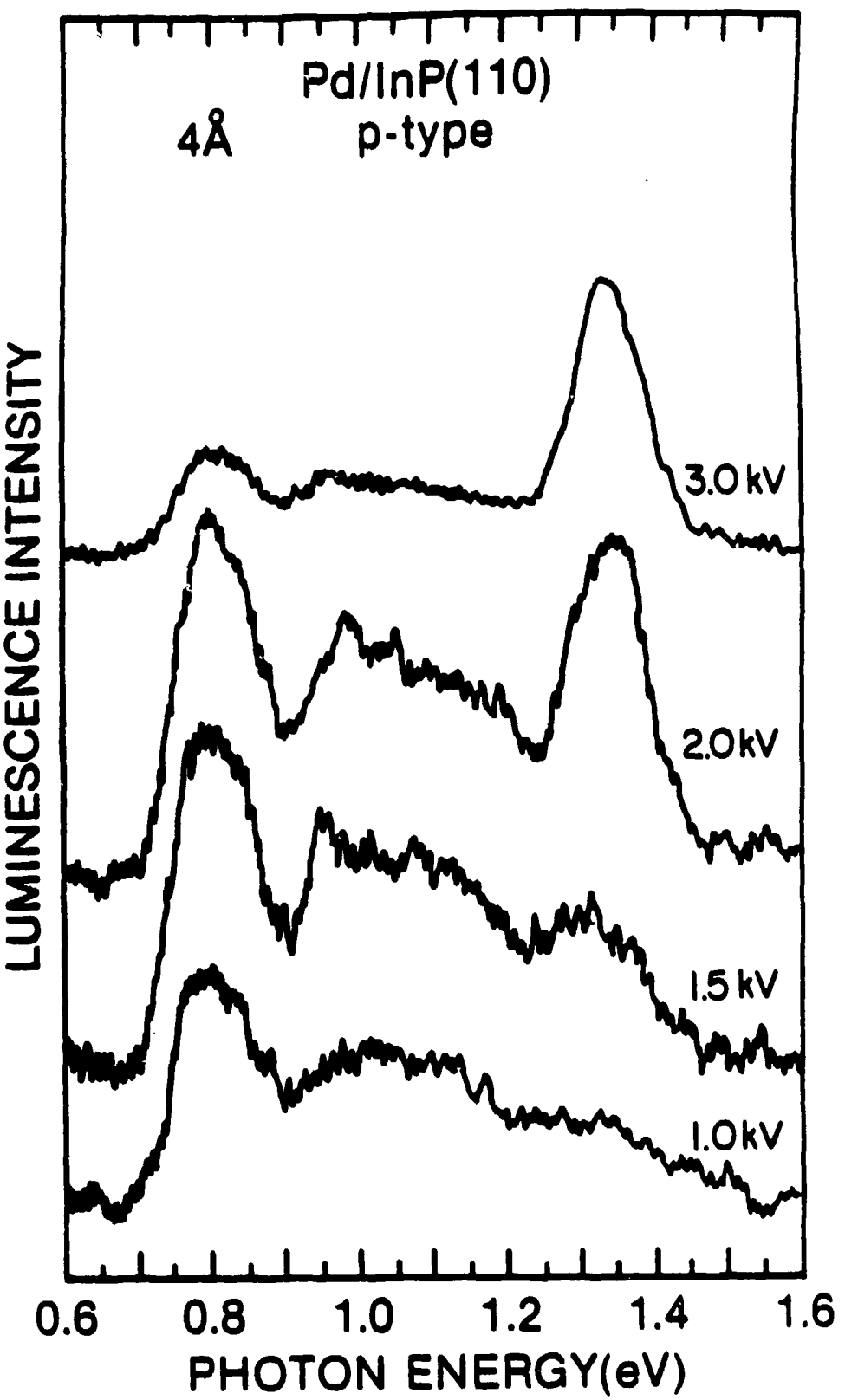
Pd/InP(110)
4Å
p-type
3.0 kV
2.0kV
1.5 kV
1.0kV
LUMINESCENCE INTENSITY
0.6
0.8
1.0
1.2
1.4
1.6
PHOTON ENERGY(eV)

Fig. 6

# Near-Ideal Schottky Barrier Formation at Metal-GaP Interfaces

L. J. Brillson, R. E. Viturro, and M. L. Slade

Xerox Webster Research Center, 800 Phillips Rd. 114-41D, Webster, NY 14580

P. Chiaradia

Istituto Struttura Material of CNR, Via E. Fermi, 00044 Frascati, Italy

D. Kilday, M. K. Kelly, and G. Margaritondo

Department of Physics, University of Wisconsin, Madison, WI 53706

## Abstract

Soft x-ray photoemission measurements of ultrahigh-vacuum-cleaved GaP (110) surfaces with In, Al, Ge, Cu and Au overlayers reveal Fermi level stabilization over a wide energy range and a near-ideal correlation between Schottky barrier height and metal work function. Coupled with recent findings for InAs (110) and $In_xGa_{1-x}As$ (100) ($x>0$) surfaces, these results demonstrate that Fermi level pinning in a narrow energy range is not representative of metal/III-V compound semiconductor interfaces.

## Introduction

The relative insensitivity of barrier heights at metal-semiconductor interfaces to differences in metal work function has formed the basis for extensive studies of Schottky barrier formation.[1] III-V compound semiconductors are widely believed to be leading examples of the strong Fermi level ($E_F$) "pinning" in a narrow range of band gap energies.[2] However, recent soft x-ray photoemission spectroscopy (SXPS) measurements of band bending for metals on clean, ordered $In_xGa_{1-x}As$ (100) ($x > 0$) and InAs (110) surfaces demonstrate that a wide range of $E_F$ movement is possible for metallization of several III-V compounds.[3] In contrast, metals on ultrahigh-vacuum (UHV)-cleaved GaAs (110) surfaces appear to give only a narrow (0.2 - 0.3 eV) range of $E_F$ positions.[4] In order to determine whether GaAs or the In-based compounds are more characteristic of III-V materials, we have investigated the $E_F$ movements of UHV-cleaved GaP during the initial stages of Schottky barrier formation. GaP is of particular relevance since: (a) $E_F$ movements induced by a wide range of metal work functions are not restricted by the band edges of this large (2.26 eV) indirect band gap semiconductor, (b) it is a binary Ga compound like GaAs rather than a ternary, and (c) Schottky barrier heights for metals on GaP exist thus far only for chemically-treated surfaces.[2,5,6] From the available data, researchers have concluded that GaP barrier height depend only weakly on metal work function:[7] for the relation $\Phi_B^n + \chi_{SC} = S\Phi_M + C$ between n-type Schottky barrier height $\Phi_B^n$, metal work function $\Phi_M$ and semiconductor electron affinity $\chi_{SC}$, the proportionality factor S is only 0.27 with a constant C = -3.76. Here $\chi_{GaP} = 3.75$ eV based on an ionization potential of 6.01 eV.[8] Besides a reevaluation of previous data, clean GaP/metal interfaces can gauge any surface state effects, since GaP is the only III-V compound semiconductor for which empty surface states are believed to be present within the band gap of the clean surface.[8]

In this Letter we report that, contrary to previous work, metal deposition does not pin the Fermi level of GaP in a narrow energy range. Instead, we observe a wide range of $E_F$ positions which correlate with metal work function. In fact, the dependence of Schottky barrier height on metal work function matches with ideal behavior on an absolute scale and with no adjustable parameters. For GaP, these results provide a clear distinction between the multiple models of Schottky barrier formation currently being proposed. Furthermore, when taken with band-bending measurements for the In-based compounds, the GaP results show that $E_F$ pinning in a narrow energy range is not a general characteristic of III-V compound semiconductors.

The GaP specimens used were bar-shaped single crystals with 5 x 5 $mm^2$ (110) cleavage faces. These were S-doped, $n \simeq 6 \times 10^{17} cm^{-3}$ for Ge, In, Au, and Cu studies and Te-doped, $n = 1.3 - 3.5 \times 10^{17} cm^{-3}$ for Au and Al. We cleaved these crystals in UHV (base pressure $8 \times 10^{-11}$ torr), evaporated metals from W filaments (pressure rise no greater than mid $10^{-9}$ Torr), and monitored depositions with a quartz crystal oscillator.

We measured the rigid P 2p and Ga 3d core level shifts as a function of Au, Al, Cu, In, and Ge depositions using 150 and 40 eV (170 and 60 eV) photons respectively to maximize (minimize) photoelectron escape depth and thereby probe core levels several monolayers below (the outermost monolayers of) the free surface. Rigid shifts of all core levels with increasing metal deposition correspond to $E_F$ shifts with respect to the band edges. In general, the relatively sharp P 2p spin-orbit split features provided clearer indications of $E_F$ movement than the Ga 3d feature. Nevertheless, both core levels were used to obtain average shifts except in cases

where additional dissociated Ga components altered the Ga 3d lineshape significantly. We used bulk-sensitive spectra to obtain these average shifts in order to minimize interference from any near-surface chemical shifts. In general, bulk and surface-sensitive core level spectra displayed similar energy shifts. We obtained the starting position of $E_F$ with respect to the band edges from the valence band edge at 60eV for the cleaved GaP surface versus similar surfaces after deposition of thick Au overlayers.

Figure 1 illustrates bulk-sensitive spectra for P 2p and Ga 3d core levels with increasing Cu deposition obtained with 150eV and 40eV respectively. Here the low kinetic energies corresponding to photoelectron escape depths of ~10-20Å.[9] Fig. 1 displays rigid shifts of both core levels to higher kinetic energy, corresponding to an increase in n-type band bending by 0.96 eV. Since the $E_F$ position of the cleaved surface was 1.95eV above the valence band edge, Fig. 1 indicates a corresponding $E_F$ stabilization energy of 0.99eV. Despite the enhanced escape depth, the Ga 3d core level feature displays an additional component shifted to higher kinetic energy due to dissociated Ga. This extra component appears at submonolayer Cu coverage and all but dominates the Ga 3d spectrum at 20Å coverage. In contrast, the P 2p core level exhibits no pronounced lineshape changes with metallization. Integrated peak areas of these structures in both bulk and surface-sensitive spectra reveal attenuation consistent with a continuous Cu overlayer versus island growth. Surface-sensitive spectra also show a slightly P-rich outdiffusion.

Figure 2 illustrates $E_F$ movements with respect to the GaP band edges as a function of Au, Al, Cu, Ge and In deposition. The $E_F$ stabilization energies extend over 1.1eV and indicate a wide range of Schottky barrier positions for metals on GaP (110). The $E_F$'s evolve to their final positions over 10-20Å, and exhibit different $E_F$

movements with metal coverage, reflecting chemical and electronic differences in the metal-GaP interaction. Each metal involves a different starting $E_F$ position which depends on the quality of cleavage. These cleavage differences appear to play at most a secondary role, as evidenced by the Ge data: two cleavages with different initial $E_F$ positions lead to almost identical stabilization energies at 5-20Å Ge coverages. Likewise, differences in n-type doping between the two GaP crystals appear to have only minor consequences: Au deposition on both crystals yields virtually the same $E_F$ behavior. Thus the SXPS data reveals a wide range in band bending for different metals, corresponding to Schottky barrier heights as low as 0.3eV and as high as 1.4 eV.

Figure 3 illustrates the dependence of $E_F$ stabilization energy on metal work function $\phi_M$. Here the energy below the GaP vacuum level appears as the electron affinity $\chi_{GaP}$ plus the n-type Schottky barrier height $\phi_B^n$. For comparison, the solid line with slope S = 1 and intercept C = 0 illustrates ideal Schottky barrier behavior - that is, $\chi_{sc} + \phi_B^n = \phi_M$. The match between the $E_F$ stabilization energy in the semiconductor and the $E_F$ below the vacuum level expected for the bulk metal is quite good, considering that these are absolute energy scales and there are no adjustable parameters. Bulk metal work function are obtained from photoemission experiments for Au[10] and Cu[10] and from internal photoemission experiments for In[11] and Al.[12] For Ge, we use the center of the Ge band gap since the overlayer is amorphous and since $E_F$ has been reported at the conduction band edge,[13] the valence band edge,[14] and energies in between,[13] depending on overlayer morphology and composition. An error bar denotes the corresponding uncertainty. We include a data point for Si on UHV-cleaved GaP crystal from a previous study.[15] The Si work function corresponds to the center of the amorphous Si band gap with error bars

extending ± 0.77eV (not shown). Vertical error bars indicate uncertainty in SXPS-determined $E_F$ energies.

A linear regression fit to the data yields slightly better agreement with S=1.07 and C=-0.22 (S=1.03 and C=-0.030 without the Si datum). However, the deviations from the S = 1, C=0 line in Fig. 3 are restricted to only two metals, Cu and Al, whose behavior can be accounted for by chemical differences. Of the metals shown, only Cu and Al can react with P to form compounds significantly more stable than GaP.[16] Because of their higher reactivity with P, these metals produce strong attenuation of the P outdiffusion, suggesting P accumulation and / or compound formation at the interface.[17,18] Such accumulation could shift $\phi_M$ toward that of P, equal to 5.04 eV.[19] In the case of Cu, $\phi_M$ = 5.0 eV produces excellent agreement with ideal Schottky behavior. Similarly, a 0.2eV increase of $\phi_M$ shifts the Al result to the expected theoretical value. Analogous deviations from ideal behavior due to chemical reactivity occur for the III-VI compound GaSe as well.[20] In contrast to GaAs[21] or InP[17], the stoichiometry of GaP outdiffusion is in general balanced or anion-rich , thereby minimizing any P accumulation at the interface.

The available data for clean metal/III-V compound semiconductor interfaces now reveal a wide range of $E_F$ behavior for GaP (110), InAs (110),[3] InAs (100),[3] $In_{0.75}Ga_{0.25}As$ (100)[3], $In_{0.50}Ga_{0.50}As$ (100)[3] and $In_{0.25}Ga_{0.75}As$ (100).[3] InP (110)[22] and GaAs (100)[3] display narrower ranges of $E_F$ stabilization, although surface treatments appear to expand these ranges significantly.[1] The range of $E_F$ stabilization for many III-V compounds (e.g., GaSb, InSb, AlSb, AlAs, and AlP) have not yet been explored. Only UHV- cleaved GaAs(110) surfaces appear to display "strong" $E_F$ pinning.[4]

Cleaved GaAs surfaces may in fact prove to be an exception rather than the rule because of the high concentration of imperfections in the bulk crystals used for actual experiments. This bulk material must be melt-grown and is known to contain the highest concentrations of deep level defects and impurities (> mid $10^{16}$ $cm^{-3}$) of all crystalline GaAs.[23] Furthermore, such bulk defects can getter to the cleaved and metallized surface, thereby increasing the local defect concentration even further. Whether GaAs grown by other techniques exhibits pinning which is just as "strong" remains to be determined, although preliminary results on GaAs (100) surfaces grown by molecular beam epitaxy suggest somewhat "weaker" pinning.[3]

These first measurements of Schottky barrier formation at clean metal-GaP interfaces provide strong distinctions between several current models of Schottky barrier formation. The large energy differences with metals do not support models based on pinning in a narrow energy range, where the effect of the metal is secondary. Included are models involving high densities of closely spaced defect energy levels[4,22] or metal-induced state pinning at a midgap position. Furthermore, a full range of classical work function behavior is difficult to interpret, much less predict, via perturbations from a single pinning position.[24] Such a model requires a substantial decrease in charge screening for GaP relative to GaAs, its III-V "pinned" counterpart, in order to account for our data. This change in charge screening must involve more than bulk dielectric properties[24,25] or electronegativity differences[25], all of which vary correspondingly by less than 20%. In contrast, the effective work function model of Woodall and Freeouf[26] predicts low densities of midgap "pinning" states for metallization of GaP, based on the expectation and observation[27] of little or no excess P at the interface. Our results confirm these expectations, with the Cu and Al deviations from classical behavior highlighting the role of interfacial P. In fact, recent microscopic analyses of metal-semiconductor interfaces suggest that

deviations from Schottky -like behaviors have their origin in atomic rather than electronic relaxations.[28]

In conclusion, we have observed a wide range of $E_F$ stabilization for metals on GaP (110) surfaces, including a good correlation with ideal Schottky barrier formation on an absolute scale. Taken with analogous results for InAs and $In_xGa_{1-x}As$ ($x>0$), these observations demonstrate that narrow-range $E_F$ pinning is not pervasive for III-V compounds and they suggest that metallization can provide greater control of III-V Schottky barriers than commonly believed.

Acknowledgements

Partial support by the Office of Naval Research (ONR N00014-80-C-0778) and conversations with J. Woodall and F. Jansen are gratefully acknowledged. We also thank the staff of the Synchrotron Radiation Center, supported by the National Science Foundation.

## Figure Captions

1. Normalized SXPS core level spectra for P 2p and Ga 3d core level spectra at hv = 150ev and 40eV respectively as a function of increasing Cu deposition.

2. Fermi level movements for ultrahigh-vacuum-cleaved GaP (110) as a function of Au, Al, Cu, Ge and In deposition. The stabilization energies at 10 or 20Å coverage span a range of 1.1eV.

3. Fermi level stabilization energies for Au, Al, Cu, Ge and In deposited on UHV-cleaved GaP (110). Left-hand scale reflects $E_F$ energy relative to GaP vacuum level. Right-hand scale indicates corresponding Schottky barrier heights. Solid line denotes ideal Schottky barrier behavior: $\chi + \phi_B^n = \phi_M$.

## References


1. L. J. Brillson, Surface Sci. Repts. 2, 123 (1982) and references therein.

2. S. M. Sze, *Physics of Semiconducting Devices*, 2nd ed. (Wiley-Interscience, New York), 1981) Ch. 5.

3. L. J. Brillson, M. L. Slade, R. E. Viturro, M. K. Kelly, N. Tache, G. Margaritondo, J. M. Woodall, P. D. Kirchner, G. D. Pettit and S. L. Wright, Appl. Phys. Lett. 48, 1458 (1986); J. Vac. Sci. Technol. B4, 919 (1986).

4. W. E. Spicer, I. Lindau, P. Skeath, and C. Y. Su, J. Vac. Sci. Technol. 17, 1019 (1980).

5. C. A. Mead, Solid State Electron. 9, 1023 (1966) and references therein.

6. G. P. Schwartz and G. J. Gualtieri, J. Appl. Phys. 58, 4621 (1985) and references therein.

7. A. M. Cowley and S. M. Sze, J. Appl. Phys. 36, 3212 (1965).

8. J. Van Laar, A. Huijser, and T. L. Van Rooy, J. Vac. Sci. Technol. 14, 894 (1977).

9. M. P. Seah and W. A. Dench, Surf. Interface Analysis 1, 2 (1979).

10. D. E. Eastman, in *Techniques of Metals Research* (Interscience, New York, 1972) Vol. VI, Pt. 1, p. 411.

11. J. Peisner, P. Roboz, and P. B. Barna, Phys. Stat. Sol. (a) 4, K187 (1971).

12. R. M. Eastment and C. H. B. Mee, J. Phys. F 3, 1738 (1973).

13. P. Chiaradia, A. D. Katnani, H. W. Sang, Jr., and R. S. Bauer, Phys. Rev. Lett. 52, 1246 (1984).

14. G. W. Gobeli and F. G. Allen, Surf. Sci, 2, 402 (1964).

15. A. D. Katnani, G. Margaritondo, R. E. Allen, and J. D. Dow, Solid State Commun. 44, 1231 (1982).

16. L. J. Brillson, Phys. Rev. Lett. 40, 260 (1978).

17. L. J. Brillson, C. F. Brucker, A. D. Katnani, N. G. Stoffel, and G. Margaritondo, Appl. Phys. Lett. 38, 784 (1981).

18. Y. Shapira and L. J. Brillson, J. Va .. Sci. Technol. B1, 618 (1983).

19. K. W. Frese, Jr., J. Vac. Sci. Technol. 16, 1042 (1979).

20. G. J. Hughes, A. McKinley, R. H. Williams, and I. T. McGovern, J. Phys. C15, L159 (1982).

21. L. J. Brillson, G. Margaritondo, and N. G. Stoffel, Phys. Rev. Lett. 44, 667 (1980).

22. R. H. Williams, J. Vac. Sci. Technol. 18, 929 (1981).

23. A. Mirceau and D. Bois, Inst. Phys. Conf. Ser. 46, 82 (1979).

24. J. Tersoff. Phys. Rev. B 32, 6968 (1985).

25. M. Schlüter, Phys. Rev. B17, 5044 (1978).

26. J. M. Woodall and J. L. Freeouf, J. Vac. Sci. Technol. 19, 794 (1981).

27. G. P. Schwartz, G. J. Gualtieri, J. E. Griffiths, C. D. Thurmond, and B. Schwartz, J. Electrochem. Soc. 127, 2488 (1980).

28. C. Mailhiot and C.B.Duke, Phys. Rev. B33,1110(1986); J. Vac. Sci. Technol. A4,869(1986).

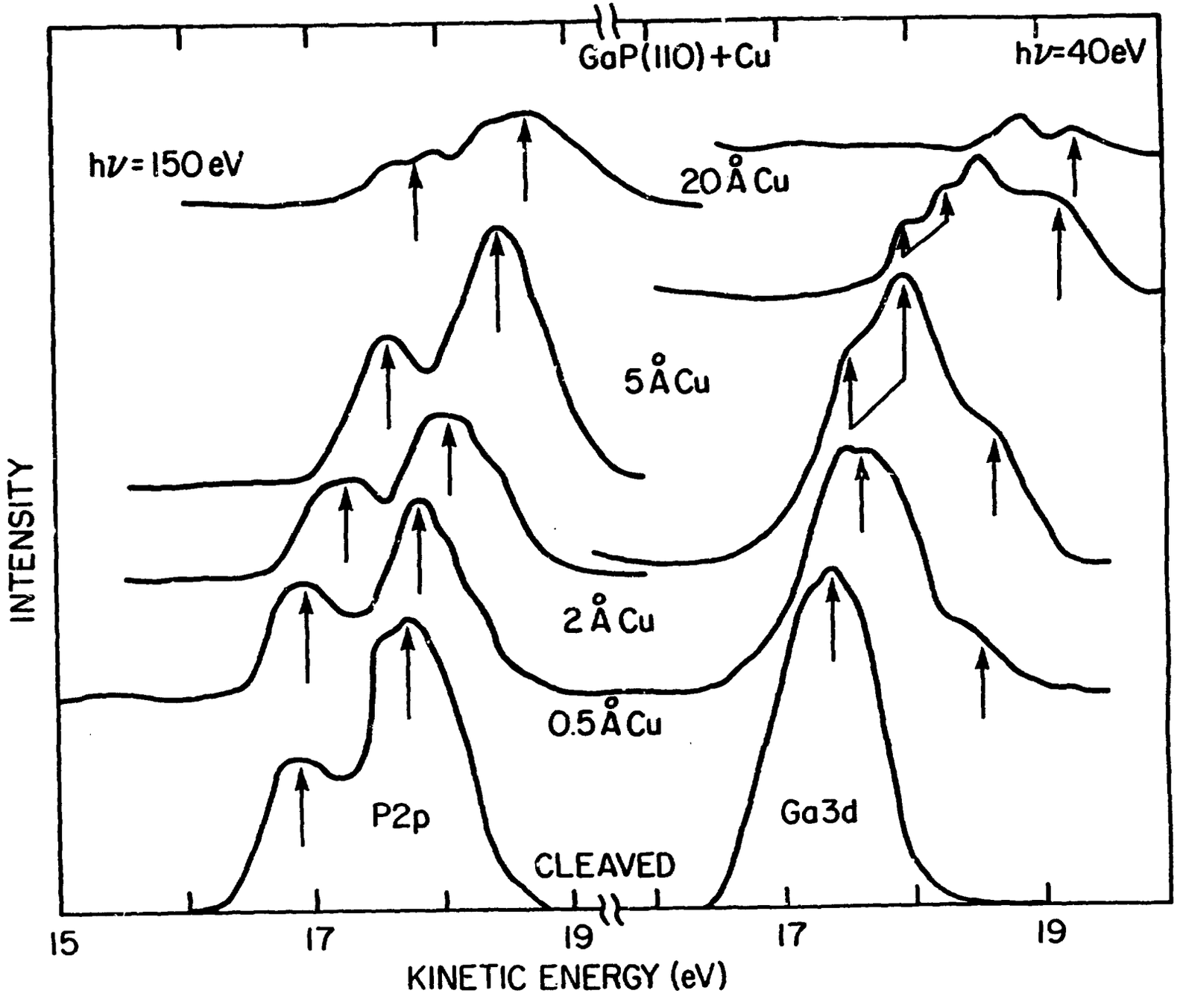
GaP(110)+Cu
hν=40eV
hν=150eV
20Å Cu
5Å Cu
2Å Cu
0.5Å Cu
P2p
Ga3d
CLEAVED
INTENSITY
15
17
19
17
19
KINETIC ENERGY (eV)

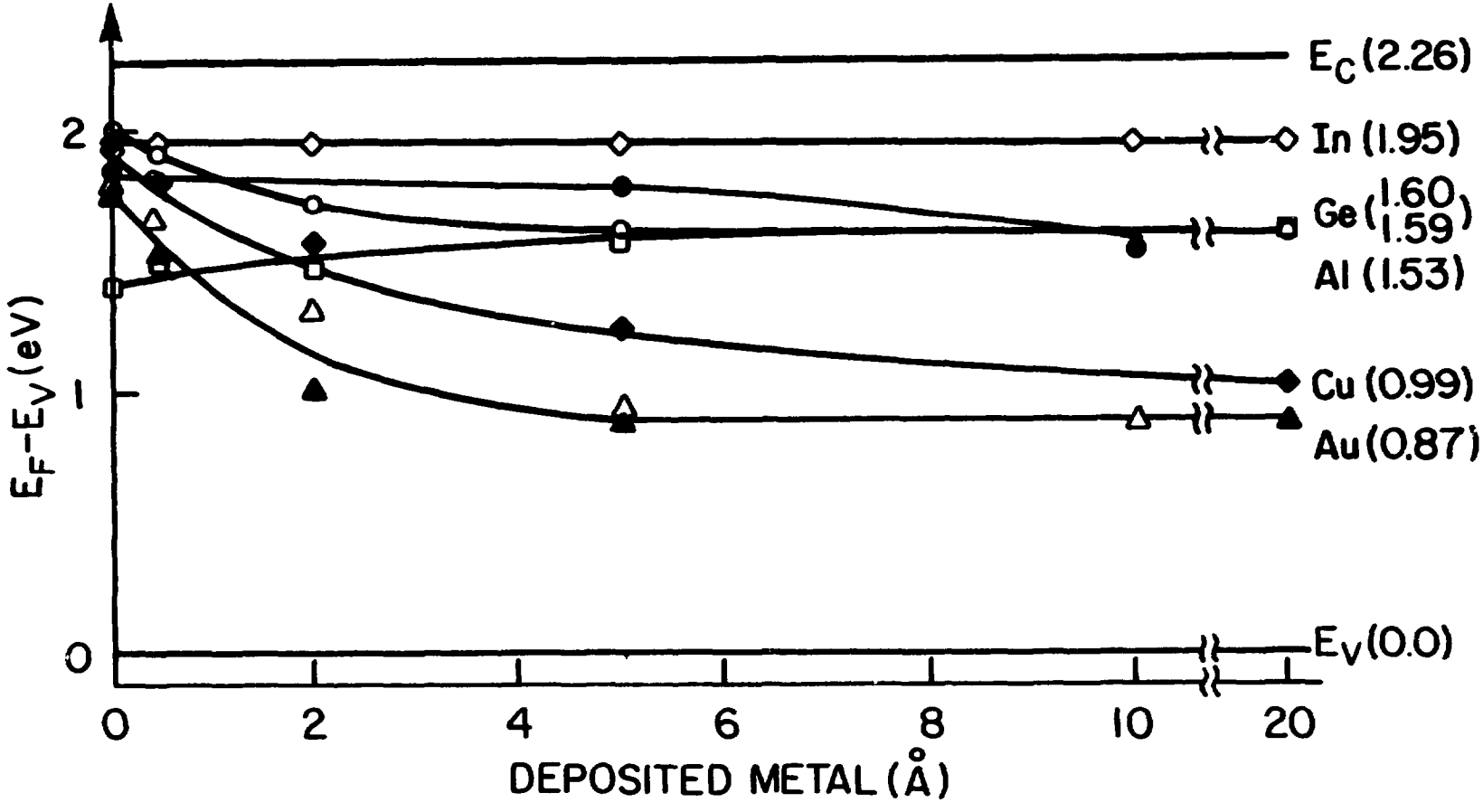
$E_C$(2.26)
In (1.95)
Ge (1.60, 1.59)
Al (1.53)
Cu (0.99)
Au (0.87)
$E_V$(0.0)
$E_F - E_V$ (eV)
2
1
0
0
2
4
6
8
10
20
DEPOSITED METAL (Å)

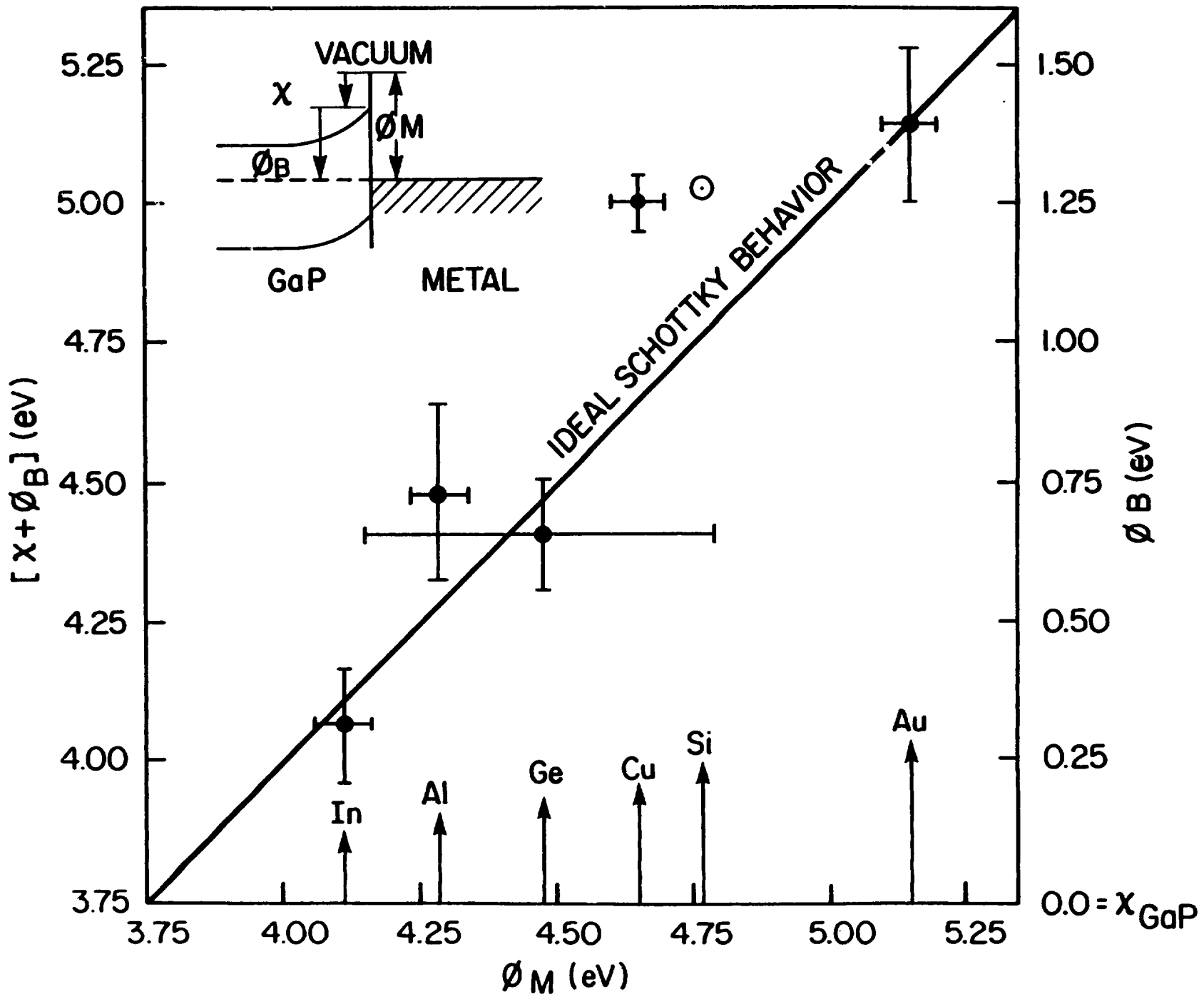
VACUUM
χ
ØM
ØB
GaP
METAL
IDEAL SCHOTTKY BEHAVIOR
5.25
5.00
4.75
4.50
4.25
4.00
3.75
[χ+ØB] (eV)
1.50
1.25
1.00
0.75
0.50
0.25
0.0 = χGaP
ØB (eV)
3.75
4.00
4.25
4.50
4.75
5.00
5.25
ØM (eV)
In
Al
Ge
Cu
Si
Au

# Unpinned Schottky Barrier Formation at Metal-GaP Interface: A Representative III-V Compound Interface

P. Chiaradia, L. J. Brillson*, M. Slade*, R. E. Viturro*, D. Kilday+, N. Tache+, M. Kelly+, and G. Margaritondo+

Istituto Struttura Material of CNR, Frascati, Italy

* Xerox Webster Research Center, Webster, NY 14580

+Department of Physics, University of Wisconsin, Madison, WI 53706

## Abstract

Metal-semiconductor interfaces obtained by deposition of In, Al, Cu, Ge and Au onto ultrahigh-vacuum cleaved GaP surfaces have been studied by photoemission with synchrotron radiation. The results indicate a wide range of Schottky barrier height. A plot of the Schottky barrier values versus metal work function reveals an almost ideal Schottky - like behavior. Among current alternative models of metal-semiconductor interfaces, only the effective-work-function model is compatible with the experimental data. The GaP data plus the absence of Fermi level pinning recently observed for In - based semiconductors indicate that GaP may be more representative than GaAs of metal / III-V compound interfaces in general.

## 1. Introduction

The mechanism of Schottky barrier (SB) formation remains a leading question in the physics of semiconductor interfaces, in spite of the large body of experimental data collected and the numerous theories developed in order to explain these results.[1] Two decades ago it was clearly recognized by Mead[2] that "it is possible to distinguish two broad classes of barrier, one in which the surface charge is dominant, and one in which the surface charge is negligible." These conditions define the well-known Bardeen surface and Schottky limits respectively.[3] For the

past two decades, it has been commonly assumed that the first limit, i.e. strong Fermi level pinning, applied to all III-V compounds[3] and was due to creation of defects[4] or other states localized near the metal-semiconductor interface. However more recent data has shown that in many cases a wide range of Schottky barrier (SB) values can be obtained, depending on the choice of the metal. In fact, such cases are now at least as numerous as the cases of strong Fermi level pinning. For instance, in the case of $In_xGa_{1-x}As(100)$ grown by molecular beam epitaxy (MBE), a large range of Fermi level stabilization energies are found to be correlated with the work functions at the interface[5]. Similar results have been obtained for the cleavage face of the small gap material InAs,[6] while the case of InP (110) is still controversial.[7] These results raise the issue of whether or not Fermi level pinning is characteristic of III-V compound semiconductor / metal interfaces.

In this paper we report on a microscopic study of SB formation on GaP (110) using soft X-ray photoemission spectroscopy which extends the early work of barriers at GaP-metal interfaces.[8] Valence band and core level spectra taken for depositions of Au, Al, Cu and In show a broad (1.1ev) range of Fermi level stabilization energies, covering half the 2.26 ev indirect band gap. This result is important both for technological and fundamental reasons. First of all it shows that rectifying as well as Ohmic contacts can be obtained on GaP (110) with a suitable choice of metal. As to current theories of metal-semiconductor interfaces, the results are in surprisingly good agreement with the classical model introduced by Schottky.[3] They are instead at variance with defect models,[4] as well as the metal-induced-gap-states (MIGS) model.[9]

Among the conventional binary III-V compounds, GaP is particularly interesting since it has a relatively large band gap, heat of formation[3] and ionicity. Furthermore, the large band gap permits a wide range of Fermi level movements, unlike those of several other III-V compounds. Previous work on metal-GaP interfaces[8] consisted of electrical and photoresponse measurements. These were performed under less-than-ideal vacuum conditions and on surfaces which were prepared by polishing and chemical etching. The so-called "index of interface behaviour" S, a proportionality factor between semiconductor barrier height and metal work function was found to be roughly 0.3 for GaP.[10,11] For comparison, S is about 0.1 for GaAs and other III-V compounds while it is close to 1 for most ionic II-VI compounds.[10] Thus it was desirable to reexamine metal-GaP interfaces with the

same and other metals in UHV conditions, making use of modern surface sensitive techniques applied to specimens cleaved under ultra-high vacuum (UHV) conditions.

Moderately doped n-type single crystals with a carrier concentration of 2 to 6 x $10^{17}$ $cm^{-3}$ were cleaved in UHV using the knife-and-anvil technique. In order to avoid any complications in the photoemission experiments due to possible charging, samples were coated with In on one side to ensure an Ohmic contact to the sample holder. Photoemission spectra were taken with a Grasshopper monochromator at the Mark II beam line of the Wisconsin Sychrotron Radiation Center. The overall spectral resolution was of the order of 0.2 - 0.3 eV. Metal deposition was obtained by evaporation from W filaments. The coverage was estimated by means of a quartz thickness monitor. During the evaporation the substrate was held at room temperature.

## 2. Results

Soft x-ray photoemission spectra revealed evidence for both chemical interactions between metal and semiconductor as well as energy shifts due to band bending. To illustrate some of the contrasts in chemical behavior, we present photemission spectra of Al and Au on UHV-cleaved GaP. These metals give rise to reactive and unreactive interfaces respectively, not only with GaP but with many other III-V compounds.[12] Energy distribution curves of valence band (VB) electrons excited by 60 eV photons are shown in Fig. 1(a) and (b) for GaP (110) as - cleaved and covered with increasing thicknesses of Al and Au, respectively. In both cases the clean (cleaved) spectra show a peak about 1 eV below the top of the VB which is due to a surface state photoemission.[13] The best cleaves yielded Fermi energies within a few tenths of an ev from the conduction band.

Fig. 1(a) shows that the VB spectrum of the substrate is attenuated very gradually with deposition of Al owing to the low cross section of Al 3s electrons. In the case of Au however, photoemission from the 5d electrons overwhelms the substrate spectra features at a coverage as low as 0.5Å. Both cases indicate that the shift of the VB edge upon metal deposition must be obtained indirectly, e.g., from the shift of the substrate core levels. For example, Fig. 2 shows photoemission spectra of Ga3d core

levels taken with a photon energy of 60 eV for increasing Al and Au coverages. Generally speaking, core level spectra require care in interpretation since they show both band bending and chemical bonding changes. For instance, inspection of Fig. 2(a) reveals that an Al coverage larger than about 5Å induces a new peak shifted to lower binding energy in the Ga 3d spectrum. This indicates formation of metallic Ga near the free Al surface due to an Al-Ga exchange reaction , resulting in Al-P bonding at the interface.Moreover the Al 2p core level spectra (not shown) indicate formation of metallic Al in the same range of coverage. We interpret this behaviour in terms of a relatively abrupt interface between Al and GaP:[12] The exchange reaction prevents intermixing of substrate and overlayer, except for the segregation of a small amount of metallic Ga to the free surface. In contrast, the case of Au shows core level spectra (see, for example Fig. 2(b)) which do not give evidence of either metallic Ga or any strong chemical reaction taking place at the interface. Upon Au coverage the interface appears interdiffused and, unlike the case of Al, is characterized by a large change in band bending, as shown in Fig. 2(b).

As in the case of Au, the deposition of In produces no evidence of strong chemical reaction from the analysis of core level lineshapes (not shown). We have also observed that in this case the initial band bending does not change appreciably upon coverage. In contrast, Cu and Al interact strongly with the substrate, giving rise to formation of free Ga . As in the case of Au, Cu induces a large increase in band bending . A summary of the band bending results is presented in Fig. 3, where the evolution of the Fermi energy relative to the valence band edge upon coverage is shown for the various interfaces we have investigated. We have noticed that the initial position of the Fermi level varies considerably from cleave to cleave. Apparently this variation is correlated with the quality of the cleave and suggests that "pinning" of the Fermi level at the clean (110) surface is dominated by extrinsic rather than intrinsic surface states.[14] In fact, we have observed a range of initial Fermi level positions ranging from 1.5 to 2.1 ev., this despite the fact that only smooth mirror-like areas are used in the photoemission experiments.

The subsequent evolution of the Fermi level has been determined by the shift of the substrate core levels. For most metals, either Ga 3d or P 2p core levels can be used consistently in this analysis. However in the case of the reacting metals Al and Cu, a systematic discrepancy between these two core levels, a few tenths of an eV or less, has been observed for coverages corresponding to Fermi level stabilization (5-20Å) in surface-sensitive spectra. Generally speaking, the Ga 3d lineshape appears to be

more strongly affected than the P 2p lineshape by metal adsorption, especially when metallic Ga forms by exchange reaction. A similar discrepancy between cation and anion rigid shifts has already been reported by other authors, both in GaP[15] and in GaAs[1]. Consequently, in our data analysis we have only used the average of the bulk - sensitive Ga 3d and P 2p core level shifts. The statistical variations in the rigid core level shifts appear as the error bars in Fig. 4. As shown in Fig. 3, Fermi level stabilization is reached at about 5Å, indicating that SB formation is a much slower process in GaP (110) than in GaAs(110).[4]

## 3. Discussion

Figure 4 summarizes our results for the SB dependence. SB values for In, Al, Cu and Au on GaP (110) are plotted against the corresponding metal work function. A comparison with the Schottky barriers of earlier works reveals a very good agreement for Cu, a reasonable agreement (within the experimental uncertainty) for Au, a disagreement for Al (most probably due to contamination in the earlier work) while In and Ge have been studied for the first time. We also include a data point for Si on UHV - cleaved GaP(110) from a previous study.[16] The Si work function corresponds to the center of the Si band gap with error bars extending $\pm$0.77ev (not shown). Fig. 4 shows a large range of SB values covering 1.1 eV. The (indirect) energy gap of GaP shown is 2.26 eV. Obviously the defect model[4] cannot account for SB formation in this material, as it does in GaAs. In the latter case the Fermi level is always pinned in a narrow energy range (about 0.2-0.3 eV), irrespective of the metal used.[17] This has been interpreted as due to two "defect' levels, the exact position of the Fermi energy being dependent on the charge transfer between metal and semiconductor.[1] In GaAs, special surface treatments are able to expand the pinning range slightly[18] but, strictly speaking, the effect of these processes is probably to modify the semiconductor doping and band structure or to produce a new interfacial dielectric structure.[18] Fig. 4 clearly shows that in metal-GaP interfaces, the SB is correlated to the metal work function, while in cleaved GaAs(110) and surface-treated GaAs(110), the small variations of SB height observed do not appear to be related to this parameter.[4,19] Another indicator of defect formation,the rate of Fermi level movement, is also quite different in GaP and GaAs. For the latter, stabilization of the Fermi energy is obtained with less than one monolayer of metal coverage.[1]

Rather than trying a functional fit of the data points of Fig. 4, we have simply compared them to what was expected from a pure Schottky - like behavior, represented by a $45^0$ line intersecting the x - axis at the origin. It is remarkable that the classical Schottky limit provides a very good fit of the experimental data. This is true in particular for the In and Au data points while for Al and Cu, there is a deviation from the classical behaviour. This can be probably explained by the complexity of chemical and metallurgical processes occurring at the interface in the case of reactive metals. This argument has been introduced and elaborated by Freeouf and Woodall in their Effective-Work-Function (EWF) model of metal-semiconductor interfaces.[20] In the spirit of this model one might say that in the case of Al and Cu an improved fit is obtained by using a modified work function, intermediate between the metal and the anion work functions (the latter is about 5.0 eV[21]). Actually, the original Schottky model provides a surprisingly good fit of the experimental data even without resorting to any refinement in the spirit of the EWF model.

The MIGS model proposed by Tersoff[9] essentially predicts a pinning of the Fermi level in a narrow range, contrary to the experimental observation in GaP. However the MIGS model plays a role only in materials having a large dielectric constant and therefore a short screening length.[9] In order for the MIGS model to apply to the GaP/metal interface, this dielectric constant must be substantially lower than that of GaAs. - in apparent disagreement with reported values for the optical dielectric constant.[9,11] The close proximity of GaP bulk dielectric constants and electronegativity to those of GaAs and other III-V compounds indicates that some other parameters must be used to gain a measure of screening in accounting for our GaP data.

In conclusion, we have performed a microscopic study of the Schottky barrier formation in GaP (110) by photoemission with synchrotron radiation. Analysis of rigid core level shifts due to band bending indicate a broad range of Fermi level stabilization energies whose absolute values are in agreement with the predictions of the classical Schottky model. These results are the most outstanding example of ideal Schottky barrier formation at a metal / III-V compound semiconductor interface and provide a strong indication that Fermi level pinning is not characteristic of III-V compound semiconductors in general.

## 4. Acknowledgments

We gratefully acknowledge the strong support of the staff of the Synchrotron Radiation Center, which is supported by the National Science Foundation. One of us (L.J.B.) wishes to acknowledge useful conversations with F. Jansen and J.M. Woodall and partial support by the Office of Naval Research under Contract N00014-C-0778 (G.B.Wright).

## Figure Captions.

1. Energy distribution curves of valence band photoelectrons for UHV-cleaved GaP with increasing coverage of Al (panel a) and Au (panel b). The excitation photon energy is 60 ev.

2. Energy distribution curves of photoelectrons excited from the Ga 3d core level with a photon energy of 60 ev. The two set of curves were obtained by progressively depositing Al (panel a) and Au (panel b) on to UHV-cleaved GaP surfaces.

3 Evolution of the Fermi level position, with respect to the top of the valence band in UHV-cleaved GaP surfaces as a function of coverage with In, Al, Cu, Ge and Au.The Fermi level position was determined by evaporating a thick layer of Au.The initial point of the curves was obtained by measuring the difference between the Fermi level position and the linearly extrapolated leading edge of the valence band spectrum. The subsequent Fermi level movement was given by the average shifts of the Ga 3d and P 2p core levels with respect to their initial position. Photon energies of 40 and 150 ev respectively were used for Ga and P in order to attain bulk sensitive conditions. The edges of the conduction and valence bands are also shown.

4 Schottky barrier height (SBH) versus metal work function $\Phi_m$ for 10 Å layers of In, Al, Cu Ge, and Au deposited onto UHV-cleaved GaP surfaces. The value of the Schottky barrier is obtained from Fig.3 For Cu, the data is interpolated between the 5Å and 20 Å values.The metal work functions are taken from Refs.22 and 23. The dashed line represents the Schottky limit as given by $SBH = \Phi_m - x_{sc}$, with $x_{sc} = 3.75$, according to Ref. 14.

## References


1. For a recent review see W. E Spicer et al., Proceedings of the International Conference on the Formation of Semiconductor Interfaces, Marseilles-Luminey, France, 1985, Surf. Sci 168, 240 (1986).

2. C. A. Mead, Solid State Electron. 9, 1023 (1966).

3. S. M. Sze, Physics of Semiconductor Devices (John Wiley & Sons, New York, 1969).

4. W. E. Spicer, I. Lindau, P. Skeath and C. Y. Su, J. Vac. Sci. Technol. 16, 1422 (1979) and 17, 1019 (1980).

5. L. J. Brillson, M. L. Slade, R. E. Viturro, M, K. Kelly, L. Tache, G. Margaritondo, J. Woodall, P. D. Kirchner, G. D. Pettit, and S. L. Wright, Appl. Phys. Lett. 48, 1458 (1986) and J. Vac. Sci. Technol, B4, 919 (1986).

6. L J. Brillson, M. L. Slade, R. E. Viturro, M. K. Kelly, L. Tache, G. Margaritondo, J. Woodall, P. D. Kirchner, G. D. Pettit, and S. L. Wright, unpublished.

7. See reference 1 and references therein.

8. A. M. Cowley and S. M. Sze, J. Appl. Phys. 36, 3212 (1965) and references therein.

9. J. Tersoff, Phys. Rev. Lett. 52, 465 (1984) and Phys. Rev. B32, 6968 (1985); W.A. Harrison and J. Tersoff, J. Vac. Sci. Technol. B4, 1068 (1986).

10. S. Kurtin, T. C. McGill and C. A. Mead, Phys. Rev. Lett. 22, 1433 (1969).

11. M. Schlüter, Phys. Rev. B17, 5044 (1978).

12. L. J. Brillson, Thin Solid Films 89, 461 (1982); L. J. Brillson, C. F. Brucker, A. D, Katnani, N. G. Stoffel, and G. Margaritondo, Appl. Phys. Lett. 38, 784 (1981).

13. F. Cerrina, A. Bommannavar, R. A. Benbow, and Z. Hurych, Phys. Rev B31, 8314 (1985).

14. A. Huijser, J. van Laar and T. L. Van Roy, Surf. Sci. 62, 472 (1977) and F. Manghi, C. M. Bertoni, C. Calandra and E. Molinari, Phys. Rev. B24, 6029 (1981).

15. P. Perfetti, F. Patella, F. Sette, C. Quaresima, C. Capasso, A. Savoia and G. Margaritondo, Phys. Rev. B30, 4533 (1984).

16. A.D.Katnani, G. Margaritondo, R.E.Allen, and J.D.Dow, Solid State Commun. 44, 1201 (1982).

17. J. R. Waldrop, J. Vac. Sci. Technol B2, 445 (1984).

18. L.J.Brillson, Surf. Sci. Repts. 2, 123 (1982) and references therein.

19. R. W. Grant, J.R.Waldrop, S.P.Kowalczyk. and E.A.Kraut, J. Vac. Sci. Technol. 19, 477 (1981).

20. J. L. Freeouf and J. M. Woodall, Appl. Phys. Lett. 39, 727, (1981); J.M.Woodall and J.L.Freeouf, J. Vac. Sci. Technol. 19, 794 (1981).

21. K. W. Frese, Jr., J. Vac. Sci. Technol. 16, 1042 (1979).

22. H.B.Michaelson, J. Appl. Phys. 11,4729 (1977).

23. D.E.Eastman, in Techniques of Metals Research (Interscience, New York,1972) Vol.VI, Pt.1,p.441.

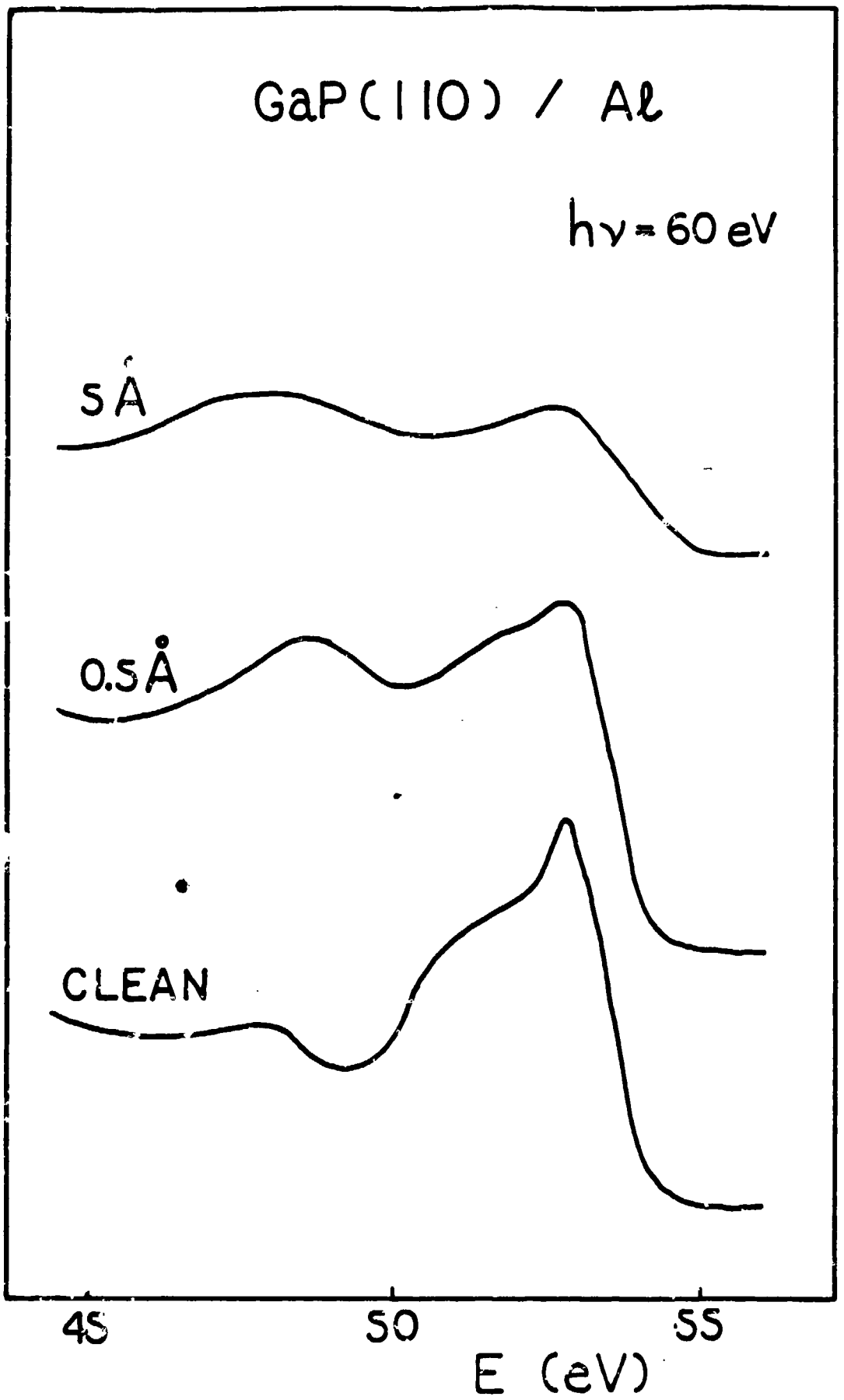


Fig. 1a

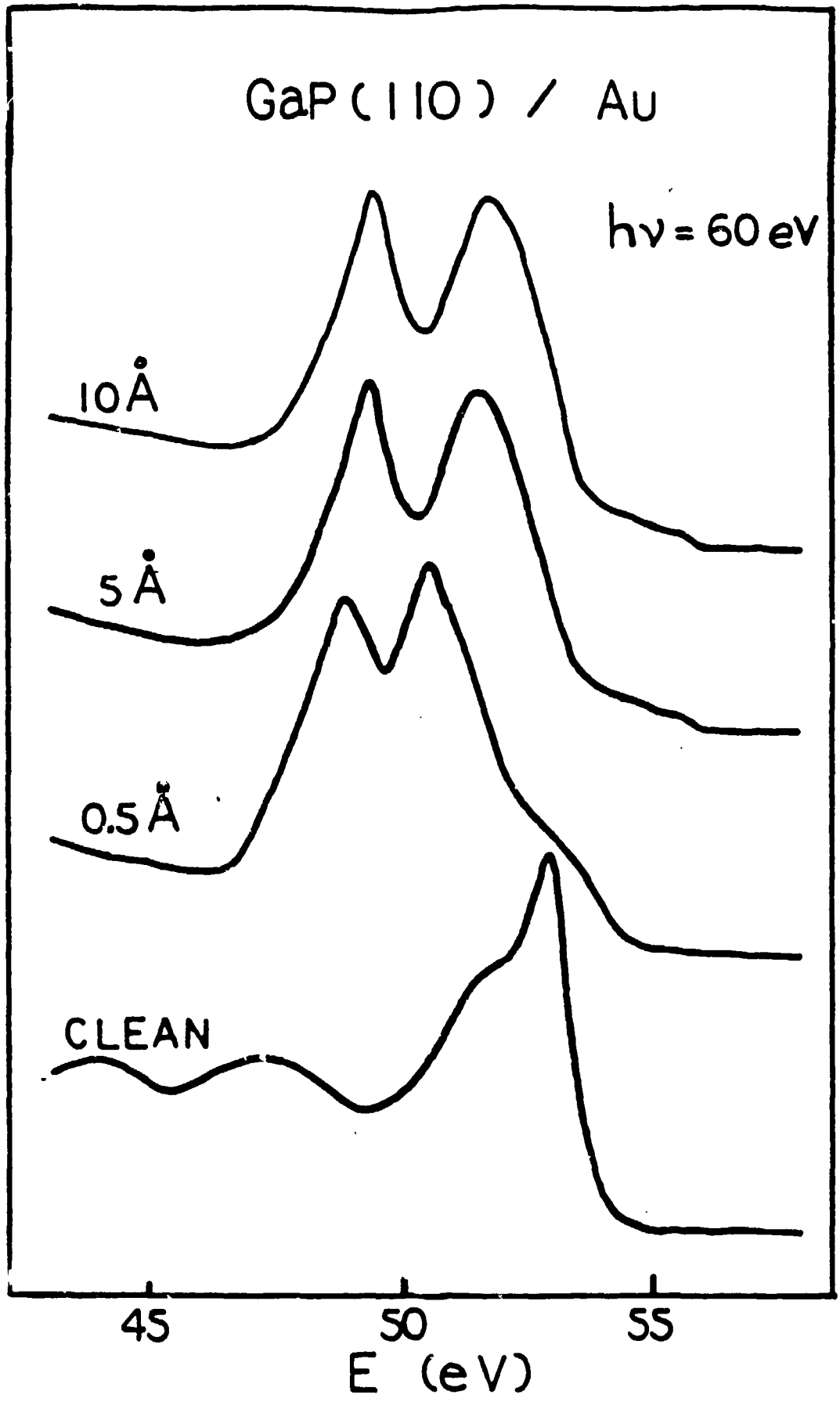


Fig. 1b

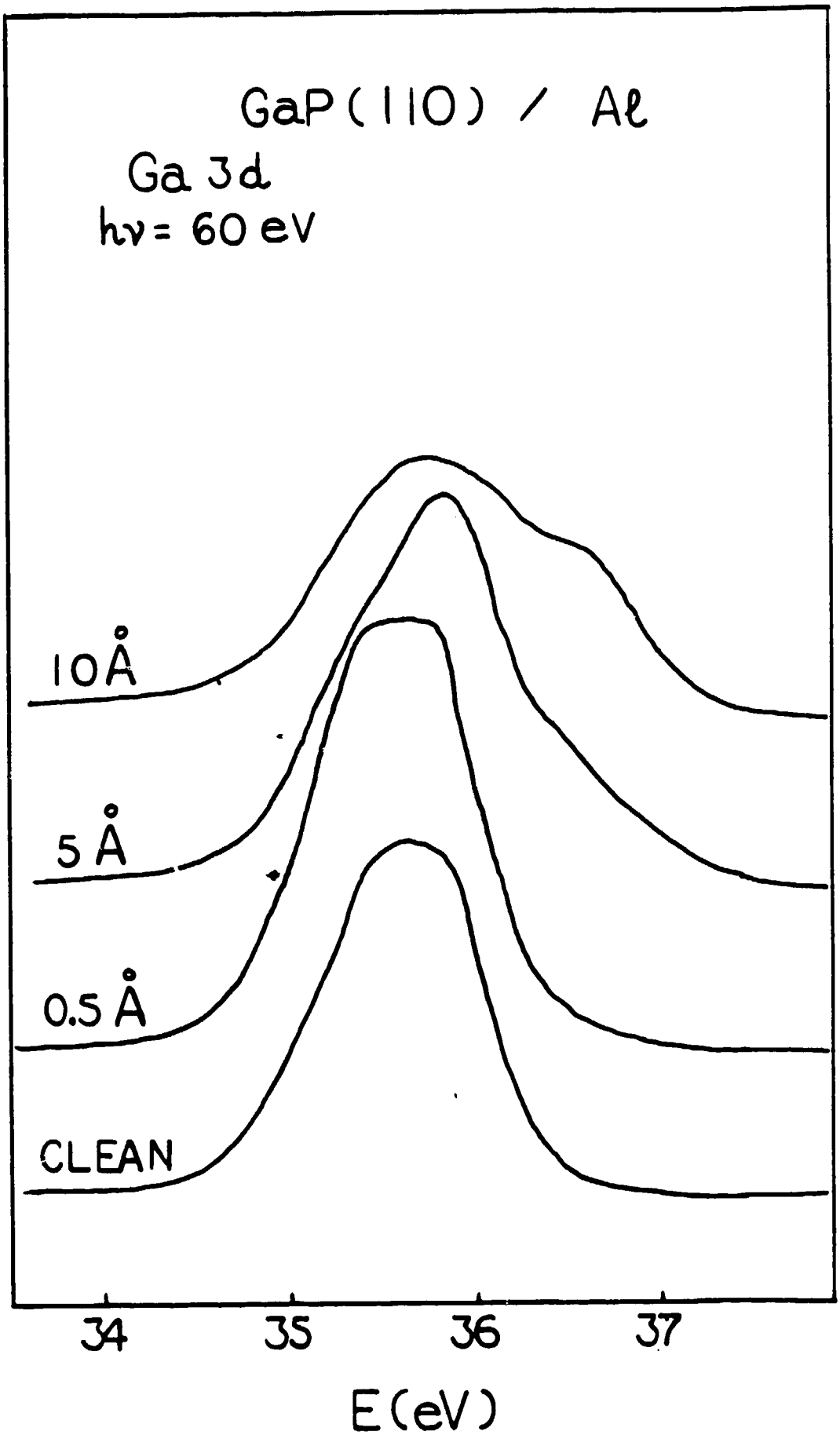


Fig. 2a

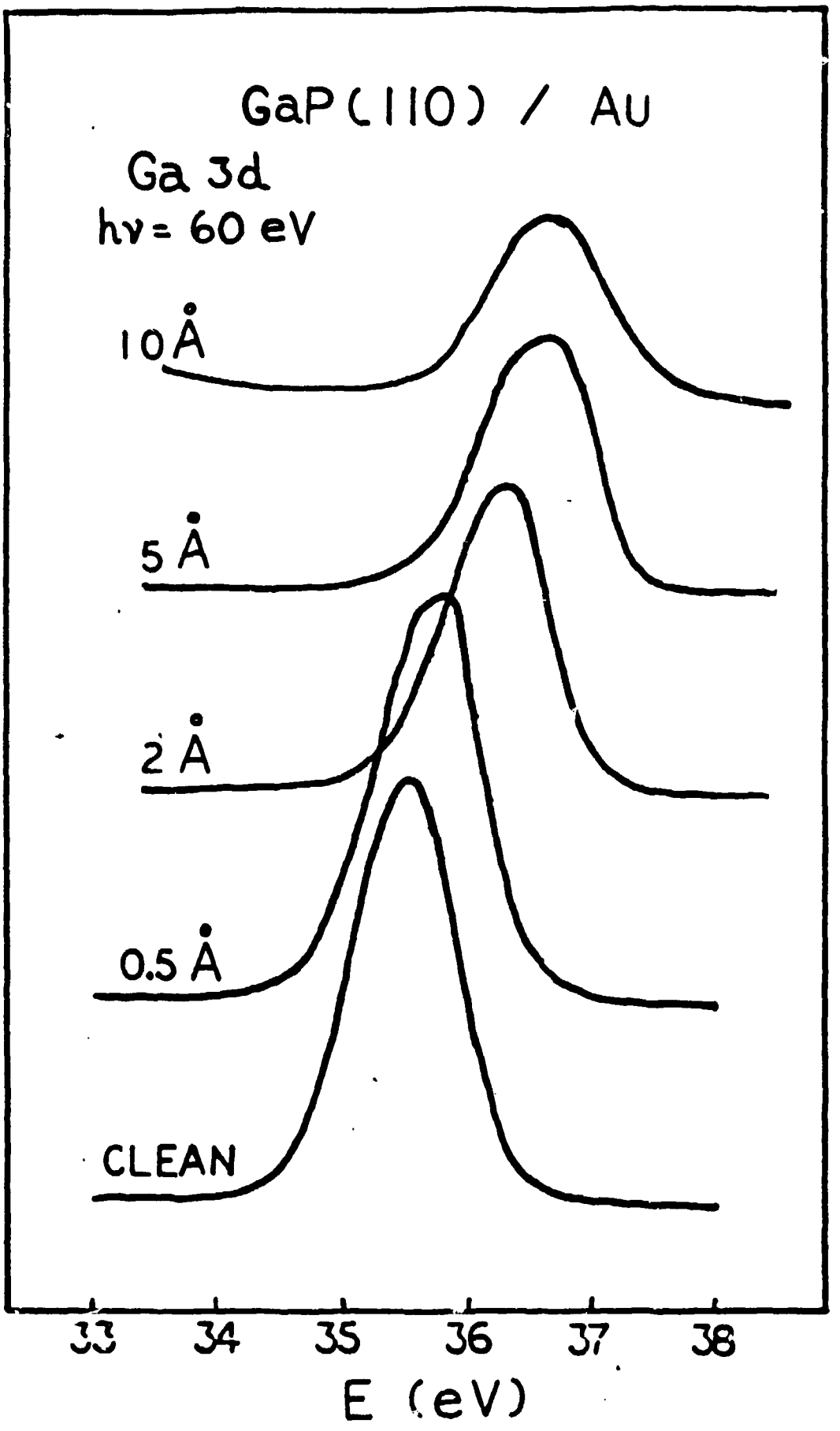


Fig.2b

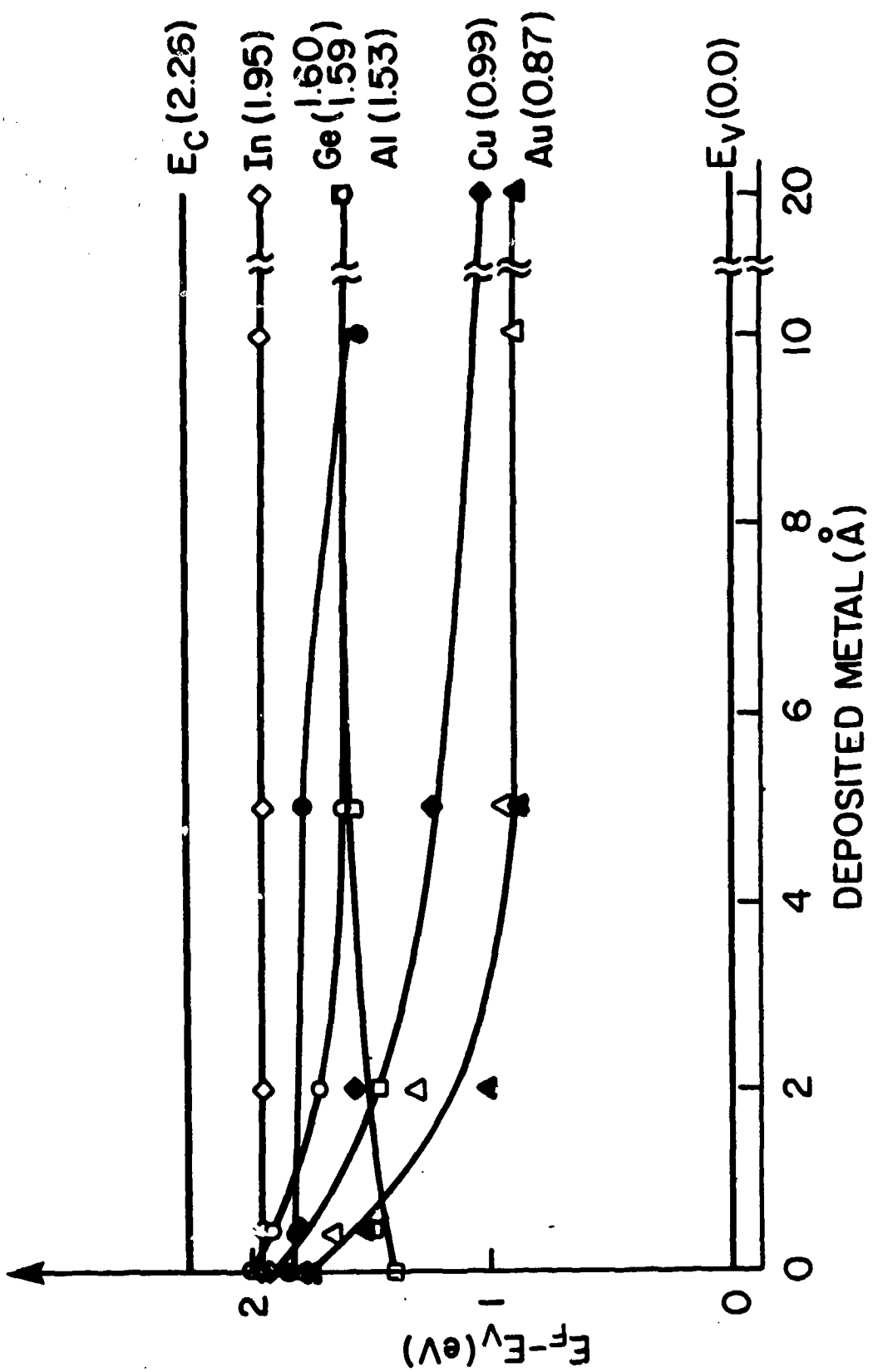
$E_C$ (2.26)
In (1.95)
Ge (1.60, 1.59)
Al (1.53)
Cu (0.99)
Au (0.87)
$E_V$ (0.0)
$E_F - E_V$ (eV)
2
1
0
0
2
4
6
8
10
20
DEPOSITED METAL (Å)

Fig. 3

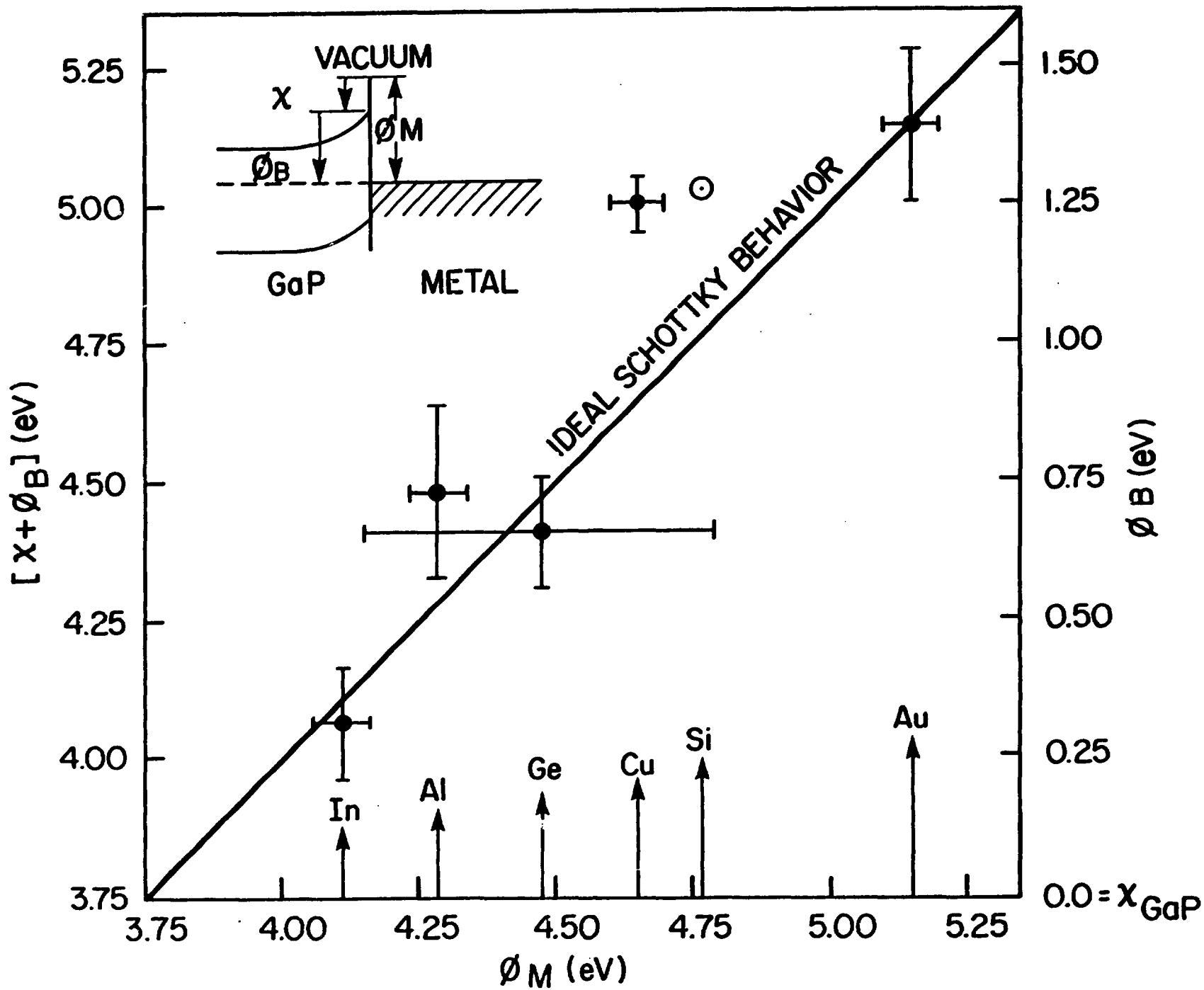
VACUUM
χ
ØM
ØB
GaP
METAL
IDEAL SCHOTTKY BEHAVIOR
[χ+ØB] (eV)
ØB (eV)
ØM (eV)
5.25
5.00
4.75
4.50
4.25
4.00
3.75
1.50
1.25
1.00
0.75
0.50
0.25
0.0 = χGaP
In
Al
Ge
Cu
Si
Au

# Cleavage-Related Electronic States of Al · InP(110) Interfaces

R. E. Viturro, J. L. Shaw, and L. J. Brillson

Xerox Webster Research Center, Webster, New York 14580

## ABSTRACT

Cathodoluminescence spectroscopy studies of III-V compound semiconductor surfaces and their metal interfaces show that the optical emission of deep level surface and interface states depend on semiconductor surface morphology. Spatially-resolved measurements reveal metal-induced interface states at cleavage steps whose optical emission properties depend on electron beam injection level. The density and spatial distribution of such metal-cleavage-related states may account for variations in electronic measurements reported for clean III-V compound semiconductor/metal interfaces.

## 1. Introduction

Cathodoluminescence spectroscopy (CLS) of metal on compound semiconductor surfaces provides a direct observation of surface and interface states within the semiconductor band gap.[1,2,3,4] For example, optical emission from deep levels of InP and GaAs provide evidence for discrete states which can stabilize the Fermi level and account for the Schottky barriers formed.[2-4] In turn, the formation of Schottky barrier for these III-V compounds is particularly interesting since they exhibit a relatively small range of Fermi level stabilization energies regardless of their metallization.[5] This Fermi level "pinning" and the absolute Schottky barrier height (SBH) -the energy barrier for carrier transport from the metal Fermi level to the semiconductor conduction(valence) band- are of high interest for both scientific and technological reasons.[6] We have now extended our CLS measurements of metal/III-V compound semiconductor interfaces to the dependence of surface and interface state optical emission on semiconductor surface morphology and electron beam

injection level. These measurements address the influence of cleavage steps and associated roughness effects on the properties of interface states and their role in Schottky barrier formation.

The metal/InP(110) interface is an ideal candidate for studying the influence of cleavage steps on electronic properties since gap states are absent for high quality (low step density) cleavage clean surfaces [7] and no optical emission is observed via CLS for such clean surfaces.[2] Gap state optical emission is observed at areas of the cleaved InP(110) surface with high step densities. These states are attributed to the presence of broken bonds at the mechanically damaged surface.[2] Strictly speaking, such surface states are present in variable concentration on any cleavage surface. Furthermore, the chemical interaction of the deposited metal on step-cleaved surfaces can cause the formation of interface states, i.e. higher concentration and/or complex defects, which are different from those formed on perfect surfaces. These interface states will affect the macroscopic value of the SBH as obtained by other techniques.[8,9,10] Here we present experimental evidence which confirms the presence of mid-gap interface states in the Al/InP(110) system whose optical emission properties are dependent on surface morphology and on injection level. The results strongly suggest that those metal induced mid-gap interface states generated on step-cleaved InP surfaces can play a role in determining the transport characteristics of M/SC junctions.

## 2. Experimental

Details of the ultrahigh vacuum (UHV) experimental apparatus can be found elsewhere.[4] Briefly, the CL excitation was produced by a chopped electron beam from a glancing incidence 500-3000 V electron gun, impinging on the semiconductor crystal face. The room temperature luminescence was focused into a Leiss double prism monochromator and the transmitted signal was phase-detected by means of a liquid nitrogen cooled Ge detector and a lock-in amplifier. Al was evaporated on UHV cleaved InP(110) ($n = 4.3 \times 10^{15}$ $cm^{-3}$), and deposited thickness was monitored by means of a quartz crystal oscillator.

The values of the maximum steady excess carrier concentration at the near surface region (N) were estimated following Pankove.[11,4] N is equal to the generation rate (G) times the carrier lifetime at the surface ($\tau$). G depends on the electron beam energy ($E_p$), the effective penetration depth (d), which depends on $E_p$, the bombarded area (A), and the beam current (I). The experiments here reported were performed at the same $E_p$ , thereby keeping d constant. For $E_p$ = 1.5 kV, the maximum electron range is about 500 A. The maximum energy loss per unit depth occurs at a depth of about 80 A,[4] and this value gives the depth at which most electron-hole pairs are generated. Thus the generation rate is proportional to the electron beam current, provided that the diameter of the electron beam does not change witn changes in the beam current. Our measurements of the bombarded area gave a spot size of about $10^{-3}$ $cm^2$ at 1.5 kV and showed that negligible changes occurred in beam dimensions with electron beam current up to 25 $\mu$A. Approximate values of G can be calculated from the expression

$$G = 2 \times 10^{24} \times I(\mu A) \text{ carriers } cm^{-3} s^{-1}$$

Where we assumed an effective excitation depth of 100 A. Values of the bulk carrier lifetime are in the nsec range. Within the depletion region the free carrier life time should be much shorter due to band bending. The life time of trap states could be much longer. For the lightly n-doped InP specimen investigated, depletion regions extend over hundreds to thousands of A, even for very low barrier heights. Thus, electron-hole pairs are mostly generated within the depletion region, and their movements are affected by internal electric fields. This effect accounts for the decrease of luminescence intensity of the near band gap (NBG) transition with band bending.

Roughness of different areas on the cleaved semiconductor surface was visually estimated and qualitatively correlated with the relative luminescence intensity of the NBG transition and with the dependence of the spectral shape on depth of excitation. [4]

## 3. Results

Recently we have reported the first study of optical emission properties associated with the formation of metal-III-V semiconductor interface states by means of cathodoluminescence spectroscopy .[2] The reported results so far did not show any injection level related phenomena in the CL characteristics of the M/III-V SC systems. In investigating the role of steps, i.e. mechanically damaged surfaces, the Al/InP(110) system is attractive because the clean, mirror-like, UHV cleaved InP surface lacks any detectable sub-band gap optical emissions, and Al deposition on these surfaces shows that no particular dominant CL radiative recombination center is created in the SC band gap. Fig. 1 shows that the NBG transition dominates the spectral shape even at multilayer metal coverage. On the other hand, CL spectra from clean step-cleaved InP areas do show a broad optical emission band at sub band gap energies and resemble those of Al/InP. We also found similarities in spectral shape between CL spectra of step-cleaved areas and those from submonolayer metal coverage on mirror-like areas, showing that the initial metal deposition causes the formation of broken bonds such as those formed during a step-cleaved process.[2] No injection level related phenomena, i.e. no change in spectral shape with increasing electron beam current were observed on those systems for electron beam currents up to 25 uA.[2]

Fig. 2 shows the CL spectra of step-cleaved Al (20 A)/InP as a function of the electron beam current. It can be seen that the mid-gap emission increases with increasing carrier generation, producing a dramatic change in the relative intensity of the optical emissions and in the spectral shape of features between 0.8 and 1.3 eV. At low injection levels, top spectrum of Fig. 2, the spectral shape resembles that of Al(20 A)/InP(110) depicted in Fig.1. With increasing injection levels the CL spectra from smooth areas scale in intensity with no changes in spectral shape, whereas those from step-cleaved patches also show changes in spectral shape. The intensity ratio of emissions between the mid-gap and the NBG transition also changes when the scanned area is moved to a different spot on the step cleaved surface. This is shown in the bottom spectra of Fig. 2, for the same electron beam current

on two rough spots on the surface. In general, the higher the step density or roughness of the surface, the higher is the mid-gap/NBG emission intensity ratio. The effect is strong at beam currents higher than 10 uA. The results are perfectly reproducible, showing that no electron beam damage has occurred. Such beam damage is expected only for order of magnitude higher beam currents where local heating can decompose the semiconductor.

Fig. 3 shows a plot of peak intensities of three main emissions as a function of electron beam current for constant excitation depth. CLS intensities which depend on injection level are found for each rough spot on the cleaved surface. These curves all have shapes similar to those shown in Fig. 2. Because the available electron beam currents extend only over one order of magnitude, the range of values is too small to certainly describe the functional dependence of peak intensity on the injection level. This range is limited by signal detection at low beam currents and the output of electron gun at high electron beam currents.

## 4. Discussion

The CL spectra of clean step-cleaved InP does show optical emission at sub band gap energies, but no change in spectral shape and in the relative intensity of the optical emissions with increasing electron beam current.[2] Thus, it is the particular interaction of Al with the step-cleaved surface which yields changes in the optical emission properties with injection level. In other words, metallization of the step cleaved surface leads to additional mid-gap CLS features.

Al has been shown to form atomically abrupt interfaces with UHV cleaved InP(110).[12] This is due to the strong metal-anion bonding that causes a formation of a thin (2-3 A) layer of AlP at the interface, causing the release of about two thirds of a monolayer of In.[12] The Al-P compound layer acts as a diffusion barrier for Al, limiting further reaction. The dissociated In segregates to the Al overlayer.[13] Rough surfaces present large amounts of unsaturated bonds and little definition of surface geometry. These disrupted surface layers presumably have a lower activation energy for reaction with a metal overlayer. Most likely

no abrupt interface would be formed on these surfaces, so that Al atoms could penetrate and react over tens of angstroms. This process enables the formation of a reacted thick layer containing complex defects which are responsible for the detected luminescence. We expect that the extent of the reaction may be related to the step density so that the higher the roughness of the surface, the more extended the reaction, thereby producing the higher densities of states responsible for mid-gap emission.

The dependence of spectral shape on steady-state excess carrier concentration is not easy to understand. A possible explanation consists of assuming that the extended Al-InP reaction causes the formation of complex defects having several charge states which lie close in energy. As the excitation increases, a second charge state is populated and radiative recombination from these centers is increased. The superlinear behavior of the 0.8 eV peak intensity supports our hypothesis of a cooperative multistate phenomenon. Flattening of the bands due to the excess carrier concentration in the depletion region cannot account for the observed behavior. This is because a reduction in band bending causes a smaller depletion region and the consequent increase in the NBG emission intensity, an effect which was not observed.

On the other hand, the sublinear behavior of the NBG transition intensity with increasing beam current is different from the linear behavior found in other CL experiments using much higher electron beam energies. Linear response was usually associated with high efficiency for spontaneous radiative recombination.[14] However, these studies investigated bulk recombination properties, using electron beam energies of about 30 kV or more.[14] Some electronic surface parameters of GaAs were determined from a qualitative and quantitative analysis of the relative photoluminescence intensity at several wavelengths of the exciting radiation.[15] The effect of the depletion layer, within the framework of the model, is to reduce the luminescence efficiency and the intensity response was shown to be linearly dependent on carrier injection.[15] However, the minimum penetration depth achieved by using photoexcitation is of the order of 1000 A. Our experiments investigated the radiative

recombination properties of the first hundred A. In this region new recombination paths are created upon formation of the metal-semiconductor interface. Possible mechanisms which explain sublinear response of the NBG transition in the near surface region with increasing excess carrier concentration are bimolecular recombination-shallow states to shallow states, and recombination through a three body process, promoted by the augmented hole concentration in the interface caused by upward band bending. The lifetime of the unrecombined electron-hole pair is thereby increased, thus increasing the probability of recombination through a different path. At this time we do not have experimental evidence to support a particular recombination mechanism which can account for the measured sublinear behavior. Experiments testing the dynamics of the recombination process should be performed in order to obtain information on recombination mechanisms at the metal/semiconductor interface.

The observed dependence of the optical emission spectra on surface morphology and on injection level can account for the scatter of the values of the macroscopic SBH obtained by electronic techniques on the cleaved surface.[8,9,10] First, our results show that the concentration of recombination centers at the M/SC interface for UHV cleaved semiconductor is a function of the roughness- cleavage quality. Second, the recombination centers formed by the interaction of Al with InP on rough patches have recombination properties not found on perfect interfaces These facts can introduce new paths for the carrier transport through the barrier and coexistence on the diode area of patches with a distribution of barrier heights. These effects are sample dependent, causing a spread in the SBH values derived from electric measurements.

In summary, we have optically detected metal/semiconductor interface states whose properties depend on surface morphology and on excitation level. The existence of discrete states provides a physical basis for the difference in transport properties between smooth and rough-cleaved surfaces, and their density and spatial distribution can account for the spread on the macroscopic SBH values.

Partial support by the Office of Naval Research (Grant No. ONR N00014-80-C-0778) and fruitful discussions with Tom Orlowsky are gratefully acknowledged.

**Figure Captions**

Fig. 1. CL spectra of clean, mirror-like n-InP (110) surface before and after Al deposition, and the clean step-cleaved surface.

Fig. 2. CL spectra of Al on UHV step-cleaved n-InP for several electron beam currents at constant excitation depth. The spectra are normalized to maximum peak intensity. The mid-gap feature at 0.8 eV increases preferentially with increasing injection level. Spectrum b is for a different patch on the surface, showing a higher NBG/mid-gap emission ratio. This higher ratio for the same injection level correlates with a smaller visual step density and a higher intensity ratio for the patch b at the clean surface.

Fig. 3. Luminescence intensity for the 0.8, 1.0, and 1.35 eV peaks (see Fig.2) vs. electron beam current for step-cleaved InP with a 20 A Al overlayer. The superlinear injection level dependence of the Al covered step-cleaved

surface is not observed for Al covered smooth surfaces or clean, step-cleaved surfaces alone.

## References


1. L. J. Brillson, H. W. Richter, M. L. Slade, B. A. Weinstein, and Y. Shapira, J. Vac. Sci. Technol. A 3, 1011 (1985).

2. R. E. Viturro, M. L. Slade, and L. J. Brillson, Phys. Rev. Lett. 57, 487 (1986).

3. R. E. Viturro, M. L. Slade and L. J. Brillson, **Procedings of the 18th ICPS**, Stockholm, Sweden 1986.

4. R. E. Viturro, M. L. Slade, and L. J. Brillson, J. Vac. Sci. Technol. A, Jul-Aug Book 2 (1987).

5. L. J. Brillson, Surf. Sci. Rept. 2, 123(1982), and references therein.

6. S. M. Sze, **Physics of Semiconductor Devices** (Wiley-Interscience, New York, 1981), 2nd ed., Chap. 5.

7. R. H. Williams, R. R. Varma, and A. McKinley, J. Phys. C.(Solid State Phys.) 10, 4545 (1977).

8. J. H. Slowik, H. W. Richter, and L. J. Brillson, J. Appl. Phys. 58, 3154(1985).

9. N. Newman, T. Kendelewicz, L. Bowman, and W. E. Spicer, Appl. Phys. Lett. **46**, 1176 (1985).

10. F. Chekir, G. N. Lu, and C. Barret, Solid-St. Electron. **29**, 519 (1986).

11. J. I. Pankove, **Optical Process in Semiconductors** (Dover, New York, 1975), page 255.

12. L. J. Brillson, Phys Rev. Lett. **46**, 838 (1981).

13. F. Houzay, M. Bensoussan, and F. Barthe, Surf. Sci. **168**, 347 (1986), and **Procedings of 18th ICPS**, Stockholm, Sweden (1986).

14. D. F. Kyser, and D. B. Wittry, **The Electron Microprobe Conference** (Electrochem. Soc., Washington, 1964), page 691.

15. K. Mettler, Appl. Phys. **12**, 75 (1977).

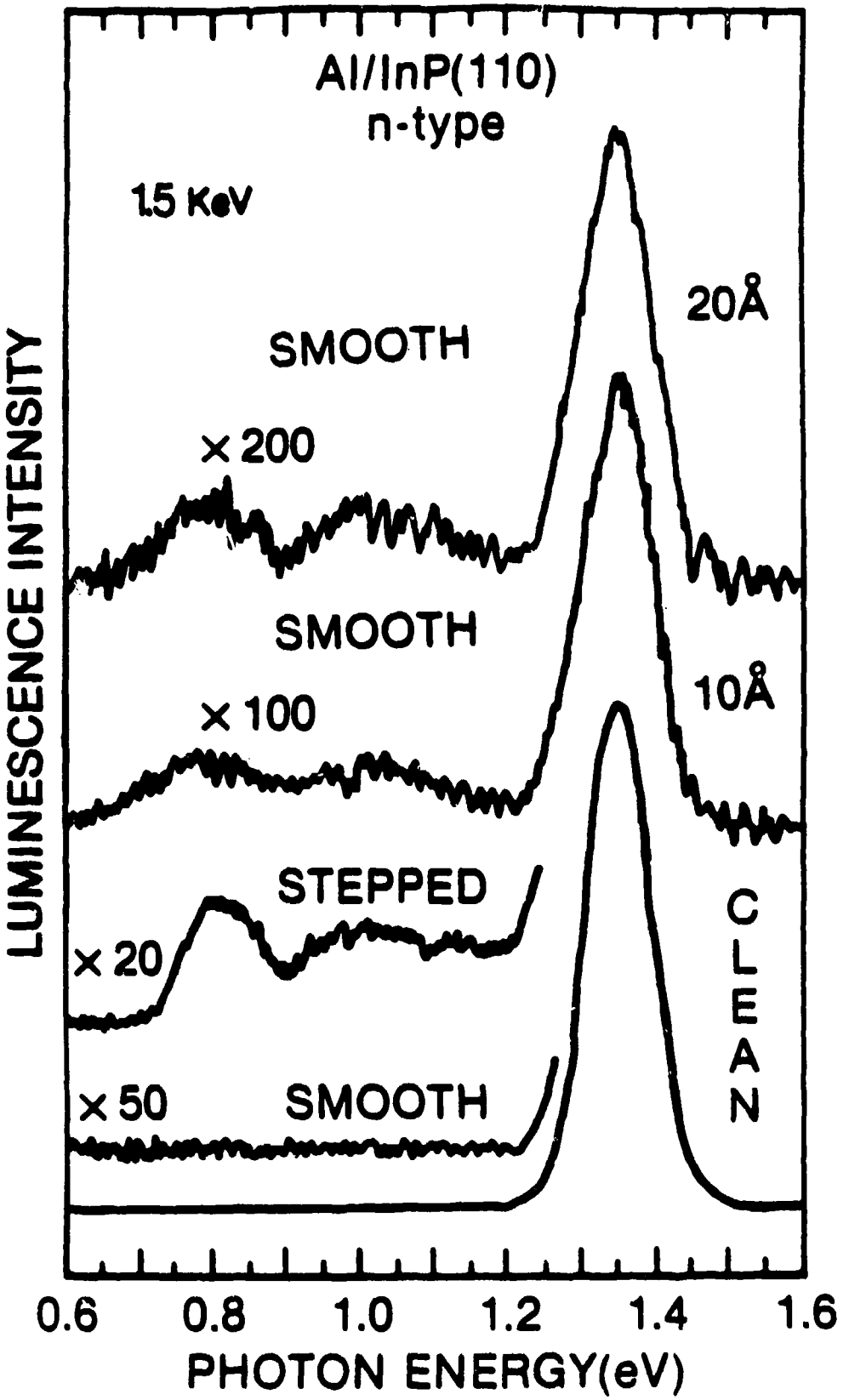
Al/InP(110)
n-type
1.5 KeV
20Å
SMOOTH
×200
SMOOTH
10Å
×100
STEPPED
×20
CLEAN
×50
SMOOTH
LUMINESCENCE INTENSITY
0.6
0.8
1.0
1.2
1.4
1.6
PHOTON ENERGY(eV)

Fig. 1

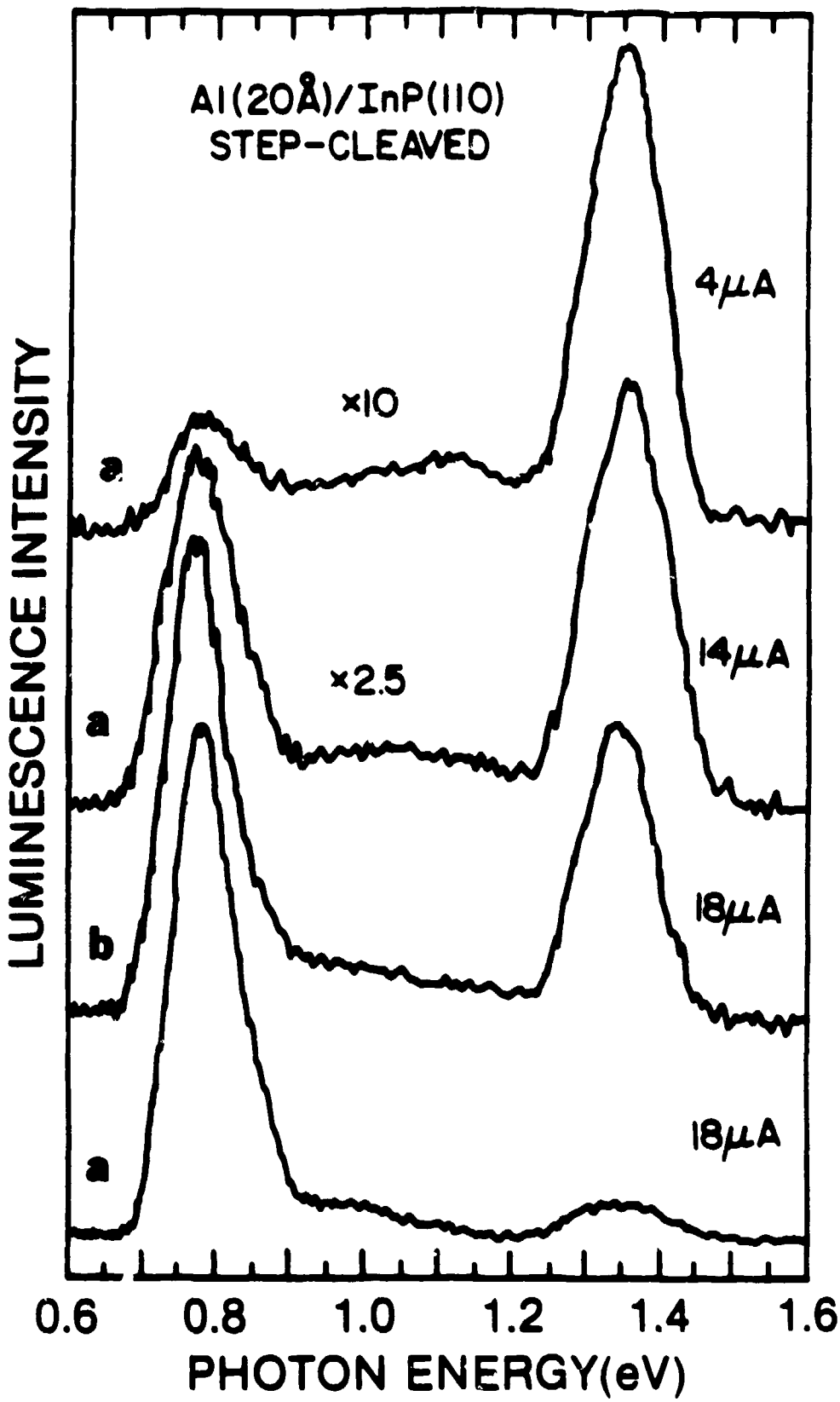
Al(20Å)/InP(110)
STEP-CLEAVED
4μA
×10
a
14μA
×2.5
a
18μA
b
18μA
a
LUMINESCENCE INTENSITY
0.6
0.8
1.0
1.2
1.4
1.6
PHOTON ENERGY(eV)

Fig. 2

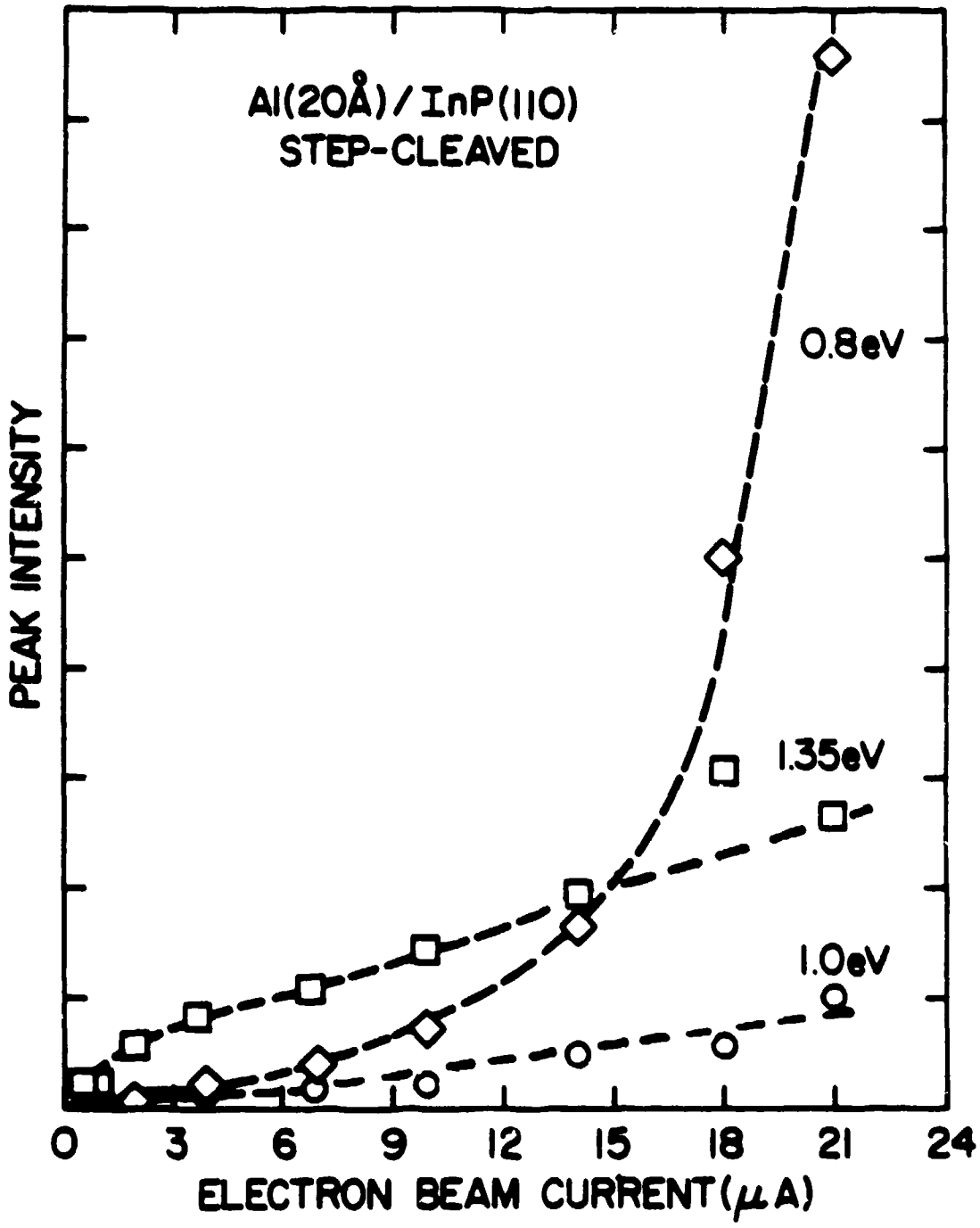
Al(20Å) / InP(110)
STEP-CLEAVED
0.8eV
1.35eV
1.0eV
PEAK INTENSITY
0
3
6
9
12
15
18
21
24
ELECTRON BEAM CURRENT(μA)

Fig. 3

# Low Energy Cathodoluminescence Spectroscopy of Semiconductor Interfaces

by L. J. Brillson and R. E. Viturro

Xerox Webster Research Center, 800 Phillips Road 114-41D, Webster, NY 14580
(716)422-6468

## ABSTRACT

Low energy cathodoluminescence spectroscopy (CLS) is a powerful new technique for characterizing the electronic structure of "buried" semiconductor interfaces. This extension of a more conventional electron microscopy technique provides information on localized states, deep level defects, and band structure of new compounds at interfaces below the free solid surface. From the energy dependence of spectral features, one can distinguish interface versus bulk state emission and assess the relative spatial distribution of states below the free surface. Low energy CLS reveals process changes in the electronic structure of semiconductor interfaces due to metallization, laser annealing, and thermal desorption. Spectral features of metal-semiconductor interfaces uncovered by CLS also provide a new perspective on physical mechanisms of Schottky barrier formation.

Key words: Cathodoluminescence, Metal-Semiconductor Interface, Schottky Barrier Formation, Interface States, Defects, Depth-Dose, Electron Range, Semiconductors, InP, GaAs, CdS, Dead Layer, Deep Levels, Interface Reaction.

## Introduction

Cathodoluminscence spectroscopy (CLS) and cathodoluminescence mapping are well-known electron microscopy techniques for studying electronic structure and free carrier recombination of bulk semiconductors.[53] Combined with photoluminescence spectroscopy, these techniques have been useful in evaluating semiconductor growth quality and its variations near grain boundaries, growth artifacts, and other microscopic imperfections of the crystalline material. See, for example references 27, 28 and 30. Included are gauges of minority carrier lifetime[10,45], diffusion length[34,50], carrier concentration,[10] and defect segregation.[29] Furthermore, CLS provides a measure of spatially-localized band structure and deep levels in modulated semiconductor structures.[17,29]

In the last several years, researchers have begun using a low energy extension of CLS to study semiconductor surfaces and "buried" metal-semiconductor interfaces. Motivating this work has been the need to probe electronic structure of metal-semiconductor junctions at metallic coverages, in order to elucidate the fundamental mechanisms involved in Schottky barrier formation. Whereas conventional surface science techniques have provided considerable information on the initial stages of contact rectification[4], they are by definition of little value in studying the "buried" interface. To investigate such interfaces, one requires the facility to probe tens of monolayers below the free surface without sampling primarily the characteristics of the bulk semiconductor. Researchers have observed clear evidence for electronic states localized near surfaces and interfaces, including metal-induced deep levels, defect levels, and band structure of localized compound layers. The ability to observe such features are due in large part to the surprisingly high near-surface sensitivity of low energy CLS. Furthermore, merely by increasing the incident electron energy, one can obtain information

from the sub-surface region and the bulk material, thereby providing a means to compare near-surface and bulk phenomena directly.

CLS results for semiconductor surfaces show dramatic differences across the same surface depending on chemical composition, roughness or bulk defect concentration. CLS results for metal films on clean semiconductor surfaces reveal discrete emission to or from states deep within the semiconductor band gap which depend on the specific metallization and/or thermal treatment employed. Hence low energy CLS represents a unique new tool for identifiying the physical mechanisms which contribute to formation of interface electronic structure and in particular the barriers to electrical charge transport.

In the following sections, we present a description of the experimental technique, the dependence of excitation depth on incident voltage in the low energy regime, CLS studies of semiconductor surfaces, CLS studies of metal-induced surface states, CLS studies of thermally-processed interfaces, implications for understanding Schottky barrier formation, and future applications.

## The Low Energy Cathodoluminescence Spectroscopy Experiment

Figure 1 illustrates schematically the low energy cathodoluminescence experiment.[6] In addition to an ultrahigh vacuum (UHV) chamber for preparing and maintaining clean and chemically-modified semiconductor surfaces, one requires a low energy (300-3000 eV) glancing incidence, a monochromator and photon detector with near-infrared sensitivity, and suitable photon collection optics. The latter consists of a quartz lens to collect the luminescence signal excited by the glancing incidence electron gun, and a sapphire vacuum viewport to pass the light through to a Leiss double prism monochromator. Both prism and grating monochromators are available which span the spectral range from the infrared to the near-ultraviolet. However, grating monochromators typically require a change of gratings over a broad spectral range as well as filters to cut out second-order diffraction.

A liquid-nitrogen-cooled S-1 photomultiplier is a common choice for sensitive light detection from the near infrared to the ultraviolet. Ge, InSb, and PbS detectors are available for detection at longer infrared wavelengths, although their detectivities are lower and are usable only over rather limited wavelength ranges. Lock-in techniques provide some improvement in signal-to-noise ratio for all of these detectors and are especially useful in removing the infrared background due to the glow of electron gun filament reflecting off the specimen. The combination of CLS with UHV conditions provides an additional benefit: by varying surface conditions in a controllable and verifable fashion, it is possible to isolate and identify electronic features related to the surface only.

Energy Dependence of Excitation Depth

The success of CLS in detecting semiconductor interface and even surface features derives mainly from the small penetration depths of the low energy incident electron beam. Whereas electron microscopies in the 100 keV to MeV energy range typically excite luminescence over depths of tens or hundreds of microns, electron beams of several hundred to several thousand eV produce luminescence from a depth of only fractions of a micron. The glancing incidence (ca. 30°) of the electron beam on the specimen provides an additional decrease in the penetration depth of the secondary electron cascade.[22,23] Hence luminescence is observable from energy levels located at "buried" interfaces many tens of monolayers below the free surface without probing appreciable depths of the underlying substrate.

The metal film on semiconductor structure serves to enhance the interface signal relative to the substrates as well. The metal overlayer serves to reduce electron penetration into the semiconductor without contributing to the luminescence. (Nevertheless CL emission from the semiconductor surface without any metal overlayer is also observable). Likewise the band bending within the semiconductor surface space charge region can separate electron-hole pairs generated by the

electron beam, thereby reducing the probability for luminescence.[51] This "dead layer" reduces luminescence from the semiconductor substrate which could otherwise dominate a small interface signal. Band bending can also enhance the interface luminescence by raising the joint density of electron and hole states near the semiconductor surface. Thus for upward (n-type) band bending, excited holes tend to accumulate at the semiconductor surface, thereby enhancing the probability for optical transitions to the valence band at the interface.

Unfortunately, quantitative data is not available for the excitation depths of the electrons employed in low energy CLS. Instead we must estimate the maximum electron range and the depth of maximum energy loss (e.g., maximum electron-hole pair creation) from expressions derived for higher kinetic energies.

Everhart and Hoff have obtained a universal range-energy relation which incorporates the average atomic weight A, average atomic number Z, and the density of the target material. The maximum range $R_B$ for a kinetic energy E is given by[37]

$$R_B = K\int_0^{\zeta(E_0)} \zeta\, d\zeta/d(\ln\zeta)\ \mathrm{gm/cm^2} \qquad (1)$$

where

$$I = (9.76 + 58.8\, z^{-1.19})\, Z\ eV \qquad (2)$$

is the "mean excitation energy",

$$\zeta = 1.1658\, E/I \qquad (3)$$

and

$$K = 9.4 \times 10^{-12} I^2 (A/Z)\ \mathrm{gm/cm^2} \qquad (4)$$

for A in grams and I in eV

$$R_B = R_B'/K \tag{5}$$

gives a universal curve of normalized range in dimensionless units which can be approximated by expressions of the form

$$R_B = C\zeta^a \tag{6}$$

In the energy range around 1 keV, a close approximation to this function for CdS is[37]

$$R_B = 1.48\,\zeta^{1.29} \tag{7}$$

The maximum energy loss per unit depth occurs at a depth $U_o$ whose energy dependence has been fitted to the experimental measurements down to kV energies. Here[37]

$$U_o = 0.069\,\zeta^{1.71} \tag{8}$$

Similarly, $R_B$ has been fitted to the expression[37]

$$R_B = 0.62\,\zeta^{1.609} \tag{9}$$

over the same energy range. The ratio of $U_o/R_B$ varies between different materials but appears to be constant for a specific material at different energies.[37] Thus from the $U_o/R_B$ ratio extracted from the fitted expressions at intermediate energy and Equation 7 at lower energies, we obtain an expression for $U_o$ at energies around 1kV equal to

$$R_B (E \leq 1kV) = 0.1647\,\zeta^{1.392} \qquad (10)$$

From these expressions, one can obtain the maximum energy range ($R_B'$) and the maximum of the depth-dose function ($U_o$) as a function of incident electron energy. For the semiconductors CdS, InP, and GaAs, I = 343. Between the kinetic energies of 500 and 5000 eV, $R_B$ varies from 150Å to 3000Å respectively while $U_o$ varies from 20Å to 400Å respectively. Hence at voltages of 500-1000 eV, the maximum energy loss occurs at depths which are orders of magnitude smaller than those of conventional MeV electron beams.

In order to analyze the intensity dependence of CLS features as a function incident voltage, the incident beam current must be normalized to maintain a constant power dissipation over the depth range - either $R_B$ ($E \leq 1kV$) or $U_o$ ($E \leq 1kV$). Thus over a 500 to 5000 eV voltage range, beam current must increase by a 1.95 {2.42} factor to maintain constant power dissipation over $R_B$ ($E \leq 1kV$) {$U_o$ ($E \leq 1kV$)}.

Comparison with experiment suggests that the energy dependence of the depth expressions are appropriate. Figure 2 illustrates the energy dependence of the near-band-edge luminescence of bulk InP (1.35 eV) along with two deep level transitions (0.8 eV and 1.0 eV) associated only with the surface (See Figure 4a).[48] Normalizing the 1.35 eV intensity at 1.0 kV to the maximum depth of energy loss $U_o$ ($E = 1kV$), one finds comparable increases for both at higher energies. Interestingly, the 1.35 eV CLS intensity increases ca.25% more slowly, in accordance with the maximum range rather than the depth of maximum energy loss. This may reflect the influence of the "dead layer," which is several thousand Å for this lightly n-doped InP crystal and whose electric field gradient weights more heavily those CLS contributions from the deeper range.

The "surface" contributions associated with this system, 2.5Å Au on InP (110), will be discussed in a later section. However, it is significant that

surface and bulk peak intensities vary in a complementary way on the same depth scale as calculated for $U_o$ ($E \leq 1kV$). As a result, the depth of maximum excitation must not be blurred appreciably by the diffusion lengths of the cascading electrons, even though the latter can easily exceed micron distances. This effect may be due to n-type band bending in the surface space charge region which repels these secondary electrons.

Cathodoluminescence Spectroscopy of Surface-Related States

Since the early 1970's, a number of researchers have used CLS to probe semiconductors. These investigations centered on $SiO_2$,[12,13,18] CdS,[25] GaAs[8,19,30,33,34], and ZnS[25]. Some work is also available for CdTe,[26] InP,[10] ZnO,[31,32] ZnSe,[14,40] Si[24] and diamond[54]. Norris et al.[25] were the first to emphasize the difference in electronic features between the semiconductor bulk and the region only a few thousand Å below the free surface. Such depth-dependent studies focussed primarily on changes in the near-surface region due to ion implantation and other damage effects. Wittry and Kyser's studies of GaAs band-edge luminescence versus incident energy[50] provided early evidence for the "dead layer" associated with band bending in the surface space charge region and indicated that the intensity of such luminescence could indeed serve as a gauge of the band bending voltage.

On the other hand, the intermediate energies of these early experiments hampered the observation of features associated with the outer few monolayers of semiconductors atoms. Likewise, the absence of UHV conditions and the use of polished and etched surfaces suggests that surface contamination and lattice damage were significant. Few if any electronic features of the clean, ordered surfaces are likely to survive under these conditions.[4]

More recent work makes use of single crystal cleavage under UHV conditions to obtain clean, ordered surfaces. Figure 3 illustrates the effect of metal adsorption on the cleaved InP (110) surface.[46,47] Prior to metallization, the UHV-cleaved surface exhibits no luminescence at

energies below the near-band-edge transition. Upon addition of approximately one-half monolayer of various metals, each of these cases results in new emission deep within the InP band gap. Also shown are features associated with a stepped portion of a similar UHV-cleaved surfaces. High densities of broken bonds are expected for the stepped surface. The similarity between the various spectra suggests that metal deposition also produces broken bonds, at least with initial coverages.

For both metal adsorption and steps, the absolute intensity of near-band-edge emission decreases, consistent with an increase in band bending. Street et al.[39] have reported similar decreases of band edge emission for oxygen adsorption on UHV-cleaved InP.

Figure 3 demonstrates the surface sensitivity of the low energy CLS technique. These features are distinctly different from any sub-band gap features of the bulk semiconductor[41-43] which, if present, are observable with higher energy CLS as well as photoluminescence spectroscopy.

Cathodoluminescence Spectroscopy of Metal-Semiconductor Interface States

Low energy CLS is also sensitive to electronic states induced by chemical interactions at the metal-semiconductor substrate. These states and their evolution with coverage can differ significantly for various metals. Figure 4 illustrates the evolution of metal-induced states for the metals Au, Al, Cu, and Pd on InP.[46] New features induced by Au in Figure 4a extend from 0.8 eV to the band edge and evolve with coverage into a relatively narrow peak centered at 0.78eV. This spectral distribution is cut off abruptly below 0.78eV due to the sharp drop in Ge detector response at 0.7-0.8eV. Cu deposition also produces a large peak in the same region but at lower coverages and with a greater attenuation of the broad peak centered at 1.1 eV. Al and Pd coverages produce qualitatively different features with no pronounced mid-gap peak.

Evolution of these different CLS features with metal coverage and the corresponding decreases in near-band edge emission reflect the rate of band bending as measured by soft x-ray photoemission spectroscopy.[5] Furthermore the positions of the CLS peaks can account for the absolute band bending measured for the macroscopic metal-semiconductor contact.[46-48] Thus Figure 4 demonstrates that discrete interface-specific features evolve during the initial stages of Schottky barrier formation which, along with the magnitude of band bending, depend on the particular metal. These optical measurements are the first direct observations of metal-semiconductor interface states.

Metals can also induce changes in the recombination of charge carriers which depend on the surface morphology of the semiconductor coated by metal. For example, Al overlayers on smooth versus stepped inP (110) portions of the same surface exhibit a substantially different dependence of CLS intensities on electron injection level. For the smooth-cleaved surface, the relative amplitudes of features in Figure 4c are independent of beam current over several orders of magnitude. Likewise, the step-cleaved surface without Al appears to be independent of beam current. However, for Al on the step-cleaved surface, one observes an increase in the 0.8 eV feature relative to the band edge emission and other features. Figure 5 illustrates the relative increase in the 0.8 eV feature with beam currents of 4 to 18μA ($2 \times 10^{17}$ - $10^{18}$ electrons/cm$^2$ - sec). These changes are reversible and therefore not due to any electron beam damage.[15,21] Such damage effects are negligible compared to those reported for MeV energies. Thermal effects are also small, as measured under comparable conditions earlier via the shift of the near-band-edge emission, whose energy increases with temperature.

The relative intensities of the midgap to near-band-edge features can vary between stepped areas and thus depends in part on the details of the step-cleaved surfaces. However, these variations occur only with metal deposition, implying an interaction between the metal and the step atoms. Since Al reacts with InP to form Al-P complexes which can

self-limit the reaction,[3] the degree of step roughness could determine the penetration of the reaction beyond the atomic interface.

Figure 6 illustrates the injection level dependence of the these major CLS features for 20Å Al on the stepped InP surface associated with Figure 5. The 1.1 eV and 1.35 eV peak intensities increase linearly with current over three orders of of magnitude. In contrast the 0.8 eV level exhibits superlinear dependence which diverges at currents of only a few μA. This behavior is representative of radiative recombination with a density of mid-gap states (a) whose cross section depends nonlinearly on the density of free carriers (e.g., multiply-excited states) or (b) which is considerably higher than those for the higher energy transition or the band-to-band transition. In either case the metal / step states created in localized patches of the interface will produce trapping and recombination of free carriers which can be considerably different from the same transport characteristics of the smooth areas. Furthermore the variation in absolute intensity of band edge emission from surface area to area indicates different band bending and therefore different Schottky barrier heights as well. Hence CLS provides evidence for nonuniformities in charge transport and rectification at metal-semiconductor junctions which depend sensitively on semiconductor surface morphology.

Bulk features of the semiconductor can also contribute to the sub-band gap CLS emission. These features typically appear for the clean surfaces and remain unchanged (albeit weaker) with metal coverages. An additional test for such bulk-related states is for one to compare CLS and photoluminescence spectroscopy features, since the latter can probe well beyond the surface space charge region.[20] As mentioned earlier, higher energy CLS can also provide evidence similar to that of photoluminescence. Preliminary results for different GaAs crystal surfaces reveals substantial mid-gap emission from the clean surface whose intensities vary considerably depending on dopant type and concentration as well as the method of crystal growth. Significantly, these widely varying results show little difference in gap state emission near the band edge, a region commonly used by researchers to assess

the quality of crystal growth. The CLS observations of bulk crystal features suggests instead that mid-gap features are a much more appropriate figure of merit for assessing crystal quality.

Cathodoluminescence of Interface Compounds and Defects via Pulsed Laser Annealing

CLS provides a measure of new compound band structure and/or deep level defects produced by thermal processing of "buried" metal-semiconductor interfaces. To promote such phenomena without substantial interdiffusion of chemical species, one can employ laser annealing with short (5nsec pulsewidth) and high absorption (hundreds of Å for a 308nm excimer laser).[7,35,36] As an example, 50 Å Cu on CdS in Figure 7 induces a new feature at 1.28 eV which is enhanced by laser annealing.[6] The resultant peak feature corresponds closely to that of the compound $Cu_2S$.[11] On the other hand, Figure 8 illustrates the different CLS features produced by a 50Å Al film on a similar CdS (1010) surface. Here laser annealing produces a pair of emission lines at 1.3 eV and 1.65 eV. The correspondence of the 1.65 eV structure with one of the bulk features observed by photoluminescence spectroscopy and the reduction of both 1.3 and 1.675 eV features with additional laser annealing suggests that both are due to lattice damage.

The incident energy dependence provides further information regarding the depth distribution of these damage-related peaks. In Figure 9a, the 2kV (more bulk sensitive) spectrum exhibits relatively equal amplitudes for both deep level emissions whereas the 500eV (more surface-sensitive) spectrum reveals a much larger 1.35 eV peak.[6] Thus the 1.35 eV emission state is located closer to the free surface within the top few hundred Å. This is consistent with melt depths of ca.200Å for laser-induced reactions at the Al-InP interface.[36] In Figure 9b, the defect features at both incident energies decrease with respect to the near-band-edge emission, consistent with a reduction in their densities at higher annealing power levels.[6] Furthermore, comparison of 2kV and 500eV CLS spectra reveals little difference in amplitude between the two deep level peaks, indicating a more uniform spatial

distribution of both states. Thus low energy CLS reveals that both metal interactions and their changes with thermal processing have major effects on electronic structure at the "buried" metal-semiconductor interface.

## Implications for Schottky Barrier Formation

Low energy CLS provides a powerful tool to examine electronic structure of metal-semiconductor interfaces. Besides probing at metal coverages well beyond the capabilities of more conventional surface science techniques, CLS provides information on band structure and deep levels which these other techniques cannot supply directly. In particular, CLS results have revealed that metals induced discrete interface states deep within the semiconductor band gap which correlate closely with the ultimate Fermi level position of the Schottky barrier.[46] These states evolve with different energies and at different rates of coverage for different metals. Such results support models of rectification which involve charge transfer to localized states defined by the chemical interaction between metal and semiconductor.[1,2,4,9,16,52] They directly contradict models based on an absence of discrete states in the semiconductor band gap[44] as well as models which predict little or no differences for different metals.[38]

Further application of the CLS technique should refine our knowledge of these interface states, especially their chemical origin, their energy dependence on particular metals, their densities of states, and their trapping cross sections. CLS will also reveal to what extent bulk defects in some semiconductors influence the Fermi level stabilization at electrical contacts. Overall, CLS provides a direct probe of interface electronic phenomena which can play a major role in understanding Schottky barrier formation.

## Future Development

CLS research thus far has utilized a straight forward combination of electron gun and photon collection optics. The relative simplicity of the

experimental technique lends itself to studies involving substantial in-situ specimen processing such as cleaning, metallization, and annealing. Nevertheless, detailed analysis of interfacial states requires more sophisticated measurements. For example, similar CLS experiments performed at cryogenic temperatures will enhance and sharpen the spectral features which, by comparison with reported photoluminescence features for known impurities and defects, may help identify the physical origin of the deep surface levels. The CLS dependence on injection current can provide evidence for differences in trapping cross sections and densities which are not otherwise apparent for different semiconductor surface morphologies. The time dependence of luminescence excitation and deexcitation may allow one to extract capture cross sections, densities, and recombination lifetimes for these deep levels. Of course, this surface-enhanced technique can also provide surface maps of electronic structure as already performed for bulk levels via high energy cathodoluminescence or photoluminescence spectroscopies.[26-30,49] Likewise, the deep levels due to impurity diffusion could be used to establish bulk and surface diffusion constants for various adsorbates on semiconductor surfaces[40] once the energy depth-dose curve is properly fitted to a given overlayer-substrate material structure.

In conclusion, low energy CLS provides a host of information on the electronic structure of semiconductor interfaces which are difficult to obtain by other techniques. In the last few years, CLS results have demonstrated that the electronic properties of the "buried" interface are sensitive to the interaction between the contact materials and that these properties play a major role in Schottky barrier formation. With wider application and increased sophistication, the low energy CLS technique promises to reveal a host of detailed electronic information about semiconductor surfaces and interfaces.

Acknowledgements

This work is supported in part by Office of Naval Research contract N00014-80-C-0778 (G. B. Wright).

## Figure Captions

1. Schematic experimental arrangement for cathodoluminescence spectroscopy under ultrahigh vacuum conditions.

2. Dependence of luminescence peak intensity and calculated excitation depth on incident electron energy for 0.8 eV, 1.0eV, and 1.35 eV features for 2.5Å Au on n-type InP (110).

3. Cathodoluminescence spectra obtained with 1.5 keV ($R_B = 600$Å, $U_0 = 80$ Å) electrons of clean, mirror-like p-type InP (110) ($p = 10^{18}$ Zn-cm$^{-3}$) before and after submonolayer deposition of Ni, Pd, or Cu. The spectrum for the clean step-cleaved surface is shown for comparison.

4. Cathodoluminescence spectra obtained with 1.0 keV ($R_B = 400$Å, $U_0 = 50$ Å) electrons of (a) Au, (b) Cu, and (c) Al on clean mirror-like n-type InP (110) ($n = 4.3 \times 10^{15}$ cm$^{-3}$ undoped), and (d) Pd on clean mirror-like p-type InP (110) ($p = 10^{18}$ Zn-cm$^{-3}$) as a function of increasing metal deposition.

5. Cathodoluminescence spectra obtained with 1.5 keV electrons of Al on step-cleaved n-type InP (110) ($n = 4.3 \times 10^{15}$ cm$^{-3}$ undoped) in ultrahigh vacuum for several incident beam currents at constant excitation depth. Spectra are normalized to maximum peak intensity. The 0.8 eV feature increases superlinearly with increasing injection level. Spectra for (a) and (b) correspond to different stepped patches of the same cleavage surface. The higher ratio of 1.35 eV versus 0.8 eV emission intensities for (b) versus (a) corresponds to a visually lower step density.

6. Luminescence intensity for the 0.8 eV, 1.0 eV, and 1.35 eV peaks in Figure 5 versus injection current for step-cleaved InP with a 20Å Al overlayer. The superlinear injection level dependence is absent for either Al-covered, smooth surfaces or for clean, step-cleaved surfaces.

7. Cathodoluminescence spectra obtained with 2keV electrons incident on UHV-cleaved CdS (1120) after deposition of 50Å Al and after in-situ laser-annealing with energy density 0.1 J/cm$^2$.

8. Cathodoluminescence spectra obtained with 2kV electrons incident on UHV-cleaved CdS (1120) after deposition of 50Å Al and after in-situ laser annealing with increasing energy density.

9. Cathodoluminescence spectra as a function incident electron energy for UHV-cleaved CdS (1120) with a 50Å Al overlayer, laser annealed with energy density (a) 0.1 J/cm$^2$ and (b) 0.2 J cm$^2$.

## References


1. Brillson LJ. (1978). Transition in Schottky barrier formation with chemical reactivity. Phys. Rev. Lett. 40, 260-263.

2. Brillson LJ, Bachrach RZ, Bauer RS. (1979). Chemically-induced charge distribution at Al-GaAs interfaces. Phys. Rev. lett. 42, 397-400.

3. Brillson LJ, Brucker CF, Katnani AD, Stoffel NG, Margaritondo G. (1981). Chemical basis for InP-metal Schottky barrier formation. Appl. Phys. Lett. 38, 784-786.

4. Brillson LJ. (1982). The structure and properties of metal-semiconductor interfaces. Surface Sci. Repts. 2, 123-326.

5. Brillson LJ, Brucker CF, Katnani AD, Stoffel NG, Daniels R, Margaritondo G. (1982). Fermi level pinning and chemical structure of InP-metal interfaces. J. Vac. Sci, Technol., 21, 564-568.

6. Brillson LJ, Richter HW, Slade ML, Weinstein BA, Shapira Y. (1985). Cathodoluminescence spectroscopy studies of laser-annealed metal-semiconductor interfaces. J. Vac. Sci. Technol. A3, 1011-1015.

7. Brillson LJ. (1986). Promoting and characterizing new chemical and electronic structure at metal-semiconductor interfaces. Surface Sci. 168, 260-274.

8. Cone ML, Hengehold RL. (1983). Characterization of ion-implanted GaAs using cathodoluminescence. J. Appl. Phys. 54, 6346-6351.

9. Freeouf JL, Woodall JM. (1981). Schottky barriers: An effective work function model. Appl. Phys. Lett. 39, 727-729.

10. Gatos CH, Vaughan JJ, Lagowski J, Gatos HC. (1981). Cathodoluminescence of InP. J. Appl. Phys. 52, 1464-1469.

11. Guastavino F, Duchemin S, Rezig B, Grault B, Savelli M. (1978). Photon and electron excitation phenomena in copper sulfides. Conf. Rec. IEEE Photovoltaic Spec. Conf. Ser. 13, 303-308.

12. Koyama H, Matsubarak, Mauri M. (1977). Cathodoluminescence study of a silicon dioxide layer on silicon with the aid of Auger electron spectroscopy. J. Appl. Phys. 48, 5380-5381.

13. Koyama H. (1979). Cathodoluminescence study of $SiO_2$. J. Appl. Phys. 51, 2228-2235.

14. Krier A, Bryant FJ. (1986). Cathodoluminescence of laser-Annealed Erbium-implanted zinc selenide. J. Phys. Chem. Solids, 47, 719-725.

15. Lang DV. (1977). Review of radiation-induced defects in III-V compounds. Inst. Phys. Conf. Ser. 31, 70-94.

16. Ludeke R, Landgren G. (1986). Electronic properties and chemistry of Ti/GaAs and Pd/GaAs interfaces. Phys. Rev. B33, 5526-5535.

17. Magnea N, Petroff PM, Capasso F, Logan RA, Alva K, Cho AY. (1985). Electric field dependence cathodoluminescence of III-V compound heterostructures: A new interface characterization technique. Appl. Phys. Lett. 46, 1074-1076.

18. McKnight SW, Palik ED. (1980). Cathodoluminescence of $SiO_2$ films. J. Noncrystalline Solids 40, 595-603.

19. McKnight SW, Palik ED, Bhar TN, (1980). Cathodoluminescence studies of anodic oxides on GaAs. J. Vac. Sci. Technol. 17, 967-970.

20. Mettler K. (1977). Photoluminescence as a tool for the study of the electronic surface properties of gallium arsenide. Appl. Phys. 12, 75-82.

21. Mircea A, Bois D. (1979). A review of deep-level defects in III-V semiconductors. Inst. Phys. Conf. Ser. 46, 82-99.

22. Murata K. (1976). Exit angle dependence of penetration depth of backscattered electrons in the scanning electron microscope. Phys. Stat. Sol. (a) 36, 197-208.

23. Murata K. (1976). Depth resolution of the low- and high-deflection backscattering electron images in the scanning electron microscope. Phys. Stat. Sol. (a) 36, 527-532.

24. Myhajlenko S, Ke W, Hamilton B. (1983). Cathodoluminescence assessment of electron beam recrystallized silicon. J. Appl. Phys. 54, 862-867.

25. Norris CB, Barnes CE, Beezhold W. (1973). Depth-resolved cathodoluminescence in undamaged and ion-implanted GaAs, ZnS, and CdS. J. Appl. Phys. 44, 3200-3221.

26. Norris CB, Barnes CE, Zanio KR. (1977). Cathodoluminescence studies of anamalous ion implantation defect introduction in CdTe. J. Appl. Phys. 48, 1659-1667.

27. Petroff PM, Lang DV, Strudel JL, Logan RA. (1978). Scanning transmission electron microscopy techniques for simultaneous electronic analysis and

observation of defects in semiconductors. Scanning Electron Microsc. 1978; I:325-332.

28. Petroff PM, Lang DV, Logan RA, Strudel JL, (1980). Analyzing semiconductor defects. Circuits Manufacturing 4, 35-54.

29. Petroff PM, Miller RC, Gossard AC, Weigmann W. (1984). Impurity trapping, interface structure, and luminescence of GaAs quantum wells grown by molecular beam epitaxy. Appl. Phys. Lett. 44, 217-219.

30. Petroff PM. (1985). Defects in III-V compound semiconductors in semiconductors and semimetals, Vol. 22A, Eds. R. K. Willardson and A. C. Beer (Academic Press, New York, 1985) 379-403.

31. Pierce BJ, Hengehold RL. (1976). Depth-resolved cathodoluminescence of ion-implanted layers in zinc oxide. J. Appl. Phys. 47, 644-651.

32. Paqlueras J, Kubalek E. (1985). Cathodoluminescence from deformed ZnO ceramics. Solid State Commun. 54, 745-746.

33. Rakshit S, Biswas SN, Chakravarti AN. (1971). Dependence of the intensity of spontaneous emission from electron-beam-excited specimens of impure GaAs on the level of excitation. Phys. Stat. Sol. (a) 7, 593-595.

34. Rao-Sahib TS, Wittry DB. (1969). Measurement of diffusion lengths in p-type gallium arsenide by electron beam excitation. J. Appl. Phys. 40, 3745-350.

35. Richter H, Brillson LJ, Daniels RR, Kelly M, Margaritondo G. (1984). Control and characterization of metal-InP and GaAs interfaces formed by laser-enhanced reactions. J. Vac. Sci. Technol. B2, 591-596.

36. Richter HW, Brillson LJ, Kelly MK, Daniels RR, Margaritondo G. (1986). Laser-induced chemical reactions at the Al / III-V compound semiconductor interface. J. Appl. Phys. 60, 1994-2002.

37. Shea SP. (1984). Energy and atomic number dependence of electron depth-dose and lateral-dose functions, in: Electron Beam Interactions With Solids, D.F.Kyser, D.E.Newbury, H. Niedrig, R. Shimizu (eds), SEM, Inc., AMF O'Hare, IL 60666, 145-151 and references therein.

38. Spicer WE, Lindau I, Skeath, Su CY. (1980). Unified defect model and beyond. J. Vac. Sci. Technol. 17, 1019-1027.

39. Street RA, Williams RH, Bauer RS. (1980). Influence of the surface on photoluminescence from indium phosphide crystals. J. Vac. Sci. Technol. 17, 1001-1004.

40. Takenoshita H, Kodo K, Sawai K. (1986). Cathodoluminescence study of diffusion coefficients of Al, Ga, and In in ZnSe. Jpn, J. Appl. Phys. 25, 1610-1611.

41. Tempkin H, Bonner WA. (1981). Photoluminescence study of melt grown InP. J. Appl. Phys 52, 397-401.

42. Tempkin H, Dutt BV, Bonner WA. (1981). Photoluminescence study of native defects in InP. Appl. Phys. Lett. 38, 431-433.

43. Tempkin H, Dutt BV, Bonner WA, Keramidas VG. (1982). Deep radiative levels for InP. J. Appl. Phys. 53, 7526-7533.

44. Tersoff J. (1985). Schottky barriers and semiconductor band structures. Phys. Rev. B32, 6968-6971.

45. Vilms J, Spicer WE. (1965). Quantum efficiency and radiative lifetime in p-type gallium arsenide. J. Appl. Phys. 36, 2815-2821.

46. Viturro RE, Slade ML, Brillson LJ. (1986). Optical-emission properties of interface states for metals in III-V compounds. Phys. Rev. Lett. 57, 487-490.

47. Viturro RE, Slade ML, Brillson LJ. (1977). Proc. 18th International Conference on the Physics of Semiconductors (Stockholm, 1976), in press.

48. Viturro RE, Slade ML, Brillson LJ. (1987). Optical emission proeprties of metal/InP and GaAs interface states. J. Vac. Sci. Technol., in press; Viturro RE, Shaw JL, Brillson LJ. unpublished.

49. Warwick CA, Brown GT. (1985). Spatial distribution of 0.68 eV emission from undoped semi-insulating gallium arsenide revealed by high resolution luminescence imaging. Appl. Phys. Lett. 46, 574-576.

50. Wittry DB, Kyser DF. (1967). Measurements of diffusion lengths in direct gap semiconductors by electron-beam excitation. J. Appl. Phys. 38, 375-382.

51. Wittry DB. (1984). Gaussian models for the energy distribution of excitation in solids: Applications to x-ray microanalysis and solid state electronics. Scanning Electron Microsc. 1984; I:99-108.

52. Woodall JM, Freeouf JL. (1981). GaAs metallization: some problems and trends. J. Vac. Sci. Technol. 19, 794-798.

53. Yacobi BG, Holt DB. (1986). Cathodoluminescence scanning electron microscopy of semiconductors. J. Appl. Phys. 59, R1-R24.

54. Yamamoto N, Spence JCH, Fathy D. (1984). Cathodoluminescence and polarization studies from individual dislocations in diamond. Phil. Mag. B49, 609-629.

## Discussion With Reviewers

### Reviewer #1

Answer

The spatial resolution of the CLS apparatus is defined by the spot size of the electron beam. In our case, the glancing incidence beam had a nominal diameter of a fraction of a millimeter. Of course, the technique can be extended to much higher resolution.

Answer

Yes, we have indeed used EBIC to map these variations. The corresponding displayed image shows darker and lighter areas that can be assigned to differences in band bending.

Answer

No, we haven't. However, this should certainly be possible to do with this technique.

### Reviewer #2

Answer

Carrier diffusion should increase rather than decrease the surface sensitivity. The random scattering of excited electrons and the diffusion of thermal carriers at depths of only a few hundred Å will result in an accumulation of electron - hole pairs near the surface (over and above any band bending effects). With increasing distance from the surface, such accumulation decreases as the excitation depth increases toward or exceeds the thermal carrier diffusion length.

Carrier diffusion is expected to reduce the depth discrimination. However, the pronounced voltage dependence of the CLS spectra

presented here suggests that extended diffusion of thermal carriers does not make a dominant contribution to the radiative recombination.

Answer

With the injection levels indicated in Figure 6 and neglecting losses due to reflection as well as lateral diffusion, we estimate our volume carrier generation to be ca. $10^{23}$-$10^{25}$ electron-hole pairs-cm$^{-3}$ for the excitation energies and depths discussed in the paper. Assuming a carrier lifetime of $10^{-9}$ sec, this means excess minority carrier concentrations of $10^{14}$ - $10^{16}$ cm$^{-3}$ versus bulk carrier concentrations of $5x10^{15}$ -$10^{18}$ cm$^{-3}$. Furthermore, only a fraction of minority carriers generated reach the surface and compensate the space charge. Thus the excess carriers may not affect the band bending significantly at these concentrations. Nevertheless, the point is well taken and we plan to explore the effect of excess free carriers on the surface band bending.

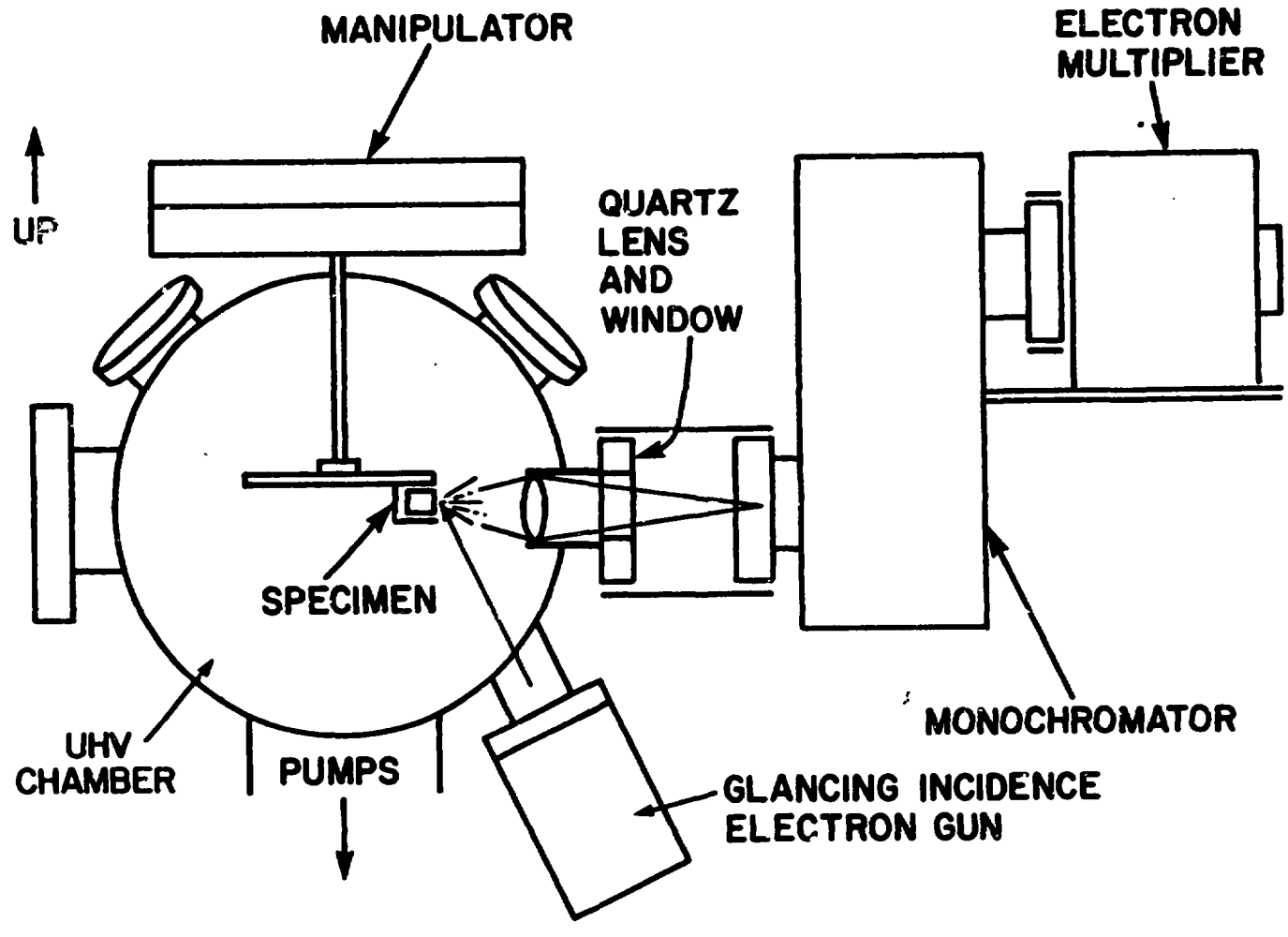
MANIPULATOR
ELECTRON MULTIPLIER
UP
QUARTZ LENS AND WINDOW
SPECIMEN
UHV CHAMBER
PUMPS
MONOCHROMATOR
GLANCING INCIDENCE ELECTRON GUN

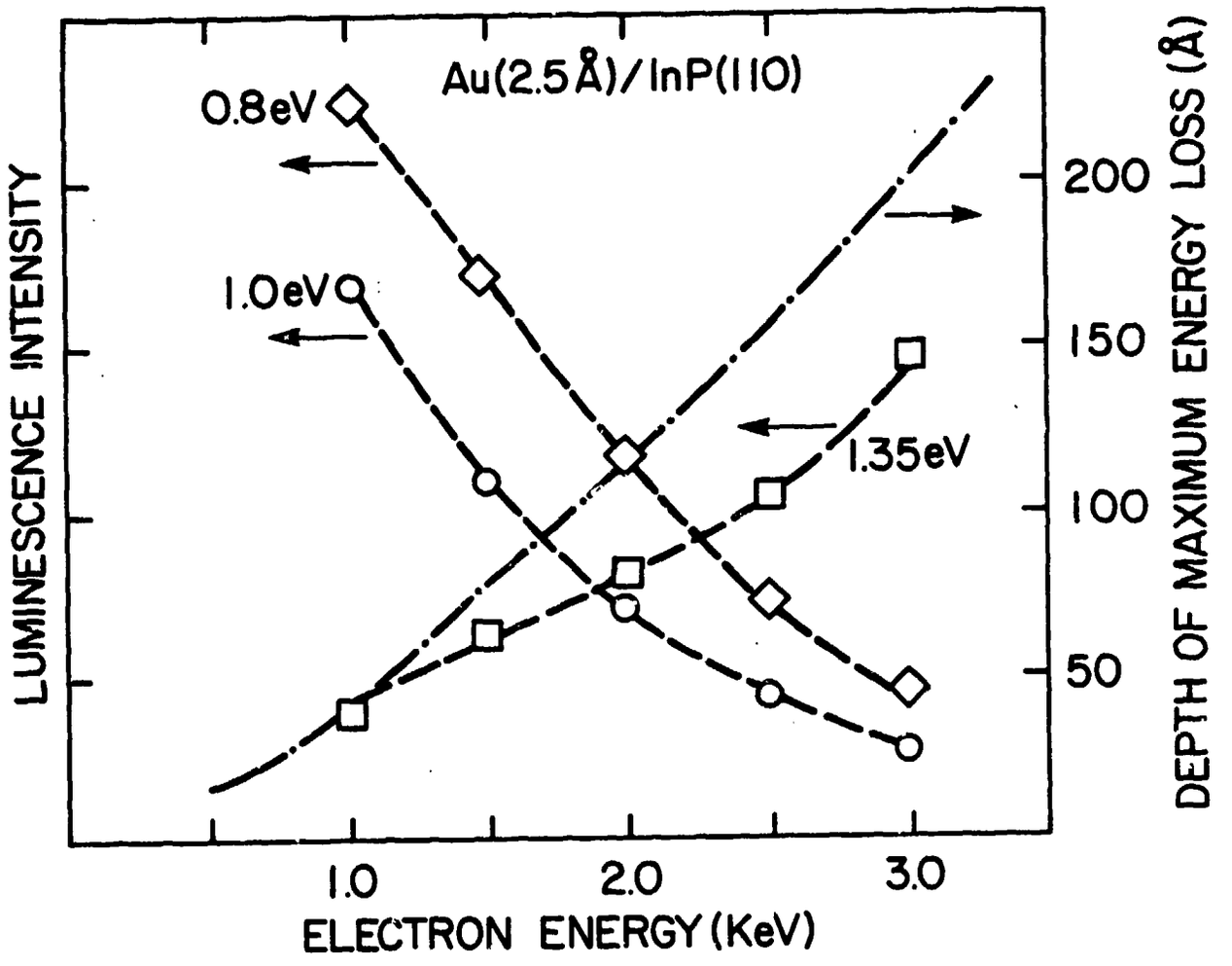
Au(2.5 Å)/InP(110)
0.8eV
1.0eV
1.35eV
LUMINESCENCE INTENSITY
DEPTH OF MAXIMUM ENERGY LOSS (Å)
200
150
100
50
1.0
2.0
3.0
ELECTRON ENERGY (KeV)

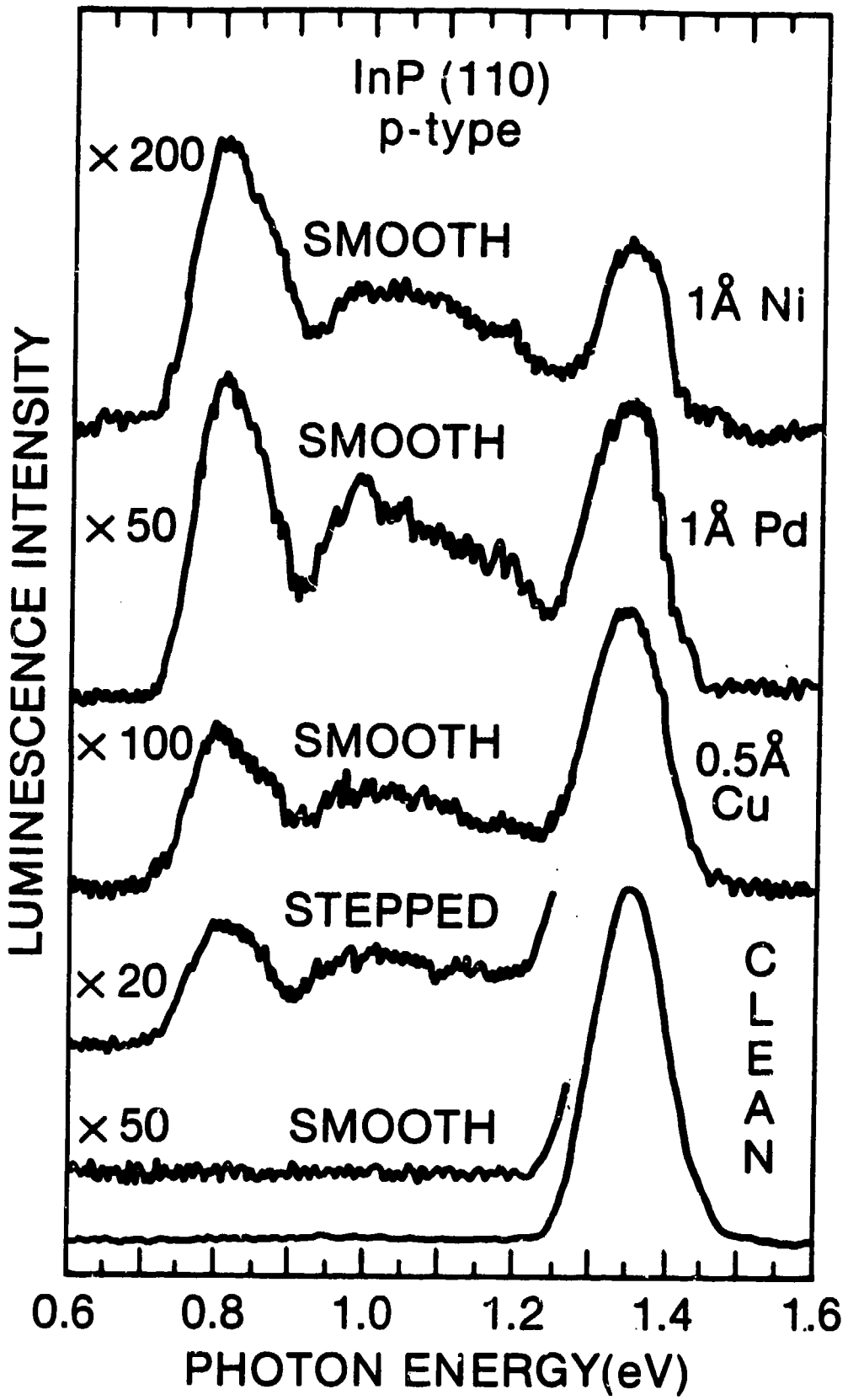
InP (110)
p-type
×200
SMOOTH
1Å Ni
SMOOTH
×50
1Å Pd
×100
SMOOTH
0.5Å
Cu
STEPPED
×20
CLEAN
×50
SMOOTH
LUMINESCENCE INTENSITY
0.6
0.8
1.0
1.2
1.4
1.6
PHOTON ENERGY(eV)

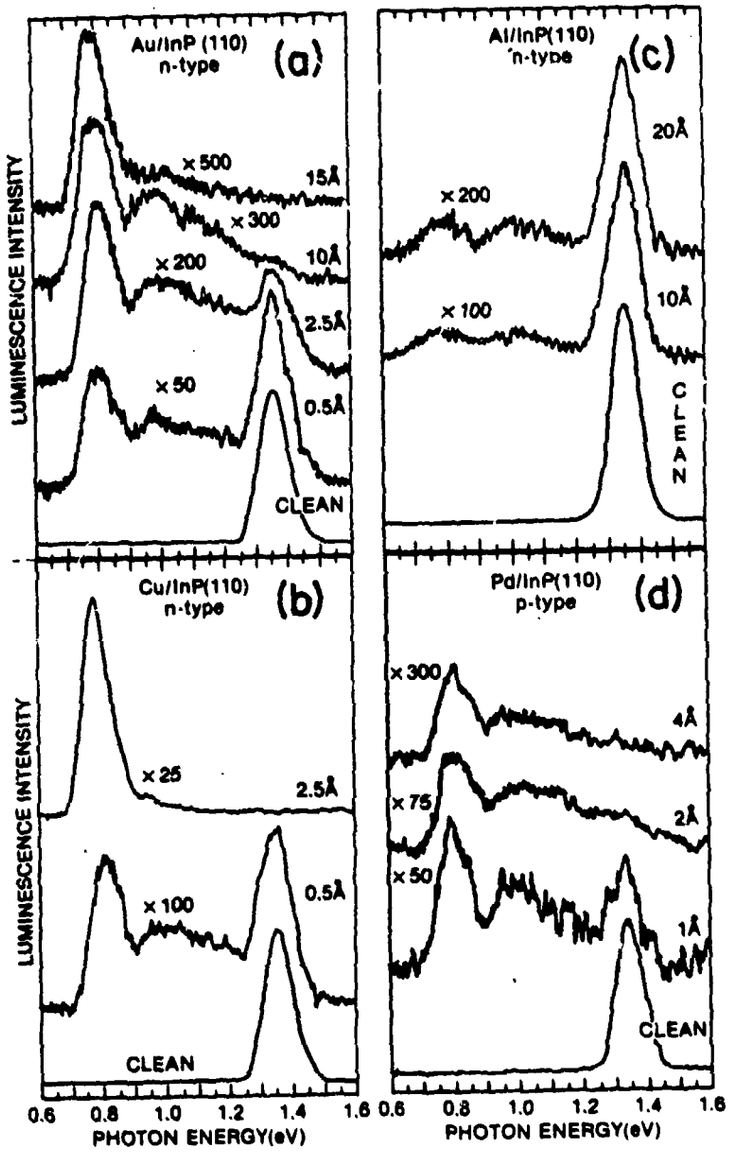
Au/InP (110)
n-type
(a)
×500
15Å
×300
10Å
×200
2.5Å
×50
0.5Å
CLEAN
Al/InP(110)
n-type
(c)
20Å
×200
×100
10Å
CLEAN
Cu/InP(110)
n-type
(b)
×25
2.5Å
×100
0.5Å
CLEAN
Pd/InP(110)
p-type
(d)
×300
4Å
×75
2Å
×50
1Å
CLEAN
LUMINESCENCE INTENSITY
LUMINESCENCE INTENSITY
0.6 0.8 1.0 1.2 1.4 1.6
PHOTON ENERGY(eV)
0.6 0.8 1.0 1.2 1.4 1.6
PHOTON ENERGY(eV)

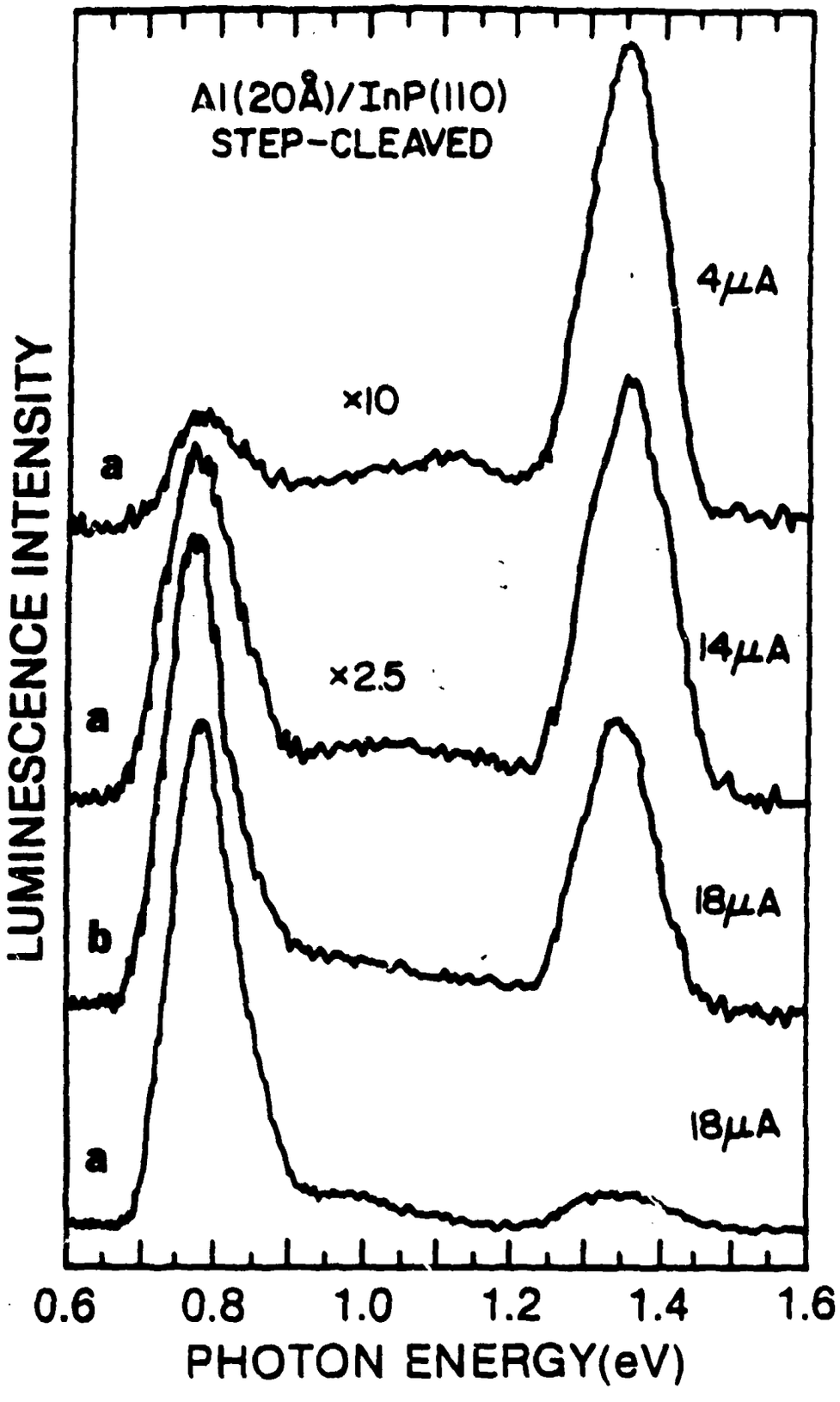
Al(20Å)/InP(110)
STEP-CLEAVED
4μA
×10
a
14μA
×2.5
a
18μA
b
18μA
a
LUMINESCENCE INTENSITY
0.6
0.8
1.0
1.2
1.4
1.6
PHOTON ENERGY(eV)

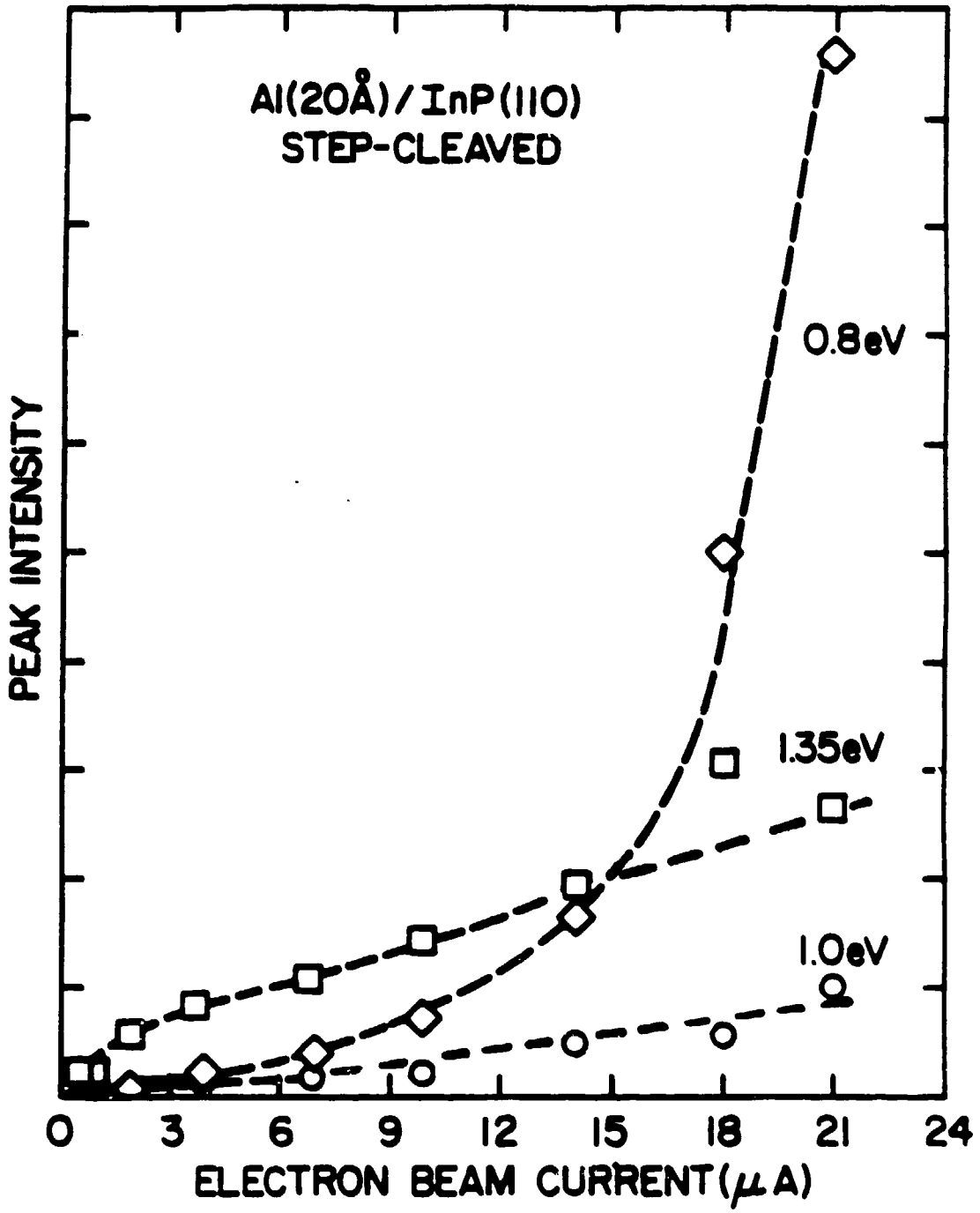
Al(20Å)/InP(110)
STEP-CLEAVED
0.8eV
1.35eV
1.0eV
PEAK INTENSITY
0
3
6
9
12
15
18
21
24
ELECTRON BEAM CURRENT(μA)

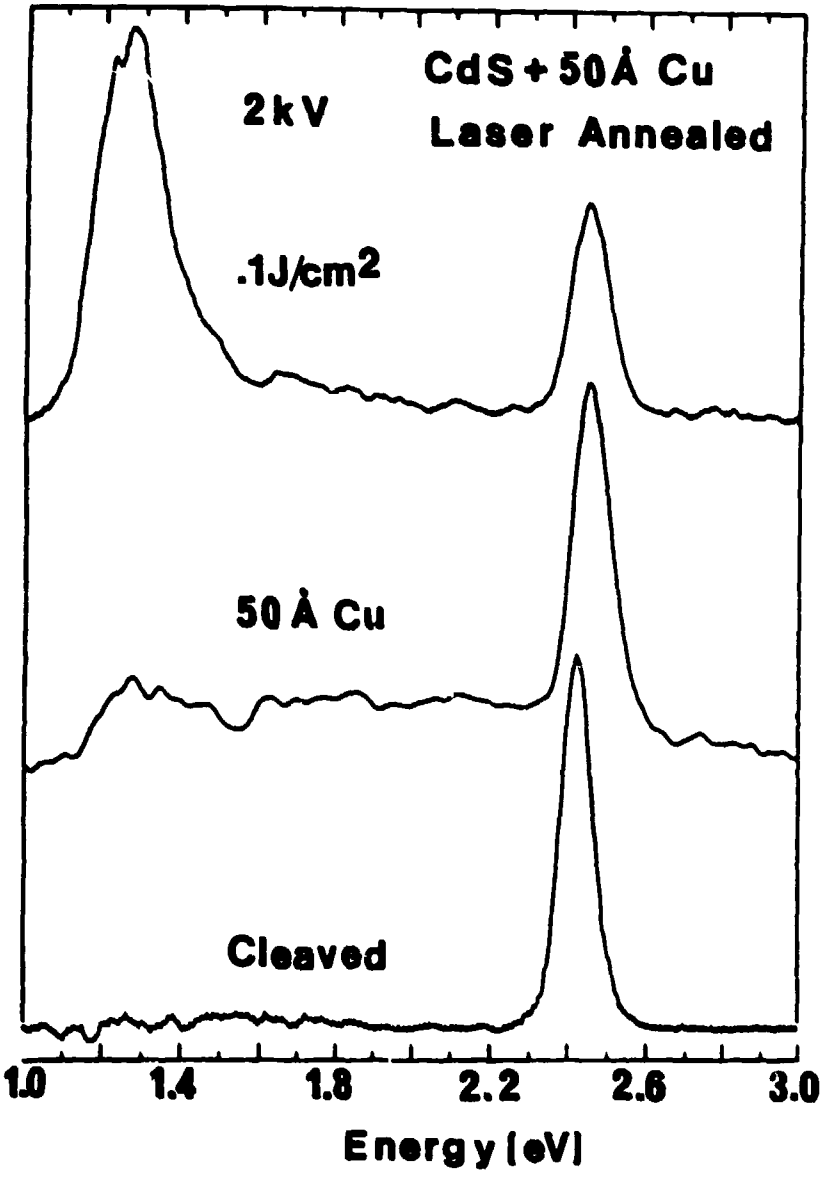
CdS + 50Å Cu
Laser Annealed
2kV
.1J/cm2
50 Å Cu
Cleaved
1.0
1.4
1.8
2.2
2.6
3.0
Energy [eV]

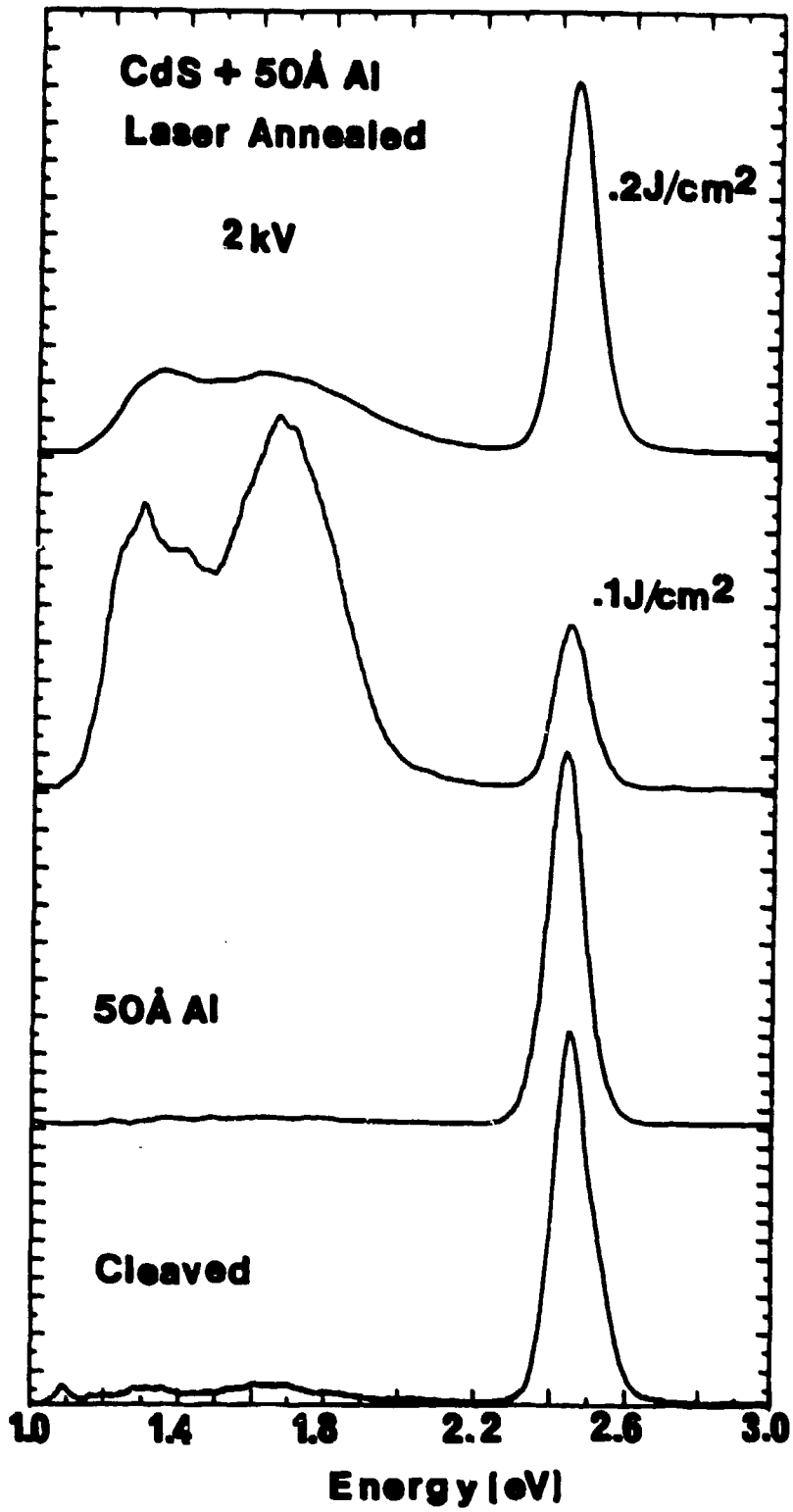
CdS + 50Å Al
Laser Annealed
2kV
.2J/cm2
.1J/cm2
50Å Al
Cleaved
1.0
1.4
1.8
2.2
2.6
3.0
Energy (eV)

Fig. 3

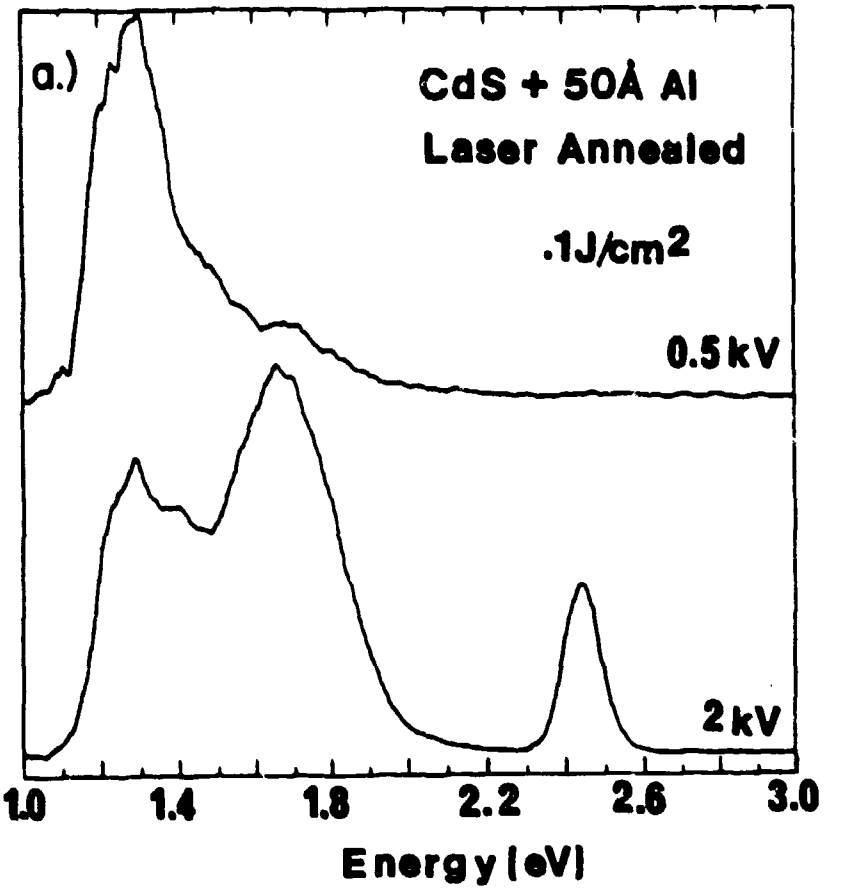
a.)
CdS + 50Å Al
Laser Annealed
.1J/cm2
0.5kV
2kV
1.0
1.4
1.8
2.2
2.6
3.0
Energy [eV]

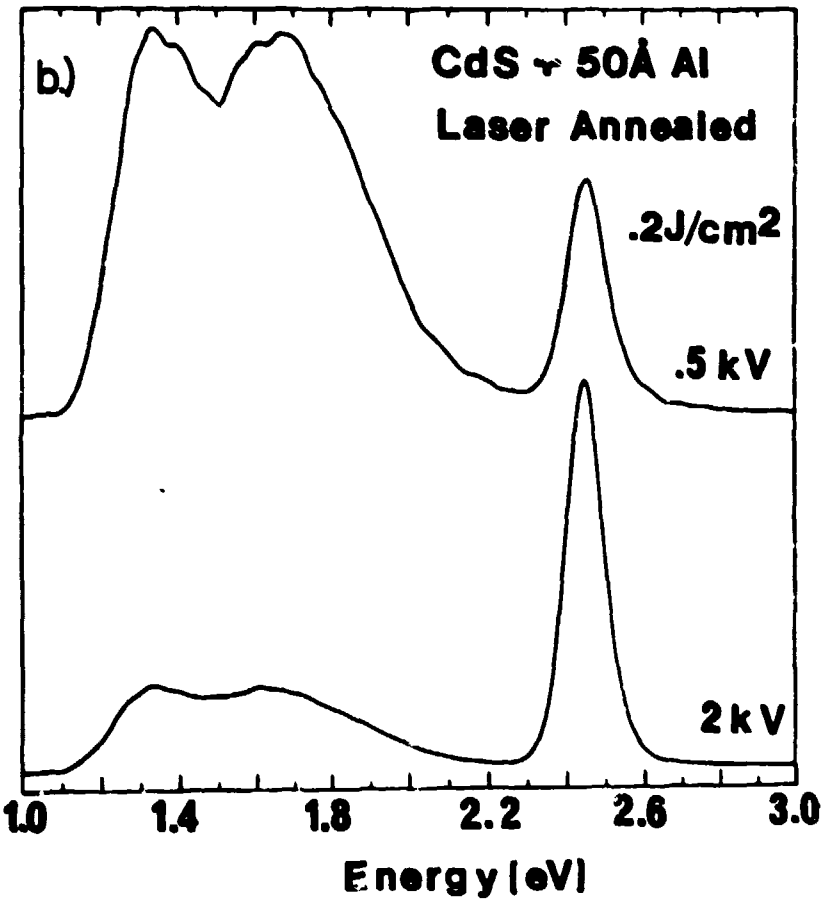
b.)
CdS + 50Å Al
Laser Annealed
.2J/cm2
.5kV
2kV
1.0
1.4
1.8
2.2
2.6
3.0
Energy [eV]

## V. Cumulative List of Publications under Navy Contract N00014-80-C-0778

80-C-0778-1. **Atomic and Electrical Structure of InP-Metal Interfaces: A Prototypical III-V Compound Semiconductor**, L.J. Brillson, C.F. Brucker, A.D. Katnani, N.G. Stoffel, and G. Margaritondo, Journal of Vacuum Science and Technology 19, 661 (1981).

80-C-0778-2. **Chemical Basis for InP-Metal Schottky Barrier Formation**, L.J. Brillson, C.F. Brucker, A.D. Katnani, N.G. Stoffel, and G. Margaritondo, Applied Physics Letters 38, 784 (1981).

80-C-0778-3. **Fermi Level Pinning and Chemical Structure of InP-Metal Interfaces**, L.J. Brillson, C.F. Brucker, A.D. Katnani, N.G. Stoffel, R. Daniels and G. Margaritondo, Journal of Vacuum Science and Technology 21, 564 (1982).

80-C-0778-4. **Leading Semiconductor Research in China**, Scientific Bulletin, Dept. Navy, Office of Naval Research Tokyo 6, 48 (1981).

80-C-0778-5. **Abruptness of Semiconductor-Metal Interfaces**, L.J. Brillson, C.F. Brucker, A.D. Katnani, N.G. Stoffel, and G. Margaritondo, Physical Review Letters 46, 838 (1981).

80-C-0778-6. **Interface Chemical Reaction and Interdiffusion of Thin Metal Films on Semiconductors**, L.J. Brillson, Thin Solid Films 89, 461 (1982).

80-C-0778-7. **Interaction of Metals with Semiconductor Surfaces**, L. J. Brillson, Applications of Surface Science, 11/12, 249 (1982).

80-C-0778-8. **Chemical and Electronic Structure of Compound Semiconductor-Metal Interfaces**, L.J. Brillson, Journal of Vacuum Science and Technology 20, 652 (1982).

80-C-0778-9. **Systematics of Chemical Structure and Schottky Barriers at Compound Semiconductor-Metal Interfaces** L.J. Brillson, C.F. Brucker, N.G. Stoffel, A.D. Katnani, R. Daniels, and G. Margaritondo, Proceedings of the Second IUPAP Semiconductor Symposium on Surfaces and Interfaces, Surface Science 132, 212 (1983).

80-C-0778-10. **Photoemission Studies of Reactive Diffusion and Localized Doping at II-VI Compound Semiconductor Interfaces**, L.J. Brillson, C.F. Brucker, N.G. Stoffel, A.D. Katnani, R. Daniels, and G. Margaritondo, Proceedings of the 16th International Conference on the Physics of Semiconductor, Physica 117B&C, 848 (1983).

80-C-0778-11. **Contact Technology in 3-5 Device Analysis and Modification of Metal-Semiconductor Contact Interface in 3-5 Devices**, L.J. Brillson, IEEE Technical Digest of the International Electron Devices Meeting, p. 111.

80-C-0778-12. **Soft X-Ray Photoemission Techniques for Characterizing Metal-Semiconductor Interfaces**, L.J. Brillson, Proceedings of the Brookhaven Conference on Advances in Soft X-Ray Science and

Technology, Eds. F.J. Himpsel and R.W. Klaffky (SPIE, Bellingham, WA, 1984) p. 89.

80-C-0778-13. **InP Surface States and Reduced Surface Recombination Velocity**, L. J. Brillson, Y. Shapira, and A. Heller, Applied Physics Letters, 43, 174 (1983).

80-C-0778-14. **Investigation of InP Surface and Metal Interfaces by Surface Photovoltage and Auger Electron Spectroscopies**, Y. Shapira, L.J. Brillson and A. Heller, Journal of Vacuum Science and Technology A1, 766 (1983).

80-C-0778-15. **Studies of Surface Recombination Velocity Reduction of InP Photoelectrochemial Solar Cells**, Y. Shapira, L.J. Brillson, and A. Heller, Proceedings of the Fifth EC Photovoltaic Solar Energy Conference, Athens, Greece (1983).

80-C-0778-16. **Origin of Surface and Metal-Induced Interface States on InP**, Y. Shapira, L.J. Brillson, and A. Heller, Physical Review B29, 6824 (1984).

80-C-0778-17. **Auger Depth Profiling Studies of Interdiffusion and Chemical Trapping at Metal-InP Interfaces**, Y. Shapira and L. J. Brillson, Journal of Vacuum Science and Technology B1, 618 (1983).

80-C-0778-18. **Reduction of Silicon-Aluminum Interdiffusion by Improved Semiconductor Ordering**, L.J. Brillson, M. Slade, A. Katnani, M. Kelly, and G. Margaritondo, Applied Physics Letters 44, 110 (1984).

80-C-0778-19. **Photoemission Studies of Atomic Redistribution at Gold-Silicon and Aluminum-Silicon Interfaces**, L.J. Brillson, A.D. Katnani, M. Kelly, and G. Margaritondo, Journal of Vacuum Science and Technology A2, 551 (1984).

80-C-0778-20. **Ultrafast UV-Laser Induced Oxidation of Silicon**, T.E.Orlowski and H. Richter, Materials Research Society Symposium Proceedings 23, 327 (1984).

80-C-0778-21. **Ultrafast Laser-Induced Oxidation of Silicon: A New Approach Towards High Quality, Low Temperature, Patterned $SiO_2$ Formation**, T.E.Orlowski and H.Richter, Applied Physics Letters 45, 241 (1984).

80-C-0778-22. **Ultrafast UV-Laser-Induced Oxidation of Silicon: Control and Characterization of the Si-$SiO_2$ Interface**, H.Richter, T.E. Orlowski, M.Kelly, and G. Margaritondo, Journal of Applied Physics 56, 2351(1984).

80-C-0778-23. **Interdiffusion and Chemical Trapping at InP (110) Interfaces with Au, Al, Ni, Cu and Ti**, Y. Shapira, L.J. Brillson, A.D. Katnani and G. Margaritondo, Physical Review B30, 4586 (1984).

80-C-0778-24. **Control and Characterization of Metal-InP and GaAs Interfaces Formed by Laser-Enhanced Reactions**, H. Richter, L.J. Brillson, R.

Daniels, M. Kelly, and G. Margaritondo, Journal of Vacuum Science and Technology B2, 591 (1984).

80-C-0778-25. **Laser-Induced Chemical Reactions at the Al/III-V Semiconductor Interface**, H. Richter and L.J. Brillson, Proceedings of the 17th International Conference on the Physics of Semiconductors (Springer-Verlag, New York, 1985), p. 137.

80-C-0778-26. **Advances in Characterizing and Controlling Metal-Semiconductor Interfaces**, L.J. Brillson, Applications of Surface Science 22/23, 948 (1985).

80-C-0778-27. **Cathodoluminescence Spectroscopy Studies of Laser-Annealed Metal-Semiconductor Interfaces**, L.J. Brillson, H.W. Richter, M.L. Slade, B.A.Weinstein, and Y. Shapira, Journal of Vacuum Science and Technology A3, 1011 (1985).

80-C-0778-28. **Laser-Induced Chemical Reaction at the Al/III-V Compound Semiconductor Interface**, H.W. Richter and L.J. Brillson, Journal of Applied Physics 60, 1994 (1986).

80-C-0778-29. **UPS, XPS and AES Studies of $CaF_2$-CdSe**, C.F. Brucker, Y. Shapira and L.J. Brillson, Thin Solid Films 135, 203 (1986).

80-C-0778-30. **Acceptor-Like Electron Traps and Thermally-Reversible Barrier Heights for Al on UHV-Cleaved (110) InP**, John H. Slowik, H.W. Richter, and L.J. Brillson, Journal of Applied Physics 58, 3154 (1985).

80-C-0778-31. **Promoting and Characterizing New Chemical and Electronic Structure at Metal-Semiconductor Interfaces**, L.J. Brillson, Surface Science 168, 260 (1986).

80-C-0778-32. **Control of Titanium-Silicon and Silicon Dioxide Reactions by Low Temperature Rapid Thermal Annealing**, L.J. Brillson, M.L. Slade, H.W. Richter, H. Vander Plas, and R.T. Fulks, Applied Physics Letters 47, 1080 (1985).

80-C-0778-33. **Titanium-Silicon and Silicon Dioxide Reactions Controlled by Low Temperature Rapid Thermal Annealing**, L.J. Brillson, M.L. Slade, H.W. Richter, H. Vander Plas, and R.T. Fulks, Journal of Vacuum Science and Technology A4, 993 (1986).

80-C-0778-34. **Chemical Reaction and Interdiffusion at III-V Compound Semiconductor-Metal Interfaces** L.J. Brillson, Materials Research Society Symposium Proceedings 54, 327 (1986).

80-C-0778-35. **Acceptor-like Electron Traps Control Effective Barrier for UHV-Cleaved and Laser Annealed Al/InP**, J. Slowik, L.J. Brillson, and H. Richter, Journal of Vacuum Science and Technology B4, 974 (1986).

80-C-0778-36. **Fermi Level Pinning and Chemical Interactions at Metal - $In_xGa_{1-x}As$ (100) Interfaces**, L.J. Brillson, M.L. Slade, R.E. Viturro, M. Kelly, N. Tache, G. Margaritondo, J. Woodall, G.D. Pettit, P.D. Kirchner and

S.L. Wright, Journal of Vacuum Science and Technology B4, 919 (1986).

80-C-0778-37. **Absence of Fermi Level Pinning at Metal - $In_xGa_{1-x}As$ (100) Interfaces,** L.J.Brillson, M.L. Slade, R.E. Viturro, M.Kelly, N. Tache, G. Margaritondo, J.M. Woodall, G.D. Pettit, P.D. Kirchner, and S.L. Wright, Applied Physics Letters 48, 1458 (1986).

80-C-0778-38. **Optical Emission Properties of Metal/III-V Compound Semiconductor Interface States,** R. E. Viturro, M. L. Slade, and L. J. Brillson, Physical Review Letters 57, 487 (1986).

80-C-0778-39. **Metallization of III-V Compounds,** L. J. Brillson, in Semiconductor-Based Heterostructures: Interfacial Structure and Stability, ed. J.E.E.Baglin, G.Y.Chin, H. W. Deckman, W. Mayo, and D. Narasinham (The Metallurgical Society,Inc.Warrendale,PA,1986) p.387.

80-C-0778-40. **Cathodoluminescence Spectroscopy of Metal/III-V Compound Semiconductor Interface States,** R. E. Viturro, M. L. Slade, and L. J. Brillson, Proceedings of the 18th International Conference on the Physics of Semiconductors (Stockholm, 1986) p. 371.

80-C-0778-41. **Optical Emission Properties of Metal / InP and GaAs Interface States,** R. E. Viturro, M. L. Slade, and L. J. Brillson, Journal of Vacuum Science and Technology, A5, 1516 (1987).

80-C-0778-42. **Near-Ideal Schottky Barrier Formation at Metal-GaP Interfaces,** L.J.Brillson, R.E.Viturro, M.L.Slade, P. Chiaradia, D. Kilday, M. Kelly, and G. Margaritondo, Applied Physics Letters 50, 1379 (1987).

80-C-0778-43. **Unpinned Schottky Barrier Formation at Metal-GaP Interfaces: A Representative III-V Compound Case,** P. Chiaradia, R. E. Viturro, M.L.Slade, L.J.Brillson, D.Kilday, M.Kelly, N.Tache, and G. Margaritondo, Journal of Vacuum Science and Technology B5, 1075 (1987).

80-C-0778-44. **Cleavage-Related Electronic States of Al - InP (110) Interfaces,** R.E.Viturro and L.J.Brillson, Journal of Vacuum Science and Technology B5, 1125 (1987).

80-C-0778-45. **Low Energy Cathodoluminescence Spectroscopy of Semiconductor Interfaces,** L.J.Brillson and R.E.Viturro, Scanning Electron Microscopy, in press.

## VI. Postdoctoral Fellows Involved in Navy Contract N0014-C-0778 Research for the Period October 1, 1986 through September 30, 1987

1. Dr. Enrique Viturro, Solid State Institute, The Technion, Israel Institute of Technology,Haifa, Israel.

2. Prof. Piero Chiaradia, Istituto Struttura Material of CNR, Frascati, Italy.

## VII. Publications / Patents / Presentations / Honors for the Period October 1, 1986 to September 30, 1987

### A. Papers Submitted to Refereed Journals (and not yet published)

1. **Low Energy Cathodoluminescence Spectroscopy of Semiconductor Interfaces,** L.J.Brillson and R.E.Viturro, Scanning Electron Microscopy, in press.

2. **Schottky Barrier Formation at Meta/MBE-Grown GaAs,** R.E.Viturro, J.L.Shaw, and L.J.Brillson, Submitted to Journal of Vacuum Science and Technology.

3. **Cathodoluminescence Spectroscopy of Metal-Semiconductor Interface Structures,** L.J.Brillson, R.E.Viturro, J.L.Shaw, and H.W.Richter, Submitted to Journal of Vacuum Science and Technology.

4. **Electronic Properties of Metal / MBE-Grown GaAs(100) Interfaces,** R.E.Viturro, J.L.Shaw, L.J.Brillson, J. McKinley, L.Tache, G.Margaritondo, J.M. Woodall, G.D. Pettit, P.D. Kirchner, and S.L. Wright, Submitted to Physical Review Letters.

### B. Papers Published in Refereed Journals

1. **Titanium-Silicon and Silicon Dioxide Reactions Controlled by Low Temperature Rapid Thermal Annealing,** L.J. Brillson, M.L. Slade, H.W. Richter, H. Vander Plas, and R.T. Fulks, Journal of Vacuum Science and Technology A4, 993 (1986).

2. **Chemical Reaction and Interdiffusion at III-V Compound Semiconductor-Metal Interfaces** L.J. Brillson, Materials Research Society Symposium Proceedings 54, 327 (1986).

3. **Acceptor-like Electron Traps Control Effective Barrier for UHV-Cleaved and Laser Annealed Al/InP,** J. Slowik, L.J. Brillson, and H. Richter, Journal of Vacuum Science and Technology B4, 974 (1986).

4. **Fermi Level Pinning and Chemical Interactions at Metal - $In_xGa_{1-x}As$ (100) Interfaces,** L.J. Brillson, M.L. Slade, R.E. Viturro, M. Kelly, N. Tache, G. Margaritondo, J. Woodall, G.D. Pettit, P.D. Kirchner and S.L. Wright, Journal of Vacuum Science and Technology B4, 919 (1986).

5. **Absence of Fermi Level Pinning at Metal - $In_xGa_{1-x}As$ (100) Interfaces,** L.J.Brillson, M.L. Slade, R.E. Viturro, M.Kelly, N. Tache, G. Margaritondo, J.M. Woodall, G.D. Pettit, P.D. Kirchner, and S.L. Wright, Applied Physics Letters 48, 1458 (1986).

6. **Optical Emission Properties of Metal/III-V Compound Semiconductor Interface States,** R. E. Viturro, M. L. Slade, and L. J. Brillson, Physical Review Letters 57, 487 (1986).

7. **Metallization of III-V Compounds,** L. J. Brillson, in Semiconductor- Based Heterostructures: Interfacial Structure and Stability, ed. J.E.E.Baglin, G.Y.Chin, H. W. Deckman, W. Mayo, and D. Narasinham (The Metallurgical Society,Inc.Warrendale,PA,1986) p.387.

8. **Cathodoluminescence Spectroscopy of Metal/III-V Compound Semiconductor Interface States,** R. E. Viturro, M. L. Slade, and L. J. Brillson, Proceedings of the 18th International Conference on the Physics of Semiconductors (Stockholm, 1986) p. 371.

9. **Optical Emission Properties of Metal / InP and GaAs Interface States,** R. E. Viturro, M. L. Slade, and L. J. Brillson, Journal of Vacuum Science and Technology, A5, 1516 (1987).

10. **Near-Ideal Schottky Barrier Formation at Metal-GaP Interfaces,** L.J.Brillson, R.E.Viturro, M.L.Slade, P. Chiaradia, D. Kilday, M. Kelly, and G. Margaritondo, Applied Physics Letters 50, 1379 (1987).

11. **Unpinned Schottky Barrier Formation at Metal-GaP Interfaces: A Representative III-V Compound Case,** P. Chiaradia, R. E. Viturro, M.L.Slade, L.J.Brillson, D.Kilday, M.Kelly, N.Tache, and G. Margaritondo, Journal of Vacuum Science and Technology B5, 1075 (1987).

12. **Cleavage-Related Electronic States of Al - InP (110) Interfaces,** R.E.Viturro and L.J.Brillson, Journal of Vacuum Science and Technology B5, 1125 (1987).

**C. Books (and Sections Thereof) Submitted for Publication**

None

**D. Books(and Sections Thereof) Published**

None

**E. Patents Filed**

None

**F. Patents Granted**

None

**G. Invited Presentations at Topical or Scientific/Technical Society Conferences**

1. **Recent Photoemission and Cathodoluminescence Spectroscopy Studies of III-V Semiconductor Interfaces,** L.J. Brillson, Workshop on 3-5 Semiconductor -Metal Interfacial Chemistry and Its Effect On Electrical Properties, Stanford University, Palo Alto, CA, November 4, 1986. Supported by Xerox Corporation.

2. **Surface Science Characterization of Metal-Semiconductor Interfaces**, American Vacuum Society Ohio Chapter Meeting, Dayton, OH, February 17, 1987. Supported by Xerox Corporation.

3. **Interface Chemical Bonding and Diffusion on an Atomic Scale at Metal-Semiconductor Interfaces**, American Physical Society Meeting , New York City, NY, March 25, 1987. Supported by Xerox Corporation.

4. **The Atomic-Scale World of Metal-Semiconductor Contacts : A Tour Via Surface Science Techniques**, Rochester Institute of Technology, Rochester, NY, April 7, 1987. Supported by Xerox Corporation.

5. **Low Energy Cathodoluminescence Spectroscopy of Metal-Semiconductor Interfaces**, Scanning Electron Microscopy Conference, Hamilton, Ontario, Canada, May 5, 1987. Supported by Xerox Corporation.

6. **Physics and Chemistry of Metal - Semiconductor Interfaces**, Electrochemical Society Meeting, Philadelphia, PA, May 11, 1987. Supported by Xerox Corporation.

7. **Atomic Scale Characterization and Processing of Semiconductor Surfaces and Interfaces**, North Coast Ohio Chapter Symposium of the American Vacuum Society, Cleveland, OH, May 21, 1987. Supported by Xerox Corporation.

8. **Electronic Structure of Metal - Semiconductor Interfaces**, Mexican National Vacuum Society Meeting, University of Morelia, Michoacan, Mexico, September 23, 1987. Supported by Xerox Corporation.

**H. Honors/Awards/Prizes**

None

**VIII. Money Spent on Equipment**

None

**IX. Transitions of Research to Industry**

None

## X. Collaborations with Workers from Academic Institutions

1. Professor Giorgio Margaritondo, Department of Physics, University of Wisconsin, Madison, WI - Soft X-Ray Photoemission Spectroscopy of Metal-Semiconductor Interfaces, Cathodoluminescence Spectroscopy of Ge-InP Interfaces.

2. Professor Piero Chiaradia, Istituto Struttura Materia CNR, Frascati, Italy - Schottky Barrier Formation at Metal-GaP Interfaces.

3. Prof. Antoine Kahn, Department of Electrical Engineering, Princeton University, Fermi Level Movements at Metal-GaAs Intefaces.

4. Prof. Harry Wieder, Department of Electrical Engineering and Computer Science, University of California at San Diego, Deep Level Luminescence and Fermi Level Pinning at Metal- InAlAs Interfaces.